Published by Institute of Physics Publishing for SISSA
Received: *May 17, 2005*
Revised: *August 12, 2005*
Accepted: *September 7, 2005*
Published: *September 20, 2005*

Antenna subtraction at NNLO

Aude Gehrmann-De Ridder
Institute for Theoretical Physics, ETH
CH-8093 Zürich, Switzerland
E-mail: gehra@phys.ethz.ch

Thomas Gehrmann
Institut für Theoretische Physik, Universität Zürich
Winterthurerstrasse 190, CH-8057 Zürich, Switzerland
E-mail: thomas.gehrmann@physik.unizh.ch

E.W. Nigel Glover
Institute of Particle Physics Phenomenology, Department of Physics
University of Durham
Durham, DH1 3LE, U.K.
E-mail: e.w.n.glover@durham.ac.uk

Abstract: The computation of exclusive QCD jet observables at higher orders requires a method for the subtraction of infrared singular configurations arising from multiple radiation of real partons. We present a subtraction scheme relevant for NNLO perturbative calculations in $e^+e^- \to$ jets. The building blocks of the scheme are antenna functions derived from the matrix elements for tree-level $1 \to 3$ and $1 \to 4$ and one-loop $1 \to 3$ processes. By construction, these building blocks have the correct infrared behaviour when one or two particles are unresolved. At the same time, their integral over the antenna phase space is straightforward. As an example of how to use the scheme we compute the NNLO contributions to the subleading colour QED-like contribution to $e^+e^- \to 3$ jets. To illustrate the application of NNLO antenna subtraction for different colour structures, we construct the integrated forms of the subtraction terms needed for the five-parton and four-parton contributions to $e^+e^- \to 3$ jets at NNLO in all colour factors, and show that their infrared poles cancel analytically with the infrared poles of the two-loop virtual correction to this observable.

Keywords: NLO Computations, Jets, QCD.

Contents

1. Introduction

Experimental measurements of jet production observables are among the most sensitive tests of the theory of Quantum Chromodynamics (QCD), and yield very accurate determinations of QCD parameters [1], especially of the strong coupling constant α_s. At present, the precision of many of these determinations is limited not by the quality of the experimental data, but by the error on the theoretical (next-to-leading order, NLO) calculations used for the extraction of the QCD parameters. To improve upon this situation, an extension of the theoretical calculations to next-to-next-to-leading order (NNLO) is therefore mandatory [2].

In the recent past, many ingredients to NNLO calculations of collider observables have been derived, including the universal three-loop QCD splitting functions [3] which govern the evolution of parton distribution functions at NNLO. The massless two-loop $2 \to 2$ and $1 \to 3$ matrix elements relevant to NNLO jet production have been computed [4, 5] using several innovative methods [6], and are now available for many processes of phenomenological relevance. The one-loop corrections to $2 \to 3$ and $1 \to 4$ matrix elements have been known for longer [7, 8] and form part of NLO calculations of the respective multi-jet observables [9, 10]. These NLO matrix elements naturally contribute to NNLO jet observables of lower multiplicity if one of the partons involved becomes unresolved (soft or collinear) [11]. In these cases, the infrared singular parts of the matrix elements need to be extracted and integrated over the phase space appropriate to the unresolved configuration to make the infrared pole structure explicit. Methods for the extraction of soft and collinear limits of one-loop matrix elements are worked out in detail in the literature [11 – 16]. As a final ingredient, the tree level $2 \to 4$ and $1 \to 5$ processes also contribute to $(2 \to 2)$- and $(1 \to 3)$-type jet observables at NNLO. These contain double real radiation singularities corresponding to two partons becoming simultaneously soft and/or collinear [17 – 20]. To determine the contribution to NNLO jet observables from these configurations, one has to find two-parton subtraction terms which coincide with the full matrix element and are still sufficiently simple to be integrated analytically in order to cancel their infrared pole structure with the two-loop virtual and the one-loop single-unresolved contributions. In the past, such configurations were only dealt with on a case-by-case basis in the context of specific calculations [17, 21 – 24], while no general method was available. Several methods have been proposed recently to accomplish this task [25 – 29]. Up to now, only one method has been fully worked through for observables of physical interest:the sector decomposition algorithm [30, 31]. In this method, both phase space and loop integrals are analytically decomposed into their Laurent expansion in dimensional regularisation, and the coefficients of the expansion are numerically integrated. Results have been obtained for $e^+e^- \to 2j$ [32], $pp \to H + X$ [33] and most recently for muon decay [34] at NNLO. In contrast to all other approaches, in the sector decomposition method one does not have to integrate the subtraction term analytically.

Following a number of pioneering calculations [35 – 37], infrared subtraction of real radiation singularities is well understood at NLO, where several generic process independent methods exist [38 – 41]. One of these methods is the so-called antenna subtraction [10, 41], which derives NLO subtraction terms from three-parton tree-level matrix elements which naturally encapsulate all singular limits due to unresolved emission of a single parton between two colour-connected [42, 43] hard partons (radiators). In [44], we described the construction of NNLO subtraction terms for $e^+e^- \to 2j$ based on full four-parton tree-level and three-parton one-loop matrix elements, which can be integrated analytically over the appropriate phase spaces [31]. If normalised appropriately, these full four-parton tree-level and three-parton one-loop matrix elements can be interpreted as antenna functions at NNLO. These NNLO antenna subtraction terms derived from four-parton matrix elements with a hard quark-antiquark pair in [44] were used subsequently [45] to compute the $\alpha_s^3 C_F^3$-correction to $e^+e^- \to 3j$ at NNLO.

The calculation presented in [44] included only antenna functions involving radiation off a hard quark-antiquark pair. We derived colour-ordered matrix elements (and thus NNLO antenna functions) for the two other partonic configurations (hard quark-gluon radiators and hard gluon-gluon radiators) by using appropriate effective lagrangian densities coupling an external current to a gluino-gluon [46] or gluon-gluon [47] system.

In the present paper, we describe the antenna subtraction method at NNLO in detail and provide an algorithm for the construction of antenna subtraction terms at NNLO from the basic three-parton and four-parton antenna functions. For the sake of clarity, we restrict ourselves to the kinematical situation of a colour-neutral particle decaying into coloured final state partons, as relevant to $e^+e^- \to m$ jets at NNLO. The basic structure of the NNLO antenna subtraction can however be carried over to configurations with partons in the initial state.

The paper is structured as follows. In section 2 we describe the antenna subtraction method at NLO and NNLO, and explain the construction of the subtraction functions for tree-level and one-loop real radiation matrix elements up to NNLO accuracy from the basic three- and four-parton antenna functions. All antenna functions are derived and integrated over their appropriate final state phase spaces in the following sections. Section 3 establishes the notation, and lists the different possible antenna configurations. In section 4, we introduce the colour-ordered infrared singularity operators [48] appearing in the integrated NLO and NNLO antenna functions. The quark-antiquark, quark-gluon and gluon-gluon antenna functions in both unintegrated and integrated forms are then derived in sections 5–7. Their behaviour in all single and double unresolved limits is summarised in section 8. As a first non-trivial application of our method, we document the calculation of the subleading colour NNLO QCD correction to the $e^+e^- \to 3j$ cross section (which was already reported briefly in [45]) in section 9. To illustrate the generality of the method, and to outline future applications of it, we reconstruct the infrared pole structure of the integrated NNLO subtraction terms for $e^+e^- \to 3j$ in all colour factors, and show that these cancel the explicit infrared poles of the two-loop virtual corrections to this observable in section 10. Finally, section 11 contains our conclusions and an outlook on applications and extensions of the method presented here.

JHEP09(2005)056

2. Infrared subtraction terms

To obtain the perturbative corrections to a jet observable at a given order, all partonic multiplicity channels contributing to that order have to be summed. In general, each partonic channel contains both ultraviolet and infrared (soft and collinear) singularities. The ultraviolet poles are removed by renormalisation, however the soft and collinear infrared poles cancel among each other when all partonic channels are summed over [49].

While infrared singularities from purely virtual corrections are obtained immediately after integration over the loop momenta, their extraction is more involved for real emission (or mixed real-virtual) contributions. Here, the infrared singularities only become explicit after integrating the real radiation matrix elements over the phase space appropriate to the jet observable under consideration. In general, this integration involves the (often iterative) definition of the jet observable, such that an analytic integration is not feasible (and also not appropriate). Instead, one would like to have a flexible method that can be easily adapted to different jet observables or jet definitions. Therefore, the infrared singularities of the real radiation contributions should be extracted using infrared subtraction terms. The crucial points that all subtraction terms must satisfy are that (a) they approximate the full real radiation matrix elements in all singular limits and (b) are still sufficiently simple to be integrated analytically over a section of phase space that encompasses all regions corresponding to singular configurations. Note that the subtraction terms should also be local and should fully account for the limit they are aimed at without introducing spurious infrared singularities in other limits.

In this paper, we shall restrict ourselves to the kinematical situation of a massive, colour-neutral particle decaying into massless coloured partons, such as multijet production in electron-position annihilation:

$$e^+e^- \to m \text{ jets}\,.$$

In this situation, infrared singularities appear only due to final state radiation. In the more general partonic scattering kinematics, coloured partons are also present in the initial state, yielding initial state and fixed initial/final state singularities. The method presented here can, like the antenna factorisation method at NLO [41], be extended to these situations. This extension is beyond the scope of this paper, and will only be commented on briefly in section 11 below.

To specify the notation, we define the tree-level n-parton contribution to the m-jet cross section (for tree level cross sections $n = m$; we leave $n \neq m$ for later reference) in d dimensions by,

$$\mathrm{d}\sigma^B = \mathcal{N} \sum_n \mathrm{d}\Phi_n(p_1,\ldots,p_n;q)\frac{1}{S_n}\,|\mathcal{M}_n(p_1,\ldots,p_n)|^2\; J_m^{(n)}(p_1,\ldots,p_n)\,, \tag{2.1}$$

the normalisation factor $\mathcal{N}$ includes all QCD-independent factors as well as the dependence on the renormalised QCD coupling constant α_s, $\sum_n$ denotes the sum over all configurations with n partons, $\mathrm{d}\Phi_n$ is the phase space for an n-parton final state with total four-momentum q^μ in $d = 4-2\epsilon$ space-time dimensions,

$$\mathrm{d}\Phi_n(p_1,\ldots,p_n;q) = \frac{\mathrm{d}^{d-1}p_1}{2E_1(2\pi)^{d-1}}\;\cdots\;\frac{\mathrm{d}^{d-1}p_n}{2E_n(2\pi)^{d-1}}\;(2\pi)^d\;\delta^d(q-p_1-\ldots-p_n)\,, \tag{2.2}$$

while S_n is a symmetry factor for identical partons in the final state. $|\mathcal{M}_n|^2$ denotes a squared, colour-ordered tree-level n-parton matrix element, where particle 1 is colour connected to particle 2 which is colour connected to particle 3 and so on as illustrated in Figure 1. Contributions to the squared matrix element which are subleading in the number of colours can equally be treated in the same context, noting that these subleading terms yield configurations where a certain number of essentially non-interacting particles are emitted between a pair of hard radiators. By carrying out the colour algebra, it becomes evident that non-ordered gluon emission inside a colour-ordered system is equivalent to

JHEP09(2005)056

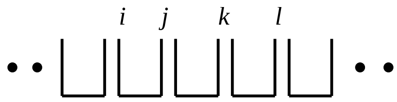

Figure 1: Illustration of colour connection.

photon emission off the outside legs of the system [18, 42]. For simplicity, these subleading colour contributions are also denoted as squared matrix elements $|\mathcal{M}_m|^2$, although they often correspond purely to interference terms between different amplitudes.

The precise definition depends on the number and types of particles involved in the process. However, all colour orderings are summed over in $\sum_m$ with the appropriate colour weighting. The jet function $J_m^{(n)}$ defines the procedure for building m jets out of n partons. The main property of $J_m^{(n)}$ is that the jet observable defined above is collinear and infrared safe as explained in [39, 40]. In general $J_m^{(n)}$ contains θ and δ-functions. $J_m^{(n)}$ can also represent the definition of the n-parton contribution to an event shape observable related to m-jet final states.

From (2.1), one obtains the leading order approximation to the m-jet cross section by integration over the appropriate phase space.

$$\mathrm{d}\sigma_{LO} = \int_{\mathrm{d}\Phi_m} \mathrm{d}\sigma^B \,. \tag{2.3}$$

Depending on the jet function used, this cross section can still be differential in certain kinematical quantities.

2.1 NLO infrared subtraction terms

At NLO, we consider the following m-jet cross section,

$$\mathrm{d}\sigma_{\mathrm{NLO}} = \int_{\mathrm{d}\Phi_{m+1}} \left(\mathrm{d}\sigma^R_{\mathrm{NLO}} - \mathrm{d}\sigma^S_{\mathrm{NLO}}\right) + \left[\int_{\mathrm{d}\Phi_{m+1}} \mathrm{d}\sigma^S_{\mathrm{NLO}} + \int_{\mathrm{d}\Phi_m} \mathrm{d}\sigma^V_{\mathrm{NLO}}\right] . \tag{2.4}$$

The cross section $\mathrm{d}\sigma^R_{\mathrm{NLO}}$ has the same expression as the Born cross section $\mathrm{d}\sigma^B_{\mathrm{NLO}}$ (2.1) above except that $m \to m+1$, while $\mathrm{d}\sigma^V_{\mathrm{NLO}}$ is the one-loop virtual correction to the m-parton Born cross section $\mathrm{d}\sigma^B$. The cross section $\mathrm{d}\sigma^S_{\mathrm{NLO}}$ is a (preferably local) counter-term for $\mathrm{d}\sigma^R_{\mathrm{NLO}}$. It has the same unintegrated singular behaviour as $\mathrm{d}\sigma^R_{\mathrm{NLO}}$ in all appropriate limits. Their difference is free of divergences and can be integrated over the $(m+1)$-parton phase space numerically. The subtraction term $\mathrm{d}\sigma^S_{\mathrm{NLO}}$ has to be integrated analytically over all singular regions of the $(m+1)$-parton phase space. The resulting cross section added to the virtual contribution yields an infrared finite result.

A systematic procedure for finding NLO infrared subtraction terms is the antenna formalism introduced in [10, 41]. The antenna subtraction terms are obtained as sum of antennae:

$$\begin{aligned}\mathrm{d}\sigma^S_{\mathrm{NLO}} = \mathcal{N} \sum_{m+1} \mathrm{d}\Phi_{m+1}(p_1,\ldots,p_{m+1};q)\frac{1}{S_{m+1}} \times \qquad\qquad (2.5)\\ \times \sum_j X^0_{ijk}\,|\mathcal{M}_m(p_1,\ldots,\tilde{p}_I,\tilde{p}_K,\ldots,p_{m+1})|^2\, J_m^{(m)}(p_1,\ldots,\tilde{p}_I,\tilde{p}_K,\ldots,p_{m+1})\,,\end{aligned}$$

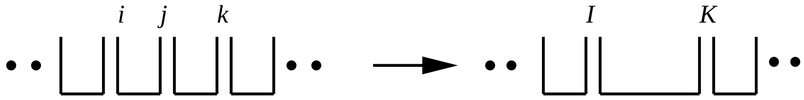

Figure 2: Colour connection of the partons showing the parent and daughter partons for the single unresolved antenna.

such that,

$$
\begin{aligned}
\mathrm{d}\sigma^{R}_{\mathrm{NLO}} - \mathrm{d}\sigma^{S}_{\mathrm{NLO}} = \mathcal{N} \sum_{m+1} \mathrm{d}\Phi_{m+1}(p_1, \ldots, p_{m+1}; q) \frac{1}{S_{m+1}} \times \\
\times \Bigg[|\mathcal{M}_{m+1}(p_1, \ldots, p_{m+1})|^2 \; J_m^{(m+1)}(p_1, \ldots, p_{m+1}) - \\
- \sum_j \; X^0_{ijk} \, |\mathcal{M}_m(p_1, \ldots, \tilde{p}_I, \tilde{p}_K, \ldots, p_{m+1})|^2 \times \\
\times \, J_m^{(m)}(p_1, \ldots, \tilde{p}_I, \tilde{p}_K, \ldots, p_{m+1}) \Bigg] . \qquad (2.6)
\end{aligned}
$$

The subtraction term involves the m-parton amplitude depending only on the redefined on-shell momenta $p_1, \ldots, \tilde{p}_I, \tilde{p}_K, \ldots, p_{m+1}$ where $\tilde{p}_I, \tilde{p}_K$ are linear combinations of p_i, p_j, p_k while the tree antenna function X^0_{ijk} depends only on p_i, p_j, p_k. X^0_{ijk} describes all of the configurations (for this colour-ordered amplitude) where parton j is unresolved. This occurs because of the particular factorisation properties of colour-ordered amplitudes. In particular, when particle j is a gluon and becomes soft, the colour-ordered matrix element undergoes QED-like factorisation so that,

$$
|\mathcal{M}_{m+1}(p_1, \ldots, p_i, p_j, p_k, \ldots, p_{m+1})|^2 \to \frac{2 s_{ik}}{s_{ij} s_{jk}} |\mathcal{M}_m(p_1, \ldots, \tilde{p}_I, \tilde{p}_K, \ldots, p_{m+1})|^2 .
$$

In this limit $\tilde{p}_I \equiv p_i$ and $\tilde{p}_K \equiv p_k$. Together particles I and K form a colour connected hard antenna that radiates particle j. In doing so, the momenta of the radiators change to form particles i and k. The type of particle may also change. For example when particle j is a gluon, the colour factor is modified at the amplitude level by,

$$
T^{a_j}_{ik} \leftrightarrow \delta_{iI} \delta_{IK} \delta_{Kk} \, ,
$$

as illustrated in figure 2. The antenna factorisation of squared matrix element and phase space can be illustrated pictorially, as displayed in figure 3.

The antenna approach described here is closely related to the commonly used dipole factorisation formalism derived by Catani and Seymour [40]. Here, the corresponding subtraction term for the same colour-ordered squared matrix element is given by

$$
\begin{aligned}
\mathrm{d}\sigma^{S}_{\mathrm{NLO}} = \mathcal{N} \sum_{m+1} \mathrm{d}\Phi_{m+1}(p_1, \ldots, p_{m+1}; q) \frac{1}{S_{m+1}} \times \qquad (2.7) \\
\times \Bigg[\sum_j \mathcal{D}_{ij,k} \, |\mathcal{M}_m((p_1, \ldots, \tilde{p}_{ij}, \tilde{p}_k, \ldots, p_{m+1})|^2 \; J_m^{(m)}(p_1, \ldots, \tilde{p}_{ij}, \tilde{p}_k, \ldots, p_{m+1}) + \\
+ \sum_j \mathcal{D}_{kj,i} |\mathcal{M}_m((p_1, \ldots, \tilde{p}_i, \tilde{p}_{kj}, \ldots, p_{m+1})|^2 J_m^{(m)}(p_1, \ldots, \tilde{p}_i, \tilde{p}_{kj}, \ldots, p_{m+1}) \Bigg] .
\end{aligned}
$$

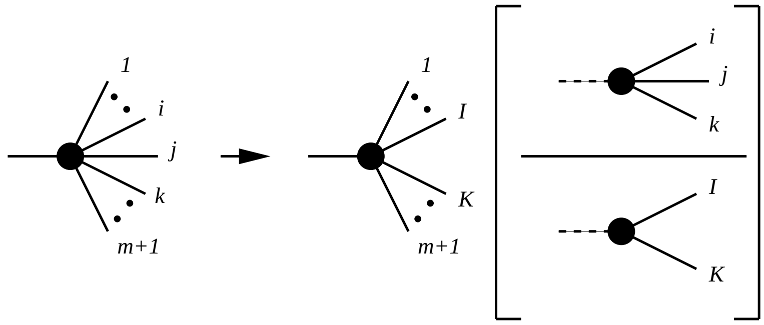

Figure 3: Illustration of NLO antenna factorisation representing the factorisation of both the squared matrix elements and the $(m+1)$-particle phase space. The term in square brackets represents both the antenna function X^0_{ijk} and the antenna phase space $\mathrm{d}\Phi_{X_{ijk}}$.

In the first term, the dipole contribution involves the m-parton amplitude which only depends on the redefined on-shell momenta $p_1, \ldots, \tilde{p}_{ij}, \tilde{p}_k, \ldots, p_{m+1}$ and the dipole function $\mathcal{D}_{ij,k}$ which depends on p_i, p_j, p_k. The momenta p_i, p_j and p_k are respectively the emitter, unresolved parton and the spectator momenta corresponding to a single dipole term. In the second term, the role of emitter and spectator are exchanged. The redefined on-shell momenta $\tilde{p}_{ij}, \tilde{p}_k$ $(\tilde{p}_{kj}, \tilde{p}_i)$ are different linear combinations of p_i, p_j and p_l for each dipole. In the antenna approach, the momentum mapping would be the same for each dipole contribution and the two terms combine to form the tree antenna, X^0_{ijk}. The two dipoles combining to an antenna have a common unresolved parton, and contain the two possible emitter/spectator combinations. In the antenna language, emitter and spectator act as radiators. Note that we can always choose to divide the antenna and use different momentum maps for the two parts.

The jet function $J_m^{(m)}$ in (2.6) does not depend on the individual momenta p_i, p_j and p_k, but only on $\tilde{p}_I, \tilde{p}_K$. One can therefore carry out the integration over the unresolved dipole phase space appropriate to p_i, p_j and p_k analytically, exploiting the factorisation of the phase space,

$$\mathrm{d}\Phi_{m+1}(p_1, \ldots, p_{m+1}; q) = \mathrm{d}\Phi_m(p_1, \ldots, \tilde{p}_I, \tilde{p}_K, \ldots, p_{m+1}; q) \cdot \mathrm{d}\Phi_{X_{ijk}}(p_i, p_j, p_k; \tilde{p}_I + \tilde{p}_K)\,. \tag{2.8}$$

The NLO antenna phase space $\mathrm{d}\Phi_{X_{ijk}}$ is proportional to the three-particle phase space, as can be seen by using $m = 2$ in the above formula and exploiting the fact that the two-particle phase space is a constant,

$$P_2 = \int \mathrm{d}\Phi_2 = 2^{-3+2\epsilon}\pi^{-1+\epsilon}\frac{\Gamma(1-\epsilon)}{\Gamma(2-2\epsilon)}\left(q^2\right)^{-\epsilon}\,, \tag{2.9}$$

such that

$$\mathrm{d}\Phi_3 = P_2\,\mathrm{d}\Phi_{X_{ijk}}\,. \tag{2.10}$$

For the analytic integration, we can use (2.8) to rewrite each of the subtraction terms in the form,

$$|\mathcal{M}_m|^2\, J_m^{(m)}\, \mathrm{d}\Phi_m \int \mathrm{d}\Phi_{X_{ijk}}\, X^0_{ijk}\,,$$

where $|\mathcal{M}_m|^2$, $J_m^{(m)}$ and $\mathrm{d}\Phi_m$ depend only on $p_1, , \ldots, \tilde{p}_I, \tilde{p}_K, \ldots, p_{m+1}$ and $\mathrm{d}\Phi_{X_{ijk}}$ and X_{ijk}^0 depend only on p_i, p_j, p_k. The analytic integral of the subtraction term is therefore defined as the antenna function integrated over the fully inclusive antenna phase space, normalised appropriately,

$$\mathcal{X}_{ijk}^0(s_{ijk}) = \left(8\pi^2\,(4\pi)^{-\epsilon}\,e^{\epsilon\gamma}\right) \int \mathrm{d}\Phi_{X_{ijk}}\, X_{ijk}^0\,. \tag{2.11}$$

This integration is performed analytically in d dimensions to make the infrared singularities explicit and added directly to the one-loop m-particle contributions. The factor $(8\pi^2\,(4\pi)^{-\epsilon}\,e^{\epsilon\gamma})$ in the above equation is related to the normalisation of the renormalised coupling constant, and its relation to the bare coupling parameter $g = \sqrt{4\pi\alpha_0}$ appearing in the QCD lagrangian density:

$$\alpha_0\mu_0^{2\epsilon}S_\epsilon = \alpha_s\mu^{2\epsilon}\left[1 - \frac{\beta_0}{\epsilon}\left(\frac{\alpha_s}{2\pi}\right) + \left(\frac{\beta_0^2}{\epsilon^2} - \frac{\beta_1}{2\epsilon}\right)\left(\frac{\alpha_s}{2\pi}\right)^2 + \mathcal{O}(\alpha_s^3)\right], \tag{2.12}$$

where

$$S_\epsilon = (4\pi)^\epsilon e^{-\epsilon\gamma} \qquad \text{with Euler constant } \gamma = 0.5772\ldots$$

and μ_0^2 is the mass parameter introduced in dimensional regularisation to maintain a dimensionless coupling in the bare QCD lagrangian density; β_0 and β_1 are the first two coefficients of the QCD β-function:

$$\beta_0 = \frac{11N - 2N_F}{6}, \qquad \beta_1 = \frac{34N^3 - 13N^2N_F + 3N_F}{12N}, \tag{2.13}$$

with $N = 3$ colours and N_F massless quark flavours.

2.2 NNLO infrared subtraction terms

At NNLO, the m-jet production is induced by final states containing up to $(m+2)$ partons, including the one-loop virtual corrections to $(m+1)$-parton final states. As at NLO, one has to introduce subtraction terms for the $(m+1)$- and $(m+2)$-parton contributions. Schematically the NNLO m-jet cross section reads,

$$\begin{aligned}\mathrm{d}\sigma_{\mathrm{NNLO}} = &\int_{\mathrm{d}\Phi_{m+2}} \left(\mathrm{d}\sigma^R_{\mathrm{NNLO}} - \mathrm{d}\sigma^S_{\mathrm{NNLO}}\right) + \int_{\mathrm{d}\Phi_{m+2}} \mathrm{d}\sigma^S_{\mathrm{NNLO}} + \\ &+ \int_{\mathrm{d}\Phi_{m+1}} \left(\mathrm{d}\sigma^{V,1}_{\mathrm{NNLO}} - \mathrm{d}\sigma^{VS,1}_{\mathrm{NNLO}}\right) + \int_{\mathrm{d}\Phi_{m+1}} \mathrm{d}\sigma^{VS,1}_{\mathrm{NNLO}} + \\ &+ \int_{\mathrm{d}\Phi_m} \mathrm{d}\sigma^{V,2}_{\mathrm{NNLO}}\,,\end{aligned} \tag{2.14}$$

where $\mathrm{d}\sigma^S_{\mathrm{NNLO}}$ denotes the real radiation subtraction term coinciding with the $(m+2)$-parton tree level cross section $\mathrm{d}\sigma^R_{\mathrm{NNLO}}$ in all singular limits. Likewise, $\mathrm{d}\sigma^{VS,1}_{\mathrm{NNLO}}$ is the one-loop virtual subtraction term coinciding with the one-loop $(m+1)$-parton cross section $\mathrm{d}\sigma^{V,1}_{\mathrm{NNLO}}$ in all singular limits. Finally, the two-loop correction to the m-parton cross section is denoted by $\mathrm{d}\sigma^{V,2}_{\mathrm{NNLO}}$.

JHEP09(2005)056

2.3 Tree-level double real radiation subtraction terms

Let us first consider the construction of the subtraction terms for the double radiation contribution $\mathrm{d}\sigma^S_{\mathrm{NNLO}}$, which shall correctly subtract all single and double unresolved singularities contained in the $(m+2)$-parton real radiation contribution to m-jet final states,

$$\begin{aligned}\mathrm{d}\sigma^R_{\mathrm{NNLO}} &= \mathcal{N} \sum_{m+2} \mathrm{d}\Phi_{m+2}(p_1, \ldots, p_{m+2}; q) \frac{1}{S_{m+2}} \times \\ &\quad \times |\mathcal{M}_{m+2}(p_1, \ldots, p_{m+2})|^2 \; J_m^{(m+2)}(p_1, \ldots, p_{m+2})\,. \end{aligned} \tag{2.15}$$

Single real radiation singularities correspond to one parton becoming soft or collinear, while double real radiation singularities occur if two partons become soft or collinear simultaneously. Singular terms in these limits can be identified by requiring a minimum number of invariants tending to zero in a given kinematical configuration. This number depends on the limit under consideration and follows from the phase space volume available to a given configuration. A detailed discussion of the kinematical definition of double unresolved limits can be found in [18, 19].

We must distinguish the following configurations:

(a) One unresolved parton but the experimental observable selects only m jets.

(b) Two colour-connected unresolved partons (colour-connected).

(c) Two unresolved partons that are not colour connected but share a common radiator (almost colour-unconnected).

(d) Two unresolved partons that are well separated from each other in the colour chain (colour-unconnected).

The first configuration was treated already in the context of antenna subtraction at NLO in section 2.1 above. In the context of the construction of $\mathrm{d}\sigma^S_{\mathrm{NNLO}}$, the same single-particle subtraction terms can be used. These do however not yet guarantee a finite $(m+2)$-parton contribution in all single unresolved regions for two reasons: (1) while the jet function in $\mathrm{d}\sigma^S_{\mathrm{NLO}}$ ensured that the subtraction term is non-zero only in the single unresolved limit it was constructed for, this is no longer the case for single unresolved radiation at NNLO; (2) the subtraction terms for the remaining three double unresolved configurations will in general be singular in the single unresolved regions, where they do not match the matrix element. Both problems will be addressed below.

The remaining three configurations (b)–(d) are illustrated in figures 4–6. The singular behaviour of the full $(m+2)$-parton matrix element in these configurations is the product of double unresolved factors (see section 8 below) and reduced m-parton matrix elements. Subtraction terms for all these configurations can be constructed using either single four-parton antenna functions or products of two three-parton antenna functions. In all cases, attention has to be paid to the matching of different double and single unresolved regions. This problem has been addressed already in several earlier publications on subtraction at NNLO [25 − 29, 44], the most concise discussion can be found in [29].

In the following, we construct the subtraction terms for all four configurations.

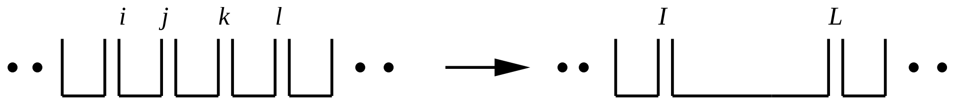

Figure 4: Colour connection of the partons showing the parent and daughter partons for the double unresolved antenna.

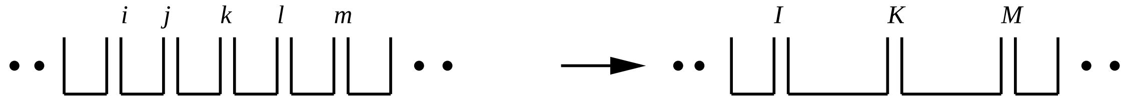

Figure 5: Colour connection of the partons showing the parent and daughter partons for two adjacent single unresolved antennae.

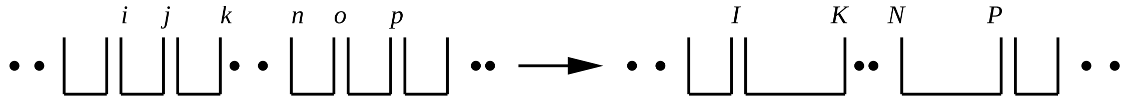

Figure 6: Colour connection of the partons showing the parent and daughter partons for two disconnected single unresolved antennae.

2.3.1 Subtraction terms for single unresolved partons

Starting point for the subtraction terms for single unresolved partons are the NLO single unresolved antenna subtraction terms (2.5),

$$\begin{aligned} \mathrm{d}\sigma_{\mathrm{NNLO}}^{S,a} = \mathcal{N} \sum_{m+2} \mathrm{d}\Phi_{m+2}(p_1,\ldots,p_{m+2};q)\frac{1}{S_{m+2}} \times \\ \times \Bigg[\sum_j X^0_{ijk}\, |\mathcal{M}_{m+1}(p_1,\ldots,\tilde{p}_I,\tilde{p}_K,\ldots,p_{m+2})|^2 \times \\ \times J_m^{(m+1)}(p_1,\ldots,\tilde{p}_I,\tilde{p}_K,\ldots,p_{m+2}) \Bigg], \end{aligned} \tag{2.16}$$

where the NLO jet function $J_m^{(m)}$ is now replaced by $J_m^{(m+1)}$. In contrast to the NLO case, subtracting these terms from the full $(m+2)$-parton matrix element does not ensure a finite contribution in all single unresolved regions. This behaviour is related to the fact that at NNLO the jet function $J_m^{(m+1)}$ allows one of the $(m+1)$ momenta to become unresolved, while at NLO $J_m^{(m)}$ required all m momenta to be hard. As a consequence, all momenta in the antenna function, including p_j, could be resolved while one of the momenta present in the reduced $(m+1)$-parton matrix element becomes unresolved. We distinguish between two cases: (1) where $\tilde{p}_I$ or $\tilde{p}_K$ become unresolved and (2) where any other momentum, p_o, in the matrix element becomes unresolved. Case (1) is necessarily a double unresolved limit since $\tilde{p}_I$ and $\tilde{p}_K$ are linear combinations of two momenta; this configuration is treated below in the discussion of the double unresolved limits of (2.16).

Case (2) is a single unresolved limit, since p_j is resolved, while p_o becomes unresolved. In this limit, $\mathrm{d}\sigma_{\mathrm{NNLO}}^{S,a}$ becomes singular. Its singular structure in this limit does not coincide with the limit of the full $(m+2)$-parton matrix element (which is already subtracted by the appropriate antenna term in $\mathrm{d}\sigma_{\mathrm{NNLO}}^{S,a}$ when $j=o$). The unresolved momentum p_o in this situation is not colour-connected to the p_j of X^0_{ijk}. The form of the spurious singular terms in $\mathrm{d}\sigma^{S,a}_{\mathrm{NNLO}}$ is therefore equal to the product of the antenna function with a singular limit of the reduced $(m+1)$-parton matrix element. It is equivalent to the product of two almost colour-unconnected or colour-unconnected antenna functions with the reduced m-parton matrix element:

$$
\begin{aligned}
& X^0_{ijk}\,|\mathcal{M}_{m+1}(p_1,\ldots,\tilde{p}_I,\tilde{p}_K,\ldots,p_n,p_o,p_p,\ldots,p_{m+2})|^2 - \\
& - X^0_{ijk}\,X^0_{nop}\,|\mathcal{M}_m(p_1,\ldots,\tilde{p}_I,\tilde{p}_K,\ldots,\tilde{p}_N,\tilde{p}_P,\ldots,p_{m+2})|^2 \stackrel{p_o \text{ unresolved}}{\longrightarrow} 0\,,
\end{aligned}
$$

where $\tilde{p}_N = \tilde{p}_K$ is allowed. Such structures appear as double unresolved subtraction terms for the configurations (c) and (d) defined above, and it will be shown in the appropriate subsections below, that the simple collinear limits of these double subtraction terms yield the correct behaviour to cancel the spurious single unresolved poles of $\mathrm{d}\sigma^{S,a}_{\mathrm{NNLO}}$.

To construct the double unresolved subtraction terms, we need to investigate the behaviour of the subtraction term (2.16) in all its double unresolved limits. We distinguish the cases of colour-connected and colour-unconnected double unresolved limits. In the colour-connected, or type (b), double unresolved limits, (2.16) can be non-vanishing only for one particular momentum configuration: two neighbouring pairs of colour-connected momenta becoming independently collinear, where one of the pairs lies inside the antenna, while the other pair consists of the remaining antenna momentum and its colour-connected neighbour. Each configuration of this type is contained precisely twice in (2.16), since there are two possibilities of attributing the inside/outside pair. Where appropriate, we shall call these limits colour-neighbouring in the following, and decompose colour-connected limits into genuinely colour-connected and colour-neighbouring limits. In the colour-unconnected, type (c,d), double unresolved limits, (2.16) is always non-vanishing and yields twice the double unresolved limit of the $(m+2)$-parton matrix element. This factor of two comes from the fact that each double unresolved limit requires both the unresolved antenna momentum p_j and one other momentum p_o appearing in the $(m+1)$-parton matrix element to become unresolved; the role of the p_j and p_o can be interchanged, resulting in two identical terms contributing to the same limit.

To summarise the above discussion, we conclude that (2.16) yields twice the $(m+2)$-parton matrix element in all colour-unconnected, almost colour-unconnected and colour-neighbouring double unresolved limits, while vanishing in all genuinely colour-connected double unresolved limits.

2.3.2 Subtraction terms for two colour-connected unresolved partons

When the two unresolved partons j and k are adjacent, we construct the subtraction term starting from the four-particle tree-level antenna X^0_{ijkl}, which is an appropriately normalised four-particle matrix element [44, 46, 47]. By construction, it contains all colour-connected double unresolved limits of the $(m+2)$-parton matrix element associated with partons j and k, but it can also be singular in *single* unresolved limits associated with j or k, where it does not coincide with limits of the matrix element. To ensure a finite subtraction term in all these single unresolved limits, we therefore subtract the appropriate

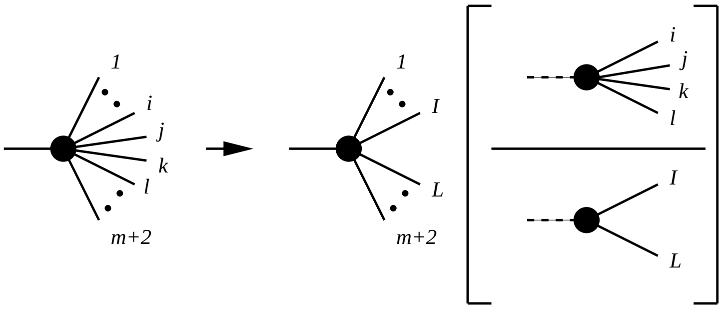

Figure 7: Illustration of NNLO antenna factorisation representing the factorisation of both the squared matrix elements and the $(m+2)$-particle phase space when the unresolved particles are colour connected. The term in square brackets represents both the antenna function X^0_{ijkl} and the antenna phase space $\mathrm{d}\Phi_{X_{ijkl}}$.

limits of the four-particle tree antennae, which are products of two tree-level three-particle antennae, such that the colour-connected double subtraction term reads:

$$
\begin{aligned}
\mathrm{d}\sigma^{S,b}_{\mathrm{NNLO}} = \mathcal{N} \sum_{m+2} \mathrm{d}\Phi_{m+2}(p_1,\ldots,p_{m+2};q)\frac{1}{S_{m+2}} \times \\
\times \Bigg[\sum_{jk} \left(X^0_{ijkl} - X^0_{ijk}X^0_{IKl} - X^0_{jkl}X^0_{iJL}\right) \times \qquad (2.17) \\
\times |\mathcal{M}_m(p_1,\ldots,\tilde{p}_I,\tilde{p}_L,\ldots,p_{m+2})|^2 \, J^{(m)}_m(p_1,\ldots,\tilde{p}_I,\tilde{p}_L,\ldots,p_{m+2})\Bigg],
\end{aligned}
$$

where the sum runs over all colour-adjacent pairs j,k and implies the appropriate selection of hard momenta i,l.

As before, the subtraction term involves the m-parton amplitude evaluated with on-shell momenta $p_1,\ldots,\tilde{p}_I,\tilde{p}_L,\ldots,p_{m+2}$ where now $\tilde{p}_I$ and $\tilde{p}_L$ are a linear combination of p_i, p_j, p_k and p_l. As for the NLO antenna of the previous section, the tree antenna function X^0_{ijkl} depends only on p_i,p_j,p_k,p_l. Particles i and l play the role of the radiators while j and k are the radiated partons. Antenna factorisation of squared matrix element and phase space in this configuration is illustrated pictorially in figure 7. Once again, the jet function $J^{(m)}_m$ in (2.17) depends only on the parent momenta $\tilde{p}_I,\tilde{p}_L$ and not $p_i,\ldots,p_l$. One can therefore carry out the integration over the unresolved antenna phase space (or part thereof) analytically, exploiting the factorisation of the phase space,

$$
\mathrm{d}\Phi_{m+2}(p_1,\ldots,p_{m+2};q) = \mathrm{d}\Phi_m(p_1,\ldots,\tilde{p}_I,\tilde{p}_L,\ldots,p_{m+1};q)\cdot \mathrm{d}\Phi_{X_{ijkl}}(p_i,p_j,p_k,p_l;\tilde{p}_I+\tilde{p}_L)\,. \qquad (2.18)
$$

The factorisation [25, 31, 21] is obtained by redefining a set of four massless on-shell momenta (radiator, two unresolved partons, radiator) into two on-shell massless momenta. The NNLO antenna phase space $\mathrm{d}\Phi_{X_{ijkl}}$ is proportional to the four-particle phase space, as can be seen by using $m=2$ in the above formula such that

$$
\mathrm{d}\Phi_4 = P_2\,\mathrm{d}\Phi_{X_{ijkl}}\,. \qquad (2.19)
$$

One suitable representation of momenta for analytic integration purposes is the tripole phase space mapping of [31] where parton i is the emitter and parton l the spectator,

$$\tilde{p}_I^\mu = p_i^\mu + p_j^\mu + p_k^\mu - \frac{y_{ijk,l}}{1-y_{ijk,l}} p_l^\mu \,, \qquad \tilde{p}_L^\mu = \frac{1}{1-y_{ijk,l}} p_l^\mu \,, \tag{2.20}$$

with

$$y_{ijk,l} = \frac{p_l{\cdot}p_i + p_l{\cdot}p_j + p_l{\cdot}p_k}{p_i{\cdot}p_j + p_i{\cdot}p_k + p_i{\cdot}p_l + p_j{\cdot}p_k + p_j{\cdot}p_l + p_k{\cdot}p_l} \,. \tag{2.21}$$

For numerical implementation the mapping of [25] is suitable.

For the analytic integration, we can use (2.18) to rewrite each of the genuine four-particle subtraction terms in the form,

$$|\mathcal{M}_m|^2 \, J_m^{(m)} \, \mathrm{d}\Phi_m \int \mathrm{d}\Phi_{X_{ijkl}} \, X^0_{ijkl} \,, \tag{2.22}$$

as before. The analytic integral of the four-particle antenna subtraction term is therefore the antenna function integrated over the fully inclusive antenna phase space, again including a normalisation factor to account for powers of the QCD coupling constant,

$$\mathcal{X}^0_{ijkl}(s_{ijkl}) = \left(8\pi^2 \, (4\pi)^{-\epsilon} \, e^{\epsilon\gamma}\right)^2 \int \mathrm{d}\Phi_{X_{ijkl}} \, X^0_{ijkl} \,. \tag{2.23}$$

This integration is performed analytically in d dimensions using the techniques explained in [31] to make the infrared singularities explicit.

The double unresolved subtraction term (2.17) correctly approximates the $(m+2)$-parton matrix element (2.15) in all double unresolved limits where colour-connected partons j and k become unresolved, except in the configuration where parton j becomes collinear with parton i, while parton k becomes collinear with parton l. In this (so-called colour-neighbouring) configuration, the tree-level four-parton antenna function X_{ijkl} correctly approximates the $(m+2)$-parton matrix element, while the products of tree-level three-parton antenna functions $X^0_{ijk}X^0_{IKl}$ and $X^0_{jkl}X^0_{iJL}$ in (2.17) are non-vanishing, and are each equal to the double unresolved limit of the matrix element. This colour-neighbouring momentum configuration was already discussed in the context of the double unresolved limits of $\mathrm{d}\sigma^{S,a}_{\mathrm{NNLO}}$ in the previous subsection. It can be seen easily that the two products of tree-level three-parton antenna functions $X^0_{ijk}X^0_{IKl}$ and $X^0_{jkl}X^0_{iJL}$ in (2.17) exactly cancel the spurious double unresolved singular terms in present in (2.16) in these colour-neighbouring double unresolved limits.

In all genuinely colour-connected limits, the four-parton tree-level antenna function X_{ijkl} in (2.17) correctly matches the singular structure of the $(m+2)$-parton matrix element, while the products of tree-level three-parton antenna functions $X^0_{ijk}X^0_{IKl}$ and $X^0_{jkl}X^0_{iJL}$ vanish (although these terms are singular at first sight, they are not sufficiently singular to overcome the small phase space volume associated with the double unresolved limits under consideration).

By construction, (2.17) vanishes in all single unresolved limits: the antenna functions cancel each other in these limits, and singularities in the m-parton matrix element are forbidden by the jet function.

JHEP09(2005)056

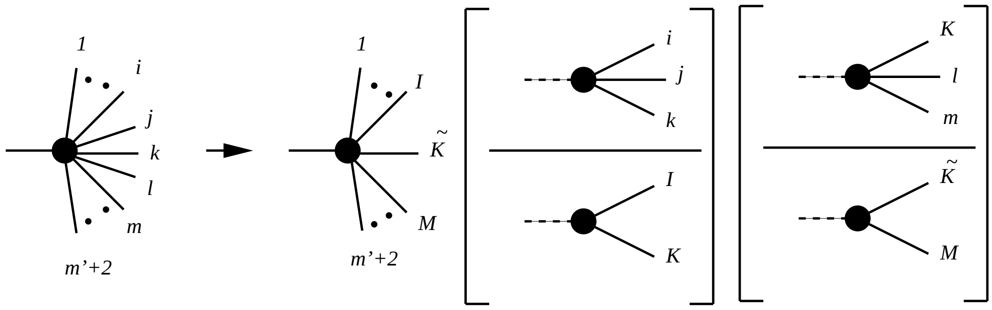

Figure 8: Illustration of NNLO antenna factorisation representing the factorisation of both the squared matrix elements and the $(m'+2)$-particle phase space when the unresolved particles are almost colour-unconnected.

2.3.3 Subtraction terms for two almost colour-unconnected unresolved partons

There are double unresolved configurations where the unresolved partons are separated by a hard radiator parton, for example, i, j, k, l, m where j and l are unresolved as illustrated in Fig. 8. These configurations are called almost colour-unconnected. In this case, we take the strongly ordered approach [41] where i, j, k form an antenna with hard partons I and K yielding an ordered amplitude involving I, K, l, m. As usual, the momenta of the hard radiator partons I and K are labelled $\tilde{p}_I$ and $\tilde{p}_K$ and are constructed from p_i, p_j, p_k. The cases where l is unresolved are then treated using an antenna K, l, m with hard partons K and L. Here the momenta of the hard radiator partons K and L are labelled $\tilde{\tilde{p}}_K$ and $\tilde{\tilde{p}}_M$ which are made from $\tilde{p}_K, p_l, p_m$. The other case where first k, l, m form an antenna followed by i, j, K is also included.

In constructing the subtraction term, we have to account for the fact that the previously defined subtraction term $\mathrm{d}\sigma^{S,a}_{\mathrm{NNLO}}$ (2.16) already contributes in the almost colour-unconnected configurations by subtracting twice the limit of the $(m'+2)$-parton matrix element in these limits (to avoid confusion between the indivial unresolved momenta and the total number of particles, we denote the latter $(m'+2)$ instead of $(m+2)$ in this subsection). Therefore, the almost colour-unconnected subtraction term reads,

$$\begin{aligned}
\mathrm{d}\sigma^{S,c}_{\mathrm{NNLO}} = -\mathcal{N} \sum_{m'+2} & \mathrm{d}\Phi_{m'+2}(p_1, \ldots, p_{m'+2}; q) \frac{1}{S_{m'+2}} \times \\
\times \Bigg[& \sum_{j,l} X^0_{ijk}\, x^0_{mlK}\, |\mathcal{M}_{m'}(p_1, \ldots, \tilde{p}_I, \tilde{\tilde{p}}_K, \tilde{\tilde{p}}_M, \ldots, p_{m'+2})|^2 \times \\
& \times J^{(m')}_{m'}(p_1, \ldots, \tilde{p}_I, \tilde{\tilde{p}}_K, \tilde{\tilde{p}}_M, \ldots, p_{m'+2}) + \\
& + \sum_{j,l} X^0_{klm}\, x^0_{ijK}\, |\mathcal{M}_{m'}(p_1, \ldots, \tilde{\tilde{p}}_I, \tilde{\tilde{p}}_K, \tilde{p}_M, \ldots, p_{m'+2})|^2 \times \\
& \times J^{(m')}_{m'}(p_1, \ldots, \tilde{\tilde{p}}_I, \tilde{\tilde{p}}_K, \tilde{p}_M, \ldots, p_{m'+2}) \Bigg],
\end{aligned} \tag{2.24}$$

where x^0_{mlK} denotes a sub-antenna, containing only the collinear limit of m with l, but not the collinear limit of l with K; in the soft limit of l, this sub-antenna yields half the soft eikonal factor. The jet function $J^{(m')}_{m'}$ and the matrix element depend only on the

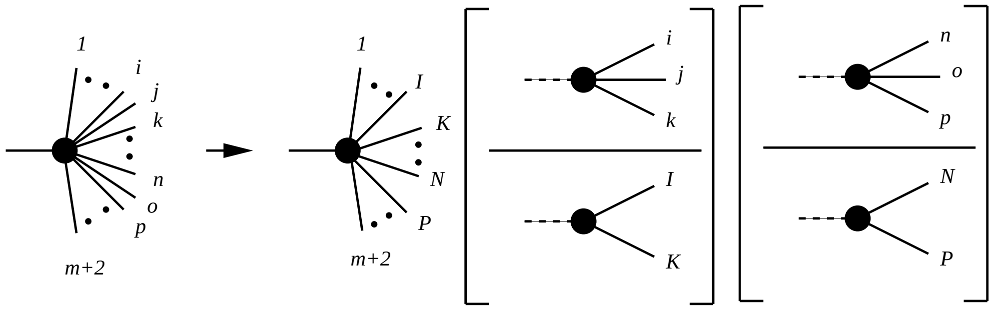

Figure 9: Illustration of NNLO antenna factorisation representing the factorisation of both the squared matrix elements and the $(m+2)$-particle phase space when the unresolved particles are colour-unconnected.

momenta associated with the m'-particle final state. Therefore, the integral over the phase space associated with the leftmost antenna function can be carried out analytically, like in the single unresolved case discussed above. After this integration, the sub-antennae can be recombined to full antenna functions again.

If required, it is also possible to carry out the integrals over both phase spaces associated with the two antenna functions. In this case, one can exploit the factorisation of the phase space to analytically perform the integrals,

$$\begin{aligned} \mathrm{d}\Phi_{m'+2}(p_1,\ldots,p_{m'+2};q) &= \mathrm{d}\Phi_{m'+1}(p_1,\ldots,\tilde{p}_I,\tilde{p}_K,\ldots,p_{m'+2};q)\cdot \mathrm{d}\Phi_{X_{ijk}}(p_i,p_j,p_k) \\ &= \mathrm{d}\Phi_{m'}(p_1,\ldots,\tilde{p}_I,\tilde{\tilde{p}}_K,\tilde{\tilde{p}}_M,\ldots,p_{m'+2};q)\cdot \\ &\quad \cdot \mathrm{d}\Phi_{X_{Klm}}(\tilde{p}_K,p_l,p_m;\tilde{\tilde{p}}_K+\tilde{\tilde{p}}_M)\cdot \\ &\quad \cdot \mathrm{d}\Phi_{X_{ijk}}(p_i,p_j,p_k;\tilde{p}_I+\tilde{p}_K)\,. \end{aligned} \tag{2.25}$$

In carrying out the analytic integration, some care has to be taken in the second dipole integral $\mathrm{d}\Phi_{X_{Klm}}$, which will pick up ϵ-dependent factors from the first integral (both integrals are fully independent only in four dimensions) related to the correlation of unit volumes involved in the two integrals. As a consequence, the analytic integration of the above formula will not yield the product of two independent integrated NLO antenna functions.

Concerning the single unresolved limits of $\mathrm{d}\sigma^{S,c}_{\mathrm{NNLO}}$, (2.24) becomes singular only if one of the antenna partons j or l is unresolved. In these cases, it exactly cancels the spurious single unresolved singularities encountered in $\mathrm{d}\sigma^{S,a}_{\mathrm{NNLO}}$ for the configuration of an unresolved momentum p_o in the $(m'+1)$-parton matrix element, which is almost colour-unconnected to the momenta in the antenna function. In the double unresolved limits of $\mathrm{d}\sigma^{S,c}_{\mathrm{NNLO}}$, momenta j and l are both unresolved, yielding minus the double unresolved limit of the $(m'+2)$-parton matrix element, as required to cancel the oversubtraction incurred by $\mathrm{d}\sigma^{S,a}_{\mathrm{NNLO}}$ in these limits.

2.3.4 Subtraction terms for two colour-unconnected unresolved partons

When two unresolved partons j and o are completely disconnected, the $(m+2)$-parton matrix element factorises into the product of two uncorrelated single unresolved factors with a reduced m-parton matrix element. In this limit, the single unresolved subtraction term $\mathrm{d}\sigma^{S,a}_{\mathrm{NNLO}}$ (2.16) subtracts a contribution which is twice the limit of the full $(m+2)$-parton matrix element. The dedicated colour-unconnected double unresolved subtraction term has to compensate for this oversubtraction. This subtraction term is a sum over independent three-particle tree-level antennae as illustrated in figure 9,

$$\begin{aligned}\mathrm{d}\sigma^{S,d}_{\mathrm{NNLO}} &= -\mathcal{N}\sum_{m+2}\mathrm{d}\Phi_{m+2}(p_1,\ldots,p_{m+2};q)\frac{1}{S_{m+2}}\times\\ &\quad\times\Bigg[\sum_{j,o} X^0_{ijk}\,X^0_{nop}\,|\mathcal{M}_m(p_1,\ldots,\tilde{p}_I,\tilde{p}_K,\ldots,\tilde{p}_N,\tilde{p}_P,\ldots,p_{m+2})|^2\times\\ &\qquad\times J^{(m)}_m(p_1,\ldots,\tilde{p}_I,\tilde{p}_K,\ldots,\tilde{p}_N,\tilde{p}_P,\ldots,p_{m+2})\Bigg],\end{aligned}\tag{2.26}$$

where the summation over o is such that it only includes colour-connected antenna configurations X^0_{nop} which have no common momentum with X^0_{ijk}.

The subtraction term involves the m-parton amplitude evaluated with on-shell momenta $p_1,\ldots,\tilde{p}_I,\tilde{p}_K,\ldots,\tilde{p}_N,\tilde{p}_P,\ldots,p_{m+2}$ where now $\tilde{p}_I$ and $\tilde{p}_K$ are a linear combination of p_i, p_j, p_k and $\tilde{p}_N$ and $\tilde{p}_P$ are made from p_n, p_o and p_p. The sum in the above equation is such that no product of two antenna configurations appears twice. Each antenna is fully independent, and the phase space factorises as,

$$\begin{aligned}\mathrm{d}\Phi_{m+2}(p_1,\ldots,p_{m+2};q) &= \mathrm{d}\Phi_m(p_1,\ldots,\tilde{p}_I,\tilde{p}_K,\ldots,\tilde{p}_N,\tilde{p}_P,\ldots,p_{m+2};q)\times\\ &\quad\times\mathrm{d}\Phi_{X_{ijk}}(p_i,p_j,p_k;\tilde{p}_I+\tilde{p}_K)\cdot\mathrm{d}\Phi_{X_{nop}}(p_n,p_o,p_p;\tilde{p}_N+\tilde{p}_P)\,.\end{aligned}\tag{2.27}$$

This contribution is either integrated only once, and then cancelled with subtraction terms present in the $(m+1)$-parton contribution, or integrated twice to make its full infrared pole structure explicit. Integration can be obtained by repeated use of (2.11), so that each term in the sum is in the form,

$$|\mathcal{M}_m|^2\,J^{(m)}_m\,\mathcal{X}^0_{ijk}(s_{ijk})\,\mathcal{X}^0_{nop}(s_{nop})\,.$$

The subtraction term (2.26) contributes to single unresolved limits if either p_j or p_o are unresolved. In these limits, it cancels precisely the spurious poles associated with the momentum p_o becoming unresolved in the $(m+1)$-parton matrix element of (2.16). In the double unresolved limits (p_j and p_o) it is designed for, it cancels the oversubtraction incurred by (2.16), thus ensuring a proper subtraction of the singular terms of the $(m+2)$-parton matrix element in these.

2.3.5 Correction terms in the m-jet region

The full double radiation subtraction term is given as sum of all subtraction terms constructed above:

$$\mathrm{d}\sigma^{S}_{\mathrm{NNLO}} = \mathrm{d}\sigma^{S,a}_{\mathrm{NNLO}} + \mathrm{d}\sigma^{S,b}_{\mathrm{NNLO}} + \mathrm{d}\sigma^{S,c}_{\mathrm{NNLO}} + \mathrm{d}\sigma^{S,d}_{\mathrm{NNLO}}\,.\tag{2.28}$$

As outlined in the previous subsections, this subtraction term correctly approximates the $(m+2)$-parton matrix element contribution to m-jet final states as defined in (2.15) in all double and single unresolved regions. Although individual terms in (2.28) contain spurious singularities in these limits, they cancel among each other in the sum.

The integrated form of (a) corresponds to an $(m+1)$-parton configuration, while the integrated forms of (b), (c) and (d) are either $(m+1)$-parton or m-parton configurations (for all but the four-parton antenna terms in (b), we can actually choose which type of configuration we want to integrate). They are added with the two-loop m-parton and the one-loop $(m+1)$-parton contributions to m-jet final states to yield integrands free of explicit infrared poles.

2.4 Single unresolved loop subtraction terms

The $(m+1)$-parton one-loop contribution to m-jet final states at NNLO is

$$
\begin{aligned}
\mathrm{d}\sigma_{\mathrm{NNLO}}^{V,1} = \mathcal{N} \sum_{m+2} & \mathrm{d}\Phi_{m+1}(p_1, \ldots, p_{m+1}; q) \frac{1}{S_{m+1}} \times \\
& \times |\mathcal{M}_{m+1}^{1}(p_1, \ldots, p_{m+1})|^2 \; J_m^{(m+1)}(p_1, \ldots, p_{m+1}) \,,
\end{aligned}
\tag{2.29}
$$

where we introduced a shorthand notation for the one-loop corrected contribution to the $(m+1)$-parton squared matrix element,

$$
|\mathcal{M}_{m+1}^{1}(p_1, \ldots, p_{m+1})|^2 = 2\,\mathrm{Re}\left(\mathcal{M}_{m+1}^{\mathrm{loop}}(p_1, \ldots, p_{m+1})\, \mathcal{M}_{m+1}^{\mathrm{tree},*}(p_1, \ldots, p_{m+1})\right), \tag{2.30}
$$

where the subleading contributions in colour are again implicit. This expression contains two types of infrared singularities. The renormalised one-loop virtual correction $\mathcal{M}_{m+1}^{\mathrm{loop}}$ to the $(m+1)$-parton matrix contains explicit infrared poles, which can be expressed using the infrared singularity operators defined in section 4 below. On the other hand, one of the $(m+1)$-partons can be unresolved, leading to infrared singularities which become explicit only after integration over the unresolved patch of the final state $(m+1)$-parton phase space. The single unresolved limits of one- and two-loop amplitudes are investigated in detail in [11−15].

To carry out the numerical integration over the $(m+1)$-parton phase, weighted by the appropriate jet function, we have to construct an infrared subtraction term $\mathrm{d}\sigma_{\mathrm{NNLO}}^{VS,1}$, which purpose is twofold: on the one hand, it should fully account for the explicit infrared singularities arising from the one-loop correction, while on the other hand it should approximate (2.29) in all single unresolved limits. After subtraction of $\mathrm{d}\sigma_{\mathrm{NNLO}}^{VS,1}$ from $\mathrm{d}\sigma_{\mathrm{NNLO}}^{V,1}$, the integrand itself should be free from explicit infrared poles, and all singular limits due to single unresolved phase space configurations must be properly accounted for. We require three types of subtraction terms:

(a) The explicit infrared poles of the $(m+1)$-parton one-loop matrix element are removed.

(b) The single unresolved limits of the $(m+1)$-parton one-loop matrix element are subtracted.

(c) Oversubtracted explicit and implicit pole terms are removed.

All three types of subtraction terms are constructed below.

2.4.1 Subtraction of explicit infrared poles

It is a well known fact from NLO calculations, that the explicit infrared poles of one-loop matrix elements cancel with the corresponding infrared poles obtained by integrating out all single unresolved configurations from the real radiation matrix elements contributing to the same (infrared safe) observable [49]. We can therefore subtract all explicit poles present in $\mathrm{d}\sigma^{V,1}_{\mathrm{NNLO}}$ with the subtraction term

$$\begin{aligned}\mathrm{d}\sigma^{VS,1,a}_{\mathrm{NNLO}} &= \mathcal{N}\sum_{m+1}\mathrm{d}\Phi_{m+1}(p_1,\dots,p_{m+1};q)\frac{1}{S_{m+1}}\times\\ &\quad\times\Bigg[\sum_{ik} -\mathcal{X}^0_{ijk}(s_{ik})\,|\mathcal{M}_{m+1}(p_1,\dots,p_i,p_k,\dots,p_{m+1})|^2\times\\ &\qquad\times J_m^{(m+1)}(p_1,\dots,p_i,p_k,\dots,p_{m+1})\Bigg],\end{aligned} \tag{2.31}$$

where the sum runs over all colour-connected pairs of momenta (p_i,p_k). The symbol $\mathcal{X}^0_{ijk}(s_{ik})$ denotes the normalised integral of the three-parton antenna function, with a parton of type j emitted between partons i and k, with the total invariant mass of the antenna particles given by the invariant mass of p_i and p_k. Since in the single unresolved mapping of the antenna phase space (2.8), $p_i+p_j+p_k=\tilde{p}_I+\tilde{p}_K$, we can identify the momenta p_i and p_k of the $(m+1)$-parton phase space with the momenta $\tilde{p}_I$ and $\tilde{p}_K$ obtained in the factorisation of the $(m+2)$-parton phase space in section 2.3.1. Consequently, using the antenna factorisation of the $(m+2)$-parton phase space in (2.16) and carrying out the phase space integral for each antenna X_{ijk}, we find

$$\mathrm{d}\sigma^{VS,1,a}_{\mathrm{NNLO}} = -\mathrm{d}\sigma^{S,a}_{\mathrm{NNLO}}\,, \tag{2.32}$$

which is of course merely a consequence of the cancellation of infrared poles at NLO.

It is evident that subtraction of $\mathrm{d}\sigma^{VS,1,a}_{\mathrm{NNLO}}$ from $\mathrm{d}\sigma^{V,1}_{\mathrm{NNLO}}$ ensures an integrand free from explicit infrared poles over the whole region of integration. In the single unresolved regions, both these functions develop further infrared singularities, which do not coincide. Therefore, we have to introduce further subtraction terms to ensure a finite integrand in all single unresolved regions.

2.4.2 Subtraction terms for one-loop single-unresolved contributions

In simple unresolved limits, the behaviour of $(m+1)$-parton one-loop amplitudes is described by the sum of two different contributions [11−15]: a simple unresolved tree level factor times a m-parton one-loop amplitude and a simple unresolved one-loop factor times a m-parton tree-level amplitude, as illustrated in figure 10. Accordingly, we construct the one-loop single unresolved subtraction term as

$$\begin{aligned}\mathrm{d}\sigma^{VS,1,b}_{\mathrm{NNLO}} &= \mathcal{N}\sum_{m+1}\mathrm{d}\Phi_{m+1}(p_1,\dots,p_{m+1};q)\frac{1}{S_{m+1}}\times\\ &\quad\times\sum_j\Bigg[X^0_{ijk}\,|\mathcal{M}^1_m(p_1,\dots,\tilde{p}_I,\tilde{p}_K,\dots,p_{m+1})|^2\,J_m^{(m)}(p_1,\dots,\tilde{p}_I,\tilde{p}_K,\dots,p_{m+1})+\\ &\qquad+X^1_{ijk}|\mathcal{M}_m(p_1,\dots,\tilde{p}_I,\tilde{p}_K,\dots,p_{m+1})|^2\,J_m^{(m)}(p_1,\dots,\tilde{p}_I,\tilde{p}_K,\dots,p_{m+1})\Bigg].\end{aligned} \tag{2.33}$$

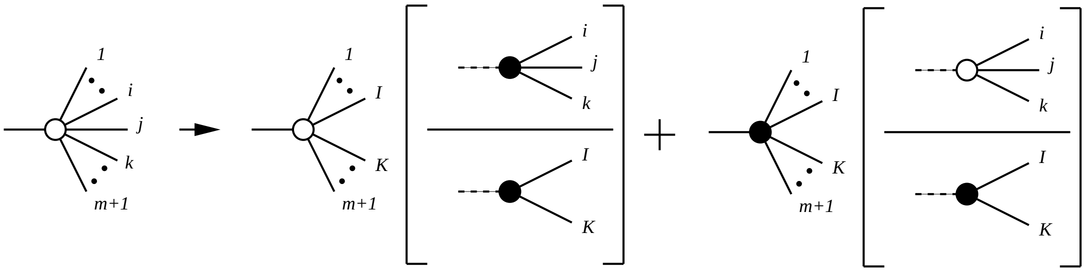

Figure 10: Illustration of NNLO antenna factorisation representing the factorisation of both the one-loop "squared" matrix elements (represented by the white blob) and the $(m+1)$-particle phase space when the unresolved particles are colour connected. The terms in square brackets represent both the three-particle tree-level antenna function X^0_{ijk} and the three-particle one-loop antenna function X^1_{ijk} and the antenna phase space.

In this expression, we have introduced the one-loop three-parton antenna function X^1_{ijk}, which depends only on the antenna momenta p_i, p_j, p_k. It correctly describes all simple unresolved limits of the difference between an $(m+1)$-parton one-loop corrected squared matrix element and the product of a tree-level antenna function with the m-parton one-loop corrected squared matrix element. It can therefore be constructed out of one-loop three-parton and two-parton matrix elements, as outlined in section 3 below. It should be noted that X^1_{ijk} is renormalised at a scale corresponding to the invariant mass of the antenna partons, s_{ijk}, while the one-loop $(m+1)$-parton matrix element is renormalised at a scale μ^2 (which is often chosen to be q^2 in jet production in e^+e^--collisions). To ensure correct subtraction of terms arising from renormalisation, we have to substitute

$$X^1_{ijk} \to X^1_{ijk} + \frac{\beta_0}{\epsilon}\frac{(4\pi)^\epsilon\, e^{-\epsilon\gamma}}{8\pi^2} X^0_{ijk} \left((s_{ijk})^{-\epsilon} - \left(\mu^2\right)^{-\epsilon} \right) \tag{2.34}$$

in (2.33). The terms arising from this substitution will in general be kept apart in the construction of the colour-ordered subtraction terms, since they all share a common colour structure β_0.

In contrast to all other expressions appearing in the construction of the one-loop single unresolved subtraction terms, X^1_{ijk} can never be related to integrals of tree-level subtraction terms. Therefore, this component of the subtraction term must cancel with parts of the two-loop m-parton contribution and we must integrate it over the three-parton antenna phase space. This can be accomplished using the techniques described in [31] and yields

$$\mathcal{X}^1_{ijk}(s_{ijk}) = \left(8\pi^2\,(4\pi)^{-\epsilon}\, e^{\epsilon\gamma}\right) \int \mathrm{d}\Phi_{X_{ijk}}\, X^1_{ijk}\,. \tag{2.35}$$

2.4.3 Compensation terms for oversubtracted poles

By construction, (2.33) correctly approximates the one-loop $(m+1)$-parton contribution to m-jet final states in all single unresolved limits. However, outside these limits, where $(m+1)$-parton configurations form m-jet final states because of the experimental jet resolution criteria, this subtraction term no longer coincides with the squared matrix element, and induces spurious explicit infrared poles.

To compensate for these explicit infrared poles outside the singular regions, we introduce a further subtraction term,

$$\begin{aligned}
\mathrm{d}\sigma_{\mathrm{NNLO}}^{VS,1,c} &= \mathcal{N} \sum_{m+1} \mathrm{d}\Phi_{m+1}(p_1,\ldots,p_{m+1};q) \frac{1}{S_{m+1}} \times \\
&\quad \times \Bigg[\sum_{ik} \mathcal{X}_{ijk}^0(s_{ik}) \sum_o X_{nop}^0 \, |\mathcal{M}_m(p_1,\ldots,p_i,p_k,\ldots,\tilde{p}_N,\tilde{p}_P,\ldots,p_{m+1})|^2 \times \\
&\qquad \times J_m^{(m)}(p_1,\ldots,p_i,p_k,\ldots,\tilde{p}_N,\tilde{p}_P,\ldots,p_{m+1}) \Bigg], \qquad (2.36)
\end{aligned}$$

where any of the two momenta p_i and p_k can be equal to p_n, p_p, $\tilde{p}_N$ or $\tilde{p}_P$, but not to the unresolved momentum p_o. Individual terms in $\mathrm{d}\sigma_{\mathrm{NNLO}}^{VS,1,c}$ cancel with individual terms in $\mathrm{d}\sigma_{\mathrm{NNLO}}^{S,b}$ (2.17), $\mathrm{d}\sigma_{\mathrm{NNLO}}^{S,c}$ (2.24) and $\mathrm{d}\sigma_{\mathrm{NNLO}}^{S,d}$ (2.26), after one of the two three-parton antenna phase space integrals is carried out. Any remaining terms of $\mathrm{d}\sigma_{\mathrm{NNLO}}^{VS,1,c}$ can be integrated over the antenna phase space $\mathrm{d}\Phi_{X_{nop}}$. In the case of p_i or p_k coinciding with one of the momenta of the antenna phase space, some care has to be taken in carrying out the integrals, which differ from the standard tree-level three-parton antenna integrals by normalisation factors coming from $\mathcal{X}_{ijk}^0(s_{ik})$.

The subtraction term (2.36) cancels the explicit infrared poles of (2.33) in the region where all $(m+1)$ partons are theoretically resolved, thus ensuring a finite integrand. In the single unresolved regions, the sum of (2.36) and (2.31) vanishes, as can be seen rather easily from the nature of NLO antenna subtraction. Consequently, only $\mathrm{d}\sigma_{\mathrm{NNLO}}^{VS,1,b}$ contributes in this region, as required to cancel the singularities of the $(m+1)$-parton squared matrix element.

2.4.4 Correction terms in the m-jet region

The full one-loop single real radiation subtraction term is the sum of all subtraction terms constructed above:

$$\mathrm{d}\sigma_{\mathrm{NNLO}}^{VS,1} = \mathrm{d}\sigma_{\mathrm{NNLO}}^{VS,1,a} + \mathrm{d}\sigma_{\mathrm{NNLO}}^{VS,1,b} + \mathrm{d}\sigma_{\mathrm{NNLO}}^{VS,1,c}. \qquad (2.37)$$

As outlined in the previous subsections, this subtraction term correctly approximates the one-loop $(m+1)$-parton squared matrix element contribution to m-jet final states as defined in (2.29) in all single unresolved regions and removes all explicit infrared poles.

While $\mathrm{d}\sigma_{\mathrm{NNLO}}^{VS,1,a}$ cancels fully with $\mathrm{d}\sigma_{\mathrm{NNLO}}^{S,a}$, parts of the remaining two terms have to be integrated to yield m-parton configurations, which are then added with the two-loop m-parton contributions $\mathrm{d}\sigma_{\mathrm{NNLO}}^{V,2}$. The precise nature of cancellations between the terms appearing in the integrated forms of $\mathrm{d}\sigma_{\mathrm{NNLO}}^{S,(bcd)}$ and terms in the unintegrated $\mathrm{d}\sigma_{\mathrm{NNLO}}^{VS,1,(bc)}$ differs considerably among the different colour structures. Therefore, no generic formula for these cancellations can be stated. In section 9, we will illustrate these cancellations on the example of the subleading colour contribution to $e^+e^- \to 3j$ at NNLO.

2.5 Comparison with other approaches

The NNLO antenna subtraction approach which we derive in detail in this section was previously sketched in our earlier publications [44, 45], where specific applications to $e^+e^- \to 2j$ and $e^+e^- \to 3j$ were considered. The case two-jet production is special in several as-

JHEP09(2005)056

pects, particularly since the double unresolved tree-level and single unresolved one-loop subtraction terms exactly coincide with the full matrix elements they are supposed to approximate. Moreover, the jet functions for two- and three-parton final states fulfil special relations which are in general not fulfilled for m- and $(m+1)$-parton final states. Most notably (see (5) in [45]),

$$J_3^{(3)}(p_i,p_j,p_k) = J_2^{(2)}(\tilde{p}_I,\tilde{p}_K) - J_2^{(3)}(p_i,p_j,p_k)\,, \tag{2.38}$$

which can be used to express [44, (3.17)] in the form of (2.28) presented in this paper.

Several other approaches to the handling of infrared singularities at NNLO have been proposed in the literature. One can distinguish two substantially different lines of making the infrared singularities in real radiation at NNLO explicit: either through a direct expansion of matrix element and phase space or through subtraction terms. In expanding the full real radiation matrix elements and the full multi-parton phase space in dimensional regularisation through sector decomposition [30, 31], one arrives at a Laurent expansion in ϵ with coefficients in terms of distributions in the Lorentz invariants associated with the process. These coefficients still contain the full phase space integration, but they are finite and the integrals can be carried out numerically. Using this approach, NNLO results have been obtained for $e^+e^- \to 2j$ [32], $pp \to H+X$ [33] and more recently muon decay [34] . In approaches invoking subtraction terms, such as the antenna subtraction proposed here, the real radiation singularities from multiparton matrix elements are removed by subtracting appropriate approximations, which coincide with the matrix elements in all singular limits, but are sufficiently simple to be integrated analytically.

A first formulation of the antenna subtraction method at NNLO was presented in refs. [25, 13]. In this work, all antenna phase space mappings required at NNLO were derived and documented. These mappings are to be used in the implementation of our formulation of NNLO antenna subtraction as well. Concerning the construction of subtraction terms, ref. [25] addresses processes involving gluons only, and restricts its results to the leading colour contributions (which are sufficient in purely gluonic processes at NNLO). The antenna subtraction terms in [25] are presented only in their unintegrated form. To implement them in an actual calculation, they still need to be integrated over the appropriate antenna phase spaces to make their infrared singularities explicit.

A generalisation of the NLO dipole subtraction formalism to NNLO was presented in [26, 14], where subtraction terms for all partonic configurations in all colour structures were derived. Again, these were presented only in their unintegrated form, while their analytical integration over the NNLO dipole phase spaces is a necessary prerequisite for their implementation into a numerical programme.

Finally, a third approach to the construction of subtraction terms at NNLO was presented in [28], where an iterative procedure of subtraction and subsequent cancellation of oversubtracted terms is invoked. Using this procedure, NNLO subtraction terms for the $C_F T_R$ colour factor in $e^+e^- \to 2j$ are constructed in [28], where they are also integrated analytically and implemented into a numerical programme. The agreement of [28] with earlier results [32, 44] illustrates the potential of this method. However, the full set of subtraction terms for all relevant partonic configurations in all colour structures is at present not yet derived (and thus not available in integrated form either) for this method.

More specific issues about subtraction at NNLO were addressed in two further works: [27] deals with overlapping collinear divergences in the initial state, and proposes a method for their systematic separation. More recently, a detailed study of the matching of single and double unresolved regions in subtraction at NNLO was presented in [29].

To implement a subtraction method at NNLO, one requires explicit expressions for all subtraction terms (double real radiation at tree level and single radiation at one-loop) in their unintegrated form, as well as the integrals of these expressions over the appropriate (double unresolved or single unresolved) phase spaces. Up to now, none of the approaches available in the literature provided these to an extent which would permit implementation for a realistic observable.

In the following sections, we will present the NLO and NNLO antenna functions for all partonic configurations and all colour factors. These are the building blocks of NLO and NNLO antenna subtraction terms required to implement our formulation of the colour-ordered antenna subtraction method. We provide the integrals of these subtraction terms for the kinematical situation of final state radiation. The method itself can in principle be extended to processes with hadrons in the initial state. In this case, the antenna subtraction terms could be constructed from the same building blocks, but different phase space factorisations and consequently different integrals are required.

3. Notation and structure of antenna functions

In this paper we derive antennae for all possible pairs of hard partons, quark-antiquark (section 5), quark-gluon (section 6) and gluon-gluon (section 7). Underlying the antenna is a colour connected pair of hard partons, that emit radiation between them. The three-particle antennae involve one unresolved parton, while the four-particle antennae involve two unresolved partons. The antenna may be at the tree or one-loop level.

Each antenna is determined by both the external state and the pair of hard partons it collapses to. In general we denote the antenna function as X. For antennae that collapse onto a hard quark-antiquark pair, $X = A$ for $qg\bar{q}$ and $qgg\bar{q}$, $X = B$ for $qq'\bar{q}'\bar{q}$ and $X = C$ for $qq\bar{q}\bar{q}$ final states. Similarly, for quark-gluon antenna, we have $X = D$ for qgg and $qggg$ and $X = E$ for $qq'\bar{q}'$ and $qq'\bar{q}'g$ final states. Finally, we characterise the gluon-gluon antennae as $X = F$ for ggg and $gggg$, $X = G$ for $gq\bar{q}$ and $gq\bar{q}g$ and $X = H$ for $q\bar{q}q'\bar{q}'$ final states. Some of these antenna functions decompose into a leading colour and a subleading colour contribution. Where appropriate, the subleading colour contribution to X is denoted as $\tilde{X}$. Finally, the one loop antenna functions also contain contributions from closed quark loops, which we denote as $\hat{X}$. The notation for the different tree-level and one-loop antenna functions is summarised in table 1.

Each antenna is a function of the invariants formed by the momenta of the final state particles.

	tree level	one loop
quark-antiquark		
$qg\bar{q}$	$A_3^0(q,g,\bar{q})$	$A_3^1(q,g,\bar{q}),\ \tilde{A}_3^1(q,g,\bar{q}),\ \hat{A}_3^1(q,g,\bar{q})$
$qgg\bar{q}$	$A_4^0(q,g,g,\bar{q}),\ \tilde{A}_4^0(q,g,g,\bar{q})$	
$qq'\bar{q}'\bar{q}$	$B_4^0(q,q',\bar{q}',\bar{q})$	
$qq\bar{q}\bar{q}$	$C_4^0(q,q,\bar{q},\bar{q})$	
quark-gluon		
qgg	$D_3^0(q,g,g)$	$D_3^1(q,g,g),\ \hat{D}_3^1(q,g,g)$
$qggg$	$D_4^0(q,g,g,g)$	
$qq'\bar{q}'$	$E_3^0(q,q',\bar{q}')$	$E_3^1(q,q',\bar{q}'),\ \tilde{E}_3^1(q,q',\bar{q}'),\ \hat{E}_3^1(q,q',\bar{q}')$
$qq'\bar{q}'g$	$E_4^0(q,q',\bar{q}',g),\ \tilde{E}_4^0(q,q',\bar{q}',g)$	
gluon-gluon		
ggg	$F_3^0(g,g,g)$	$F_3^1(g,g,g),\ \hat{F}_3^1(g,g,g)$
$gggg$	$F_4^0(g,g,g,g)$	
$gq\bar{q}$	$G_3^0(g,q,\bar{q})$	$G_3^1(g,q,\bar{q}),\ \tilde{G}_3^1(g,q,\bar{q}),\ \hat{G}_3^1(g,q,\bar{q})$
$gq\bar{q}g$	$G_4^0(g,q,\bar{q},g),\ \tilde{G}_4^0(g,q,\bar{q},g)$	
$q\bar{q}q'\bar{q}'$	$H_4^0(q,\bar{q},q',\bar{q}')$	

Table 1: List of tree-level and one-loop colour-ordered antenna functions. The tilde denotes subleading colour contributions, and the hat flavour-number dependent corrections.

It will prove useful to introduce the operators $\mathcal{P}oles$ and $\mathcal{F}inite$ that select either the singular or finite contribution from a particular antenna. For example,

$$\mathcal{P}oles(\mathcal{X})$$

extracts the singular contribution from the antenna X after integration over the unresolved phase space in terms of the infrared singularity operators of section 4. It should be noted that $\mathcal{P}oles(\mathcal{X})$ also contains finite terms arising from the expansion of the infrared singularity operators. These terms are on the one hand of the type $(\epsilon \ln s)^n$ (where s is the invariant mass of any pair of particles contained in the antenna, or the total invariant mass of all antenna particles), on the other hand they contain transcendental constants resulting from the expansion of the normalisation factors appearing in the different infrared singularity operators. To extract the *remaining* finite contribution, we introduce

$$\mathcal{F}inite(\mathcal{X}) \equiv \mathcal{X} - \mathcal{P}oles(\mathcal{X})\,.$$

Generally,

$$\mathcal{X} = \mathcal{P}oles(\mathcal{X}) + \mathcal{F}inite(\mathcal{X}) + \mathcal{O}(\epsilon)\,. \tag{3.1}$$

The one-loop antenna functions contain explicit poles from the loop integration. Therefore, the operators $\mathcal{P}oles$ and $\mathcal{F}inite$ can also be applied to their unintegrated forms X. The action of these operators is again to decompose the unintegrated antenna in terms of infrared singularity operators describing the pole terms and a finite remainder.

All antenna functions are derived from physical matrix elements: the quark-antiquark antenna functions from $\gamma^* \to q\bar{q}$ + (partons) [44], the quark-gluon antenna functions from

$\tilde{\chi} \to \tilde{g}$ + (partons) [46] and the gluon-gluon antenna functions from $H \to$ (partons) [47]. The tree-level antenna functions are obtained by normalising the colour-ordered three- and four-parton tree-level squared matrix elements to the squared matrix element for the basic two-parton process,

$$\begin{aligned} X^0_{ijk} &= S_{ijk,IK} \, \frac{|\mathcal{M}^0_{ijk}|^2}{|\mathcal{M}^0_{IK}|^2} \,, \\ X^0_{ijl} &= S_{ijkl,IL} \, \frac{|\mathcal{M}^0_{ijkl}|^2}{|\mathcal{M}^0_{IL}|^2} \,, \end{aligned} \tag{3.2}$$

where S denotes the symmetry factor associated to the antenna, which accounts both for potential identical particle symmetries and for the presence of more than one antenna in the basic two-parton process. The one-loop antenna functions are obtained from the colour-ordered renormalised one-loop three-parton matrix elements as

$$X^1_{ijk} = S_{ijk,IK} \, \frac{|\mathcal{M}^1_{ijk}|^2}{|\mathcal{M}^0_{IK}|^2} - X^0_{ijk} \, \frac{|\mathcal{M}^1_{IK}|^2}{|\mathcal{M}^0_{IK}|^2} \,. \tag{3.3}$$

The numerical implementation of the three- and four-parton antenna phase space [25] requires the partonic emissions to be ordered. Ordering of emissions means that the two hard radiator partons defining the antenna are identified, and that each unresolved parton can become singular only with the two particles which are adjacent to it, i.e. with the two radiators for three-parton antenna functions and with one radiator and with the other unresolved parton for the four-parton antenna functions. For the sake of numerical implementation, this implies two requirements: (1) the separation of multiple antenna configurations present in a single antenna function for three- and four-parton antenna functions and (2) the separation of non-ordered emissions (present only at subleading colour in the four-parton antenna functions) into terms that can be identified with a particular ordering of the momenta.

In the colour-ordered quark-gluon and gluon-gluon antenna functions derived from physical matrix elements for neutralino decay [46] and Higgs boson decay [47], it is in general not possible to identify the hard radiators and the unresolved partons in a unique manner. The reason for this ambiguity is in the cyclic nature of the colour orderings, which becomes evident already in the three-parton antenna functions: each pair of two partons can in principle act as hard radiators, resulting in more than one antenna configuration present in a single antenna function. For the three-parton antenna functions D^0_3 and F^0_3, we illustrate in (6.13) and (7.13) below how these different antenna configurations can be disentangled, resulting in new sub-antenna functions where the hard radiators can be uniquely identified. Such a decomposition is also possible for four-parton antenna functions which display the same ambiguity. However, in the four-parton case repeated partial fractioning is required to extract individual sub-antenna configurations. Since this procedure introduces new denominators in the antenna terms, we will use it only for the numerical implementation. At this point, it should be pointed out that the cyclic ambiguity is inevitable if physical matrix elements involving gluons as radiators are used to derive the antenna functions, since the cyclic symmetry in colour space is enforced by gauge invariance.

The decomposition of non-ordered emissions into different terms is discussed in detail in section 5 using the quark-antiquark antenna function $\tilde{A}_4^0$, which describes the emission of two gluons at subleading colour, as an example. In this antenna the gluons behave effectively like photons, coupling only to the quark and the antiquark. Consequently, each gluon can become collinear with both hard radiators. In (5.28) below, we illustrate how this antenna function can be decomposed into individual terms corresponding to different well-defined orderings by repeated partial fractioning in the invariants. The same procedure has to be applied for all other antenna functions which are not sufficiently ordered. Since this repeated partial fractioning yields increases the number of terms in the analytic expressions for the antenna functions quite considerably, we restrict ourselves to quoting only the full antenna functions, not their ordered decompositions.

Repeated partial fractioning generates denominators which do not correspond to physical propagators of four-parton matrix elements. Therefore, it is in general not possible to integrate the ordered terms analytically, at least not by merely applying the methods of [31]. Analytical phase space integration of functions involving non-propagator-type denominators is in principle possible [16, 15] and requires a more involved reduction procedure and a larger set of master integrals. To avoid this problem we use the ordered sub-antenna functions in the numerical implementation, and ensure that all ordered contributions to a given antenna function are taken together with the same phase space factorisation (but different phase space mappings). With this procedure, the ordered contributions to the sub-antenna functions can be recombined to form the full antenna functions (related to physical matrix elements) quoted in the following three sections, which are then integrated analytically to make their infrared pole structure explicit. This recombination may be obtained by considering more than one colour-ordering for the full $(m+2)$-parton matrix element, and by explicit subtraction of unwanted spurious singularities. This problem is discussed more explicitly using the four-parton quark-gluon antenna function D_4^0 of sections 6 and 8.3.2 as an example.

4. Colour-ordered infrared singularity operators

In order to express the singularity structure in a way that cancellations between real radiation and virtual radiation can be made explicit, it is convenient to extract the infrared singularity structure using the $\mathbf{I}^{(1)}$-operator [48]. This operator describes the singularity structure of virtual one-loop amplitudes. At the two-loop level, the infrared singularity structure is described by $\mathbf{I}^{(1)}$-operators, a hard radiation operator $\mathbf{H}^{(2)}$, the QCD β-function and the gluon splitting constant K. The same pole structure is recovered [44, 46, 47] in the sum of double real radiation and one-loop single real radiation contributions, such that the sum of double-virtual, virtual single-unresolved and double-unresolved corrections is finite. Some cancellations, related to the one-loop correction to the soft gluon current $\mathbf{S}^{(2)}$, take place only between virtual single-unresolved and double-unresolved corrections.

In the formulation of [48], $\mathbf{I}^{(1)}$ is a tensor in colour space, and contains imaginary parts from the analytic continuation of loop amplitudes from the euclidean to the minkowskian region. In the following, we will only consider colour-ordered matrix elements, for which

$\mathbf{I}^{(1)}$ is a scalar in colour space. Moreover, using the $\mathbf{I}^{(1)}$-operator to describe real radiation singularities, only its real part is relevant, since contributions from its imaginary part cancel once the double-virtual two-loop-times-tree-level and one-loop-times-one-loop parts are added together.

The real radiation infrared singularity operators that appear in the integrated form of an antenna function are denoted by $(ij = q\bar{q}, qg, g\bar{q}, gg)$

$$\mathbf{I}^{(1)}_{ij}(\epsilon, s_{ij}) \qquad \text{and} \qquad \mathbf{I}^{(1)}_{ij,F}(\epsilon, s_{ij})\,,$$

where the second operator describes contributions arising from the splitting of a gluon into a quark-antiquark pair and which are proportional to the number of light quark flavours N_F.

The operators are given by

$$\begin{aligned}
\mathbf{I}^{(1)}_{q\bar{q}}(\epsilon, s_{q\bar{q}}) &= -\frac{e^{\epsilon\gamma}}{2\Gamma(1-\epsilon)}\left[\frac{1}{\epsilon^2}+\frac{3}{2\epsilon}\right]\mathrm{Re}(-s_{q\bar{q}})^{-\epsilon}\,,\\
\mathbf{I}^{(1)}_{qg}(\epsilon, s_{qg}) &= -\frac{e^{\epsilon\gamma}}{2\Gamma(1-\epsilon)}\left[\frac{1}{\epsilon^2}+\frac{5}{3\epsilon}\right]\mathrm{Re}(-s_{qg})^{-\epsilon}\,,\\
\mathbf{I}^{(1)}_{gg}(\epsilon, s_{gg}) &= -\frac{e^{\epsilon\gamma}}{2\Gamma(1-\epsilon)}\left[\frac{1}{\epsilon^2}+\frac{11}{6\epsilon}\right]\mathrm{Re}(-s_{gg})^{-\epsilon}\,,\\
\mathbf{I}^{(1)}_{q\bar{q},F}(\epsilon, s_{q\bar{q}}) &= 0\,,\\
\mathbf{I}^{(1)}_{qg,F}(\epsilon, s_{qg}) &= \frac{e^{\epsilon\gamma}}{2\Gamma(1-\epsilon)}\,\frac{1}{6\epsilon}\,\mathrm{Re}(-s_{qg})^{-\epsilon}\,,\\
\mathbf{I}^{(1)}_{gg,F}(\epsilon, s_{gg}) &= \frac{e^{\epsilon\gamma}}{2\Gamma(1-\epsilon)}\,\frac{1}{3\epsilon}\,\mathrm{Re}(-s_{gg})^{-\epsilon}\,.
\end{aligned} \tag{4.1}$$

The antiquark-gluon operators are obtained by charge conjugation:

$$\mathbf{I}^{(1)}_{g\bar{q}}(\epsilon, s_{g\bar{q}}) = \mathbf{I}^{(1)}_{qg}(\epsilon, s_{g\bar{q}}) \qquad \text{and} \qquad \mathbf{I}^{(1)}_{g\bar{q},F}(\epsilon, s_{g\bar{q}}) = \mathbf{I}^{(1)}_{qg,F}(\epsilon, s_{g\bar{q}})\,.$$

At NNLO, several new infrared singularity operators appear; the one-loop soft gluon current $\mathbf{S}^{(2)}(\epsilon, q^2)$ [12],

$$\begin{aligned}
\mathbf{S}^{(2)}(\epsilon, q^2) = \Bigg[&-\frac{1}{4\epsilon^4}-\frac{3}{4\epsilon^3}+\frac{1}{\epsilon^2}\left(-\frac{13}{4}+\frac{7\pi^2}{24}\right)+\frac{1}{\epsilon}\left(-\frac{51}{4}+\frac{7\pi^2}{8}+\frac{14}{3}\zeta_3\right)+\\
&+\left(-\frac{205}{4}+\frac{91\pi^2}{24}+14\zeta_3+\frac{7\pi^4}{480}\right)+\mathcal{O}(\epsilon)\Bigg](q^2)^{-2\epsilon}\,,
\end{aligned} \tag{4.2}$$

and the hard radiation functions $\mathbf{H}^{(2)}_{ij}(\epsilon, q^2)$, which decompose into virtual contributions $\mathbf{H}^{(2)}_{ij,V}(\epsilon, q^2)$ and real contributions $\mathbf{H}^{(2)}_{ij,R}(\epsilon, q^2)$. For the antenna functions presented here, the virtual contributions are given by,

$$\begin{aligned}
\mathbf{H}^{(2)}_{V,A}(\epsilon, q^2) &= \frac{e^{\epsilon\gamma}}{\Gamma(1-\epsilon)}\left[\frac{1}{\epsilon^2}\left(\frac{43}{8}-\frac{\pi^2}{6}\right)+\frac{1}{\epsilon}\left(\frac{839}{24}-\frac{\pi^2}{2}-11\zeta_3\right)\right](q^2)^{-2\epsilon}\,,\\
\mathbf{H}^{(2)}_{V,\tilde{A}}(\epsilon, q^2) &= \frac{e^{\epsilon\gamma}}{\Gamma(1-\epsilon)}\left[\frac{1}{\epsilon^2}\left(\frac{43}{8}-\frac{\pi^2}{6}\right)+\frac{1}{\epsilon}\left(\frac{51}{2}-\frac{\pi^2}{4}-15\zeta_3\right)\right](q^2)^{-2\epsilon}\,,
\end{aligned}$$

$$
\begin{aligned}
\mathbf{H}^{(2)}_{V,\hat{A}}(\epsilon,q^2) &= \frac{e^{\epsilon\gamma}}{\Gamma(1-\epsilon)}\left[-\frac{19}{12\epsilon}\right](q^2)^{-2\epsilon}\,,\\
\mathbf{H}^{(2)}_{V,D}(\epsilon,q^2) &= \frac{e^{\epsilon\gamma}}{\Gamma(1-\epsilon)}\left[\frac{1}{6\epsilon^3}+\frac{1}{\epsilon^2}\left(\frac{109}{4}-\frac{2\pi^2}{3}\right)+\right.\\
&\qquad\left.+\frac{1}{\epsilon}\left(\frac{17791}{108}-\frac{133\pi^2}{72}-52\zeta_3\right)\right](q^2)^{-2\epsilon}\,,\\
\mathbf{H}^{(2)}_{V,\hat{D}}(\epsilon,q^2) &= \frac{e^{\epsilon\gamma}}{\Gamma(1-\epsilon)}\left[-\frac{275}{36\epsilon}\right](q^2)^{-2\epsilon}\,,\\
\mathbf{H}^{(2)}_{V,E}(\epsilon,q^2) &= \frac{e^{\epsilon\gamma}}{\Gamma(1-\epsilon)}\left[-\frac{2}{\epsilon^2}+\frac{1}{\epsilon}\left(-\frac{326}{27}+\frac{\pi^2}{9}\right)\right](q^2)^{-2\epsilon}\,,\\
\mathbf{H}^{(2)}_{V,\tilde{E}}(\epsilon,q^2) &= \frac{e^{\epsilon\gamma}}{\Gamma(1-\epsilon)}\left[-\frac{1}{6\epsilon^3}-\frac{35}{36\epsilon^2}+\frac{1}{\epsilon}\left(-\frac{509}{108}+\frac{17\pi^2}{72}\right)\right](q^2)^{-2\epsilon}\,,\\
\mathbf{H}^{(2)}_{V,F}(\epsilon,q^2) &= \frac{e^{\epsilon\gamma}}{\Gamma(1-\epsilon)}\left[\frac{1}{3\epsilon^3}+\frac{1}{\epsilon^2}\left(30-\frac{2\pi^2}{3}\right)+\right.\\
&\qquad\left.+\frac{1}{\epsilon}\left(\frac{20009}{108}-\frac{79\pi^2}{36}-52\zeta_3\right)\right](q^2)^{-2\epsilon}\,,\\
\mathbf{H}^{(2)}_{V,\hat{F}}(\epsilon,q^2) &= \frac{e^{\epsilon\gamma}}{\Gamma(1-\epsilon)}\left[-\frac{37}{3\epsilon}\right](q^2)^{-2\epsilon}\,,\\
\mathbf{H}^{(2)}_{V,G}(\epsilon,q^2) &= \frac{e^{\epsilon\gamma}}{\Gamma(1-\epsilon)}\left[-\frac{14}{3\epsilon^2}+\frac{1}{\epsilon}\left(-\frac{805}{27}+\frac{2\pi^2}{9}\right)\right](q^2)^{-2\epsilon}\,,\\
\mathbf{H}^{(2)}_{V,\tilde{G}}(\epsilon,q^2) &= \frac{e^{\epsilon\gamma}}{\Gamma(1-\epsilon)}\left[-\frac{1}{3\epsilon^3}-\frac{41}{18\epsilon^2}+\frac{1}{\epsilon}\left(-\frac{325}{27}+\frac{17\pi^2}{36}\right)\right](q^2)^{-2\epsilon}\,,\\
\mathbf{H}^{(2)}_{V,\hat{G}}(\epsilon,q^2) &= \frac{e^{\epsilon\gamma}}{\Gamma(1-\epsilon)}\left[-\frac{2}{9\epsilon^2}+\frac{7}{9\epsilon}\right](q^2)^{-2\epsilon}\,,
\end{aligned}
\tag{4.3}
$$

while the real radiation contributions are,

$$
\begin{aligned}
\mathbf{H}^{(2)}_{R,A}(\epsilon,q^2) &= \frac{e^{\epsilon\gamma}}{\Gamma(1-\epsilon)}\left[\frac{1}{\epsilon^2}\left(-\frac{43}{8}+\frac{\pi^2}{6}\right)+\frac{1}{\epsilon}\left(-\frac{29795}{864}+\frac{37\pi^2}{96}+\frac{51}{4}\zeta_3\right)\right](q^2)^{-2\epsilon}\,,\\
\mathbf{H}^{(2)}_{R,\tilde{A}}(\epsilon,q^2) &= \frac{e^{\epsilon\gamma}}{\Gamma(1-\epsilon)}\left[\frac{1}{\epsilon^2}\left(-\frac{43}{8}+\frac{\pi^2}{6}\right)+\frac{1}{\epsilon}\left(-\frac{845}{32}+\frac{\pi^2}{2}+13\zeta_3\right)\right](q^2)^{-2\epsilon}\,,\\
\mathbf{H}^{(2)}_{R,B}(\epsilon,q^2) &= \frac{e^{\epsilon\gamma}}{\Gamma(1-\epsilon)}\left[\frac{1}{\epsilon}\left(\frac{317}{216}+\frac{\pi^2}{48}\right)\right](q^2)^{-2\epsilon}\,,\\
\mathbf{H}^{(2)}_{R,C}(\epsilon,q^2) &= \frac{e^{\epsilon\gamma}}{\Gamma(1-\epsilon)}\left[\frac{1}{\epsilon}\left(\frac{13}{16}-\frac{\pi^2}{8}+\frac{1}{2}\zeta_3\right)\right](q^2)^{-2\epsilon}\,,\\
\mathbf{H}^{(2)}_{R,D}(\epsilon,q^2) &= \frac{e^{\epsilon\gamma}}{\Gamma(1-\epsilon)}\left[-\frac{1}{6\epsilon^3}+\frac{1}{\epsilon^2}\left(-\frac{109}{4}+\frac{2\pi^2}{3}\right)+\right.\\
&\qquad\left.+\frac{1}{\epsilon}\left(-\frac{71261}{432}+\frac{97\pi^2}{48}+52\zeta_3\right)\right](q^2)^{-2\epsilon}\,,\\
\mathbf{H}^{(2)}_{R,E}(\epsilon,q^2) &= \frac{e^{\epsilon\gamma}}{\Gamma(1-\epsilon)}\left[\frac{2}{\epsilon^2}+\frac{1}{\epsilon}\left(\frac{518}{27}-\frac{7\pi^2}{72}\right)\right](q^2)^{-2\epsilon}\,,
\end{aligned}
$$

$$
\begin{aligned}
\mathbf{H}^{(2)}_{R,\tilde{E}}(\epsilon,q^2) &= \frac{e^{\epsilon\gamma}}{\Gamma(1-\epsilon)}\left[\frac{1}{6\epsilon^3}+\frac{35}{36\epsilon^2}+\frac{1}{\epsilon}\left(\frac{1045}{216}-\frac{17\pi^2}{72}\right)\right](q^2)^{-2\epsilon}\,,\\
\mathbf{H}^{(2)}_{R,F}(\epsilon,q^2) &= \frac{e^{\epsilon\gamma}}{\Gamma(1-\epsilon)}\Bigg[-\frac{1}{3\epsilon^3}+\frac{1}{\epsilon^2}\left(-30+\frac{2\pi^2}{3}\right)+\\
&\qquad +\frac{1}{\epsilon}\left(-\frac{4991}{27}+\frac{109\pi^2}{48}+\frac{105}{2}\zeta_3\right)\Bigg](q^2)^{-2\epsilon}\,,\\
\mathbf{H}^{(2)}_{R,G}(\epsilon,q^2) &= \frac{e^{\epsilon\gamma}}{\Gamma(1-\epsilon)}\left[\frac{14}{3\epsilon^2}+\frac{1}{\epsilon}\left(\frac{4463}{108}-\frac{17\pi^2}{72}\right)\right](q^2)^{-2\epsilon}\,,\\
\mathbf{H}^{(2)}_{R,\tilde{G}}(\epsilon,q^2) &= \frac{e^{\epsilon\gamma}}{\Gamma(1-\epsilon)}\left[\frac{1}{3\epsilon^3}+\frac{41}{18\epsilon^2}+\frac{1}{\epsilon}\left(\frac{1327}{108}-\frac{17\pi^2}{36}\right)\right](q^2)^{-2\epsilon}\,,\\
\mathbf{H}^{(2)}_{R,H}(\epsilon,q^2) &= \frac{e^{\epsilon\gamma}}{\Gamma(1-\epsilon)}\left[\frac{2}{9\epsilon^2}-\frac{16}{27\epsilon}\right](q^2)^{-2\epsilon}\,. \qquad (4.4)
\end{aligned}
$$

Combining the real and virtual hard radiation functions yields the hard radiation terms from the two-loop virtual corrections [4, 5, 44, 46, 47],

$$
\begin{aligned}
\mathbf{H}^{(2)}_{q\bar{q}}(\epsilon,q^2) &= N^2\,\mathbf{H}^{(2)}_{q\bar{q},N^2}(\epsilon,q^2)+\mathbf{H}^{(2)}_{q\bar{q},1}(\epsilon,q^2)+\frac{1}{N^2}\,\mathbf{H}^{(2)}_{q\bar{q},1/N^2}(\epsilon,q^2)+\\
&\quad +NN_F\,\mathbf{H}^{(2)}_{q\bar{q},NN_F}(\epsilon,q^2)+\frac{N_F}{N}\mathbf{H}^{(2)}_{q\bar{q},N_F/N}(\epsilon,q^2)\,, \qquad (4.5)\\
\mathbf{H}^{(2)}_{qg}(\epsilon,q^2) &= N^2\,\mathbf{H}^{(2)}_{qg,N^2}(\epsilon,q^2)+NN_F\,\mathbf{H}^{(2)}_{qg,NN_F}(\epsilon,q^2)+\frac{N_F}{N}\mathbf{H}^{(2)}_{qg,N_F/N}(\epsilon,q^2)+\\
&\quad +N_F^2\,\mathbf{H}^{(2)}_{qg,N_F^2}(\epsilon,q^2)\,, \qquad (4.6)\\
\mathbf{H}^{(2)}_{gg}(\epsilon,q^2) &= N^2\,\mathbf{H}^{(2)}_{gg,N^2}(\epsilon,q^2)+NN_F\,\mathbf{H}^{(2)}_{gg,NN_F}(\epsilon,q^2)+\frac{N_F}{N}\mathbf{H}^{(2)}_{gg,N_F/N}(\epsilon,q^2)+\\
&\quad +N_F^2\,\mathbf{H}^{(2)}_{gg,N_F^2}(\epsilon,q^2)\,, \qquad (4.7)
\end{aligned}
$$

with

$$
\begin{aligned}
\mathbf{H}^{(2)}_{q\bar{q},N^2}(\epsilon,q^2) &= \frac{1}{2}\left(\mathbf{H}^{(2)}_{V,A}(\epsilon,q^2)+\mathbf{H}^{(2)}_{R,A}(\epsilon,q^2)\right)\\
&= \frac{e^{\epsilon\gamma}}{4\epsilon\Gamma(1-\epsilon)}\left(\frac{409}{432}-\frac{11\pi^2}{48}+\frac{7}{2}\zeta_3\right)(q^2)^{-2\epsilon}\,, \qquad (4.8)\\
\mathbf{H}^{(2)}_{q\bar{q},1/N^2}(\epsilon,q^2) &= \frac{1}{2}\left(\mathbf{H}^{(2)}_{V,\hat{A}}(\epsilon,q^2)+\mathbf{H}^{(2)}_{R,\hat{A}}(\epsilon,q^2)+\mathbf{H}^{(2)}_{R,C}(\epsilon,q^2)\right)\\
&= \frac{e^{\epsilon\gamma}}{4\epsilon\Gamma(1-\epsilon)}\left(-\frac{3}{16}+\frac{\pi^2}{4}-3\zeta_3\right)(q^2)^{-2\epsilon}\,, \qquad (4.9)\\
\mathbf{H}^{(2)}_{q\bar{q},1}(\epsilon,q^2) &= -\mathbf{H}^{(2)}_{qq,N^2}(\epsilon,q^2)-\mathbf{H}^{(2)}_{q\bar{q},1/N^2}(\epsilon,q^2)\,, \qquad (4.10)\\
\mathbf{H}^{(2)}_{q\bar{q},NN_F}(\epsilon,q^2) &= \frac{1}{2}\left(\mathbf{H}^{(2)}_{V,\hat{A}}(\epsilon,q^2)+\mathbf{H}^{(2)}_{R,B}(\epsilon,q^2)\right)\\
&= \frac{e^{\epsilon\gamma}}{4\epsilon\Gamma(1-\epsilon)}\left(-\frac{25}{108}+\frac{\pi^2}{24}\right)(q^2)^{-2\epsilon}\,, \qquad (4.11)\\
\mathbf{H}^{(2)}_{q\bar{q},N_F/N}(\epsilon,q^2) &= -\mathbf{H}^{(2)}_{q\bar{q},NN_F}(\epsilon,q^2)\,, \qquad (4.12)\\
\mathbf{H}^{(2)}_{qg,N^2}(\epsilon,q^2) &= \frac{1}{2}\left(\mathbf{H}^{(2)}_{V,D}(\epsilon,q^2)+\mathbf{H}^{(2)}_{R,D}(\epsilon,q^2)\right)
\end{aligned}
$$

$$= \frac{e^{\epsilon\gamma}}{4\epsilon\Gamma(1-\epsilon)} \left(-\frac{97}{216} + \frac{25\pi^2}{72}\right) (q^2)^{-2\epsilon}\,, \tag{4.13}$$

$$\mathbf{H}^{(2)}_{qg,NN_F}(\epsilon, q^2) = \frac{1}{2}\left(\mathbf{H}^{(2)}_{V,\hat{D}}(\epsilon, q^2) + \mathbf{H}^{(2)}_{V,E}(\epsilon, q^2) + \mathbf{H}^{(2)}_{R,E}(\epsilon, q^2)\right)$$
$$= \frac{e^{\epsilon\gamma}}{4\epsilon\Gamma(1-\epsilon)} \left(-\frac{19}{18} + \frac{\pi^2}{36}\right) (q^2)^{-2\epsilon}\,, \tag{4.14}$$

$$\mathbf{H}^{(2)}_{qg,N_F/N}(\epsilon, q^2) = -\frac{1}{2}\left(\mathbf{H}^{(2)}_{V,\tilde{E}}(\epsilon, q^2) + \mathbf{H}^{(2)}_{R,\tilde{E}}(\epsilon, q^2)\right)$$
$$= \frac{e^{\epsilon\gamma}}{4\epsilon\Gamma(1-\epsilon)} \left(-\frac{1}{4}\right) (q^2)^{-2\epsilon}\,, \tag{4.15}$$

$$\mathbf{H}^{(2)}_{qg,N_F^2}(\epsilon, q^2) = \frac{e^{\epsilon\gamma}}{4\epsilon\Gamma(1-\epsilon)} \frac{5}{27} (q^2)^{-2\epsilon}\,, \tag{4.16}$$

$$\mathbf{H}^{(2)}_{gg,N^2}(\epsilon, q^2) = \frac{1}{2}\left(\mathbf{H}^{(2)}_{V,F}(\epsilon, q^2) + \mathbf{H}^{(2)}_{R,F}(\epsilon, q^2)\right)$$
$$= \frac{e^{\epsilon\gamma}}{4\epsilon\Gamma(1-\epsilon)} \left(\frac{5}{6} + \frac{11\pi^2}{72} + \zeta_3\right) (q^2)^{-2\epsilon}\,, \tag{4.17}$$

$$\mathbf{H}^{(2)}_{gg,NN_F}(\epsilon, q^2) = \frac{1}{2}\left(\mathbf{H}^{(2)}_{V,\hat{F}}(\epsilon, q^2) + \mathbf{H}^{(2)}_{V,G}(\epsilon, q^2) + \mathbf{H}^{(2)}_{R,G}(\epsilon, q^2)\right)$$
$$= \frac{e^{\epsilon\gamma}}{4\epsilon\Gamma(1-\epsilon)} \left(-\frac{89}{54} - \frac{\pi^2}{36}\right) (q^2)^{-2\epsilon}\,, \tag{4.18}$$

$$\mathbf{H}^{(2)}_{gg,N_F/N}(\epsilon, q^2) = -\frac{1}{2}\left(\mathbf{H}^{(2)}_{V,\tilde{G}}(\epsilon, q^2) + \mathbf{H}^{(2)}_{R,\tilde{G}}(\epsilon, q^2)\right)$$
$$= \frac{e^{\epsilon\gamma}}{4\epsilon\Gamma(1-\epsilon)} \left(-\frac{1}{2}\right) (q^2)^{-2\epsilon}\,, \tag{4.19}$$

$$\mathbf{H}^{(2)}_{gg,N_F^2}(\epsilon, q^2) = -\frac{1}{2}\left(\mathbf{H}^{(2)}_{V,\hat{G}}(\epsilon, q^2) + \mathbf{H}^{(2)}_{R,H}(\epsilon, q^2)\right)$$
$$= \frac{e^{\epsilon\gamma}}{4\epsilon\Gamma(1-\epsilon)} \frac{10}{27} (q^2)^{-2\epsilon}\,. \tag{4.20}$$

The relation of these operators to the singularity structure of physical multi-parton two-loop matrix elements was discussed in [4, 5, 44, 46, 47]

Finally, the NNLO singularity structures also contain the QCD β-function (2.13) and the collinear coefficient K. In a colour-ordered decomposition, these are

$$\beta_0 = b_0 N + b_{0,F} N_F \qquad \text{with} \qquad b_0 = \frac{11}{6}\,, b_{0,F} = -\frac{1}{3} \tag{4.21}$$

and

$$K = k_0 N + k_{0,F} N_F \qquad \text{with} \qquad k_0 = \frac{67}{18} - \frac{\pi^2}{6}\,, k_{0,F} = -\frac{5}{9}. \tag{4.22}$$

5. Quark-antiquark antennae

The quark-antiquark antenna functions are derived by appropriately normalising the colour-ordered QCD real radiation corrections to $\gamma^* \to q\bar{q}$, described to NNLO accuracy in [44].

The overall normalisation is given by defining the tree-level two-parton quark-antiquark antenna function

$$\mathcal{A}_2^0(s_{12}) \equiv 1\,. \tag{5.1}$$

The one-loop two-parton quark-antiquark antenna is then:

$$\begin{aligned}\mathcal{A}_2^1(s_{12}) &= (s_{12})^{-\epsilon}\Bigg[-\frac{1}{\epsilon^2}-\frac{3}{2\epsilon}-4+\frac{7\pi^2}{12}+\left(-8+\frac{7\pi^2}{8}+\frac{7}{3}\zeta_3\right)\epsilon+\\ &\quad+\left(-16+\frac{7\pi^2}{3}+\frac{7}{2}\zeta_3-\frac{73\pi^4}{1440}\right)\epsilon^2+\mathcal{O}(\epsilon^3)\Bigg]\,, \end{aligned} \tag{5.2}$$

with

$$\mathcal{P}oles\left(\mathcal{A}_2^1(s_{12})\right) = 2\mathbf{I}^{(1)}_{q\bar{q}}\left(\epsilon, s_{12}\right), \tag{5.3}$$

$$\mathcal{F}inite\left(\mathcal{A}_2^1(s_{12})\right) = -4. \tag{5.4}$$

5.1 Three-parton tree-level antenna functions

The tree-level three-parton quark-antiquark antenna is:

$$A_3^0(1_q, 3_g, 2_{\bar{q}}) = \frac{1}{s_{123}}\left(\frac{s_{13}}{s_{23}}+\frac{s_{23}}{s_{13}}+2\frac{s_{12}s_{123}}{s_{13}s_{23}}\right)+\mathcal{O}(\epsilon)\,, \tag{5.5}$$

yielding the integrated antenna function according to (2.11):

$$\begin{aligned}\mathcal{A}_3^0(s_{123}) &= (s_{123})^{-\epsilon}\Bigg[\frac{1}{\epsilon^2}+\frac{3}{2\epsilon}+\frac{19}{4}-\frac{7\pi^2}{12}+\left(\frac{109}{8}-\frac{7\pi^2}{8}-\frac{25}{3}\zeta_3\right)\epsilon+\\ &\quad+\left(\frac{639}{16}-\frac{133\pi^2}{48}-\frac{25}{2}\zeta_3-\frac{71\pi^4}{1440}\right)\epsilon^2+\mathcal{O}(\epsilon^3)\Bigg]\,, \end{aligned} \tag{5.6}$$

with

$$\mathcal{P}oles\left(\mathcal{A}_3^0(s_{123})\right) = -2\mathbf{I}^{(1)}_{q\bar{q}}\left(\epsilon, s_{123}\right)\,, \tag{5.7}$$

$$\mathcal{F}inite\left(\mathcal{A}_3^0(s_{123})\right) = \frac{19}{4}\,. \tag{5.8}$$

This antenna can be split symmetrically into two sub-antennae, which coincide with the $q \to qg$ dipole functions:

$$A_3^0(1,3,2) = a_3^0(1,3,2) + a_3^0(2,3,1)\,, \tag{5.9}$$

with

$$a_3^0(1,3,2) = \frac{1}{s_{123}}\left(\frac{s_{23}}{s_{13}}+2\frac{s_{12}s_{123}}{(s_{13}+s_{23})s_{13}}\right)+\mathcal{O}(\epsilon)\,. \tag{5.10}$$

5.2 Three-parton one-loop antenna functions

At one loop, one finds three different three-particle antenna functions, corresponding to the leading and subleading colour structures $A_3^1(1_q,3_g,2_{\bar{q}})$, $\tilde{A}_3^1(1_q,3_g,2_{\bar{q}})$ and to the contribution from a closed quark loop $\hat{A}_3^1(1_q,3_g,2_{\bar{q}})$.

Introducing

$$R(y,z) = \log y \log z - \log y \log(1-y) - \log z \log(1-z) + \frac{\pi^2}{6} - \mathrm{Li}_2(y) - \mathrm{Li}_2(z) \qquad (5.11)$$

and $y_{ij} = s_{ij}/s_{123}$, the one-loop antenna functions are given by:

$$\begin{aligned}
\mathcal{P}oles\left(A_3^1(1_q,3_g,2_{\bar{q}})\right) &= 2\left(\mathbf{I}^{(1)}_{qg}(\epsilon,s_{13}) + \mathbf{I}^{(1)}_{qg}(\epsilon,s_{23}) - \mathbf{I}^{(1)}_{q\bar{q}}(\epsilon,s_{123})\right) A_3^0(1,3,2)\,, && (5.12)\\
\mathcal{F}inite\left(A_3^1(1_q,3_g,2_{\bar{q}})\right) &= -\left(R(y_{13},y_{23}) + \frac{5}{3}\log y_{13} + \frac{5}{3}\log y_{23}\right) A_3^0(1,3,2) + \\
&\quad + \frac{1}{s_{123}} + \frac{s_{12}+s_{23}}{2s_{123}s_{13}} + \frac{s_{12}+s_{13}}{2s_{123}s_{23}} - \frac{s_{13}}{2s_{123}(s_{12}+s_{13})} - \\
&\quad - \frac{s_{23}}{2s_{123}(s_{12}+s_{23})} + \frac{\log y_{13}}{s_{123}}\left(2 - \frac{1}{2}\frac{s_{13}s_{23}}{(s_{12}+s_{23})^2} + 2\frac{s_{13}-s_{23}}{s_{12}+s_{23}}\right) + \\
&\quad + \frac{\log y_{23}}{s_{123}}\left(2 - \frac{1}{2}\frac{s_{13}s_{23}}{(s_{12}+s_{13})^2} + 2\frac{s_{23}-s_{13}}{s_{12}+s_{13}}\right), && (5.13)\\
\mathcal{P}oles\left(\tilde{A}_3^1(1_q,3_g,2_{\bar{q}})\right) &= 2\left(\mathbf{I}^{(1)}_{q\bar{q}}(\epsilon,s_{12}) - \mathbf{I}^{(1)}_{q\bar{q}}(\epsilon,s_{123})\right) A_3^0(1,3,2)\,, && (5.14)\\
\mathcal{F}inite\left(\tilde{A}_3^1(q,g,\bar{q})\right) &= -\left(R(y_{12},y_{13}) + R(y_{12},y_{23}) + \frac{3}{2}\log y_{12}\right) A_3^0(1,3,2) - \\
&\quad - \frac{s_{12}+s_{23}}{2s_{123}s_{13}} - \frac{s_{12}+s_{13}}{2s_{123}s_{23}} + \frac{s_{12}}{2s_{123}(s_{12}+s_{13})} + \frac{s_{12}}{2s_{123}(s_{12}+s_{23})} + \\
&\quad + \frac{2s_{12}}{s_{123}(s_{13}+s_{23})} + \frac{2\log y_{12}}{s_{123}}\left(2\frac{s_{12}}{s_{13}+s_{23}} + \frac{s_{12}^2}{(s_{13}+s_{23})^2}\right) + \\
&\quad + \frac{\log y_{13}}{2s_{123}}\left(\frac{s_{12}s_{13}}{(s_{12}+s_{23})^2} + 4\frac{s_{12}}{s_{12}+s_{23}} + \frac{s_{13}}{s_{12}+s_{23}}\right) + \\
&\quad + \frac{\log y_{23}}{2s_{123}}\left(\frac{s_{12}s_{23}}{(s_{12}+s_{13})^2} + 4\frac{s_{12}}{s_{12}+s_{13}} + \frac{s_{23}}{s_{12}+s_{13}}\right) + \\
&\quad + R(y_{12},y_{13})\frac{2s_{12}+s_{13}}{s_{123}s_{23}} + R(y_{12},y_{23})\frac{2s_{12}+s_{23}}{s_{123}s_{13}}\,, && (5.15)\\
\mathcal{P}oles\left(\hat{A}_3^1(1_q,3_g,2_{\bar{q}})\right) &= 2\left(\mathbf{I}^{(1)}_{qg,F}(\epsilon,s_{13}) + \mathbf{I}^{(1)}_{qg,F}(\epsilon,s_{23})\right) A_3^0(1,3,2)\,, && (5.16)\\
\mathcal{F}inite\left(\hat{A}_3^1(1_q,3_g,2_{\bar{q}})\right) &= \frac{1}{6}\left(\log y_{13} + \log y_{23}\right) A_3^0(1,3,2)\,. && (5.17)
\end{aligned}$$

Note that application of the $\mathcal{F}inite$-operator in the above expression yields only the $\mathcal{O}(\epsilon^0)$-terms of the antenna functions. These antenna functions contain higher powers in ϵ as well, and these are relevant to the integrated antennae listed below.

The integrated antennae are defined in (2.35). They read:

$$\mathcal{A}_3^1(s_{123}) = (s_{123})^{-2\epsilon}\Bigg[-\frac{1}{4\epsilon^4} - \frac{31}{12\epsilon^3} + \frac{1}{\epsilon^2}\left(-\frac{53}{8} + \frac{11\pi^2}{24}\right) + \frac{1}{\epsilon}\left(-\frac{647}{24} + \frac{22\pi^2}{9} + \frac{23}{3}\zeta_3\right) +$$

$$+\left(-\frac{5231}{48}+\frac{17\pi^2}{2}+\frac{689}{18}\zeta_3-\frac{41\pi^4}{480}\right)+\mathcal{O}(\epsilon)\Bigg], \tag{5.18}$$

$$\tilde{\mathcal{A}}_3^1(s_{123}) = (s_{123})^{-2\epsilon}\Bigg[\frac{1}{\epsilon^2}\left(-\frac{5}{8}+\frac{\pi^2}{6}\right)+\frac{1}{\epsilon}\left(-\frac{19}{4}+\frac{\pi^2}{4}+7\zeta_3\right)+$$
$$+\left(-\frac{105}{4}+\frac{27\pi^2}{16}+\frac{27}{2}\zeta_3+\frac{7\pi^4}{90}\right)+\mathcal{O}(\epsilon)\Bigg], \tag{5.19}$$

$$\hat{\mathcal{A}}_3^1(s_{123}) = (s_{123})^{-2\epsilon}\Bigg[\frac{1}{3\epsilon^3}+\frac{1}{2\epsilon^2}+\frac{1}{\epsilon}\left(\frac{19}{12}-\frac{7\pi^2}{36}\right)+$$
$$+\left(\frac{109}{24}-\frac{7\pi^2}{24}-\frac{25}{9}\zeta_3\right)+\mathcal{O}(\epsilon)\Bigg], \tag{5.20}$$

with

$$\mathcal{P}oles\left(\mathcal{A}_3^1(s_{123})\right) = -\mathcal{A}_2^1(s_{123})\left(2\mathbf{I}_{q\bar{q}}^{(1)}(\epsilon,s_{123})+\mathcal{A}_3^0(s_{123})\right)+\frac{2b_0}{\epsilon}(s_{123})^{-\epsilon}\,\mathbf{I}_{q\bar{q}}^{(1)}(\epsilon,s_{123})-$$
$$-\mathbf{H}_{V,A}^{(2)}(\epsilon,s_{123})+\mathbf{S}_V^{(2)}(\epsilon,s_{123}), \tag{5.21}$$

$$\mathcal{F}inite\left(\mathcal{A}_3^1(s_{123})\right) = -\frac{6581}{48}+\frac{787\pi^2}{96}+\frac{17\pi^4}{360}+\frac{143}{3}\zeta_3, \tag{5.22}$$

$$\mathcal{P}oles\left(\tilde{\mathcal{A}}_3^1(s_{123})\right) = -\mathcal{A}_2^1(s_{123})\left(2\mathbf{I}_{q\bar{q}}^{(1)}(\epsilon,s_{123})+\mathcal{A}_3^0(s_{123})\right)-\mathbf{H}_{V,\tilde{A}}^{(2)}(\epsilon,s_{123}), \tag{5.23}$$

$$\mathcal{F}inite\left(\tilde{\mathcal{A}}_3^1(s_{123})\right) = -\frac{845}{8}+\frac{217\pi^2}{32}+\frac{9\pi^4}{40}+\frac{75}{2}\zeta_3, \tag{5.24}$$

$$\mathcal{P}oles\left(\hat{\mathcal{A}}_3^1(s_{123})\right) = \frac{2b_{0,F}}{\epsilon}(s_{123})^{-\epsilon}\,\mathbf{I}_{q\bar{q}}^{(1)}(\epsilon,s_{123})-\mathbf{H}_{V,\hat{A}}^{(2)}(s_{123}), \tag{5.25}$$

$$\mathcal{F}inite\left(\hat{\mathcal{A}}_3^1(\epsilon,s_{123})\right) = \frac{109}{24}-\frac{8}{3}\zeta_3. \tag{5.26}$$

5.3 Four-parton tree-level antenna functions

The tree-level four-parton quark-antiquark antenna contains three final states: quark-gluon-gluon-antiquark at leading and subleading colour, A_4^0 and $\tilde{A}_4^0$ and quark-antiquark-quark-antiquark for non-identical quark flavours B_4^0 as well as the identical-flavour-only contribution C_4^0. The quark-antiquark-quark-antiquark final state with identical quark flavours is thus described by the sum of antennae for non-identical flavour and identical-flavour-only. The antennae for the $qgg\bar{q}$ final state are:

$$A_4^0(1_q,3_g,4_g,2_{\bar{q}}) = a_4^0(1,3,4,2)+a_4^0(2,4,3,1), \tag{5.27}$$
$$\tilde{A}_4^0(1_q,3_g,4_g,2_{\bar{q}}) = \tilde{a}_4^0(1,3,4,2)+\tilde{a}_4^0(2,4,3,1)+\tilde{a}_4^0(1,4,3,2)+\tilde{a}_4^0(2,3,4,1), \tag{5.28}$$

where the sub-antennae are given by

$$a_4^0(1,3,4,2) = \frac{1}{s_{1234}}\Bigg\{\frac{1}{s_{13}s_{24}s_{34}}\left[2s_{12}s_{14}+2s_{12}s_{23}+2s_{12}^2+s_{14}^2+s_{23}^2\right]+$$
$$+\frac{1}{s_{13}s_{24}s_{234}}\left[3s_{12}s_{14}-3s_{12}s_{34}+4s_{12}^2-s_{14}s_{34}+s_{14}^2+s_{34}^2\right]+$$
$$+\frac{1}{s_{13}s_{24}}\left[6s_{12}+3s_{14}+3s_{23}\right]+$$
$$+\frac{1}{s_{13}s_{34}s_{234}}\left[2s_{12}s_{14}-2s_{12}s_{24}+2s_{12}^2-2s_{14}s_{24}+s_{14}^2+s_{24}^2\right]+$$

$$
\begin{aligned}
&+\frac{1}{s_{13}s_{34}}\left[6s_{12}+2s_{14}+4s_{23}+s_{24}\right]+\\
&+\frac{1}{s_{13}s_{234}}\left[-6s_{12}-3s_{14}+3s_{24}+3s_{34}\right]-\\
&-\frac{2}{s_{13}}+\frac{1}{s_{24}s_{34}}\left[4s_{12}+2s_{13}+3s_{14}\right]+\frac{1}{s_{24}s_{234}^2}\left[s_{12}s_{34}+s_{13}s_{34}+s_{14}s_{34}\right]+\\
&+\frac{1}{s_{24}s_{234}}\left[-3s_{12}-2s_{13}-2s_{14}\right]+\frac{1}{s_{34}^2s_{234}^2}\left[2s_{12}s_{24}^2+2s_{13}s_{24}^2+2s_{14}s_{24}^2\right]+\\
&+\frac{1}{s_{34}^2s_{234}}\left[-4s_{14}s_{24}+2s_{24}^2\right]+\frac{1}{s_{34}s_{234}^2}\left[4s_{12}s_{24}+4s_{13}s_{24}+4s_{14}s_{24}\right]+\\
&+\frac{1}{s_{34}s_{234}}\left[-8s_{12}-3s_{13}-5s_{14}+2s_{24}\right]-\frac{2}{s_{34}}+\\
&+\frac{1}{s_{234}^2}\left[3s_{12}+3s_{13}+3s_{14}\right]+\mathcal{O}(\epsilon)\Bigg\},
\end{aligned}
\tag{5.29}
$$

$$
\begin{aligned}
\tilde{a}_4^0(1,3,4,2) = \frac{1}{s_{1234}}\Bigg\{&\frac{1}{s_{13}s_{24}s_{134}s_{234}}\left[\frac{3}{2}s_{12}s_{34}^2-2s_{12}^2s_{34}+s_{12}^3-\frac{1}{2}s_{34}^3\right]+\\
&+\frac{1}{s_{13}s_{24}s_{134}}\left[3s_{12}s_{23}-3s_{12}s_{34}+4s_{12}^2-s_{23}s_{34}+s_{23}^2+s_{34}^2\right]+\\
&+\frac{s_{12}^3}{s_{13}s_{24}(s_{13}+s_{23})(s_{14}+s_{24})}+\frac{1}{s_{13}s_{24}(s_{13}+s_{23})}\left[\frac{1}{2}s_{12}s_{14}+s_{12}^2\right]+\\
&+\frac{1}{s_{13}s_{24}(s_{14}+s_{24})}\left[\frac{1}{2}s_{12}s_{23}+s_{12}^2\right]+\frac{1}{s_{13}s_{24}}\left[3s_{12}+\frac{3}{2}s_{14}+\frac{3}{2}s_{23}\right]+\\
&+\frac{1}{s_{13}s_{134}^2}\left[s_{12}s_{34}+s_{23}s_{34}+s_{24}s_{34}\right]+\frac{2s_{12}^3}{s_{13}s_{134}s_{234}(s_{13}+s_{23})}+\\
&+\frac{1}{s_{13}s_{134}s_{234}}\left[3s_{12}s_{34}-s_{24}s_{34}-2s_{34}^2\right]+\\
&+\frac{1}{s_{13}s_{134}(s_{13}+s_{23})}\left[s_{12}s_{24}+s_{12}s_{34}+2s_{12}^2\right]+\\
&+\frac{1}{s_{13}s_{134}}\left[-s_{23}-s_{24}+2s_{34}\right]+\frac{1}{s_{13}s_{234}(s_{13}+s_{23})}\left[s_{12}s_{14}+s_{12}s_{34}+2s_{12}^2\right]+\\
&+\frac{1}{s_{13}s_{234}}\left[-2s_{12}-2s_{14}+s_{24}+2s_{34}\right]+\\
&+\frac{s_{12}^3}{s_{13}(s_{13}+s_{23})(s_{14}+s_{24})(s_{13}+s_{14})}+\\
&+\frac{1}{s_{13}(s_{13}+s_{23})(s_{13}+s_{14})}\left[s_{12}s_{24}+2s_{12}^2\right]+\\
&+\frac{1}{s_{13}(s_{14}+s_{24})(s_{13}+s_{14})}\left[s_{12}s_{23}+2s_{12}^2\right]+\\
&+\frac{2s_{12}}{s_{13}(s_{13}+s_{14})}-\frac{2}{s_{13}}+\frac{1}{s_{134}^2}\left[s_{12}+s_{23}+s_{24}\right]+\\
&+\frac{1}{s_{134}s_{234}}\left[s_{12}-s_{34}\right]+\frac{1}{s_{134}}+\mathcal{O}(\epsilon)\Bigg\}.
\end{aligned}
\tag{5.30}
$$

In A_4^0 the gluonic emissions are colour-ordered, while in $\tilde{A}_4^0$ the gluons are photon-like, implying no ordering. Because of colour-ordering, A_4^0 can be used with a single ordered phase space mapping. In contrast, $\tilde{A}_4^0$ can not be used with a unique ordered phase space mapping. The above decomposition into $\tilde{a}_4^0$ yields however ordered terms, since the combination $\tilde{a}_4^0(1,3,4,2)+\tilde{a}_4^0(2,4,3,1)$ contains only single emission singularities in $1/s_{13}$ and

$1/s_{24}$, corresponding to the ordered $(1,3,4,2)$ phase space mapping. On the other hand $\tilde{a}_4^0(1,4,3,2)+\tilde{a}_4^0(2,3,4,1)$ contains only single emission singularities in $1/s_{14}$ and $1/s_{23}$, corresponding to the ordered $(1,4,3,2)$ phase space mapping. Since the decomposition of $\tilde{A}_4^0$ is symmetric, all four $\tilde{a}_4^0$ yield identical integrals if integrated over the tripole phase space. It should be noted that it is not possible to analytically integrate an individual $\tilde{a}_4^0$ over the tripole phase space using the reduction and integration techniques described in [31], since the extra polynomial denominators present there enlarge the set of basis integrals considerably. When the four $\tilde{a}_4^0$ are added together these polynomial denominators cancel, and the tripole integrals can be carried out.

The integrals of these antenna functions are according to (2.23):

$$\begin{aligned}\mathcal{A}_4^0(s_{1234}) &= (s_{1234})^{-2\epsilon}\left[\frac{3}{4\epsilon^4}+\frac{65}{24\epsilon^3}+\frac{1}{\epsilon^2}\left(\frac{217}{18}-\frac{13\pi^2}{12}\right)+\right.\\ &\quad+\frac{1}{\epsilon}\left(\frac{43223}{864}-\frac{589\pi^2}{144}-\frac{71}{4}\zeta_3\right)+\\ &\quad\left.+\left(\frac{1076717}{5184}-\frac{7955\pi^2}{432}-\frac{1327}{18}\zeta_3+\frac{373\pi^4}{1440}\right)+\mathcal{O}(\epsilon)\right], \end{aligned}\tag{5.31}$$

$$\begin{aligned}\tilde{\mathcal{A}}_4^0(s_{1234}) &= 2\ (s_{1234})^{-2\epsilon}\left[\frac{1}{2\epsilon^4}+\frac{3}{2\epsilon^3}+\frac{1}{\epsilon^2}\left(\frac{13}{2}-\frac{3\pi^2}{4}\right)+\right.\\ &\quad+\frac{1}{\epsilon}\left(\frac{845}{32}-\frac{9\pi^2}{4}-\frac{40}{3}\zeta_3\right)+\\ &\quad\left.+\left(\frac{6921}{64}-\frac{473\pi^2}{48}-40\zeta_3+\frac{17\pi^4}{144}\right)+\mathcal{O}(\epsilon)\right], \end{aligned}\tag{5.32}$$

with

$$\begin{aligned}\mathcal{P}oles\left(\mathcal{A}_4^0(s_{1234})\right) &= 2\left[\mathbf{I}_{q\bar{q}}^{(1)}(\epsilon,s_{1234})\right]^2-2\,e^{-\epsilon\gamma}\frac{\Gamma(1-2\epsilon)}{\Gamma(1-\epsilon)}\left(\frac{b_0}{\epsilon}+k_0\right)\mathbf{I}_{q\bar{q}}^{(1)}(2\epsilon,s_{1234})-\\ &\quad-\mathbf{H}_{R,A}^{(2)}(\epsilon,s_{1234})-\mathbf{S}_V^{(2)}(\epsilon,s_{1234}),\end{aligned}\tag{5.33}$$

$$\mathcal{F}inite\left(\mathcal{A}_4^0(s_{1234})\right) = \frac{811037}{5184}-\frac{2321\pi^2}{288}-\frac{13\pi^4}{160}-\frac{4217}{72}\zeta_3,\tag{5.34}$$

$$\mathcal{P}oles\left(\tilde{\mathcal{A}}_4^0(s_{1234})\right) = 4\left[\mathbf{I}_{q\bar{q}}^{(1)}(\epsilon,s_{1234})\right]^2-2\,\mathbf{H}_{R,\tilde{A}}^{(2)}(\epsilon,s_{1234}),\tag{5.35}$$

$$\mathcal{F}inite\left(\tilde{\mathcal{A}}_4^0(s_{1234})\right) = \frac{6921}{32}-\frac{259\pi^2}{16}-\frac{3\pi^4}{10}-78\zeta_3.\tag{5.36}$$

The non-identical quark antenna is:

$$B_4^0(1_q,3_{q'},4_{\bar{q}'},2_{\bar{q}}) = b_4^0(1,3,4,2)+b_4^0(2,3,4,1)+b_4^0(1,4,3,2)+b_4^0(2,4,3,1)\ ,\tag{5.37}$$

with a sub-antenna function given by

$$\begin{aligned}b_4^0(1,3,4,2) &= \frac{1}{s_{1234}}\left\{\frac{1}{s_{34}^2s_{234}^2}\left[-2s_{12}s_{24}^2-2s_{13}s_{24}^2-2s_{14}s_{24}^2\right]+\frac{1}{s_{34}^2s_{234}}\left[4s_{14}s_{24}-2s_{24}^2\right]+\right.\\ &\quad+\frac{1}{s_{34}s_{234}^2}\left[-2s_{12}s_{24}-2s_{13}s_{24}-2s_{14}s_{24}\right]+\frac{1}{s_{34}s_{234}}\times\\ &\quad\left.\times\left[2s_{12}+s_{13}+s_{14}\right]+\frac{1}{s_{234}^2}\left[-s_{12}-s_{13}-s_{14}\right]+\mathcal{O}(\epsilon)\right\}.\end{aligned}\tag{5.38}$$

In B_4^0, the secondary quark emission is ordered, such that a single ordered phase space mapping can be used.

This subtraction term yields the integral

$$\mathcal{B}_4^0(s_{1234}) = (s_{1234})^{-2\epsilon}\left[-\frac{1}{12\epsilon^3}-\frac{7}{18\epsilon^2}+\frac{1}{\epsilon}\left(-\frac{407}{216}+\frac{11\pi^2}{72}\right)+\right.$$
$$\left.+\left(-\frac{11753}{1296}+\frac{77\pi^2}{108}+\frac{67}{18}\zeta_3\right)+\mathcal{O}(\epsilon)\right], \qquad (5.39)$$

with

$$\mathcal{P}oles\left(\mathcal{B}_4^0(s_{1234})\right) = -2e^{-\epsilon\gamma}\frac{\Gamma(1-2\epsilon)}{\Gamma(1-\epsilon)}\left(\frac{b_{0,F}}{\epsilon}+k_{0,F}\right)\mathbf{I}_{q\bar{q}}^{(1)}(2\epsilon,s_{1234})-$$
$$-\mathbf{H}_{R,B}^{(2)}(\epsilon,s_{1234}), \qquad (5.40)$$
$$\mathcal{F}inite\left(\mathcal{B}_4^0(s_{1234})\right) = -\frac{11753}{1296}-\frac{7\pi^2}{72}+\frac{133}{36}\zeta_3\,. \qquad (5.41)$$

The identical-flavour-only quark-antiquark-quark-antiquark antenna is:

$$C_4^0(1_q,3_q,4_{\bar{q}},2_{\bar{q}}) = c_4^0(1,2,3,4)+c_4^0(1,4,3,2)\;, \qquad (5.42)$$

with

$$c_4^0(1,2,3,4) = \frac{1}{s_{1234}}\left\{\frac{s_{14}^3}{4s_{23}s_{34}s_{123}s_{234}}+\frac{1}{4s_{23}s_{34}s_{123}}\left[s_{13}s_{14}-s_{13}^2-2s_{14}^2\right]+\right.$$
$$+\frac{1}{4s_{23}s_{34}}\left[-s_{12}-s_{13}-s_{14}\right]+\frac{1}{2s_{34}s_{123}s_{234}}\left[s_{13}^2+s_{14}^2\right]+$$
$$+\frac{1}{s_{34}s_{234}^2}\left[s_{12}s_{24}+s_{13}s_{24}+s_{14}s_{24}\right]+$$
$$+\frac{1}{2s_{34}s_{234}}\left[s_{12}+s_{13}+s_{24}\right]+\frac{1}{2s_{123}s_{234}}\left[-2s_{13}+2s_{14}+s_{34}\right]+$$
$$\left.+\frac{1}{s_{234}^2}\left[-s_{12}-s_{13}-s_{14}\right]-\frac{1}{2s_{234}}+\mathcal{O}(\epsilon)\right\}. \qquad (5.43)$$

It integrates to

$$\mathcal{C}_4^0(s_{1234}) = \frac{1}{2}\,(s_{1234})^{-2\epsilon}\left[\frac{1}{\epsilon}\left(-\frac{13}{16}+\frac{\pi^2}{8}-\frac{1}{2}\zeta_3\right)+\right.$$
$$\left.+\left(-\frac{339}{32}+\frac{17\pi^2}{24}+\frac{21}{4}\zeta_3-\frac{2\pi^4}{45}\right)+\mathcal{O}(\epsilon)\right], \qquad (5.44)$$

with

$$\mathcal{P}oles\left(\mathcal{C}_4^0(s_{1234})\right) = -\frac{1}{2}\mathbf{H}_{R,C}^{(2)}(\epsilon,s_{1234}), \qquad (5.45)$$
$$\mathcal{F}inite\left(\mathcal{C}_4^0(s_{1234})\right) = -\frac{339}{64}+\frac{17\pi^2}{48}+\frac{21}{8}\zeta_3-\frac{\pi^4}{45}\,. \qquad (5.46)$$

All antenna functions listed in this section agree with the four-parton matrix elements in the Appendix of [35], taking account of the different normalisation used here.

6. Quark-gluon antennae

The quark-gluon antenna functions are obtained from the QCD real radiation corrections to the decay of a heavy neutralino into a massless gluino and a gluon, $\tilde{\chi} \to \tilde{g}g$, which is described in detail in [46].

The overall normalisation is given by defining the tree-level two-parton quark-gluon antenna function

$$\mathcal{D}_2^0(s_{13}) \equiv 1\,. \tag{6.1}$$

In this equation, and in all subsequent equations in the section, we label the primary quark momentum as $(1)_q$ and the momenta of gluons or of a secondary quark-antiquark pair as $(3)_i$, $(4)_j$ and $(5)_k$. This non-consecutive labelling of momenta is introduced in view of applying the quark-gluon antenna functions in an actual calculation, where they will always appear in a pair: quark-gluon antenna and antiquark-gluon antenna, with $(1)_q$ and $(2)_{\bar{q}}$ denoting the primary quark and antiquark momenta.

The one-loop two-parton quark-gluon antenna contains two contributions, corresponding to the different colour and flavour structures:

$$\mathcal{D}_2^1(s_{13}) = 2(s_{13})^{-\epsilon}\left[-\frac{1}{\epsilon^2}-\frac{5}{3\epsilon}+\frac{7\pi^2}{12}+\left(-1+\frac{7}{3}\zeta_3\right)\epsilon+\left(-3-\frac{73\pi^4}{1440}\right)\epsilon^2+\mathcal{O}(\epsilon^3)\right], \tag{6.2}$$

$$\hat{\mathcal{D}}_2^1(s_{13}) = 2\,(s_{13})^{-\epsilon}\frac{1}{6\epsilon}\,, \tag{6.3}$$

with

$$\mathcal{P}oles\left(\mathcal{D}_2^1(s_{13})\right) = 4\mathbf{I}^{(1)}_{qg}(\epsilon, s_{13})\,, \tag{6.4}$$

$$\mathcal{F}inite\left(\mathcal{D}_2^1(s_{13})\right) = 0\,, \tag{6.5}$$

$$\mathcal{P}oles\left(\hat{\mathcal{D}}_2^1(s_{13})\right) = 4\mathbf{I}^{(1)}_{qg,F}(\epsilon, s_{13})\,, \tag{6.6}$$

$$\mathcal{F}inite\left(\hat{\mathcal{D}}_2^1(s_{13})\right) = 0\,. \tag{6.7}$$

The pole terms in the above expression have to be compared to the pole terms of the one-loop correction to the quark-antiquark antenna function $\mathcal{A}_2^1$ in (5.3), containing $2\mathbf{I}^{(1)}_{q\bar{q}}$. The factor 4 in (6.4), (6.6) appears since the tree level quark-gluon antenna function $\mathcal{D}_2^0(s_{13})$ contains two distinct quark-gluon antennae, in contrast to the single quark-antiquark antenna contained in $\mathcal{A}_2^0(s_{12})$, as will be seen below in constructing the three-parton tree-level antenna functions.

6.1 Three-parton tree-level antenna functions

The tree-level three-parton quark-gluon antenna contains two final states: quark-gluon-gluon and quark-quark-antiquark. The antenna corresponding to the first final state is:

$$D_3^0(1_q, 3_g, 4_g) = \frac{1}{s_{134}^2}\left(\frac{2s_{134}^2 s_{14}}{s_{13}s_{34}}+\frac{2s_{134}^2 s_{13}}{s_{14}s_{34}}+\frac{s_{14}s_{34}+s_{34}^2}{s_{13}}+\right.$$
$$\left.+\frac{s_{13}s_{34}+s_{34}^2}{s_{14}}+\frac{2s_{13}s_{14}}{s_{34}}+5s_{134}+s_{34}\right)+\mathcal{O}(\epsilon)\,. \tag{6.8}$$

Its integrated form is

$$\mathcal{D}_3^0(s_{134}) = 2\,(s_{134})^{-\epsilon}\left[\frac{1}{\epsilon^2}+\frac{5}{3\epsilon}+\frac{17}{3}-\frac{7\pi^2}{12}+\left(\frac{209}{12}-\frac{35\pi^2}{36}-\frac{25}{3}\zeta_3\right)\epsilon+\right.$$
$$\left.+\left(\frac{421}{8}-\frac{119\pi^2}{36}-\frac{125}{9}\zeta_3-\frac{71\pi^4}{1440}\right)\epsilon^2+\mathcal{O}(\epsilon^3)\right], \tag{6.9}$$

with

$$\mathcal{P}oles\left(\mathcal{D}_3^0(s_{134})\right) = -4\mathbf{I}_{qg}^{(1)}(\epsilon, s_{134}), \tag{6.10}$$
$$\mathcal{F}inite\left(\mathcal{D}_3^0(s_{134})\right) = \frac{34}{3}. \tag{6.11}$$

This tree-level antenna function contains two antennae, corresponding to the configurations: (gluon (3_g) radiated between quark and gluon (4_g)) and (gluon (4_g) radiated between quark and gluon (3_g)). The separation between these is not free from an ambiguity, since the collinear limit of the two gluons has be split between the two configurations. We decompose

$$D_3^0(1,3,4) = d_3^0(1,3,4) + d_3^0(1,4,3), \tag{6.12}$$

where the sub-antenna is given by

$$d_3^0(1,3,4) = \frac{1}{s_{134}^2}\left(\frac{2s_{134}^2 s_{14}}{s_{13}s_{34}}+\frac{s_{14}s_{34}+s_{34}^2}{s_{13}}+\frac{s_{13}s_{14}}{s_{34}}+\frac{5}{2}s_{134}+\frac{1}{2}s_{34}\right)+\mathcal{O}(\epsilon). \tag{6.13}$$

The function could be further decomposed into two dipoles if needed for configurations discussed in section 2.3.2.

The tree-level three-parton quark-gluon antenna corresponding to the quark-quark-antiquark final state is:

$$E_3^0(1_q, 3_{q'}, 4_{\bar{q}'}) = \frac{1}{s_{134}^2}\left(\frac{s_{13}^2+s_{14}^2}{s_{34}}+s_{13}+s_{14}\right)+\mathcal{O}(\epsilon). \tag{6.14}$$

Phase space integration yields:

$$\mathcal{E}_3^0(s_{134}) = 2\,(s_{134})^{-\epsilon}\left[-\frac{1}{6\epsilon}-\frac{1}{2}+\left(-\frac{3}{2}+\frac{7\pi^2}{72}\right)\epsilon+\left(-\frac{9}{2}+\frac{7\pi^2}{24}-\frac{25}{18}\zeta_3\right)\epsilon^2+\mathcal{O}(\epsilon^3)\right], \tag{6.15}$$

with

$$\mathcal{P}oles\left(\mathcal{E}_3^0(s_{134})\right) = -4\mathbf{I}_{qg,F}^{(1)}(\epsilon, s_{134}), \tag{6.16}$$
$$\mathcal{F}inite\left(\mathcal{E}_3^0(s_{134})\right) = -1. \tag{6.17}$$

6.2 Three-parton one-loop antenna functions

At one loop, the correction to the quark-gluon-gluon antenna contains a leading colour term $D_3^1(1_q, 3_g, 4_g)$ and a quark loop term $\hat{D}_3^1(1_q, 3_g, 4_g)$. These read:

$$\mathcal{P}oles\left(D_3^1(1_q,3_g,4_g)\right) = 2\Big(\mathbf{I}_{qg}^{(1)}(\epsilon, s_{13})+\mathbf{I}_{qg}^{(1)}(\epsilon, s_{14})+\mathbf{I}_{gg}^{(1)}(\epsilon, s_{34})-$$

$$- 2\mathbf{I}^{(1)}_{qg}(\epsilon, s_{134})\Big) D_3^0(1,3,4)\,, \tag{6.18}$$

$$\mathcal{F}inite\left(D_3^1(1_q,3_g,4_g)\right) = -\Big(R(y_{13},y_{34}) + R(y_{14},y_{34}) + R(y_{13},y_{14}) + \frac{5}{3}\log y_{13} + + \frac{5}{3}\log y_{14} + \frac{11}{6}\log y_{34}\Big) D_3^0(1,3,4) + \frac{1}{3s_{34}}\,, \tag{6.19}$$

$$\mathcal{P}oles\left(\hat{D}_3^1(1_q,3_g,4_g)\right) = 2\Big(\mathbf{I}^{(1)}_{qg,F}(\epsilon,s_{13}) + \mathbf{I}^{(1)}_{qg,F}(\epsilon,s_{14}) + + \mathbf{I}^{(1)}_{gg,F}(\epsilon,s_{34}) - 2\mathbf{I}^{(1)}_{qg,F}(\epsilon,s_{134})\Big) D_3^0(1,3,4)\,, \tag{6.20}$$

$$\mathcal{F}inite\left(\hat{D}_3^1(1_q,3_g,4_g)\right) = \frac{1}{6}\left(\log y_{13} + \log y_{14} + 2\log y_{34}\right) D_3^0(1,3,4) - \frac{1}{3s_{34}}\,. \tag{6.21}$$

Integration of these antenna functions yields

$$\mathcal{D}_3^1(s_{134}) = (s_{134})^{-2\epsilon}\Bigg[-\frac{1}{2\epsilon^4} - \frac{16}{3\epsilon^3} + \frac{1}{\epsilon^2}\left(-\frac{619}{36} + \frac{5\pi^2}{4}\right) + \frac{1}{\epsilon}\left(-\frac{8941}{108} + \frac{23\pi^2}{4} + \frac{88}{3}\zeta_3\right) + + \left(-\frac{20353}{54} + \frac{5473\pi^2}{216} + 105\zeta_3 - \frac{11\pi^4}{720}\right) + \mathcal{O}(\epsilon)\Bigg]\,, \tag{6.22}$$

$$\hat{\mathcal{D}}_3^1(s_{134}) = (s_{134})^{-2\epsilon}\left[\frac{2}{3\epsilon^3} + \frac{10}{9\epsilon^2} + \frac{1}{\epsilon}\left(\frac{139}{36} - \frac{7\pi^2}{18}\right) + \left(\frac{443}{36} - \frac{35\pi^2}{54} - \frac{50}{9}\zeta_3\right) + \mathcal{O}(\epsilon)\right], \tag{6.23}$$

with

$$\mathcal{P}oles\left(\mathcal{D}_3^1(s_{134})\right) = -\mathcal{D}_2^1(s_{134})\left(4\mathbf{I}^{(1)}_{qg}(\epsilon,s_{134}) + \mathcal{D}_3^0(s_{134})\right) + \frac{2b_0}{\epsilon}(s_{134})^{-\epsilon}\left[2\,\mathbf{I}^{(1)}_{qg}(\epsilon,s_{134})\right] - - \mathbf{H}^{(2)}_{V,D}(\epsilon,s_{134}) + 2\mathbf{S}^{(2)}(\epsilon,s_{134})\,, \tag{6.24}$$

$$\mathcal{F}inite\left(\mathcal{D}_3^1(s_{134})\right) = -\frac{32455}{54} + \frac{16573\pi^2}{432} + \frac{49\pi^4}{90} + \frac{3283}{18}\zeta_3\,, \tag{6.25}$$

$$\mathcal{P}oles\left(\hat{\mathcal{D}}_3^1(s_{134})\right) = -\hat{\mathcal{D}}_2^1(s_{134})\left(4\mathbf{I}^{(1)}_{qg}(\epsilon,s_{134}) + \mathcal{D}_3^0(s_{134})\right) + + \frac{2b_{0,F}}{\epsilon}(s_{134})^{-\epsilon}\left[2\,\mathbf{I}^{(1)}_{qg}(\epsilon,s_{134})\right] - \mathbf{H}^{(2)}_{V,\hat{D}}(\epsilon,s_{134})\,, \tag{6.26}$$

$$\mathcal{F}inite\left(\hat{\mathcal{D}}_3^1(s_{134})\right) = \frac{287}{12} - \frac{32}{3}\zeta_3\,. \tag{6.27}$$

Again, the factors of 2 in front of the infrared singularity operators and of the soft gluon current arise from the fact that the basic two-parton process contains two quark-gluon antennae.

At one loop, the correction to the quark-quark-antiquark antenna contains a leading colour and a subleading colour term $E_3^1(1_q,3_{q'},4_{\bar{q}'})$, $\tilde{E}_3^1(1_q,3_{q'},4_{\bar{q}'})$ as well as a quark loop term $\hat{E}_3^1(1_q,3_{q'},4_{\bar{q}'})$. These read:

$$\mathcal{P}oles\left(E_3^1(1_q,3_{q'},4_{\bar{q}'})\right) = 2\left(\mathbf{I}^{(1)}_{q\bar{q}}(\epsilon,s_{13}) + \mathbf{I}^{(1)}_{q\bar{q}}(\epsilon,s_{14}) - 2\mathbf{I}^{(1)}_{qg}(\epsilon,s_{134})\right) E_3^0(1,3,4)\,, \tag{6.28}$$

$$\mathcal{F}inite\left(E_3^1(1_q,3_{q'},4_{\bar{q}'})\right) = -\Big(R(y_{13},y_{34}) + R(y_{14},y_{34}) + \frac{3}{2}\log y_{14} + \frac{3}{2}\log y_{14} +$$

$$
\begin{aligned}
&\quad + \frac{13}{6}\log y_{34} - \frac{40}{9}\bigg) E_3^0(1,3,4) + \\
&\quad + R(y_{13},y_{34})\frac{s_{13}}{s_{134}^2} + R(y_{14},y_{34})\frac{s_{14}}{s_{134}^2}\,, \qquad (6.29)\\
\mathcal{P}oles\left(\tilde{E}_3^1(1_q,3_{q'},4_{\bar{q}'})\right) &= 2\left(\mathbf{I}^{(1)}_{q\bar{q}}(\epsilon,s_{34})\right) E_3^0(1,3,4)\,, \qquad (6.30)\\
\mathcal{F}inite\left(\tilde{E}_3^1(1_q,3_{q'},4_{\bar{q}'})\right) &= -4E_3^0(1,3,4)\,, \qquad (6.31)\\
\mathcal{P}oles\left(\hat{E}_3^1(1_q,3_{q'},4_{\bar{q}'})\right) &= -4\mathbf{I}^{(1)}_{qg,F}(\epsilon,s_{134})E_3^0(1,3,4)\,, \qquad (6.32)\\
\mathcal{F}inite\left(\hat{E}_3^1(1_q,3_{q'},4_{\bar{q}'})\right) &= \left(-\frac{10}{9}+\frac{2}{3}\log y_{34}\right) E_3^0(1,3,4)\,. \qquad (6.33)
\end{aligned}
$$

Integration of these antenna functions yields

$$
\begin{aligned}
\mathcal{E}_3^1(s_{134}) &= (s_{134})^{-2\epsilon}\left[\frac{11}{18\epsilon^2}+\frac{1}{\epsilon}\left(\frac{74}{27}-\frac{\pi^2}{9}\right)+\left(\frac{3023}{216}-\frac{181\pi^2}{216}-\frac{130}{9}\zeta_3\right)+\mathcal{O}(\epsilon)\right], \qquad (6.34)\\
\tilde{\mathcal{E}}_3^1(s_{134}) &= (s_{134})^{-2\epsilon}\left[\frac{1}{6\epsilon^3}+\frac{35}{36\epsilon^2}+\frac{1}{\epsilon}\left(\frac{509}{108}-\frac{\pi^2}{4}\right)+\left(\frac{1670}{81}-\frac{35\pi^2}{24}-\frac{31}{9}\zeta_3\right)+\mathcal{O}(\epsilon)\right], \qquad (6.35)\\
\hat{\mathcal{E}}_3^1(s_{134}) &= (s_{134})^{-2\epsilon}\left[\frac{1}{3\epsilon}+\left(\frac{172}{81}-\frac{11\pi^2}{108}\right)+\mathcal{O}(\epsilon)\right], \qquad (6.36)
\end{aligned}
$$

with

$$
\begin{aligned}
\mathcal{P}oles\left(\mathcal{E}_3^1(s_{134})\right) &= -\mathcal{D}_2^1(s_{134})\left(4\mathbf{I}^{(1)}_{qg,F}(\epsilon,s_{134})+\mathcal{E}_3^0(s_{134})\right)+\\
&\quad+\frac{2b_0}{\epsilon}(s_{134})^{-\epsilon}\,2\,\mathbf{I}^{(1)}_{qg,F}(\epsilon,s_{134})-\mathbf{H}^{(2)}_{V,E}(\epsilon,s_{134})\,, \qquad (6.37)\\
\mathcal{F}inite\left(\mathcal{E}_3^1(s_{134})\right) &= \frac{9071}{216}-\frac{143\pi^2}{54}-\frac{26}{3}\zeta_3\,, \qquad (6.38)\\
\mathcal{P}oles\left(\tilde{\mathcal{E}}_3^1(s_{134})\right) &= -\mathbf{H}^{(2)}_{V,\tilde{E}}(\epsilon,s_{134})\,, \qquad (6.39)\\
\mathcal{F}inite\left(\tilde{\mathcal{E}}_3^1(s_{134})\right) &= \frac{1670}{81}-\frac{595\pi^2}{432}-\frac{61}{18}\zeta_3\,, \qquad (6.40)\\
\mathcal{P}oles\left(\hat{\mathcal{E}}_3^1(s_{134})\right) &= -\hat{\mathcal{D}}_2^1(s_{134})\left(4\mathbf{I}^{(1)}_{qg,F}(\epsilon,s_{134})+\mathcal{E}_3^0(s_{134})\right)+\\
&\quad+\frac{2b_{0,F}}{\epsilon}(s_{134})^{-\epsilon}\left[2\,\mathbf{I}^{(1)}_{qg,F}(\epsilon,s_{134})\right]+2\left[2\,\mathbf{I}^{(1)}_{qg,F}(\epsilon,s_{134})\right]^2-\\
&\quad-2e^{-\epsilon\gamma}\frac{\Gamma(1-2\epsilon)}{\Gamma(1-\epsilon)}\left(\frac{b_{0,F}}{\epsilon}+k_{0,F}\right)\left[2\,\mathbf{I}^{(1)}_{qg,F}(2\epsilon,s_{134})\right]-\\
&\quad-2\,\mathbf{H}^{(2)}_{qg,N_F^2}(\epsilon,s_{134})\,, \qquad (6.41)\\
\mathcal{F}inite\left(\hat{\mathcal{E}}_3^1(s_{134})\right) &= \frac{91}{81}+\frac{\pi^2}{72}\,. \qquad (6.42)
\end{aligned}
$$

The last contribution corresponds to the quark loop correction to the quark-quark-antiquark antenna, and enters into physical cross sections multiplied with a factor N_F^2. In the case of quark-gluon antenna functions, there is no contribution with this factor coming from four-parton tree-level antennae. Therefore, $\mathcal{P}oles(\hat{\mathcal{E}}_3^1)$ contains the full infrared singularity structure of the two-loop two-parton quark-gluon antenna at N_F^2. Note that the full hard radiation factor $\mathbf{H}^{(2)}_{qg,N_F^2}$ (and not only the virtual hard radiation) is present here.

6.3 Four-parton tree-level antenna functions

The tree-level four-parton quark-gluon antenna contains two final states: quark-gluon-gluon-gluon, D_4^0 and quark-quark-antiquark-gluon at leading and subleading colour, E_4^0 and $\tilde{E}_4^0$. The antenna for the $qggg$ final state is:

$$D_4^0(1_q,3_g,4_g,5_g) = d_4^0(1,3,4,5) + d_4^0(1,5,4,3)\,, \tag{6.43}$$

with

$$\begin{aligned}
d_4^0(1,3,4,5) = \frac{1}{s_{1345}}\Bigg\{ & \frac{s_{14}}{2s_{13}s_{15}s_{34}s_{45}}\left[3s_{14}s_{35}^2+3s_{14}^2s_{35}+2s_{14}^3+s_{35}^3\right]+\\
&+\frac{s_{14}}{s_{13}s_{15}s_{34}}\left[6s_{14}s_{35}+3s_{14}s_{45}+4s_{14}^2+3s_{35}s_{45}+3s_{35}^2+s_{45}^2\right]+\\
&+\frac{s_{14}}{s_{13}s_{15}}\left[3s_{14}+3s_{35}+3s_{45}\right]+\frac{s_{14}}{s_{13}s_{34}s_{135}s_{345}}\times\\
&\times\left[3s_{14}s_{45}^2+3s_{14}^2s_{45}+2s_{14}^3+s_{45}^3\right]+\\
&+\frac{s_{14}}{s_{13}s_{135}s_{345}}\left[3s_{14}s_{45}+3s_{14}^2-2s_{35}s_{45}-s_{35}^2+s_{45}^2\right]+\\
&+\frac{s_{14}^3}{s_{13}s_{34}s_{135}}+\frac{s_{35}^3s_{45}}{2s_{13}s_{15}s_{134}s_{145}}-\frac{s_{35}^3}{2s_{13}s_{15}s_{134}}+\\
&+\frac{s_{15}}{s_{13}s_{45}s_{134}s_{145}}\left[3s_{15}s_{35}^2+3s_{15}^2s_{35}+s_{15}^3+s_{35}^3\right]+\\
&+\frac{1}{s_{13}s_{34}s_{45}}\Big[9s_{14}s_{15}s_{35}+4s_{14}s_{15}^2+6s_{14}s_{35}^2+6s_{14}^2s_{15}+\\
&\qquad+9s_{14}^2s_{35}+4s_{14}^3+3s_{15}s_{35}^2+4s_{15}^2s_{35}+2s_{15}^3+s_{35}^3\Big]+\\
&+\frac{1}{s_{13}s_{34}s_{345}}\Big[s_{14}s_{15}s_{45}+4s_{14}s_{15}^2+s_{14}s_{45}^2+6s_{14}^2s_{15}+\\
&\qquad+3s_{14}^2s_{45}+4s_{14}^3+s_{15}s_{45}^2-2s_{15}^2s_{45}+2s_{15}^3\Big]+\\
&+\frac{1}{s_{13}s_{34}}\Big[17s_{14}s_{15}+16s_{14}s_{35}+11s_{14}s_{45}+15s_{14}^2+12s_{15}s_{35}+\\
&\qquad+5s_{15}s_{45}+10s_{15}^2+5s_{35}s_{45}+5s_{35}^2+2s_{45}^2\Big]+\\
&+\frac{s_{34}}{s_{13}s_{134}^2}\left[2s_{15}s_{35}+2s_{15}s_{45}+s_{15}^2+2s_{35}s_{45}+s_{35}^2+s_{45}^2\right]+\\
&+\frac{s_{35}}{s_{13}s_{45}s_{145}s_{135}}\left[3s_{34}s_{35}^2+3s_{34}^2s_{35}+s_{34}^3+s_{35}^3\right]+\\
&+\frac{s_{35}}{s_{13}s_{145}s_{135}}\left[-6s_{34}s_{35}+3s_{34}s_{45}-3s_{34}^2+3s_{35}s_{45}-3s_{35}^2-s_{45}^2\right]+
\end{aligned}$$

$$
\begin{aligned}
&+\frac{s_{35}}{s_{13}s_{135}^2}\left[2s_{14}s_{34}+2s_{14}s_{45}+s_{14}^2+2s_{34}s_{45}+s_{34}^2+s_{45}^2\right]+\\
&+\frac{1}{s_{13}s_{45}s_{134}s_{345}}\left[5s_{15}s_{35}^3+9s_{15}^2s_{35}^2+7s_{15}^3s_{35}+2s_{15}^4+s_{35}^4\right]+\\
&+\frac{1}{s_{13}s_{45}s_{134}}\Big[2s_{15}s_{34}s_{35}-4s_{15}s_{35}^2+s_{15}^2s_{34}-5s_{15}^2s_{35}-2s_{15}^3+\\
&\qquad\qquad+s_{34}s_{35}^2-s_{35}^3\Big]+\frac{1}{s_{13}s_{45}s_{145}}\times\\
&\times\Big[3s_{15}s_{34}s_{35}+2s_{15}s_{34}^2+2s_{15}s_{35}^2-s_{15}^2s_{34}+s_{15}^2s_{35}+s_{15}^3-\\
&\quad-3s_{34}s_{35}^2-3s_{34}^2s_{35}-s_{34}^3-s_{35}^3\Big]+\\
&+\frac{1}{s_{13}s_{45}s_{135}s_{345}}\left[-5s_{14}s_{35}^3+9s_{14}^2s_{35}^2-7s_{14}^3s_{35}+2s_{14}^4+s_{35}^4\right]+\\
&+\frac{1}{s_{13}s_{45}s_{135}}\Big[4s_{14}s_{34}^2+6s_{14}s_{35}^2+7s_{14}^2s_{34}-7s_{14}^2s_{35}+\\
&\qquad\qquad+6s_{14}^3+4s_{34}s_{35}^2+3s_{34}^2s_{35}+s_{34}^3\Big]+\frac{1}{s_{13}s_{45}s_{345}}\times\\
&\times\Big[10s_{14}s_{15}^2+6s_{14}s_{35}^2+10s_{14}^2s_{15}-7s_{14}^2s_{35}+6s_{14}^3+6s_{15}s_{35}^2+\\
&\quad+7s_{15}^2s_{35}+6s_{15}^3\Big]+\frac{1}{s_{13}s_{45}}\times\\
&\times\Big[17s_{14}s_{15}+8s_{14}s_{34}+6s_{14}s_{35}+18s_{14}^2+5s_{15}s_{34}+\\
&\quad+4s_{15}s_{35}+5s_{15}^2-s_{34}s_{35}-s_{34}^2+2s_{35}^2\Big]+\frac{1}{s_{13}s_{134}s_{145}}\times\\
&\times\Big[3s_{15}s_{35}s_{45}+6s_{15}s_{35}^2+6s_{15}^2s_{35}+s_{15}^2s_{45}+2s_{15}^3+3s_{35}^2s_{45}+\frac{3}{2}s_{35}^3\Big]+\\
&+\frac{1}{s_{13}s_{134}s_{345}}\Big[6s_{15}s_{35}s_{45}+9s_{15}s_{35}^2+s_{15}s_{45}^2+9s_{15}^2s_{35}+3s_{15}^2s_{45}+\\
&\qquad\qquad+3s_{15}^3+s_{35}s_{45}^2+3s_{35}^2s_{45}+3s_{35}^3\Big]+\frac{1}{s_{13}s_{134}}\times\\
&\times\Big[4s_{15}s_{34}-13s_{15}s_{35}-6s_{15}s_{45}-7s_{15}^2+4s_{34}s_{35}+3s_{34}s_{45}-\\
&\quad-5s_{35}s_{45}-7s_{35}^2-2s_{45}^2\Big]+\frac{1}{s_{13}s_{145}}\times\\
&\times\Big[-2s_{15}s_{34}-s_{15}s_{35}+s_{15}^2+6s_{34}s_{35}-s_{34}s_{45}+2s_{34}^2-\\
&\quad-3s_{35}s_{45}+4s_{35}^2\Big]+\frac{1}{s_{13}s_{135}}\times
\end{aligned}
$$

$$
\begin{aligned}
&\times\left[2s_{14}s_{34}-s_{14}s_{35}+6s_{14}^2-s_{34}s_{35}-2s_{34}s_{45}+3s_{35}s_{45}-s_{35}^2-s_{45}^2\right]+\\
&+\frac{1}{s_{13}s_{345}}\Big[2s_{14}s_{15}+2s_{14}s_{35}+2s_{14}s_{45}+s_{14}^2+4s_{15}s_{35}+\\
&\qquad\qquad+2s_{15}s_{45}+s_{15}^2+s_{35}s_{45}+2s_{35}^2\Big]+\frac{1}{s_{13}}\times\\
&\times\left[14s_{14}+2s_{15}+2s_{34}+3s_{35}-2s_{45}\right]-\\
&-\frac{4s_{13}s_{15}^2}{s_{45}s_{145}s_{345}}+\frac{s_{14}s_{15}}{s_{34}s_{134}^2}\left[-4s_{35}-4s_{45}\right]-\frac{4s_{14}s_{15}^2s_{45}}{s_{34}^2s_{134}s_{345}}+\frac{s_{14}}{s_{34}^2s_{134}}\times\\
&\times\left[2s_{14}s_{15}+2s_{14}s_{35}+2s_{14}s_{45}+4s_{15}s_{35}-4s_{15}s_{45}-2s_{35}s_{45}-2s_{45}^2\right]+\\
&+\frac{s_{14}^2}{s_{34}^2s_{134}^2}\left[2s_{15}s_{35}+2s_{15}s_{45}+2s_{15}^2+2s_{35}s_{45}+s_{35}^2+s_{45}^2\right]+\\
&+\frac{s_{15}}{2s_{34}s_{45}s_{134}s_{145}}\left[3s_{15}s_{35}^2+3s_{15}^2s_{35}+2s_{15}^3+s_{35}^3\right]+\\
&+\frac{s_{15}}{s_{34}s_{45}s_{145}}\left[2s_{13}s_{15}+2s_{15}s_{35}+\frac{3}{2}s_{35}^2\right]+\\
&+\frac{s_{15}}{s_{34}s_{134}s_{345}}\left[-4s_{14}s_{15}-2s_{14}s_{45}-4s_{14}^2-8s_{15}^2-2s_{45}^2\right]+\\
&+\frac{s_{15}s_{35}}{s_{45}^2s_{345}}\left[-4s_{14}-4s_{15}+4s_{35}\right]+\frac{s_{15}s_{35}}{s_{45}s_{135}s_{345}}\left[2s_{14}+s_{15}+\frac{1}{2}s_{35}\right]+\\
&+\frac{s_{15}s_{35}^2}{s_{45}^2s_{345}^2}\left[4s_{14}+2s_{15}\right]+\frac{s_{15}}{s_{45}^2s_{145}}\times\\
&\times\left[2s_{13}s_{15}+2s_{15}s_{34}+2s_{15}s_{35}-2s_{34}s_{35}-2s_{35}^2\right]+\\
&+\frac{s_{15}}{s_{45}^2}\left[2s_{15}+2s_{34}-6s_{35}\right]+\frac{s_{15}}{s_{45}s_{134}s_{345}}\times\\
&\times\left[-6s_{14}s_{15}-2s_{14}s_{35}-2s_{14}^2-6s_{15}s_{35}-4s_{15}^2-8s_{35}^2\right]+\\
&+\frac{s_{15}}{s_{45}s_{134}}\left[-s_{14}+\frac{5}{2}s_{15}+\frac{1}{2}s_{34}+\frac{15}{2}s_{35}\right]+\frac{s_{15}}{s_{45}s_{145}^2}\times\\
&\times\left[4s_{34}s_{35}+2s_{34}^2+2s_{35}^2\right]+\frac{s_{15}}{s_{45}s_{145}s_{135}}\times\\
&\times\left[\frac{3}{2}s_{15}s_{34}-\frac{1}{2}s_{15}s_{35}-s_{15}^2-\frac{3}{2}s_{34}s_{35}-\frac{3}{2}s_{34}^2-s_{35}^2\right]+\\
&+\frac{s_{15}}{s_{45}s_{145}}\left[-2s_{15}+\frac{11}{2}s_{34}+4s_{35}\right]+\frac{s_{15}}{s_{45}s_{135}}\times\\
&\times\left[-2s_{14}-2s_{34}\right]+\frac{s_{15}}{s_{45}s_{345}}\times\\
&\times\left[-6s_{14}-6s_{15}-6s_{35}\right]+\frac{15s_{15}}{2s_{45}}+\frac{s_{15}^2}{s_{45}^2s_{145}^2}\times\\
&\times\left[2s_{13}s_{34}+2s_{13}s_{35}+2s_{34}s_{35}+s_{34}^2+s_{35}^2\right]+\frac{s_{45}}{s_{34}^2s_{345}}\times
\end{aligned}
$$

$$
\begin{aligned}
&\times\left[-8s_{14}s_{15}+4s_{14}s_{45}-4s_{14}^2+4s_{15}s_{45}\right]+\frac{s_{45}^2}{s_{34}^2s_{345}^2}\times\\
&\times\left[4s_{13}s_{15}+4s_{14}s_{15}+2s_{14}^2+2s_{15}^2\right]+\frac{1}{s_{34}^2}\times\\
&\times\Bigg[-2s_{13}s_{15}+2s_{14}s_{15}+2s_{14}s_{35}-6s_{14}s_{45}+2s_{14}^2-\\
&\quad-2s_{15}s_{35}-2s_{15}s_{45}+s_{35}^2+s_{45}^2\Bigg]+\frac{1}{s_{34}s_{45}s_{134}}\times\\
&\times\left[\frac{1}{2}s_{14}s_{15}s_{35}+3s_{14}s_{15}^2+s_{14}^2s_{15}+\frac{1}{2}s_{14}^2s_{35}+s_{14}^3+\frac{3}{2}s_{15}s_{35}^2+\right.\\
&\quad\left.+\frac{5}{2}s_{15}^2s_{35}+s_{15}^3+\frac{1}{2}s_{35}^3\right]+\frac{1}{s_{34}s_{45}}\times\\
&\times\left[4s_{13}s_{15}+16s_{14}s_{15}+11s_{14}s_{35}+7s_{14}^2+16s_{15}s_{35}+8s_{15}^2+\frac{9}{2}s_{35}^2\right]+\\
&+\frac{s_{45}}{s_{34}s_{135}s_{345}}\left[2s_{14}s_{15}-6s_{14}s_{45}-6s_{14}^2++\frac{3}{2}s_{15}s_{45}-s_{15}^2-\frac{5}{2}s_{45}^2\right]+\\
&+\frac{s_{45}}{s_{34}s_{345}^2}\left[8s_{13}s_{15}+8s_{14}s_{15}+4s_{14}^2+4s_{15}^2\right]+\\
&+\frac{1}{s_{34}s_{134}s_{145}}\left[9s_{15}s_{35}s_{45}+\frac{9}{2}s_{15}s_{35}^2+5s_{15}s_{45}^2+6s_{15}^2s_{35}+\frac{11}{2}s_{15}^2s_{45}+\right.\\
&\qquad\left.+\frac{7}{2}s_{15}^3+6s_{35}s_{45}^2+\frac{9}{2}s_{35}^2s_{45}+s_{35}^3+\frac{5}{2}s_{45}^3\right]+\\
&+\frac{1}{s_{34}s_{134}s_{135}}\left[\frac{9}{2}s_{15}s_{35}s_{45}+3s_{15}s_{35}^2+\frac{3}{2}s_{15}s_{45}^2+\frac{5}{2}s_{15}^2s_{35}+\frac{3}{2}s_{15}^2s_{45}+\right.\\
&\qquad\left.+s_{15}^3+\frac{9}{2}s_{35}s_{45}^2+6s_{35}^2s_{45}+\frac{5}{2}s_{35}^3+s_{45}^3\right]+\\
&+\frac{1}{2s_{34}s_{134}}\Big[-5s_{14}s_{15}+5s_{14}s_{35}-3s_{14}s_{45}-7s_{14}^2-22s_{15}s_{35}-19s_{15}s_{45}-\\
&\qquad-35s_{15}^2-27s_{35}s_{45}-17s_{35}^2-13s_{45}^2\Big]+\\
&+\frac{1}{s_{34}s_{145}s_{345}}\Big[-6s_{13}s_{15}s_{45}-2s_{13}s_{15}^2+6s_{15}s_{45}^2\\
&\qquad+5s_{15}^2s_{45}+2s_{15}^3+4s_{45}^3\Big]+\frac{1}{s_{34}s_{145}}\times\\
&\times\left[\frac{13}{2}s_{13}s_{15}+\frac{13}{2}s_{15}s_{35}+\frac{1}{2}s_{15}^2+7s_{35}s_{45}+3s_{35}^2-s_{45}^2\right]+\\
&+\frac{1}{s_{34}s_{135}}\left[+s_{14}s_{35}+7s_{14}s_{45}+4s_{14}^2+\frac{3}{2}s_{15}s_{35}+\right.\\
&\qquad\left.+\frac{1}{2}s_{15}s_{45}+s_{15}^2+\frac{7}{2}s_{35}s_{45}+\frac{5}{2}s_{35}^2+\frac{11}{2}s_{45}^2\right]+
\end{aligned}
$$

$$
\begin{aligned}
&+\frac{1}{s_{34}s_{345}}\bigg[-8s_{13}s_{15}-14s_{14}s_{15}+7s_{14}s_{45}-8s_{14}^2+\\
&\qquad\qquad+7s_{15}s_{45}-16s_{15}^2-\frac{9}{2}s_{45}^2\bigg]+\frac{1}{2s_{34}}\times\\
&\times\left[23s_{14}-13s_{15}+5s_{35}+4s_{45}\right]+\frac{1}{2s_{45}s_{134}s_{145}}\times\\
&\times\bigg[-3s_{15}s_{34}s_{35}-s_{15}s_{34}^2-3s_{15}s_{35}^2-3s_{15}^2s_{35}-3s_{15}^3-\\
&\quad-3s_{34}s_{35}^2-3s_{34}^2s_{35}-s_{34}^3-s_{35}^3\bigg]+\frac{1}{s_{134}^2}\times\\
&\times\left[s_{15}^2+4s_{35}s_{45}+2s_{35}^2+2s_{45}^2\right]+\frac{1}{s_{134}s_{145}}\times\\
&\times\bigg[\frac{3}{2}s_{15}s_{34}-3s_{15}s_{35}-6s_{15}s_{45}-\frac{9}{2}s_{15}^2+\frac{3}{2}s_{34}s_{45}+\\
&\quad+\frac{1}{2}s_{34}^2-3s_{35}s_{45}-\frac{3}{2}s_{35}^2-4s_{45}^2\bigg]+\frac{1}{s_{134}s_{135}}\times\\
&\times\left[+\frac{3}{2}s_{15}s_{34}-\frac{9}{2}s_{15}s_{35}-\frac{3}{2}s_{15}^2-9s_{35}s_{45}-6s_{35}^2\right]+\frac{1}{2s_{134}s_{345}}\times\\
&\times\bigg[-5s_{14}s_{35}-3s_{14}s_{45}+3s_{14}^2-22s_{15}s_{35}-12s_{15}s_{45}+12s_{15}^2+\\
&\quad+s_{35}s_{45}-s_{35}^2+s_{45}^2\bigg]+\frac{1}{2s_{134}}\times\\
&\times\left[-3s_{14}+29s_{15}+18s_{35}+23s_{45}\right]+\frac{1}{2s_{145}s_{135}}\times\\
&\times\left[3s_{15}s_{35}-3s_{15}s_{45}-3s_{15}^2+9s_{35}s_{45}-2s_{45}^2\right]+\\
&+\frac{1}{2s_{145}s_{345}}\left[-2s_{15}s_{35}+3s_{15}s_{45}+s_{15}^2-3s_{35}s_{45}+s_{35}^2+5s_{45}^2\right]+\\
&+\frac{1}{s_{145}}\left[-4s_{15}-4s_{45}\right]+\frac{1}{s_{135}^2}\left[4s_{14}s_{45}+s_{14}^2+2s_{34}s_{45}+2s_{45}^2\right]+\\
&+\frac{1}{s_{135}s_{345}}\bigg[2s_{14}s_{15}+7s_{14}s_{35}-6s_{14}s_{45}-4s_{14}^2-\frac{3}{2}s_{15}s_{35}+\\
&\qquad\qquad+\frac{3}{2}s_{15}s_{45}-s_{15}^2+\frac{5}{2}s_{35}s_{45}-\frac{5}{2}s_{35}^2-\frac{5}{2}s_{45}^2\bigg]+\\
&+\frac{1}{s_{135}}\left[2s_{14}-2s_{35}+7s_{45}\right]+\\
&+\frac{1}{s_{345}^2}\left[6s_{13}s_{15}+8s_{14}s_{15}+3s_{14}^2+4s_{15}^2\right]+\\
&+\frac{1}{s_{345}}\left[\frac{7}{2}s_{14}+\frac{15}{2}s_{15}+3s_{35}-\frac{5}{2}s_{45}\right]+8+\mathcal{O}(\epsilon)\bigg\}\,.
\end{aligned}
\tag{6.44}
$$

In $D_4^0(1,3,4,5)$, the gluonic emissions are colour-ordered. However, as explained in [46], both possible colour-orderings (normal and reverse) are contained in the same colour-ordered squared matrix element. Moreover, since this squared matrix element originates from an amplitude which is cyclic in the partonic colour indices, it also contains singular limits in the momentum configuration $(5_g, 1_q, 3_g)$, as outlined in detail in section 8.3.2 below. Using this antenna function as NNLO subtraction term, this limit has to be accounted for properly.

For the above reasons, it is not possible to use a single ordered phase space parametrisation in the numerical implementation of $D_4^0(1,3,4,5)$. Instead, $D_4^0(1,3,4,5)$ has to be split into different ordered pieces by repeated partial fractioning on pairs of invariants. Since this decomposition is not symmetric, the individual pieces can no longer be integrated analytically. Therefore the full $D_4^0(1,3,4,5)$ and not the sub-antennae must be used as a subtraction term.

The integral of this antenna function is

$$\begin{aligned}\mathcal{D}_4^0(s_{1345}) = (s_{1345})^{-2\epsilon}\Bigg[&\frac{5}{2\epsilon^4}+\frac{37}{4\epsilon^3}+\frac{1}{\epsilon^2}\left(\frac{398}{9}-\frac{11\pi^2}{3}\right)+\\ &+\frac{1}{\epsilon}\left(\frac{28319}{144}-\frac{55\pi^2}{4}-\frac{188}{3}\zeta_3\right)+\\ &+\left(\frac{2201527}{2592}-\frac{529\pi^2}{8}+\frac{511\pi^4}{720}-\frac{722}{3}\zeta_3\right)+\mathcal{O}(\epsilon)\Bigg], \qquad (6.45)\end{aligned}$$

with

$$\begin{aligned}\mathcal{P}oles\left(\mathcal{D}_4^0(s_{1345})\right) =\; & 2\left[2\mathbf{I}_{qg}^{(1)}(\epsilon,s_{1345})\right]^2 - 2e^{-\epsilon\gamma}\frac{\Gamma(1-2\epsilon)}{\Gamma(1-\epsilon)}\left(\frac{b_0}{\epsilon}+k_0\right)\left[2\mathbf{I}_{qg}^{(1)}(2\epsilon,s_{1345})\right]-\\ &-\mathbf{H}_{R,D}^{(2)}(\epsilon,s_{1345})-2\,\mathbf{S}_V^{(2)}(\epsilon,s_{1345}), \qquad (6.46)\\ \mathcal{F}inite\left(\mathcal{D}_4^0(s_{1345})\right) =\; & \frac{1935847}{2592}-\frac{4271\pi^2}{108}-\frac{73\pi^4}{144}-\frac{7483}{36}\zeta_3\,. \qquad (6.47)\end{aligned}$$

The leading colour and subleading colour quark-quark-antiquark-gluon antennae are:

$$\begin{aligned}E_4^0(1_q,3_{q'},4_{\bar{q}'},5_g) = \frac{1}{s_{1345}^2}\Bigg\{&-\frac{s_{13}s_{14}}{s_{15}s_{345}}+\frac{s_{14}}{s_{15}s_{34}s_{45}}\left[s_{13}s_{35}+s_{13}^2+s_{14}^2\right]+\\ &+\frac{s_{14}}{s_{15}s_{34}s_{134}}\left[2s_{14}s_{35}+2s_{14}s_{45}-s_{35}^2+s_{45}^2\right]+\\ &+\frac{s_{14}}{s_{15}s_{45}s_{345}}\left[s_{13}s_{35}+s_{13}^2+s_{14}^2\right]+\\ &+\frac{s_{14}}{s_{15}s_{45}}\left[2s_{13}+2s_{14}+s_{35}\right]-\frac{4s_{14}s_{15}^2s_{35}}{s_{34}^2s_{134}s_{345}}+\frac{s_{14}}{s_{34}^2s_{134}}\times\\ &\times\Big[-4s_{14}s_{15}-4s_{14}s_{35}-4s_{14}s_{45}+8s_{15}s_{45}+4s_{15}^2+\\ &\quad+4s_{35}s_{45}+4s_{45}^2\Big]+\frac{s_{14}}{s_{34}s_{45}s_{134}}\times\\ &\times\left[-2s_{14}s_{15}-s_{14}s_{35}-2s_{14}^2-s_{15}s_{35}-s_{15}^2\right]+\frac{s_{14}}{s_{34}s_{134}^2}\times\end{aligned}$$

$$
\begin{aligned}
&\times\left[-4s_{15}s_{35}-4s_{15}s_{45}-2s_{15}^2-4s_{35}s_{45}-2s_{35}^2-2s_{45}^2\right]-\\
&-\frac{s_{14}}{s_{345}}+\frac{s_{14}^2}{s_{34}^2s_{134}^2}\times\\
&\times\left[-4s_{15}s_{35}-4s_{15}s_{45}-2s_{15}^2-4s_{35}s_{45}-2s_{35}^2-2s_{45}^2\right]+\\
&+\frac{1}{s_{15}s_{34}s_{345}}\left[s_{13}s_{14}^2+s_{13}^2s_{14}+s_{13}^2s_{35}+s_{13}^3-s_{14}^2s_{35}+s_{14}^3\right]+\\
&+\frac{1}{s_{15}s_{34}}\Big[s_{13}s_{14}+3s_{13}s_{35}+s_{13}s_{45}+2s_{13}^2-s_{14}s_{35}+s_{14}s_{45}+\\
&\qquad\qquad+4s_{14}^2+s_{35}s_{45}+s_{35}^2\Big]+\frac{1}{s_{15}s_{134}}\times\\
&\times\left[-s_{13}s_{45}+s_{14}s_{35}+2s_{14}s_{45}-s_{35}s_{45}+s_{45}^2\right]+\\
&+\frac{1}{s_{15}}\left[s_{13}+2s_{14}+s_{35}+s_{45}\right]+\frac{1}{s_{15}}s_{34}s_{134}s_{345}\times\\
&\times\left[-2s_{14}s_{35}+8s_{14}^2-2s_{15}s_{35}+2s_{15}^2+2s_{35}^2\right]+\\
&+\frac{s_{35}}{s_{34}^2s_{345}}\Big[4s_{13}s_{14}+8s_{13}s_{15}-4s_{13}s_{35}+4s_{13}^2-\\
&\qquad\qquad-4s_{14}s_{35}-4s_{15}s_{35}+4s_{15}^2\Big]+\frac{s_{35}^2}{s_{34}^2s_{345}^2}\times\\
&\times\left[-4s_{13}s_{14}-4s_{13}s_{15}-2s_{13}^2-4s_{14}s_{15}-2s_{14}^2-2s_{15}^2\right]+\\
&+\frac{1}{s_{34}^2}\Big[-4s_{13}s_{15}+4s_{13}s_{35}-4s_{13}s_{45}-2s_{13}^2+4s_{14}s_{15}+\\
&\qquad+4s_{14}s_{35}+4s_{14}s_{45}+4s_{15}s_{35}-4s_{15}s_{45}-2s_{15}^2-2s_{45}^2\Big]+\\
&+\frac{1}{s_{34}s_{134}}\Big[-s_{14}s_{15}-7s_{14}s_{35}+s_{14}s_{45}+7s_{14}^2+\\
&\qquad\qquad+s_{15}s_{35}+7s_{15}s_{45}+6s_{15}^2+2s_{35}s_{45}+s_{35}^2+3s_{45}^2\Big]+\\
&+\frac{1}{s_{34}s_{345}}\left[6s_{13}s_{15}+2s_{13}s_{35}+4s_{13}^2-4s_{14}s_{35}+6s_{14}^2+5s_{15}^2\right]+\\
&+\frac{1}{s_{34}}\left[3s_{13}+2s_{14}+6s_{15}+6s_{35}+s_{45}\right]+\\
&+\frac{s_{35}}{s_{45}s_{345}^2}\left[2s_{13}s_{14}+2s_{13}s_{15}+s_{13}^2+2s_{14}s_{15}+s_{14}^2+s_{15}^2\right]+\\
&+\frac{1}{s_{45}s_{134}s_{345}}\Big[-s_{13}s_{14}s_{15}+s_{13}s_{14}s_{35}-s_{13}s_{14}^2+s_{13}s_{15}s_{35}+\\
&\qquad\qquad\quad+3s_{14}s_{15}^2+3s_{14}^2s_{15}+s_{14}^3+s_{15}^3\Big]+\frac{1}{s_{45}s_{134}}\times\\
&\times\left[-s_{13}s_{15}+s_{14}s_{15}-s_{14}^2+s_{15}^2\right]+\frac{1}{s_{45}s_{345}}\times
\end{aligned}
$$

$$
\begin{aligned}
&\times\left[-2s_{13}s_{15}+2s_{13}s_{35}-s_{13}^2+3s_{14}s_{15}+s_{14}s_{35}+4s_{14}^2+s_{15}s_{35}\right]+\\
&+\frac{1}{s_{45}}\left[-2s_{13}+2s_{14}-s_{34}\right]+\\
&+\frac{1}{s_{134}^2}\left[-2s_{15}s_{35}-2s_{15}s_{45}-s_{15}^2-2s_{35}s_{45}-s_{35}^2-s_{45}^2\right]+\\
&+\frac{1}{s_{134}s_{345}}\left[s_{13}s_{14}-3s_{13}s_{15}-s_{13}^2+4s_{14}s_{15}-s_{14}^2-3s_{15}^2\right]+\\
&+\frac{1}{s_{134}}\left[-3s_{13}+6s_{14}-3s_{35}+2s_{45}\right]+2+\mathcal{O}(\epsilon)\Bigg\},
\end{aligned}
\tag{6.48}
$$

$$
\tilde{E}_4^0(1_q,3_{q'},4_{\bar{q}'},5_g) = \tilde{e}_4^0(1,3,4,5)+\tilde{e}_4^0(1,4,3,5)\,,
\tag{6.49}
$$

with

$$
\begin{aligned}
\tilde{e}_4^0(1,3,4,5) = \frac{1}{s_{1345}^2}\Bigg\{&\frac{1}{s_{35}s_{45}}\left[2s_{13}s_{34}+2s_{13}s_{15}+2s_{13}^2+s_{34}s_{15}+s_{15}^2\right]+\\
&+\frac{s_{35}}{s_{45}s_{345}^2}\left[2s_{13}s_{14}+2s_{13}s_{15}+s_{13}^2+2s_{14}s_{15}+s_{14}^2+s_{15}^2\right]+\\
&+\frac{1}{s_{45}s_{345}}\Big[-2s_{13}s_{14}-4s_{13}s_{15}+s_{13}s_{35}-2s_{13}^2-2s_{14}s_{15}+\\
&\qquad+s_{14}s_{35}+s_{15}s_{35}-2s_{15}^2\Big]+\mathcal{O}(\epsilon)\Bigg\}.
\end{aligned}
\tag{6.50}
$$

Concerning the phase space mapping, E_4^0 can be decomposed into ordered contributions, which can use an ordered parametrisation of the phase space, by repeated partial fractioning of the invariants (like in $\tilde{A}_4^0$). Due to the lack of symmetry, the result is considerably larger than the above expression and not very instructive. It is therefore not quoted here. $\tilde{E}_4^0$ is already ordered (since quark (1) decouples from all singular limits).

In the leading colour term, the gluonic emission is colour-ordered (either in the $q,\bar{q}'$-antenna denoted here, or in the q,q'-antenna). The second colour-ordering is obtained by interchanging $q' \leftrightarrow \bar{q}'$. Note, in particular, that gluon emission inside the $q',\bar{q}'$-antenna is only possible at subleading colour (and constitutes in fact the full subleading colour contribution).

Integration yields

$$
\begin{aligned}
\mathcal{E}_4^0(s_{1345}) = \frac{1}{2}\left(s_{1345}\right)^{-2\epsilon}\Bigg[&-\frac{5}{6\epsilon^3}-\frac{17}{4\epsilon^2}+\frac{1}{\epsilon}\left(-\frac{2239}{108}+\frac{5\pi^2}{4}\right)\\
&+\left(-\frac{20521}{216}+\frac{51\pi^2}{8}+\frac{200}{9}\zeta_3\right)+\mathcal{O}(\epsilon)\Bigg],
\end{aligned}
\tag{6.51}
$$

$$
\begin{aligned}
\tilde{\mathcal{E}}_4^0(s_{1345}) = \left(s_{1345}\right)^{-2\epsilon}\Bigg[&-\frac{1}{6\epsilon^3}-\frac{35}{36\epsilon^2}+\frac{1}{\epsilon}\left(-\frac{1045}{216}+\frac{\pi^2}{4}\right)+\\
&+\left(-\frac{28637}{1296}+\frac{35\pi^2}{24}+\frac{40}{9}\zeta_3\right)+\mathcal{O}(\epsilon)\Bigg],
\end{aligned}
\tag{6.52}
$$

with

$$
\mathcal{P}oles\left(\mathcal{E}_4^0(s_{1345})\right) = 2\left[2\mathbf{I}_{qg}^{(1)}(\epsilon,s_{1345})\right]\left[2\mathbf{I}_{qg,F}^{(1)}(\epsilon,s_{1345})\right]-e^{-\epsilon\gamma}\frac{\Gamma(1-2\epsilon)}{\Gamma(1-\epsilon)}\times
$$

$$\times\left[\left(\frac{b_{0,F}}{\epsilon}+k_{0,F}\right)\left[2\mathbf{I}^{(1)}_{qg}(2\epsilon,s_{1345})\right]+\left(\frac{b_0}{\epsilon}+k_0\right)\left[2\mathbf{I}^{(1)}_{qg,F}(2\epsilon,s_{1345})\right]\right]-$$
$$-\frac{1}{2}\mathbf{H}^{(2)}_{R,E}(\epsilon,s_{1345})\,, \tag{6.53}$$
$$\mathcal{F}inite\left(\mathcal{E}_4^0(s_{1345})\right) = -\frac{20521}{432}+\frac{1097\pi^2}{864}+\frac{391}{36}\zeta_3\,, \tag{6.54}$$
$$\mathcal{P}oles\left(\tilde{\mathcal{E}}_4^0(s_{1345})\right) = -\mathbf{H}^{(2)}_{R,\tilde{E}}(\epsilon,s_{1345})\,, \tag{6.55}$$
$$\mathcal{F}inite\left(\tilde{\mathcal{E}}_4^0(s_{1345})\right) = -\frac{28637}{1296}+\frac{595\pi^2}{432}+\frac{79}{18}\zeta_3\,. \tag{6.56}$$

7. Gluon-gluon antennae

The gluon-gluon antenna functions are obtained from the QCD real radiation corrections to the decay of a massive Higgs boson into two gluons, $H \to gg$, which is described in detail in [47].

The overall normalisation is given by defining the tree-level two-parton gluon-gluon antenna function

$$\mathcal{F}_2^0(s_{12}) \equiv 1\,. \tag{7.1}$$

The one-loop two-parton gluon-gluon antenna contains two contributions, corresponding to the different colour and flavour structures:

$$\mathcal{F}_2^1(s_{12}) = 2(s_{12})^{-\epsilon}\left[-\frac{1}{\epsilon^2}-\frac{11}{6\epsilon}+\frac{7\pi^2}{12}+\left(-1+\frac{7}{3}\zeta_3\right)\epsilon+\left(-3-\frac{73\pi^4}{1440}\right)\epsilon^2+\mathcal{O}(\epsilon^3)\right], \tag{7.2}$$
$$\hat{\mathcal{F}}_2^1(s_{12}) = 2\,(s_{12})^{-\epsilon}\frac{1}{3\epsilon}\,, \tag{7.3}$$

with

$$\mathcal{P}oles\left(\mathcal{F}_2^1(s_{12})\right) = 4\,\mathbf{I}^{(1)}_{gg}(\epsilon,s_{12})\,, \tag{7.4}$$
$$\mathcal{F}inite\left(\mathcal{F}_2^1(s_{12})\right) = 0\,, \tag{7.5}$$
$$\mathcal{P}oles\left(\hat{\mathcal{F}}_2^1(s_{12})\right) = 4\,\mathbf{I}^{(1)}_{gg,F}(\epsilon,s_{12})\,, \tag{7.6}$$
$$\mathcal{F}inite\left(\hat{\mathcal{F}}_2^1(s_{12})\right) = 0\,. \tag{7.7}$$

The pole terms in the above expression have to be compared to the pole terms of the one-loop correction to the quark-antiquark antenna function $\mathcal{A}_2^1$ in (5.3), and the quark-gluon antenna functions $\mathcal{D}_2^1$ in (6.4) and $\hat{\mathcal{D}}_2^1$ in (6.6). The factor 4 in (7.4), (7.6) appears since the tree-level gluon-gluon antenna function $\mathcal{F}_2^0$ contains two distinct gluon-gluon antennae. This situation is like for $\mathcal{D}_2^0$, which contains two quark-gluon antennae, but in contrast to the single quark-antiquark antenna contained in $\mathcal{A}_2^0$.

7.1 Three-parton tree-level antenna functions

The tree-level three-parton gluon-gluon antenna contains two final states: gluon-gluon-gluon and gluon-quark-antiquark. The antenna corresponding to the first final state is:

$$F_3^0(g_1,g_2,g_3)=\frac{2}{s_{123}^2}\left(\frac{s_{123}^2 s_{12}}{s_{13}s_{23}}+\frac{s_{123}^2 s_{13}}{s_{12}s_{23}}+\frac{s_{123}^2 s_{23}}{s_{12}s_{13}}+\frac{s_{12}s_{13}}{s_{23}}+\frac{s_{12}s_{23}}{s_{13}}+\frac{s_{13}s_{23}}{s_{12}}+4s_{123}+\mathcal{O}(\epsilon)\right). \tag{7.8}$$

It yields the integral:

$$\begin{aligned}\mathcal{F}_3^0(s_{123}) &= 3\,(s_{123})^{-\epsilon}\left[\frac{1}{\epsilon^2}+\frac{11}{6\epsilon}+\frac{73}{12}-\frac{7\pi^2}{12}+\left(\frac{451}{24}-\frac{77\pi^2}{72}-\frac{25}{3}\zeta_3\right)\epsilon+\right.\\ &\quad\left.+\left(\frac{2729}{48}-\frac{511\pi^2}{144}-\frac{275}{18}\zeta_3-\frac{71\pi^4}{1440}\right)\epsilon^2+\mathcal{O}(\epsilon^3)\right], \end{aligned}\tag{7.9}$$

with

$$\mathcal{P}oles\left(\mathcal{F}_3^0(s_{123})\right) = -6\mathbf{I}_{gg}^{(1)}(\epsilon,s_{123}), \tag{7.10}$$

$$\mathcal{F}inite\left(\mathcal{F}_3^0(s_{123})\right) = \frac{73}{4}. \tag{7.11}$$

As can be seen from the pole structure, this tree-level antenna function contains three antenna configurations, corresponding to the three possible configurations of emitting a gluon in between a gluon pair. The separation between these is not free from an ambiguity, but is in fact fixed by the decomposition used in the case of the quark-gluon-gluon antenna in (6.13) above. We decompose

$$F_3^0(1,2,3) = f_3^0(1,3,2)+f_3^0(3,2,1)+f_3^0(2,1,3), \tag{7.12}$$

where

$$f_3^0(1,3,2) = \frac{1}{s_{123}^2}\left(2\frac{s_{123}^2 s_{12}}{s_{13}s_{23}}+\frac{s_{12}s_{13}}{s_{23}}+\frac{s_{12}s_{23}}{s_{13}}+\frac{2}{3}s_{123}+\mathcal{O}(\epsilon)\right). \tag{7.13}$$

The tree-level three-parton gluon-gluon antenna corresponding to the gluon-quark-antiquark final state is:

$$G_3^0(1_g,3_q,4_{\bar q}) = \frac{1}{s_{134}^2}\left(\frac{s_{13}^2+s_{14}^2}{s_{34}}+\mathcal{O}(\epsilon)\right). \tag{7.14}$$

Its integrated form reads:

$$\begin{aligned}\mathcal{G}_3^0(s_{134}) &= (s_{134})^{-\epsilon}\left[-\frac{1}{3\epsilon}-\frac{7}{6}+\left(-\frac{15}{4}+\frac{7\pi^2}{36}\right)\epsilon+\right.\\ &\quad\left.+\left(-\frac{93}{8}+\frac{49\pi^2}{72}-\frac{25}{9}\zeta_3\right)\epsilon^2+\mathcal{O}(\epsilon^3)\right], \end{aligned}\tag{7.15}$$

with

$$\mathcal{P}oles\left(\mathcal{G}_3^0(s_{134})\right) = -2\mathbf{I}_{gg,F}^{(1)}(\epsilon,s_{134}), \tag{7.16}$$

$$\mathcal{F}inite\left(\mathcal{G}_3^0(s_{134})\right) = -\frac{7}{6}. \tag{7.17}$$

JHEP09(2005)056

7.2 Three-parton one-loop antenna functions

At one loop, the correction to the gluon-gluon-gluon antenna contains a leading colour term $F_3^1(g_1,g_2,g_3)$ and a quark loop term $\hat{F}_3^1(g_1,g_2,g_3)$. These read:

$$\begin{aligned}
\mathcal{P}oles\left(F_3^1(g_1,g_2,g_3)\right) &= 2\Big(\mathbf{I}^{(1)}_{gg}(\epsilon,s_{12})+\mathbf{I}^{(1)}_{gg}(\epsilon,s_{13})+\mathbf{I}^{(1)}_{gg}(\epsilon,s_{23})-2\,\mathbf{I}^{(1)}_{gg}(\epsilon,s_{123})\Big)\times \\
&\quad\times F_3^0(1,2,3)\,, \qquad (7.18)\\
\mathcal{F}inite\left(F_3^1(1,2,3)\right) &= -\Big(R(y_{12},y_{13})+R(y_{13},y_{23})+R(y_{12},y_{23})+\frac{11}{6}\log y_{12}+ \\
&\quad+\frac{11}{6}\log y_{13}+\frac{11}{6}\log y_{23}\Big)F_3^0(1,2,3)+ \\
&\quad+\frac{1}{3s_{12}}+\frac{1}{3s_{13}}+\frac{1}{3s_{23}}+\frac{1}{3s_{123}}\,, \qquad (7.19)\\
\mathcal{P}oles\left(\hat{F}_3^1(g_1,g_2,g_3)\right) &= 2\Big(\mathbf{I}^{(1)}_{gg,F}(\epsilon,s_{12})+\mathbf{I}^{(1)}_{gg,F}(\epsilon,s_{13})+\mathbf{I}^{(1)}_{gg,F}(\epsilon,s_{23})- \\
&\quad-2\,\mathbf{I}^{(1)}_{gg,F}(\epsilon,s_{123})\Big)F_3^0(1,2,3)\,, \qquad (7.20)\\
\mathcal{F}inite\left(\hat{F}_3^1(g_1,g_2,g_3)\right) &= \frac{1}{3}\Big[(\log y_{12}+\log y_{13}+\log y_{23})\,F_3^0(1,2,3)-\frac{1}{s_{12}}- \\
&\quad-\frac{1}{s_{13}}-\frac{1}{s_{23}}-\frac{1}{s_{123}}\Big]. \qquad (7.21)
\end{aligned}$$

Integration of these antenna functions yields

$$\begin{aligned}
\mathcal{F}_3^1(s_{123}) &= (s_{123})^{-2\epsilon}\Big[-\frac{3}{4\epsilon^4}-\frac{33}{4\epsilon^3}+\frac{1}{\epsilon^2}\left(-\frac{85}{3}+\frac{15\pi^2}{8}\right)+\frac{1}{\epsilon}\left(-\frac{9827}{72}+\frac{55\pi^2}{6}+44\,\zeta_3\right)+ \\
&\quad+\left(-\frac{90185}{144}+\frac{6005\pi^2}{144}+\frac{506}{3}\zeta_3-\frac{11\pi^4}{480}\right)+\mathcal{O}(\epsilon)\Big]\,, \qquad (7.22)\\
\hat{\mathcal{F}}_3^1(s_{123}) &= (s_{123})^{-2\epsilon}\left[\frac{1}{\epsilon^3}+\frac{11}{6\epsilon^2}+\frac{1}{\epsilon}\left(\frac{19}{3}-\frac{7\pi^2}{12}\right)+\left(\frac{499}{24}-\frac{77\pi^2}{72}-\frac{25}{3}\zeta_3\right)+\mathcal{O}(\epsilon)\right], \qquad (7.23)
\end{aligned}$$

with

$$\begin{aligned}
\mathcal{P}oles\left(\mathcal{F}_3^1(s_{123})\right) &= -\mathcal{F}_2^1(s_{123})\left(6\mathbf{I}^{(1)}_{gg}(\epsilon,s_{123})+\mathcal{F}_3^0(s_{123})\right)+\frac{2b_0}{\epsilon}\,(s_{123})^{-\epsilon}\left[3\,\mathbf{I}^{(1)}_{gg}(\epsilon,s_{123})\right]- \\
&\quad-\frac{3}{2}\,\mathbf{H}^{(2)}_{V,F}(\epsilon,s_{123})+3\mathbf{S}^{(2)}(\epsilon,s_{123})\,, \qquad (7.24)\\
\mathcal{F}inite\left(\mathcal{F}_3^1(s_{123})\right) &= -\frac{146933}{144}+\frac{1139\pi^2}{18}+\frac{49\pi^4}{60}+\frac{902}{3}\zeta_3\,, \qquad (7.25)\\
\mathcal{P}oles\left(\hat{\mathcal{F}}_3^1(s_{123})\right) &= -\hat{\mathcal{F}}_2^1(s_{123})\left(6\mathbf{I}^{(1)}_{gg}(\epsilon,s_{123})+\mathcal{F}_3^0(s_{123})\right)+ \\
&\quad+\frac{2b_{0,F}}{\epsilon}\,(s_{123})^{-\epsilon}\left[3\,\mathbf{I}^{(1)}_{gg}(\epsilon,s_{123})\right]-\frac{3}{2}\,\mathbf{H}^{(2)}_{V,\hat{F}}(\epsilon,s_{123})\,, \qquad (7.26)\\
\mathcal{F}inite\left(\hat{\mathcal{F}}_3^1(s_{123})\right) &= \frac{467}{8}-24\zeta_3\,. \qquad (7.27)
\end{aligned}$$

The factors of 3 in front of the infrared singularity operators and of the soft gluon current arise from the fact that the tree-level three-parton antenna function contains three antenna configurations.

At one loop, the correction to the quark-quark-antiquark antenna contains a leading colour and a subleading colour term $G_3^1(1_g,3_q,4_{\bar{q}})$, $\tilde{G}_3^1(1_g,3_q,4_{\bar{q}})$ as well as a quark loop term $\hat{G}_3^1(1_g,3_q,4_{\bar{q}})$. These read:

$$\begin{aligned}
\mathcal{P}oles\left(G_3^1(1_g,3_q,4_{\bar{q}})\right) &= 2\left(\mathbf{I}^{(1)}_{qg}(\epsilon,s_{13})+\mathbf{I}^{(1)}_{qg}(\epsilon,s_{14})-2\,\mathbf{I}^{(1)}_{gg}(\epsilon,s_{134})\right)G_3^0(1,3,4), && (7.28)\\
\mathcal{F}inite\left(G_3^1(1_g,3_q,4_{\bar{q}})\right) &= -\Bigg(R(y_{13},y_{34})+R(y_{14},y_{34})+\frac{5}{3}\log y_{13}+\frac{5}{3}\log y_{14}+\\
&\quad+\frac{13}{6}\log y_{34}-\frac{40}{9}\Bigg)G_3^0(1,3,4)-\frac{s_{13}+s_{14}}{2\,s_{134}^2}\,, && (7.29)\\
\mathcal{P}oles\left(\tilde{G}_3^1(1_g,3_q,4_{\bar{q}})\right) &= 2\left(\mathbf{I}^{(1)}_{q\bar{q}}(\epsilon,s_{34})\right)G_3^0(1,3,4)\,, && (7.30)\\
\mathcal{F}inite\left(\tilde{G}_3^1(1_g,3_q,4_{\bar{q}})\right) &= -\left(4+R(y_{13},y_{14})\right)G_3^0(1,3,4)+\frac{s_{13}+s_{14}}{2\,s_{134}^2}\,, && (7.31)\\
\mathcal{P}oles\left(\hat{G}_3^1(1_g,3_q,4_{\bar{q}})\right) &= -4\mathbf{I}^{(1)}_{gg,F}(\epsilon,s_{134})G_3^0(1,3,4)\,, && (7.32)\\
\mathcal{F}inite\left(\hat{G}_3^1(1_g,3_q,4_{\bar{q}})\right) &= \left(-\frac{10}{9}+\frac{2}{3}\log y_{34}+\frac{1}{6}\log y_{13}+\frac{1}{6}\log y_{14}\right)G_3^0(1,3,4)\,. && (7.33)
\end{aligned}$$

Integration of these antenna functions yields

$$\begin{aligned}
\mathcal{G}_3^1(s_{134}) &= (s_{134})^{-2\epsilon}\left[\frac{11}{18\epsilon^2}+\frac{1}{\epsilon}\left(\frac{169}{54}-\frac{\pi^2}{9}\right)+\left(\frac{446}{27}-\frac{205\pi^2}{216}-\frac{130}{9}\zeta_3\right)+\mathcal{O}(\epsilon)\right], && (7.34)\\
\tilde{\mathcal{G}}_3^1(s_{134}) &= (s_{134})^{-2\epsilon}\left[\frac{1}{6\epsilon^3}+\frac{41}{36\epsilon^2}+\frac{1}{\epsilon}\left(\frac{325}{54}-\frac{\pi^2}{4}\right)+\left(\frac{18457}{648}-\frac{41\pi^2}{24}-\frac{37}{9}\zeta_3\right)+\mathcal{O}(\epsilon)\right], && (7.35)\\
\hat{\mathcal{G}}_3^1(s_{134}) &= (s_{134})^{-2\epsilon}\left[\frac{7}{18\epsilon}+\left(\frac{895}{324}-\frac{11\pi^2}{108}\right)+\mathcal{O}(\epsilon)\right], && (7.36)
\end{aligned}$$

with

$$\begin{aligned}
\mathcal{P}oles\left(\mathcal{G}_3^1(s_{134})\right) &= -\mathcal{F}_2^1(s_{134})\left(2\mathbf{I}^{(1)}_{gg,F}(\epsilon,s_{134})+\mathcal{G}_3^0(s_{134})\right)+\\
&\quad+\frac{2b_0}{\epsilon}(s_{134})^{-\epsilon}\,\mathbf{I}^{(1)}_{gg,F}(\epsilon,s_{134})-\frac{1}{2}\mathbf{H}^{(2)}_{V,G}(\epsilon,s_{134})\,, && (7.37)\\
\mathcal{F}inite\left(\mathcal{G}_3^1(s_{134})\right) &= \frac{1445}{27}-\frac{337\pi^2}{108}-\frac{26}{3}\zeta_3\,, && (7.38)\\
\mathcal{P}oles\left(\tilde{\mathcal{G}}_3^1(s_{134})\right) &= -\frac{1}{2}\mathbf{H}^{(2)}_{V,\tilde{G}}(\epsilon,s_{134})\,, && (7.39)\\
\mathcal{F}inite\left(\tilde{\mathcal{G}}_3^1(s_{134})\right) &= \frac{18457}{648}-\frac{697\pi^2}{432}-\frac{73}{18}\zeta_3\,, && (7.40)\\
\mathcal{P}oles\left(\hat{\mathcal{G}}_3^1(s_{134})\right) &= -\hat{\mathcal{F}}_2^1(s_{134})\left(2\mathbf{I}^{(1)}_{gg,F}(\epsilon,s_{134})+\mathcal{G}_3^0(s_{134})\right)+\\
&\quad+\frac{2b_{0,F}}{\epsilon}(s_{134})^{-\epsilon}\,\mathbf{I}^{(1)}_{gg,F}(\epsilon,s_{134})-\frac{1}{2}\mathbf{H}^{(2)}_{V,\hat{G}}(\epsilon,s_{134})\,, && (7.41)
\end{aligned}$$

$$\mathcal{F}inite\left(\hat{\mathcal{G}}_3^1(s_{134})\right) = \frac{85}{324} - \frac{17\pi^2}{108}\,. \tag{7.42}$$

In contrast to the N_F^2 one-loop three-parton quark-gluon antenna function $\hat{\mathcal{E}}_3^1$, which had no corresponding tree-level four-parton antenna function with the same colour and flavour structure, $\hat{\mathcal{G}}_3^1$ is complemented by an antenna function containing two quark-antiquark pairs, $\mathcal{H}_4^0$, which is derived below. Correspondingly, $\hat{\mathcal{G}}_3^1$ does not contain the full N_F^2-terms for gluon-gluon final states.

7.3 Four-parton tree-level antenna functions

The tree-level four-parton quark-gluon antenna contains three final states: gluon-gluon-gluon-gluon, F_4^0, and gluon-quark-antiquark-gluon at leading and subleading colour, G_4^0 and $\tilde{G}_4^0$ and quark-antiquark-quark-antiquark, H_4^0. The antenna for the $gggg$ final state is:

$$\begin{aligned} F_4^0(g_1,g_2,g_3,g_4) = \;& f_4^0(1,2,3,4) + f_4^0(4,3,2,1) + f_4^0(2,3,4,1) + f_4^0(1,4,3,2) + \\ & + f_4^0(3,4,1,2) + f_4^0(2,1,4,3) + f_4^0(4,1,2,3) + f_4^0(3,2,1,4)\;, \end{aligned} \tag{7.43}$$

with

$$\begin{aligned} f_4^0(1,2,3,4) = \frac{1}{s_{1234}^2}\Bigg\{ & -\frac{2s_{34}s_{13}s_{14}^2}{s_{23}^2 s_{123} s_{234}} + \frac{1}{s_{23}^2}\times \\ & \times\Big[2s_{12}s_{14} - 2s_{12}s_{24} + 2s_{12}s_{34} + s_{12}^2 - 2s_{13}s_{14} - 2s_{13}s_{24} - \\ & - 2s_{13}s_{34} - 2s_{14}s_{24} + 2s_{14}s_{34} + s_{14}^2 + s_{34}^2\Big] + \frac{s_{13}}{s_{23}^2 s_{123}}\times \\ & \times\left[4s_{13}s_{14} + 4s_{13}s_{24} + 4s_{13}s_{34} - 8s_{14}s_{34} - 2s_{14}^2 - 4s_{24}s_{34} - 4s_{34}^2\right] + \\ & + \frac{s_{13}^2}{s_{23}^2 s_{123}^2}\left[4s_{14}s_{24} + 4s_{14}s_{34} + 2s_{14}^2 + 4s_{24}s_{34} + 2s_{24}^2 + 2s_{34}^2\right] + \\ & + \frac{1}{4s_{23}s_{12}s_{34}s_{14}}\left[2s_{13}s_{24}^3 + 3s_{13}^2 s_{24}^2 + 2s_{13}^3 s_{24} + s_{13}^4 + s_{24}^4\right] + \\ & + \frac{1}{s_{23}s_{12}s_{34}}\Big[6s_{13}s_{14}s_{24} + 2s_{13}s_{14}^2 + 6s_{13}s_{24}^2 + 3s_{13}^2 s_{14} + 6s_{13}^2 s_{24} + \\ & + 2s_{13}^3 + 3s_{14}s_{24}^2 + 2s_{14}^2 s_{24} + s_{14}^3 + 2s_{24}^3\Big] + \\ & + \frac{s_{24}}{s_{23}s_{12}s_{124}}\left[s_{24}s_{34} + s_{24}^2 + 2s_{34}^2\right] + \\ & + \frac{1}{s_{23}s_{12}s_{234}s_{124}}\left[2s_{13}s_{34}^3 + 3s_{13}^2 s_{34}^2 + 2s_{13}^3 s_{34} + s_{13}^4 + s_{34}^4\right] + \\ & + \frac{1}{s_{23}s_{12}s_{234}}\Big[2s_{13}s_{14}s_{34} + 2s_{13}s_{14}^2 + 2s_{13}s_{34}^2 + 3s_{13}^2 s_{14} + \\ & + 3s_{13}^2 s_{34} + 2s_{13}^3 + 2s_{14}s_{34}^2 - s_{14}^2 s_{34} + s_{14}^3\Big] + \frac{1}{s_{23}s_{12}}\times \\ & \times\Big[20s_{13}s_{14} + 14s_{13}s_{24} + 9s_{13}^2 + 16s_{14}s_{24} + 4s_{14}s_{34} + 19s_{14}^2 + \end{aligned}$$

$$
\begin{aligned}
&\quad + 7s_{24}^2 - 10s_{34}^2\Bigg] + \frac{s_{14}}{s_{23}s_{123}s_{234}} \times \\
&[-s_{13}s_{14} - 4s_{13}s_{34} - 4s_{13}^2 + s_{14}s_{34} - 4s_{14}^2 - 4s_{34}^2] + \\
&+ \frac{1}{s_{23}s_{123}s_{134}}\Bigg[6s_{14}s_{24}s_{34} + 6s_{14}s_{24}^2 + 6s_{14}^2s_{24} + s_{14}^3 + 6s_{24}s_{34}^2 + \\
&\qquad\qquad + 9s_{24}^2s_{34} + 6s_{24}^3 + s_{34}^3\Bigg] + \frac{1}{s_{23}s_{123}s_{124}} \times \\
&\times \Bigg[-3s_{14}s_{24}s_{34} - \frac{3}{2}s_{14}s_{24}^2 - \frac{3}{2}s_{14}s_{34}^2 - s_{14}^2s_{24} - s_{14}^2s_{34} + \\
&\quad + \frac{3}{4}s_{14}^3 - 3s_{24}s_{34}^2 - 3s_{24}^2s_{34} - s_{24}^3 - s_{34}^3\Bigg] + \frac{1}{4s_{23}s_{123}} \times \\
&\times \Bigg[-7s_{13}s_{14} + 18s_{13}s_{24} - 16s_{13}s_{34} - 11s_{13}^2 - 41s_{14}s_{24} - 36s_{14}s_{34} - \\
&\quad - 63s_{14}^2 - 16s_{24}s_{34} - 21s_{24}^2 - 18s_{34}^2\Bigg] + \frac{1}{s_{23}s_{134}} \times \\
&\times \Bigg[7s_{12}s_{14} + 2s_{12}s_{24} + 8s_{12}s_{34} - 4s_{12}^2 + 4s_{14}s_{24} - 3s_{14}s_{34} - \\
&\quad - s_{14}^2 + 2s_{24}s_{34} + 3s_{24}^2 - 3s_{34}^2\Bigg] + \\
&+ \frac{1}{8s_{23}}[21s_{12} + 69s_{13} + 14s_{14} + 69s_{24} + 21s_{34}] + \\
&+ \frac{1}{2s_{12}^2s_{34}^2}[-2s_{13}s_{14}s_{23}s_{24} + s_{13}^2s_{24}^2 + s_{14}^2s_{23}^2] + \\
&+ \frac{1}{s_{12}s_{34}s_{123}s_{234}}[4s_{14}s_{24}^3 + 6s_{14}^2s_{24}^2 + 4s_{14}^3s_{24} + s_{14}^4 + s_{24}^4] + \\
&+ \frac{1}{s_{12}s_{34}s_{123}s_{134}}[4s_{14}s_{24}^3 + 6s_{14}^2s_{24}^2 + 4s_{14}^3s_{24} + s_{14}^4 + s_{24}^4] + \\
&+ \frac{1}{8s_{12}s_{34}s_{123}}\Bigg[12s_{14}s_{23}s_{24} + 12s_{14}s_{23}^2 - \\
&\qquad\qquad - 12s_{14}s_{24}^2 - 6s_{14}^2s_{23} - 18s_{14}^2s_{24} - \\
&\qquad\qquad -4s_{14}^3 + 27s_{23}s_{24}^2 + 21s_{23}^2s_{24} + 3s_{23}^3 + 5s_{24}^3\Bigg] + \\
&+ \frac{1}{8s_{12}s_{34}s_{234}}\Bigg[12s_{13}s_{14}s_{24} + 18s_{13}s_{14}^2 + \\
&\qquad\qquad + 3s_{13}s_{24}^2 + 12s_{13}^2s_{14} + 3s_{13}^2s_{24} + \\
&\qquad\qquad + 3s_{13}^3 + 12s_{14}s_{24}^2 + 18s_{14}^2s_{24} + 12s_{14}^3 + 3s_{24}^3\Bigg] + \\
&+ \frac{1}{8s_{12}s_{34}}\Bigg[16s_{13}s_{14} + 31s_{13}s_{23} + 45s_{13}s_{24} + 25s_{13}^2 - 8s_{14}s_{23} +
\end{aligned}
$$

$$
\begin{aligned}
&\quad + 16s_{14}s_{24} + 6s_{14}^2 + 31s_{23}s_{24} + 21s_{23}^2 + 25s_{24}^2\Big] + \\
&+ \frac{5}{8s_{12}s_{123}s_{234}}\Big[12s_{14}s_{24}s_{34} + 12s_{14}s_{24}^2 + \\
&\quad + 4s_{14}s_{34}^2 + 12s_{14}^2s_{24} + 6s_{14}^2s_{34} + \\
&\quad + 4s_{14}^3 + 4s_{24}s_{34}^2 + 6s_{24}^2s_{34} + 4s_{24}^3 + s_{34}^3\Big] + \\
&+ \frac{5}{8s_{12}s_{123}}\Big[4s_{14}s_{23} - 8s_{14}s_{24} - 4s_{14}s_{34} - 6s_{14}^2 + 2s_{23}s_{24} + s_{23}s_{34} - \\
&\quad - s_{23}^2 - 3s_{24}s_{34} - 3s_{24}^2 - s_{34}^2\Big] + \frac{3}{8s_{12}s_{234}} \times \\
&\times \Big[4s_{13}s_{14} + 2s_{13}s_{24} + s_{13}s_{34} + s_{13}^2 + 8s_{14}s_{24} + 4s_{14}s_{34} + 6s_{14}^2 + \\
&\quad + 3s_{24}s_{34} + 3s_{24}^2 + s_{34}^2\Big] + \frac{3}{8s_{12}}\left[-s_{13} - 4s_{14} + s_{23} - 2s_{24} - s_{34}\right] + \\
&+ \frac{3}{8s_{34}s_{123}s_{234}}\Big[-4s_{13}s_{14}s_{24} - 6s_{13}s_{14}^2 - s_{13}s_{24}^2 - 4s_{13}^2s_{14} - \\
&\quad - s_{13}^2s_{24} - s_{13}^3 - 4s_{14}s_{24}^2 - 6s_{14}^2s_{24} - 4s_{14}^3 - s_{24}^3\Big] + \\
&+ \frac{3}{8s_{34}s_{123}}\Big[4s_{13}s_{14} - s_{13}s_{23} + s_{13}s_{24} + s_{13}^2 - 4s_{14}s_{23} + 4s_{14}s_{24} + \\
&\quad + 6s_{14}^2 - s_{23}s_{24} + s_{23}^2 + s_{24}^2\Big] + \\
&+ \frac{1}{s_{24}s_{123}s_{134}}\left[-2s_{14} + s_{24} - 2s_{34}\right] + \\
&+ \frac{1}{s_{123}^2}\left[2s_{14}s_{24} + 2s_{14}s_{34} + s_{14}^2 + 2s_{24}s_{34} + s_{24}^2 + s_{34}^2\right] + \\
&+ \frac{1}{8s_{123}s_{234}}\Big[-12s_{13}s_{14} - 6s_{13}s_{24} - 3s_{13}s_{34} - 3s_{13}^2 - 24s_{14}s_{24} - \\
&\quad - 12s_{14}s_{34} + 38s_{14}^2 - 9s_{24}s_{34} - 9s_{24}^2 - 3s_{34}^2\Big] + \\
&+ \frac{1}{8s_{123}}\left[-6s_{13} + 45s_{14} - 3s_{23} + 58s_{24} + 36s_{34}\right] + \frac{35}{8} + \mathcal{O}(\epsilon)\Big\}. \qquad (7.44)
\end{aligned}
$$

In F_4^0, the gluonic emissions are colour-ordered. Since the original colour structure is a trace over the gluon colour indices [47], F_4^0 is symmetric under cyclic interchanges of the momenta. Therefore, each pair of adjacent momenta can act as hard emitter pair for the antenna function. F_4^0 thus contains four different colour-ordered antennae. For numerical implementation, these have to be separated from each other by repeated partial fractioning of the associated invariants. This fractioning is not made explicit in the above expression f_4^0.

The integral of this antenna function is

$$\mathcal{F}_4^0(s_{1234}) = 2\,(s_{1234})^{-2\epsilon}\left[\frac{5}{2\epsilon^4}+\frac{121}{12\epsilon^3}+\frac{1}{\epsilon^2}\left(\frac{436}{9}-\frac{11\pi^2}{3}\right)+\right.$$
$$+\frac{1}{\epsilon}\left(\frac{23455}{108}-\frac{1067\pi^2}{72}-\frac{379}{6}\zeta_3\right)+$$
$$\left.+\left(\frac{304951}{324}-\frac{7781\pi^2}{108}-\frac{2288}{9}\zeta_3+\frac{479\pi^4}{720}\right)+\mathcal{O}(\epsilon)\right], \quad (7.45)$$

with

$$\mathcal{P}oles\left(\mathcal{F}_4^0(s_{1234})\right) = 4\left[2\mathbf{I}_{gg}^{(1)}(\epsilon,s_{1234})\right]^2 - 4\,e^{-\epsilon\gamma}\frac{\Gamma(1-2\epsilon)}{\Gamma(1-\epsilon)}\left(\frac{b_0}{\epsilon}+k_0\right)\left[2\mathbf{I}_{gg}^{(1)}(2\epsilon,s_{1234})\right]-$$
$$-2\,\mathbf{H}_{R,F}^{(2)}(\epsilon,s_{1234}) - 4\,\mathbf{S}_V^{(2)}(\epsilon,s_{1234})\,, \quad (7.46)$$
$$\mathcal{F}inite\left(\mathcal{F}_4^0(s_{1234}\right) = \frac{271741}{162}-\frac{2335\pi^2}{27}-\frac{397\pi^4}{360}-\frac{2651}{6}\zeta_3\,. \quad (7.47)$$

The leading colour and subleading colour gluon-quark-antiquark-gluon antennae are:

$$G_4^0(1_g,3_q,4_{\bar{q}},2_g) = g_4^0(1,3,4,2)+g_4^0(2,4,3,1)\,, \quad (7.48)$$
$$\tilde{G}_4^0(1_g,3_q,4_{\bar{q}},2_g) = \tilde{g}_4^0(1,3,4,2)+\tilde{g}_4^0(1,4,3,2)+\tilde{g}_4^0(2,3,4,1)+\tilde{g}_4^0(2,4,3,1)\,, \quad (7.49)$$

with

$$g_4^0(1,3,4,2) = \frac{1}{s_{1234}^2}\left\{\frac{1}{s_{12}^2s_{34}^2}\left[2s_{13}s_{14}s_{23}s_{24}-s_{13}^2s_{24}^2-s_{14}^2s_{23}^2\right]+\frac{s_{23}}{s_{12}s_{13}s_{34}}\left[s_{23}^2+s_{24}^2\right]+\right.$$
$$+\frac{s_{23}}{s_{12}s_{13}s_{134}}\left[s_{23}^2-2s_{24}s_{34}+s_{24}^2+s_{34}^2\right]+$$
$$+\frac{s_{23}}{s_{12}s_{13}}\left[s_{14}+2s_{24}-s_{34}\right]-\frac{s_{13}}{s_{12}}+\frac{1}{s_{12}s_{34}s_{134}}\times$$
$$\times\left[-2s_{14}s_{23}^2+2s_{14}s_{24}^2+2s_{14}^2s_{23}+2s_{14}^2s_{24}+\right.$$
$$\left.+s_{23}s_{24}^2+s_{23}^2s_{24}+s_{23}^3+s_{24}^3\right]+\frac{1}{s_{12}s_{34}}\times$$
$$\times\left[2s_{13}s_{14}+4s_{13}s_{23}+3s_{13}s_{24}+2s_{13}^2-s_{14}s_{23}+4s_{14}^2\right]+$$
$$+\frac{1}{s_{12}s_{134}}\left[2s_{14}s_{24}-4s_{23}s_{24}+s_{23}s_{34}+s_{24}s_{34}\right]+$$
$$+\frac{s_{12}}{s_{34}s_{134}s_{234}}\left[2s_{12}s_{14}+s_{12}^2+4s_{14}s_{24}+4s_{14}^2+4s_{24}^2\right]+$$
$$+\frac{s_{12}}{s_{134}s_{234}}\left[6s_{14}+6s_{24}+3s_{34}\right]+$$
$$+\frac{2s_{12}^2s_{14}s_{24}}{s_{34}^2s_{134}s_{234}}+\frac{1}{2s_{13}s_{24}}\left[s_{12}s_{34}-s_{14}s_{23}\right]+$$
$$+\frac{s_{24}}{s_{13}s_{34}s_{234}}\left[-2s_{12}s_{24}+s_{12}^2+s_{24}^2\right]+\frac{1}{s_{13}s_{34}}\times$$

$$
\begin{aligned}
&\times\left[-2s_{12}s_{23}+2s_{12}s_{24}-s_{12}^2+2s_{23}s_{24}-2s_{23}^2-2s_{24}^2\right]+\\
&+\frac{s_{34}}{s_{13}s_{134}^2}\Big[-2s_{12}s_{23}-2s_{12}s_{24}-s_{12}^2-\\
&\qquad\qquad-2s_{23}s_{24}-s_{23}^2-s_{24}^2\Big]+\frac{1}{s_{13}s_{134}s_{234}}\times\\
&\times\Big[6s_{12}s_{24}s_{34}+4s_{12}s_{24}^2+3s_{12}s_{34}^2-3s_{12}^2s_{24}-3s_{12}^2s_{34}+\\
&\quad+s_{12}^3-3s_{24}s_{34}^2-4s_{24}^2s_{34}-2s_{24}^3-s_{34}^3\Big]+\frac{1}{s_{13}s_{134}}\times\\
&\times\Big[8s_{12}s_{23}-4s_{12}s_{24}-4s_{12}s_{34}+4s_{12}^2-2s_{23}s_{34}+\\
&\quad+6s_{23}^2+2s_{24}^2+2s_{34}^2\Big]+\frac{1}{s_{13}s_{234}}\times\\
&\times\left[-4s_{12}s_{24}-2s_{12}s_{34}+s_{12}^2+3s_{24}s_{34}+4s_{24}^2+s_{34}^2\right]+\\
&+\frac{1}{s_{13}}\left[2s_{12}+2s_{23}-2s_{24}-2s_{34}\right]+\\
&+\frac{s_{14}}{s_{34}^2s_{134}}\Big[-4s_{12}s_{14}+8s_{12}s_{24}+2s_{12}^2-4s_{14}s_{23}\\
&\qquad\qquad-4s_{14}s_{24}+4s_{23}s_{24}+4s_{24}^2\Big]+\frac{s_{14}^2}{s_{34}^2s_{134}^2}\times\\
&\times\left[-4s_{12}s_{23}-4s_{12}s_{24}-2s_{12}^2-4s_{23}s_{24}-2s_{23}^2-2s_{24}^2\right]+\frac{1}{s_{34}^2}\times\\
&\times\left[-4s_{12}s_{13}+4s_{12}s_{14}-s_{12}^2+4s_{13}s_{23}-2s_{13}s_{24}-2s_{13}^2+2s_{14}s_{23}\right]+\\
&+\frac{1}{s_{34}s_{134}}\Big[4s_{12}s_{23}+2s_{12}s_{24}+5s_{12}^2-8s_{14}s_{23}+\\
&\qquad\qquad+6s_{14}s_{24}+6s_{14}^2+6s_{23}^2+4s_{24}^2\Big]+\\
&+\frac{1}{s_{34}}\left[2s_{12}+2s_{13}+6s_{14}\right]+\\
&+\frac{1}{s_{134}^2}\left[-2s_{12}s_{23}-2s_{12}s_{24}-s_{12}^2-2s_{23}s_{24}-s_{23}^2-s_{24}^2\right]+\\
&+\frac{1}{s_{134}}\left[-4s_{12}+4s_{14}-4s_{23}-2s_{24}+3s_{34}\right]-\frac{7}{2}+\mathcal{O}(\epsilon)\Bigg\}, \qquad (7.50)
\end{aligned}
$$

$$
\begin{aligned}
\tilde{g}_4^0(1,3,4,2)\;=\;\frac{1}{s_{1234}^2}\Bigg\{&\frac{(s_{12}+s_{23})^2}{s_{13}s_{14}}+\frac{s_{12}s_{24}}{2s_{13}s_{23}s_{134}s_{234}}\left[s_{24}^2+s_{12}^2\right]+\\
&+\frac{s_{12}}{2s_{13}s_{23}s_{134}}\left[s_{24}s_{34}-s_{24}^2-s_{34}^2-s_{12}^2\right]+\\
&+\frac{1}{2s_{13}s_{24}}\left[s_{12}s_{34}-s_{14}s_{23}\right]+
\end{aligned}
$$

$$
\begin{aligned}
&+\frac{s_{34}}{s_{13}s_{134}^2}\left[-2s_{12}s_{23}-2s_{12}s_{24}-s_{12}^2-2s_{23}s_{24}-s_{23}^2-s_{24}^2\right]+\\
&+\frac{1}{s_{13}s_{134}s_{234}}\left[\frac{7}{2}s_{12}s_{24}s_{34}+\frac{1}{2}s_{12}s_{24}^2+\frac{5}{2}s_{12}s_{34}^2+\right.\\
&\qquad\left.-3s_{12}^2s_{34}+\frac{1}{2}s_{12}^3-2s_{24}s_{34}^2-2s_{24}^2s_{34}-s_{34}^3\right]+\\
&+\frac{1}{s_{13}s_{134}}\left[-2s_{12}s_{24}-4s_{12}s_{34}-s_{12}^2-2s_{23}s_{34}+s_{23}^2+\right.\\
&\qquad\left.+2s_{24}s_{34}-s_{24}^2\right]+\\
&+\frac{1}{s_{13}s_{234}}\left[-2s_{12}s_{24}-2s_{12}s_{34}+s_{12}^2+2s_{24}s_{34}+2s_{24}^2+s_{34}^2\right]+\\
&+\frac{1}{s_{13}}\left[2s_{12}+2s_{23}-2s_{24}\right]+\frac{1}{s_{134}^2}\times\\
&\times\left[-2s_{12}s_{23}-2s_{12}s_{24}-s_{12}^2-2s_{23}s_{24}-s_{23}^2-s_{24}^2\right]+\\
&+\frac{s_{12}}{s_{134}s_{234}}\left[-2s_{34}-s_{12}\right]+\\
&+\left.\frac{1}{s_{134}}\left[-2s_{12}-s_{23}-s_{24}-s_{34}\right]-1+\mathcal{O}(\epsilon)\right\}. \qquad (7.51)
\end{aligned}
$$

In the leading colour contribution G_4^0, the gluonic emissions are colour-ordered in between the quark-antiquark pair. However, like all gluon-gluon antenna functions at leading colour, G_4^0 is cyclic in the colour indices, such that it also contains a configuration where the two gluons form the hard emitter pair, emitting the quark-antiquark pair inside the antenna. As before, the different antenna configurations can be separated from each other for the numerical integration by repeated partial fractioning of the invariants.

Integration yields

$$
\begin{aligned}
\mathcal{G}_4^0(s_{1234}) &= \frac{1}{2}\,(s_{1234})^{-2\epsilon}\left[-\frac{3}{2\epsilon^3}-\frac{155}{18\epsilon^2}+\frac{1}{\epsilon}\left(-\frac{523}{12}+\frac{79\pi^2}{36}\right)+\right.\\
&\qquad\left.+\left(-\frac{16579}{81}+\frac{1385\pi^2}{108}+37\zeta_3\right)+\mathcal{O}(\epsilon)\right], \qquad (7.52)\\
\tilde{\mathcal{G}}_4^0(s_{1234}) &= (s_{1234})^{-2\epsilon}\left[-\frac{1}{3\epsilon^3}-\frac{41}{18\epsilon^2}+\frac{1}{\epsilon}\left(-\frac{1327}{108}+\frac{\pi^2}{2}\right)+\right.\\
&\qquad\left.+\left(-\frac{4864}{81}+\frac{41\pi^2}{12}+\frac{86}{9}\zeta_3\right)+\mathcal{O}(\epsilon)\right], \qquad (7.53)
\end{aligned}
$$

with

$$
\begin{aligned}
\mathcal{P}oles\left(\mathcal{G}_4^0(s_{1234})\right) &= 2\left[2\mathbf{I}_{gg}^{(1)}(\epsilon,s_{1234})\right]\left[2\mathbf{I}_{gg,F}^{(1)}(\epsilon,s_{1234})\right]-e^{-\epsilon\gamma}\frac{\Gamma(1-2\epsilon)}{\Gamma(1-\epsilon)}\times\\
&\times\left[\left(\frac{b_{0,F}}{\epsilon}+k_{0,F}\right)\left[2\mathbf{I}_{gg}^{(1)}(2\epsilon,s_{1234})\right]+\right.\\
&\qquad\left.+\left(\frac{b_0}{\epsilon}+k_0\right)\left[2\mathbf{I}_{gg,F}^{(1)}(2\epsilon,s_{1234})\right]\right]-\frac{1}{2}\mathbf{H}_{R,G}^{(2)}(\epsilon,s_{1234}), \qquad (7.54)
\end{aligned}
$$

$$\mathcal{F}inite\left(\mathcal{G}_4^0(s_{1234})\right) = -\frac{16579}{162} + \frac{155\pi^2}{48} + \frac{649}{36}\zeta_3\,, \tag{7.55}$$

$$\mathcal{P}oles\left(\tilde{\mathcal{G}}_4^0(s_{1234})\right) = -\mathbf{H}^{(2)}_{R,\tilde{G}}(\epsilon, s_{1234})\,, \tag{7.56}$$

$$\mathcal{F}inite\left(\tilde{\mathcal{G}}_4^0(s_{1234})\right) = -\frac{4864}{81} + \frac{697\pi^2}{216} + \frac{85}{9}\zeta_3\,. \tag{7.57}$$

The quark-antiquark-quark-antiquark antenna is

$$\begin{aligned} H_4^0(1_q, 2_{\bar{q}}, 3_{q'}, 4_{\bar{q}'}) = \frac{1}{s_{1234}^2}\Bigg\{ & \frac{2}{s_{12}^2 s_{34}^2}\left[s_{13}s_{24} - s_{14}s_{23}\right]^2 + \frac{1}{s_{12}s_{34}} \times \\ & \left[-2s_{13}s_{24} + s_{13}^2 - 2s_{14}s_{23} + s_{14}^2 + s_{23}^2 + s_{24}^2\right] + \\ & + 2 + \mathcal{O}(\epsilon)\Bigg\}\,, \end{aligned} \tag{7.58}$$

where only different quark flavours need to be considered, since the identical flavour contribution to this final state is finite.

The integral of this antenna term is

$$\mathcal{H}_4^0(s_{1234}) = (s_{1234})^{-2\epsilon}\left[\frac{1}{9\epsilon^2} + \frac{7}{9\epsilon} + \left(\frac{677}{162} - \frac{\pi^2}{6}\right)\right]\,, \tag{7.59}$$

with

$$\begin{aligned} \mathcal{P}oles\left(\mathcal{H}_4^0(s_{1234})\right) = & \; 2\left[2\mathbf{I}^{(1)}_{gg,F}(\epsilon, s_{1234})\right]^2 - \\ & - 2e^{-\epsilon\gamma}\frac{\Gamma(1-2\epsilon)}{\Gamma(1-\epsilon)}\left(\frac{b_{0,F}}{\epsilon} + k_{0,F}\right)\left[2\mathbf{I}^{(1)}_{gg,F}(2\epsilon, s_{1234})\right] - \\ & - \mathbf{H}^{(2)}_{R,H}(\epsilon, s_{1234})\,, \end{aligned} \tag{7.60}$$

$$\mathcal{F}inite\left(\mathcal{H}_4^0(s_{1234})\right) = \frac{677}{162} + \frac{11\pi^2}{36}\,. \tag{7.61}$$

The contribution from identical quarks only to this final state is finite, and thus no gluon-gluon antenna function is defined for two identical quark-antiquark pairs.

8. Infrared limits of the antenna subtraction terms

The antenna subtraction terms defined in the three previous sections encapsulate all single and double unresolved limits of tree-level QCD matrix elements and all single unresolved limits of one-loop QCD matrix elements. In this section, we list the behaviour of all tree-level three-parton and four-parton antenna functions. Using this information, it is then possible to employ these antenna functions in the construction of complete infrared subtraction functions for QCD matrix elements at NNLO.

8.1 Generalised collinear and soft factors

The factorisation properties of tree-level QCD squared matrix elements at NLO and NNLO have been investigated in detail in [38, 40, 17–20]. At NLO, only a single particle can become unresolved, either soft or collinear. In these limits, the $(m+1)$-parton matrix element factorises into a reduced m-parton matrix element times a soft eikonal factor or a collinear splitting function. At NNLO, two particles can become unresolved in several possible configurations: double soft, soft/collinear, double single collinear, triple collinear. In each of these limits, the $(m+2)$-parton matrix element factorises into a reduced m-parton matrix element times a generalised double unresolved factor (double soft factor, soft/collinear splitting function, double single collinear splitting function, triple collinear splitting function). In the following, we list all generalised single and double unresolved factors.

8.1.1 Single unresolved factors

When deriving limits of the three-parton antenna functions in single unresolved configurations, we encounter well-known soft eikonal factors when a gluon is soft and three different Altarelli-Parisi splitting functions when two partons are collinear. These are listed below.

When a soft gluon (b) is emitted between two hard partons (a and c), the eikonal factor S_{abc} factorises off the squared matrix element:

$$S_{abc} \equiv \frac{2s_{ac}}{s_{ab}s_{bc}}\,. \tag{8.1}$$

When two partons become collinear, we have different splitting functions corresponding to various final state configurations: a quark splits into a quark and a gluon ($P_{qg\to Q}$), a gluon splits into a quark-antiquark pair ($P_{q\bar{q}\to G}$) or a gluon splits into two gluons ($P_{gg\to G}$). These are given by:

$$\begin{aligned}
P_{qg\to Q}(z) &= \left(\frac{1+(1-z)^2-\epsilon z^2}{z}\right), \\
P_{q\bar{q}\to G}(z) &= \left(\frac{z^2+(1-z)^2-\epsilon}{1-\epsilon}\right), \\
P_{gg\to G}(z) &= 2\left(\frac{z}{1-z}+\frac{1-z}{z}+z(1-z)\right).
\end{aligned} \tag{8.2}$$

In these equations, z is the momentum fraction of one of the collinear partons and the label q appearing in these splitting function can stand for a quark or antiquark: $P_{qg\to Q} = P_{\bar{q}g\to\bar{Q}}$ by charge conjugation. Q or G appearing in the collinear splitting functions denotes the parent particle of the two collinear partons i and j. In the discussion below, the momentum associated with this parent particle will be denoted by (ij).

8.1.2 Double unresolved factors

To describe the limiting behaviours of the four-parton antenna functions in double unresolved configurations, we require generalised soft and collinear factors. These were first derived in [17 − 20], and are listed below. We follow largely the notation of [18].

1. Double soft factors

When two colour connected gluons (b) and (c) are simultaneously soft, the double soft gluon function for four partons in the final state is given by

$$\begin{aligned} S_{abcd}(s_{ad}, s_{ab}, s_{cd}, s_{bc}, s_{abc}, s_{bcd}) = &\frac{2s_{ad}^2}{s_{ab}s_{bcd}s_{abc}s_{cd}} + \\ &+\frac{2s_{ad}}{s_{bc}}\left(\frac{1}{s_{ab}s_{cd}} + \frac{1}{s_{ab}s_{bcd}} + \frac{1}{s_{cd}s_{abc}} - \frac{4}{s_{abc}s_{bcd}}\right) + \\ &+\frac{2(1-\epsilon)}{s_{bc}^2}\left(\frac{s_{ab}}{s_{abc}} + \frac{s_{cd}}{s_{bcd}} - 1\right)^2 . \end{aligned} \tag{8.3}$$

Here a and d are the hard partons surrounding the soft pair.

In the case when two unconnected gluons become simultaneously soft the corresponding double soft gluon factor is the product of two eikonal factors S_{abc}, given in (8.1).

For the emission of a soft quark-antiquark pair resulting from the splitting of an intermediate gluon emitted itself from a primary pair of hard partons, the soft factor takes the form,

$$\begin{aligned} S_{ab}(c_q, d_{\bar{q}}) = &\frac{2}{s_{cd}^2\,(s_{ac}+s_{ad})(s_{bc}+s_{bd})}\,(s_{ab}s_{cd} - s_{ac}s_{bd} - s_{bc}s_{ad}) + \\ &+\frac{2}{s_{cd}^2}\left(\frac{s_{ac}s_{ad}}{(s_{ac}+s_{ad})^2} + \frac{s_{bc}s_{bd}}{(s_{bc}+s_{bd})^2}\right), \end{aligned} \tag{8.4}$$

with a and b the adjacent hard partons. Note that this formula is different from the one that can be found in [19] for this limit, where the second line of the above formula is absent.

2. Soft-collinear factors

   When a gluon (a) is soft, partons (d,a,b,c) are colour connected and partons b and c are collinear then the limiting behaviour of the squared matrix element is described by the soft-collinear factor, which is subsequently multiplied with the appropriate simple collinear splitting function

$$S_{d;abc}(z, s_{ab}, s_{bc}, s_{abc}, s_{ad}, s_{bd}, s_{cd}) = \frac{(s_{bd}+s_{cd})}{s_{ab}s_{ad}}\left(z + \frac{s_{ab}+zs_{bc}}{s_{abc}}\right). \tag{8.5}$$

   In here, z is always the collinear momentum fraction of parton b in the collinear pair (bc), with b being colour-connected to the soft parton a.

3. Triple collinear splitting functions

   There are five different triple collinear splitting functions depending on the nature of the partons which become collinear.

   The colour-ordered triple collinear splitting function $P_{ggg\to G}$ is given by

$$\begin{aligned} &P_{abc\to G}(w, x, y, s_{ab}, s_{bc}, s_{abc}) = \\ &= 2\times\left\{+\frac{(1-\epsilon)}{s_{ab}^2 s_{abc}^2}\frac{(xs_{abc}-(1-y)s_{bc})^2}{(1-y)^2} + \frac{2(1-\epsilon)s_{bc}}{s_{ab}s_{abc}^2} + \frac{3(1-\epsilon)}{2s_{abc}^2} + \right.\end{aligned}$$

$$+\frac{1}{s_{ab}s_{abc}}\left(\frac{(1-y(1-y))^2}{yw(1-w)}-2\frac{x^2+xy+y^2}{1-y}+\frac{xw-x^2y-2}{y(1-y)}+2\epsilon\frac{x}{(1-y)}\right)+$$
$$+\frac{1}{2s_{ab}s_{bc}}\left(3x^2-\frac{2(2-w+w^2)(x^2+w(1-w))}{y(1-y)}+\frac{1}{yw}+\frac{1}{(1-y)(1-w)}\right)\Bigg\}+$$
$$+(s_{ab}\leftrightarrow s_{bc}, w\leftrightarrow y)\,, \tag{8.6}$$

with w, x and y being the momentum fractions carried by the collinear gluons a, b, c, and with $w=(1-x-y)$. This splitting function is symmetric under the exchange of the outer gluons (a and c), and contains poles only in s_{ab} and s_{bc}.

$\tilde{P}_{qg_1g_2\to Q}$ is the triple collinear splitting function obtained when quark q is collinear to two gluons, g_1 and g_2, which are not colour connected, i.e. behave like photons [17]. It reads,

$$\begin{aligned}
&\tilde{P}_{qg_1g_2\to Q}(w,x,y,s_{qg_1},s_{qg_2},s_{qg_1g_2}) = \\
&\quad = +\frac{1}{2s_{qg_1}s_{qg_2}}\frac{w}{xy}\left(1+w^2-\epsilon(x^2+xy+y^2)-\epsilon^2xy\right)+\frac{1}{s_{qg_1}s_{qg_1g_2}}\times \\
&\quad\quad \times\frac{1}{xy}\left(w(1-x+\epsilon^2xy)+(1-y)^3-\epsilon(1-y)(x^2+xy+y^2)+\epsilon^2xy\right)- \\
&\quad\quad -\frac{(1-\epsilon)}{s_{qg_1g_2}^2}\left((1-\epsilon)\frac{s_{qg_1}}{s_{qg_2}}-\epsilon\right)+(s_{qg_1}\leftrightarrow s_{qg_2}, x\leftrightarrow y),
\end{aligned} \tag{8.7}$$

with x,y and w the momentum fractions carried by the collinear particles and with $w=(1-x-y)$. For the case when the two gluons are instead colour connected, the colour-ordered splitting function reads,

$$\begin{aligned}
&P_{qg_1g_2\to Q}(w,x,y,s_{qg_1},s_{qg_2},s_{g_1g_2},s_{qg_1g_2}) = \\
&\quad = +\frac{1}{s_{qg_1}s_{g_1g_2}}\left((1-\epsilon)\left(\frac{1+w^2}{y}+\frac{1+(1-y)^2}{(1-w)}\right)+2\epsilon\left(\frac{w}{y}+\frac{1-y}{1-w}\right)\right)+ \\
&\quad\quad +\frac{1}{s_{qg_1}s_{qg_1g_2}}\left((1-\epsilon)\left(\frac{(1-y)^3+w(1-x)-2y}{y(1-w)}\right)-\right. \\
&\quad\quad\quad \left.-\epsilon\left(\frac{2(1-y)(y-w)}{y(1-w)}-x\right)-\epsilon^2x\right)+ \\
&\quad\quad +\frac{1}{s_{g_1g_2}s_{qg_1g_2}}\left((1-\epsilon)\left(\frac{(1-y)^2(2-y)+x^3+2xw-2-y}{y(1-w)}\right)+\right. \\
&\quad\quad\quad \left.+2\epsilon\frac{(xw-y-2yw)}{y(1-w)}\right)+ \\
&\quad\quad +(1-\epsilon)\left(\frac{2\left(xs_{qg_1g_2}-(1-w)s_{qg_1}\right)^2}{s_{g_1g_2}^2s_{qg_1g_2}^2(1-w)^2}+\right. \\
&\quad\quad\quad \left.+\frac{1}{s_{qg_1g_2}^2}\left(4\frac{s_{qg_1}}{s_{g_1g_2}}+(1-\epsilon)\frac{s_{g_1g_2}}{s_{qg_1}}+(3-\epsilon)\right)\right).
\end{aligned} \tag{8.8}$$

Similarly the clustering of a gluon with a quark-antiquark pair into a parent gluon again has two distinct functions depending on whether the final state is colour-ordered or not, In the colour connected case, the gluon is emitted outside the quark-antiquark pair, and one obtains the colour-ordered splitting function,

$$\begin{aligned}
&P_{g\bar{q}q\to G}(w,x,y,s_{g\bar{q}},s_{\bar{q}q},s_{g\bar{q}q}) = \\
&= -\frac{1}{s^2_{g\bar{q}q}}\left(4\frac{s_{g\bar{q}}}{s_{\bar{q}q}}+(1-\epsilon)\frac{s_{\bar{q}q}}{s_{g\bar{q}}}+(3-\epsilon)\right)-\frac{2\left(xs_{g\bar{q}q}-(1-w)s_{g\bar{q}}\right)^2}{s^2_{\bar{q}q}s^2_{g\bar{q}q}(1-w)^2}+ \\
&\quad+\frac{1}{s_{g\bar{q}}s_{g\bar{q}q}}\left(\frac{(1-y)}{w(1-w)}-y-2w-\epsilon-\frac{2x(1-y)(y-w)}{(1-\epsilon)w(1-w)}\right)+ \\
&\quad+\frac{1}{s_{g\bar{q}}s_{\bar{q}q}}\left(\frac{x\left((1-w)^3-w^3\right)}{w(1-w)}-\frac{2x^2\left(1-yw-(1-y)(1-w)\right)}{(1-\epsilon)w(1-w)}\right)+ \\
&\quad+\frac{1}{s_{\bar{q}q}s_{g\bar{q}q}}\left(\frac{(1+w^3+4xw)}{w(1-w)}+\frac{2x\left(w(x-y)-y(1+w)\right)}{(1-\epsilon)w(1-w)}\right), \qquad (8.9)
\end{aligned}$$

while in the case where the gluon is emitted between the quark-antiquark pair, which is subleading in colour, one obtains a QED-like splitting function,

$$\begin{aligned}
&\tilde{P}_{qg\bar{q}\to G}(w,x,y,s_{qg},s_{g\bar{q}},s_{\bar{q}q},s_{qg\bar{q}}) = \\
&= -\frac{1}{s^2_{qg\bar{q}}}\left((1-\epsilon)\frac{s_{q\bar{q}}}{s_{qg}}+1\right)+\frac{1}{s_{g\bar{q}}s_{qg}}\left((1+x^2)-\frac{x+2wy}{1-\epsilon}\right)- \\
&\quad-\frac{1}{s_{qg}s_{qg\bar{q}}}\left(1+2x+\epsilon-\frac{2(1-y)}{(1-\epsilon)}\right)+(s_{qg}\leftrightarrow s_{g\bar{q}},w\leftrightarrow y)\,. \qquad (8.10)
\end{aligned}$$

Lastly, the clustering of a quark-antiquark pair ($q'\bar{q}'$) and a quark (q) to form a parent quark Q with the same flavour as q. The splitting function depends upon whether or not the quarks are of identical flavour,

$$P_{q\bar{q}'q'\to Q} = P^{\rm non-ident.}_{q\bar{q}'q'\to Q} - \frac{\delta_{qq'}}{N}P^{\rm ident.}_{q\bar{q}'q'\to Q}, \qquad (8.11)$$

where $\delta_{qq'}=1$ for identical flavour quarks. If quarks q_1, ${q'}_3$ and ${\bar{q}'}_4$ are clustered to form Q,

$$\begin{aligned}
&P^{\rm non-ident.}_{q\bar{q}'q'\to Q}(w,x,y,s_{q\bar{q}'},s_{q'\bar{q}'},s_{qq'\bar{q}'}) = \\
&= -\frac{1}{s^2_{qq'\bar{q}'}}\left((1-\epsilon)+\frac{2s_{q\bar{q}'}}{s_{q'\bar{q}'}}\right)-\frac{2\left(xs_{qq'\bar{q}'}-(1-w)s_{q\bar{q}'}\right)^2}{s^2_{q'\bar{q}'}s^2_{qq'\bar{q}'}(1-w)^2}+ \\
&\quad+\frac{1}{s_{q'\bar{q}'}s_{qq'\bar{q}'}}\left(\frac{1+x^2+(x+w)^2}{(1-w)}-\epsilon(1-w)\right). \qquad (8.12)
\end{aligned}$$

When the flavours of the clustering quarks are the same, there is an additional contribution coming from the interference terms of the four-quark matrix elements, which reads

$$\begin{aligned}
&P^{\rm ident.}_{q\bar{q}'q'\to Q}(w,x,y,s_{q\bar{q}'},s_{q\bar{q}'},s_{qq'\bar{q}'}) = \\
&= -\frac{(1-\epsilon)}{s^2_{qq'\bar{q}'}}\left(\frac{2s_{q\bar{q}'}}{s_{q'\bar{q}'}}+2+\epsilon\right)-\frac{1}{2s_{q\bar{q}'}s_{q'\bar{q}'}}\left(\frac{x(1+x^2)}{(1-y)(1-w)}-\epsilon x\left(\frac{2(1-y)}{(1-w)}+1+\epsilon\right)\right)+ \\
&\quad+\frac{1}{s_{q'\bar{q}'}s_{qq'\bar{q}'}}\left(\frac{1+x^2}{(1-y)}+\frac{2x}{(1-w)}-\epsilon\left(\frac{(1-w)^2}{(1-y)}+(1+x)+\frac{2x}{(1-w)}+\epsilon(1-w)\right)\right)+ \\
&\quad+(s_{q\bar{q}'}\leftrightarrow s_{q'\bar{q}'},y\leftrightarrow w)\,. \qquad (8.13)
\end{aligned}$$

This identical flavour splitting function contains poles when $\overline{q}'$ clusters with both q' and q. It is symmetric under $q_1 \leftrightarrow {q'}_3$.

4. Double collinear splitting functions

   If two distinct pairs of partons become simultaneously collinear, the $(m+2)$-parton squared matrix element factorises into the product of two simple collinear splitting functions (8.2) with the m-parton squared matrix element.

8.2 Quark-antiquark antennae

The three-parton and four-parton quark-antiquark antenna functions were derived in section 5 from the real radiation corrections to $\gamma^* \to q\bar{q}$. Their behaviour in all limits where one or two partons become unresolved are described below.

8.2.1 Three-parton antenna functions

We have only one three-parton quark-antiquark antenna function: $A_3^0(1_q, 3_g, 2_{\bar{q}})$, which has the following limits:

1. Soft limit:
$$A_3^0(1,3,2) \xrightarrow{3_g \to 0} S_{132}\,. \tag{8.14}$$

2. Collinear limit:
$$A_3^0(1,3,2) \xrightarrow{1_q \| 3_g} \frac{1}{s_{13}}\, P_{qg\to Q}(z). \tag{8.15}$$
   where the momenta of the quark (1_q) and the antiquark $(2_{\bar{q}})$ can be interchanged.

8.2.2 Four-parton antenna functions

The NNLO real radiation corrections to $\gamma^* \to q\bar{q}$ yield four different four-parton quark-antiquark antenna functions: the leading and subleading colour quark-antiquark-gluon-gluon antennae $A_4^0(1_q, 3_g, 4_g, 2_{\bar{q}})$, $\tilde{A}_4^0(1_q, 3_g, 4_g, 2_{\bar{q}})$, as well as the antennae with two quark-antiquark pairs of different and identical flavour $B_4^0(1_q, 3_{q'}, 4_{\bar{q}'}, 2_{\bar{q}})$ and $C_4^0(1_q, 3_q, 4_{\bar{q}}, 2_{\bar{q}})$. Their single and double unresolved limits are described in the following. We shall always restrict ourselves to the non-vanishing limits only.

In $A_4^0(1,3,4,2)$, the colour-ordering of the gluonic emissions ensures that only neighbouring partons can form singular configurations. While singularities are present in $1/s_{13}$ and $1/s_{24}$, no singularities in $1/s_{14}$ and $1/s_{23}$ appear.

For this colour-ordered antenna function, we find the following non-vanishing double unresolved limits:

1. Double soft and soft-collinear limits:
$$\begin{aligned}
A_4^0(1,3,4,2) &\xrightarrow{3_g\to 0, 4_g\to 0} S_{1342}\,,\\
A_4^0(1,3,4,2) &\xrightarrow{3_g\to 0, 4_g\| 2_{\bar{q}}} S_{1;342}(z)\, \frac{1}{s_{24}}\, P_{qg\to Q}(z)\,,\\
A_4^0(1,3,4,2) &\xrightarrow{4_g\to 0, 3_g\| 1_q} S_{2;431}(z)\, \frac{1}{s_{13}}\, P_{qg\to Q}(z)\,.
\end{aligned} \tag{8.16}$$

2. Triple collinear limits

$$A_4^0(1,3,4,2) \stackrel{1_q\|3_g\|4_g}{\longrightarrow} P_{134\to Q}(w,z,y)\,, \tag{8.17}$$

with quark (1_q) and antiquark ($2_{\bar{q}}$) being interchangeable.

3. Double collinear limits:

$$A_4^0(1,3,4,2) \stackrel{1_q\|3_g,2_{\bar{q}}\|g_4}{\longrightarrow} \frac{1}{s_{13}}\,P_{qg\to Q}(z)\,\frac{1}{s_{24}}\,P_{\bar{q}g\to\bar{Q}}(y)\,. \tag{8.18}$$

We find the following non-vanishing single unresolved limits:

1. Soft limits:

$$\begin{aligned} A_4^0(1,i,j,2) &\stackrel{i_g\to 0}{\longrightarrow} S_{1ij}\;A_3^0(1,j,2)\,,\\ A_4^0(1,i,j,2) &\stackrel{j_g\to 0}{\longrightarrow} S_{ij2}\;A_3^0(1,i,2)\,. \end{aligned} \tag{8.19}$$

2. Collinear limits (quark-gluon):

$$\begin{aligned} A_4^0(1,3,4,2) &\stackrel{1_q\|3_g}{\longrightarrow} \frac{1}{s_{13}}\,P_{qg\to Q}(z)\;A_3^0((13),4,2)\,,\\ A_4^0(1,3,4,2) &\stackrel{2_{\bar{q}}\|4_g}{\longrightarrow} \frac{1}{s_{24}}\,P_{qg\to Q}(z)\;A_3^0(1,3,(24))\,, \end{aligned} \tag{8.20}$$

where the parent parton of the collinear partons (1) and (3) (or (2) and (4)) is denoted (13) (or (24)) in the three-parton antenna function A_3^0.

3. Collinear limit (gluon-gluon):

$$A_4^0(1,3,4,2) \stackrel{3_g\|4_g}{\longrightarrow} \frac{1}{s_{34}}\,P_{gg\to G}(z)\;A_3^0(1,(34),2)\;+\;\text{ang.}\,, \tag{8.21}$$

where (ang.) means that angular terms are also present here. These do however cancel after integration over the unresolved phase space. A detailed discussion of these angular terms can be found in section 8.5 below.

The limits of the other colour-ordered subtraction term, $A_4^0(1,4,3,2)$, can be inferred from the limits of $A_4^0(1,3,4,2)$ listed above by interchanging the momenta of the two final state gluons (3_g) and (4_g).

The subleading colour contribution $\tilde{A}_4^0(1,3,4,2)$ is not colour-ordered, and therefore symmetric under the interchange of the two gluon momenta 3 and 4. We find the following non-vanishing double unresolved limits:

1. Double soft and soft-collinear limits:

$$\begin{aligned} \tilde{A}_4^0(1,3,4,2) &\stackrel{3_g\to 0,4_g\to 0}{\longrightarrow} S_{132}S_{142}\,,\\ \tilde{A}_4^0(1,i,j,2) &\stackrel{g_i\to 0,g_j\|q_2}{\longrightarrow} \tilde{S}_{1;ij2}(z)\,\frac{1}{s_{j2}}\,P_{qg\to Q}(z)\,, \end{aligned} \tag{8.22}$$

with i,j standing each for one of the two intermediate gluons. Quark (1_q) and antiquark ($2_{\bar{q}}$) are interchangeable.

JHEP09(2005)056

2. Triple collinear limits:

$$\tilde{A}_4^0(1,3,4,2) \stackrel{1_q\|3_g\|4_g}{\longrightarrow} \tilde{P}_{134\to Q}(w,x,y)\,, \tag{8.23}$$

with quark (1_q) and antiquark ($2_{\bar{q}}$) being interchangeable.

3. Double collinear limits:

$$\tilde{A}_4^0(1,i,j,2) \stackrel{1_q\|i_g,2_{\bar{q}}\|j_g}{\longrightarrow} \frac{1}{s_{1i}}\, P_{qg\to Q}(z)\, \frac{1}{s_{2j}}\, P_{\bar{q}g\to\bar{Q}}(y)\,, \tag{8.24}$$

with i and j each standing for one of the two gluons (3_g) or (4_g); quark (1_q) and antiquark ($2_{\bar{q}}$) can also be exchanged.

The non-vanishing single unresolved limits are:

1. Soft limits:

$$\tilde{A}_4^0(1,i,j,2) \stackrel{i_g\to 0}{\longrightarrow} S_{1i2}\, A_3^0(1,j,2)\,, \tag{8.25}$$

where i and j represent the two gluons (3_g) and (4_g).

2. Collinear limits:

$$\tilde{A}_4^0(1,i,j,2) \stackrel{1_q\|i_g}{\longrightarrow} \frac{1}{s_{1i}}\, P_{qg\to Q}(z)\, A_3^0((1i),j,2)\,. \tag{8.26}$$

Again, (1_q) and ($2_{\bar{q}}$) can be interchanged and i can stand for one of the two gluons (3_g) or (4_g).

For the antenna function containing two quark-antiquark pairs of non-identical flavours, $B_4^0(1_q,3_{q'},4_{\bar{q}'},2_{\bar{q}})$, we find the following double unresolved limits:

1. Double soft limit:

$$B_4^0(1,3,4,2) \stackrel{3_{q'}\to 0,4_{\bar{q}'}\to 0}{\longrightarrow} S_{12}(3,4)\,. \tag{8.27}$$

2. Triple collinear limit:

$$B_4^0(1,3,4,2) \stackrel{1_q\|3_{q'}\|4_{\bar{q}'}}{\longrightarrow} P^{\text{non-ident.}}_{143\to Q}(x,y)\,. \tag{8.28}$$

The quark (1_q) and antiquark ($2_{\bar{q}}$) momenta can be interchanged.

$B_4^0(1,3,4,2)$ contains only one single unresolved limit ($3_q \parallel 4_{\bar{q}}$):

$$B_4^0(1,3,4,2) \stackrel{3_{q'}\|4_{\bar{q}'}}{\longrightarrow} \frac{1}{s_{34}}\, P_{q\bar{q}\to G}(z)\, A_3^0(1,(34),2) + \text{ang.}\,, \tag{8.29}$$

where (ang.) means that angular terms are also obtained here.

Finally we consider the identical-flavour-only antenna function denoted by $C_4^0(1_q,3_q,4_{\bar{q}},2_{\bar{q}})$. This function is proportional has only one non-vanishing double unresolved limit: triple collinear ($2_{\bar{q}} \parallel 4_{\bar{q}} \parallel 3_q$),

$$C_4^0(1,3,4,2) \stackrel{2_{\bar{q}}\|3_q\|4_{\bar{q}}}{\longrightarrow} \frac{1}{2}\, P^{\text{ident.}}_{234\to\bar{Q}}(w,x,y)\,. \tag{8.30}$$

This antenna function has no further non-vanishing (double or single unresolved) limits, although terms in $1/s_{24}$ and $1/s_{34}$ are present in the function. In the respective limits, the coefficients of these terms vanish.

8.3 Quark-gluon antennae

The quark-gluon antenna functions were derived in section 6 above. We describe their behaviour in all single and double unresolved limits in the following. Again, we will only list the non-vanishing contributions. In all these functions, the quark (1_q) can also represent an antiquark.

8.3.1 Three-parton antenna functions

The tree-level three-parton quark-gluon antenna functions represent two final states: quark-gluon-gluon ($D_3^0(1_q, 3_g, 4_g)$) and quark-quark-antiquark ($E_3^0(1_q, 3_{q'}, 4_{\bar{q}'})$).

The tree-level antenna function $D_3^0(1_q, 3_g, 4_g)$ contains two colour orderings corresponding to the following configurations: gluon (3_g) radiated between quark (1_q) and gluon (4_g) denoted by $d_3^0(1,3,4)$ and gluon (3_g) radiated between quark (1_q) and gluon (4_g) denoted by $d_3^0(1,4,3)$, such that

$$D_3^0(1,3,4) = d_3^0(1,3,4) + d_3^0(1,4,3)\,.$$

The separation between these is not free from an ambiguity. It is constructed in such a way that the collinear limit of the two gluons has to be split between the two configurations. The decomposition used here is stated in (6.13).

The simple unresolved limits of $D_3^0(1,3,4)$ and $d_3^0(1,3,4)$ are stated below. For the sake of clarity, we also list some non-trivial vanishing limits:

1. Soft limits:

$$\begin{aligned}
D_3^0(1,i,j) &\xrightarrow{i_g\to 0} S_{1ij}\,,\\
D_3^0(1,i,j) &\xrightarrow{j_g\to 0} S_{1ji}\,,\\
d_3^0(1,i,j) &\xrightarrow{i_g\to 0} S_{1ij}\,,\\
d_3^0(1,i,j) &\xrightarrow{j_g\to 0} 0\,.
\end{aligned}\tag{8.31}$$

2. Collinear limits:

$$\begin{aligned}
D_3^0(1,3,4) &\xrightarrow{3_g\|4_g} \frac{1}{s_{34}}\,P_{gg\to G}(z)\,,\\
d_3^0(1,3,4) &\xrightarrow{3_g\|4_g} \frac{1}{s_{34}}\left(P_{gg\to G}(z) - \frac{2z}{1-z} - z(1-z)\right)\,,\\
d_3^0(1,4,3) &\xrightarrow{3_g\|4_g} \frac{1}{s_{34}}\left(P_{gg\to G}(z) - \frac{2(1-z)}{z} - z(1-z)\right)\,,\\
D_3^0(1,i,j) &\xrightarrow{1_q\|i_g} \frac{1}{s_{1i}}\,P_{qg\to Q}(z)\,,\\
D_3^0(1,i,j) &\xrightarrow{1_q\|j_g} \frac{1}{s_{1j}}\,P_{qg\to Q}(z)\,,\\
d_3^0(1,i,j) &\xrightarrow{1_q\|i_g} \frac{1}{s_{1i}}\,P_{qg\to Q}(z)\,,\\
d_3^0(1,i,j) &\xrightarrow{1_q\|j_g} 0\,.
\end{aligned}\tag{8.32}$$

The antenna function $E_3^0(1_q, 3_{q'}, 4_{\bar{q}'})$ has only one singular behaviour, when the quark-antiquark pair becomes collinear:

$$E_3^0(1,3,4) \stackrel{3_{q'}\|4_{\bar{q}'}}{\longrightarrow} \frac{1}{s_{34}}\, P_{q\bar{q}\to G}(z)\,. \tag{8.33}$$

8.3.2 Four-parton antenna functions

The NNLO real radiation corrections to $\tilde{\chi} \to \tilde{g}g$ yield three different four-parton quark-gluon antenna functions: the quark-gluon-gluon-gluon antenna contains only a leading colour (colour-ordered) term $D_4^0(1_q, 3_g, 4_g, 5_g)$, while the quark-quark-antiquark-gluon antennae have leading colour and subleading colour contributions $E_4^0(1_q, 3_{q'}, 4_{\bar{q}'}, 5_g)$ and $\tilde{E}_4^0(1_q, 3_{q'}, 4_{\bar{q}'}, 5_g)$. By construction, no identical-flavour contribution appears. The non-vanishing single and double unresolved limits of these antenna functions are described in the following. As before, some of the single unresolved limits also contain angular terms, which will be discussed in more detail in section 8.5 below.

The colour-ordered quark-gluon-gluon-gluon antenna function $D_4^0(1_q, 3_g, 4_g, 5_g)$ contains several different antenna configurations: due to the cyclic nature of the colour indices of the $\tilde{\chi} \to \tilde{g}ggg$ matrix element [46], each pair of two neighbouring partons can represent the two hard partons forming the antenna. This behaviour is in contrast to the quark-antiquark antennae described in the previous subsection, where the colour-ordering ensures that the primary quark-antiquark pair always forms the hard partons. Consequently, D_4^0 contains considerably more double and single unresolved limits than the four-parton quark-antiquark antenna functions studied above.

For the double unresolved limits we find:

1. Double soft and soft-collinear limits:

$$\begin{aligned}
D_4^0(1,3,4,5) &\stackrel{3_g\to 0, 4_g\to 0}{\longrightarrow} S_{1345}\,,\\
D_4^0(1,3,4,5) &\stackrel{4_g\to 0, 5_g\to 0}{\longrightarrow} S_{1543}\,,\\
D_4^0(1,3,4,5) &\stackrel{3_g\to 0, 5_g\to 0}{\longrightarrow} S_{134}\, S_{154}\,,
\end{aligned} \tag{8.34}$$

$$\begin{aligned}
D_4^0(1,3,4,5) &\stackrel{1_q\|5_g, 3_g\to 0}{\longrightarrow} S_{4;315}(z)\, \frac{1}{s_{15}}\, P_{qg\to Q}(1-z)\,,\\
D_4^0(1,3,4,5) &\stackrel{4_g\|5_g, 3_g\to 0}{\longrightarrow} S_{1;345}(z)\, \frac{1}{s_{45}}\, P_{gg\to G}(z)\,,\\
D_4^0(1,3,4,5) &\stackrel{1_q\|3_g, 4_g\to 0}{\longrightarrow} S_{5;431}(z)\, \frac{1}{s_{13}}\, P_{qg\to Q}(z)\,,\\
D_4^0(1,3,4,5) &\stackrel{1_q\|5_g, 4_g\to 0}{\longrightarrow} S_{3;451}(z)\, \frac{1}{s_{15}}\, P_{qg\to Q}(z)\,,\\
D_4^0(1,3,4,5) &\stackrel{1_q\|3_g, 5_g\to 0}{\longrightarrow} S_{4;513}(z)\, \frac{1}{s_{13}}\, P_{qg\to Q}(1-z)\,,\\
D_4^0(1,3,4,5) &\stackrel{3_g\|4_g, 5_g\to 0}{\longrightarrow} S_{1;543}(z)\, \frac{1}{s_{34}}\, P_{gg\to G}(z)\,.
\end{aligned} \tag{8.35}$$

2. Triple collinear limits:

$$
\begin{aligned}
D_4^0(1,3,4,5) &\xrightarrow{1_q\|3_g\|4_g} P_{134\to Q}(w,x,y)\,,\\
D_4^0(1,3,4,5) &\xrightarrow{1_q\|5_g\|4_g} P_{154\to Q}(w,x,y)\,,\\
D_4^0(1,3,4,5) &\xrightarrow{1_q\|3_g\|5_g} \tilde{P}_{135\to Q}(w,x,y)\,,\\
D_4^0(1,3,4,5) &\xrightarrow{3_g\|4_g\|5_g} P_{345\to G}(w,x,y)\,.
\end{aligned}
\tag{8.36}
$$

In these, the presence of the triple collinear limit ($1_q \parallel 3_g \parallel 5_g$) is particularly noteworthy. This limit appears due to the cyclic nature of the D_4^0 antenna function. In contrast to the other two triple collinear limits involving (1_q), where the leading colour triple collinear splitting function $P_{1ij\to Q}$ appears, this limit is controlled by the subleading colour splitting function $\tilde{P}_{135\to Q}$, since the gluons (3_g) and (5_g) are not directly colour-connected. Applying D_4^0 as antenna subtraction term to a physical multi-parton matrix element, special care has to be taken about this particular limit, which is a priori oversubtracted.

3. Double collinear limits:

$$
\begin{aligned}
D_4^0(1,3,4,5) &\xrightarrow{1_q\|3_g,4_g\|5_g} \frac{1}{s_{13}s_{45}}\,P_{qg\to Q}(z)\;P_{gg\to G}(y)\,,\\
D_4^0(1,3,4,5) &\xrightarrow{1_q\|5_g,3_g\|4_g} \frac{1}{s_{15}s_{34}}\,P_{qg\to Q}(z)\;P_{gg\to G}(y)\,.
\end{aligned}
\tag{8.37}
$$

For the single unresolved limits we obtain:

1. Soft limits:

$$
\begin{aligned}
D_4^0(1,3,4,5) &\xrightarrow{3_g\to 0} S_{134}\;D_3^0(1,4,5)\,,\\
D_4^0(1,3,4,5) &\xrightarrow{4_g\to 0} S_{345}\;D_3^0(1,3,5)\,,\\
D_4^0(1,3,4,5) &\xrightarrow{5_g\to 0} S_{154}\;D_3^0(1,3,4)\,.
\end{aligned}
\tag{8.38}
$$

2. Collinear limits

$$
\begin{aligned}
D_4^0(1,3,4,5) &\xrightarrow{1_q\|3_g} \frac{1}{s_{13}}\,P_{qg\to Q}(z)\;D_3^0((13),4,5)\,,\\
D_4^0(1,3,4,5) &\xrightarrow{1_q\|5_g} \frac{1}{s_{15}}\,P_{qg\to Q}(z)\;D_3^0((15),3,4)\,,\\
D_4^0(1,3,4,5) &\xrightarrow{3_g\|4_g} \frac{1}{s_{34}}\,P_{gg\to G}(z)\;D_3^0((1,(34),5)+\text{ang.}\,,\\
D_4^0(1,3,4,5) &\xrightarrow{4_g\|5_g} \frac{1}{s_{45}}\,P_{gg\to G}(z)\;D_3^0((1,3,(45))+\text{ang.}\,.
\end{aligned}
\tag{8.39}
$$

The leading colour quark-quark-antiquark-gluon antenna function $E_4^0(1_q,3_{q'},4_{\bar{q}'},5_g)$ is colour-ordered: the gluon 5_g is emitted only between the primary quark (1_q) and the secondary antiquark ($4_{\bar{q}'}$). The second colour-ordering $E_4^0(1_q,4_{\bar{q}'},3_{q'},5_g)$ is obtained by exchanging the secondary quark and antiquark momenta.

For the double unresolved limits of this antenna function we find:

1. Double soft and soft-collinear limits:

$$E_4^0(1,3,4,5) \stackrel{3_{q'}\to 0, 4_{\bar{q}'}\to 0}{\longrightarrow} S_{15}(3,4)\,,$$
$$E_4^0(1,3,4,5) \stackrel{3_{q'}\|4_{\bar{q}'}, 5_g\to 0}{\longrightarrow} S_{1;543}(z)\,\frac{1}{s_{34}}\,P_{q\bar{q}\to G}(z)\,. \tag{8.40}$$

2. Triple collinear limits:

$$E_4^0(1,3,4,5) \stackrel{1_q\|3_{q'}\|4_{\bar{q}'}}{\longrightarrow} P^{\text{non-ident.}}_{134\to Q}(w,x,y)\,,$$
$$E_4^0(1,3,4,5) \stackrel{3_{q'}\|4_{\bar{q}'}\|5_g}{\longrightarrow} P_{543\to G}(w,x,y)\,. \tag{8.41}$$

3. Double collinear limit:

$$E_4^0(1,3,4,5) \stackrel{1_q\|5_g, 3_{q'}\|4_{\bar{q}'}}{\longrightarrow} \frac{1}{s_{34}s_{15}}\,P_{qg\to Q}(z)\,P_{q\bar{q}\to G}(y)\,. \tag{8.42}$$

For the single unresolved limits we obtain:

1. Soft limit:

$$E_4^0(1,3,4,5) \stackrel{5_g\to 0}{\longrightarrow} S_{154}\,E_3^0(1,3,4)\,, \tag{8.43}$$

2. Collinear limits:

$$E_4^0(1,3,4,5) \stackrel{3_{q'}\|4_{\bar{q}'}}{\longrightarrow} \frac{1}{s_{34}}\,P_{q\bar{q}\to G}(z)\,D_3^0(1,(34),5) + \text{ang.}\,,$$
$$E_4^0(1,3,4,5) \stackrel{4_{\bar{q}'}\|5_g}{\longrightarrow} \frac{1}{s_{45}}\,P_{qg\to Q}(z)\,E_3^0(1,3,(45))\,,$$
$$E_4^0(1,3,4,5) \stackrel{1_q\|5_g}{\longrightarrow} \frac{1}{s_{15}}\,P_{qg\to Q}(z)\,E_3^0((15),3,4)\,. \tag{8.44}$$

In the subleading colour antenna $\tilde{E}_4^0(1_q, 3_{q'}, 4_{\bar{q}'}, 5_g)$ the gluon (5_g) is radiated between the secondary quark-antiquark pair$(3_{q'}, 4_{\bar{q}'})$. As a consequence, no singular structure involves the primary quark (1_q), thus limiting the number of singular configurations contained in this antenna. It contains only one double unresolved configuration, triple collinear $(3_{q'} \parallel 4_{\bar{q}'} \parallel 5_g)$:

$$\tilde{E}_4^0(1,3,4,5) \stackrel{3_{q'}\|4_{\bar{q}'}\|5_g}{\longrightarrow} \tilde{P}_{534\to G}(w,x,y). \tag{8.45}$$

The single unresolved limits always involve the gluon (5_g). They read:

1. Soft limit:

$$\tilde{E}_4^0(1,3,4,5) \stackrel{g_5\to 0}{\longrightarrow} S_{354}\,E_3^0(1,3,4)\,. \tag{8.46}$$

2. Collinear limits:

$$\tilde{E}_4^0(1,i,j,5) \stackrel{i\|g_5}{\longrightarrow} \frac{1}{s_{i5}}\,P_{qg\to Q}(z)\,E_3^0(1,(i5),j)\,, \tag{8.47}$$

where i and j can both play the role of the quark $(3_{q'})$ or the antiquark $(4_{\bar{q}'})$.

8.4 Gluon-gluon antennae

The gluon-gluon antenna functions were derived in section 7 above. Their behaviour in all single and double unresolved limits is summarised in the following, where only the non-vanishing contributions are given.

8.4.1 Three-parton antenna functions

There are two tree-level three-parton gluon-gluon antenna functions: gluon-gluon-gluon $F_3^0(1_g, 2_g, 3_g)$ and gluon-quark-antiquark $G_3^0(1_g, 3_q, 4_{\bar{q}})$.

The tree-level antenna function $F_3^0(1_g, 2_g, 3_g)$ contains three antenna configurations since each pair of gluons can represent the hard partons, emitting the remaining third gluon. Each of these configurations is denoted by $f_3^0(i, j, k)$:

$$F_3^0(1,2,3) = f_3^0(1,2,3) + f_3^0(1,3,2) + f_3^0(2,1,3)\,.$$

As with the quark-gluon-gluon antenna function, this decomposition into antenna configurations is not unambiguous, the decomposition used here is stated in (7.13).

The simple unresolved limits of $F_3^0(1,2,3)$ and $f_3^0(1,2,3)$ are:

1. Soft limits:

$$\begin{aligned}
F_3^0(1,2,3) &\xrightarrow{1_g\to 0} S_{213}\,,\\
F_3^0(1,2,3) &\xrightarrow{2_g\to 0} S_{123}\,,\\
F_3^0(1,2,3) &\xrightarrow{3_g\to 0} S_{132}\,,\\
f_3^0(1,2,3) &\xrightarrow{2_g\to 0} S_{123}\,,\\
f_3^0(1,2,3) &\xrightarrow{1_g\to 0} 0\,,\\
f_3^0(1,2,3) &\xrightarrow{3_g\to 0} 0\,,
\end{aligned} \tag{8.48}$$

   where we also include the non-trivial vanishing limits for clarity.

2. Collinear limits:

$$\begin{aligned}
F_3^0(1,2,3) &\xrightarrow{1_g\|1_g} \frac{1}{s_{12}}\,P_{gg\to G}(z)\,,\\
F_3^0(1,2,3) &\xrightarrow{1_g\|2_g} \frac{1}{s_{13}}\,P_{gg\to G}(z)\,,\\
F_3^0(1,2,3) &\xrightarrow{2_g\|3_g} \frac{1}{s_{23}}\,P_{gg\to G}(z)\,,\\
f_3^0(1,2,3) &\xrightarrow{1_g\|2_g} \frac{1}{s_{12}}\left(P_{gg\to G}(z) - \frac{2z}{1-z} - z(1-z)\right)\,,\\
f_3^0(1,2,3) &\xrightarrow{2_g\|3_g} \frac{1}{s_{23}}\left(P_{gg\to G}(z) - \frac{2(1-z)}{z} - z(1-z)\right)\,,\\
f_3^0(1,2,3) &\xrightarrow{1_g\|3_g} 0\,.
\end{aligned} \tag{8.49}$$

JHEP09(2005)056

The gluon-quark-antiquark antenna function has only one unresolved configuration: if quark and antiquark are collinear. In this case,

$$G_3^0(1,3,4) \stackrel{3_q\|4_{\bar{q}}}{\longrightarrow} \frac{1}{s_{34}} P_{q\bar{q}\to G}(z). \tag{8.50}$$

8.4.2 Four-parton antenna functions

The NNLO real radiation corrections to $H \to gg$ yield four different four-parton gluon-gluon antenna functions: the gluon-gluon-gluon-gluon antenna contains only a leading colour (colour-ordered) term $F_4^0(1_g, 2_g, 3_g, 4_g)$, while the gluon-quark-antiquark-gluon antennae contain both leading colour and subleading colour contributions $G_4^0(1_g, 3_q, 4_{\bar{q}}, 2_g)$ and $\tilde{G}_4^0(1_g, 3_q, 4_{\bar{q}}, 2_g)$. Finally, there is also a quark-antiquark-quark-antiquark antenna function $H_4^0(1_q, 2_{\bar{q}}, 3_{q'}, 4_{\bar{q}'})$, where the quarks are of different flavour. Angular terms are indicated where appropriate and will be discussed in detail in section 8.5 below.

Like already observed in the quark-gluon case, the colour-ordered gluon-gluon-gluon-gluon antenna function $F_4^0(1_g, 2_g, 3_g, 4_g)$ contains several different antenna configurations: due to the cyclic nature of the colour indices of the $H \to gggg$ matrix element [47], each pair of two neighbouring partons can represent the two hard partons forming the antenna. In the following, the set $(ijkl)$ represents any of the ordered permutations $(1234, 2341, 3412, 4123)$.

The double unresolved limits are:

1. Double soft and soft-collinear limits:

$$\begin{aligned}
F_4^0(1,2,3,4) &\stackrel{j_g\to 0, k_g\to 0}{\longrightarrow} S_{ijkl}\,, \\
F_4^0(1,2,3,4) &\stackrel{j_g\to 0, l_g\to 0}{\longrightarrow} S_{ijk}\, S_{kli}\,, && (8.51)\\
F_4^0(1,2,3,4) &\stackrel{i_g\|j_g, k_g\to 0}{\longrightarrow} S_{l;kji}(z)\, \frac{1}{s_{ij}}\, P_{gg\to G}(z)\,, \\
F_4^0(1,2,3,4) &\stackrel{i_g\|j_g, l_g\to 0}{\longrightarrow} S_{k;lij}(z)\, \frac{1}{s_{ij}}\, P_{gg\to G}(z)\,. && (8.52)
\end{aligned}$$

2. Triple collinear limits:

$$F_4^0(1,2,3,4) \stackrel{i_g\|j_g\|k_g}{\longrightarrow} P_{ijk\to G}(w,x,y)\,. \tag{8.53}$$

3. Double collinear limits:

$$F_4^0(1,2,3,4) \stackrel{i_g\|j_g, k_g\|l_g}{\longrightarrow} \frac{1}{s_{ij}s_{kl}}\, P_{gg\to G}(z)\, P_{gg\to G}(y)\,. \tag{8.54}$$

In the single unresolved limits we have:

1. Soft limits:

$$F_4^0(1,2,3,4) \stackrel{j_g\to 0}{\longrightarrow} S_{ijk}\, F_3^0(i,k,l)\,. \tag{8.55}$$

2. Collinear limits:

$$F_4^0(1,2,3,4) \stackrel{i_g\|j_g}{\longrightarrow} \frac{1}{s_{ij}}\, P_{gg\to G}(z)\, F_3^0((ij),k,l) + \text{ang.}\,. \tag{8.56}$$

The leading colour gluon-gluon-quark-antiquark antenna function $G_4^0(1_g, 3_q, 4_{\bar{q}}, 2_g)$ is colour-ordered: the gluon (1_g) is emitted between gluon (2_g) and the quark (3_q), while (again due to the cyclic nature of the colour indices) gluon (2_g) is emitted between gluon (1_g) and the antiquark $(4_{\bar{q}})$. The second colour-ordering $G_4^0(1_g, 4_{\bar{q}}, 3_q, 2_g)$ is obtained by exchanging the quark and antiquark momenta.

The double unresolved limits of this antenna function are:

1. Double soft and soft-collinear limits:

$$G_4^0(1,3,4,2) \xrightarrow{3_q\to 0, 4_{\bar{q}}\to 0} S_{12}(3,4)\,, \tag{8.57}$$

$$\begin{aligned} G_4^0(1,3,4,2) &\xrightarrow{3_q\|4_{\bar{q}}, 2_g\to 0} S_{1;243}(z)\, \frac{1}{s_{34}}\, P_{q\bar{q}\to G}(z)\,,\\ G_4^0(1,2,3,4) &\xrightarrow{3_q\|4_{\bar{q}}, 1_g\to 0} S_{2;134}(z)\, \frac{1}{s_{34}}\, P_{q\bar{q}\to G}(z)\,. \end{aligned} \tag{8.58}$$

2. Triple collinear limits:

$$\begin{aligned} G_4^0(1,3,4,2) &\xrightarrow{1_g\|3_q\|4_{\bar{q}}} P_{134\to G}(w,x,y)\,,\\ G_4^0(1,3,4,2) &\xrightarrow{2_g\|3_q\|4_{\bar{q}}} P_{243\to G}(w,x,y)\,. \end{aligned} \tag{8.59}$$

3. Double collinear limit:

$$G_4^0(1,3,4,2) \xrightarrow{1_g\|2_g, 3_q\|4_{\bar{q}}} \frac{1}{s_{12}s_{34}}\, P_{gg\to G}(z)\, P_{q\bar{q}\to G}(y)\,. \tag{8.60}$$

For the single unresolved limits we have:

1. Soft limits:

$$\begin{aligned} G_4^0(1,3,4,2) &\xrightarrow{1_g\to 0} S_{213}\, G_3^0(2,3,4)\,,\\ G_4^0(1,3,4,2) &\xrightarrow{2_g\to 0} S_{124}\, G_3^0(1,3,4)\,. \end{aligned} \tag{8.61}$$

2. Collinear limits:

$$\begin{aligned} G_4^0(1,3,4,2) &\xrightarrow{1_g\|2_g} \frac{1}{s_{12}}\, P_{gg\to G}(z)\, G_3^0((12),3,4) + \text{ang.}\,,\\ G_4^0(1,3,4,2) &\xrightarrow{3_q\|4_{\bar{q}}} \frac{1}{s_{34}}\, P_{q\bar{q}\to G}(z)\, F_3^0(1,(34),2) + \text{ang.}\,,\\ G_4^0(1,3,4,2) &\xrightarrow{1_g\|3_q} \frac{1}{s_{13}}\, P_{qg\to Q}(z)\, G_3^0(2,(13),4)\,,\\ G_4^0(1,3,4,2) &\xrightarrow{4_{\bar{q}}\|2_g} \frac{1}{s_{24}}\, P_{qg\to Q}(z)\, G_3^0(1,3,(24))\,. \end{aligned} \tag{8.62}$$

In the subleading colour antenna $\tilde{G}_4^0(1_q, 3_q, 4_{\bar{q}}, 2_g)$ one of the gluons is radiated between the quark-antiquark pair$(3_q, 4_{\bar{q}})$, while the other is outside the quark-antiquark system. As a consequence, no singular structure involves both gluons at once.

This antenna function contains only one type of double unresolved configuration, the triple collinear limit:

$$\begin{aligned}
\tilde{G}_4^0(1,3,4,2) &\stackrel{1_g\|3_q\|4_{\bar{q}}}{\longrightarrow} \tilde{P}_{314\to G}(w,x,y)\,,\\
\tilde{G}_4^0(1,3,4,2) &\stackrel{2_g\|3_q\|4_{\bar{q}}}{\longrightarrow} \tilde{P}_{324\to G}(w,x,y). \qquad (8.63)
\end{aligned}$$

The single unresolved limits always involve one of the gluons. They read:

1. Soft limits:

$$\begin{aligned}
\tilde{G}_4^0(1,3,4,2) &\stackrel{g_1\to 0}{\longrightarrow} S_{314}\; G_3^0(2,3,4)\,,\\
\tilde{G}_4^0(1,3,4,2) &\stackrel{g_2\to 0}{\longrightarrow} S_{324}\; G_3^0(1,3,4)\,. \qquad (8.64)
\end{aligned}$$

2. Collinear limits:

$$\begin{aligned}
\tilde{G}_4^0(1,i,j,2) &\stackrel{i\|g_1}{\longrightarrow} \tfrac{1}{s_{1i}}\; P_{qg\to Q}(z)\; G_3^0(2,(i1),j)\;,\\
\tilde{G}_4^0(1,i,j,2) &\stackrel{i\|g_2}{\longrightarrow} \tfrac{1}{s_{2i}}\; P_{qg\to Q}(z)\; G_3^0(1,(i2),j)\,, \qquad (8.65)
\end{aligned}$$

   where i and j can both play the role of the quark or the antiquark.

The antenna function containing two quark-antiquark pairs of non-identical flavours, $H_4^0(1_q,2_{\bar{q}},3_{q'},4_{\bar{q}'})$ contains only one double unresolved limit, the double single collinear configuration:

$$H_4^0(1,2,3,4) \stackrel{1_q\|2_{\bar{q}},3_{q'}\|4_{\bar{q}'}}{\longrightarrow} \frac{1}{s_{12}s_{34}}\; P_{q\bar{q}\to G}(z)\; P_{q\bar{q}\to G}(y)\,. \qquad (8.66)$$

The two single collinear limits are:

$$\begin{aligned}
H_4^0(1,2,3,4) &\stackrel{1_q\|2_{\bar{q}}}{\longrightarrow} \frac{1}{s_{12}}\; P_{q\bar{q}\to G}(z)\; G_3^0((12),3,4) + \text{ang.}\,,\\
H_4^0(1,2,3,4) &\stackrel{3_{q'}\|4_{\bar{q}'}}{\longrightarrow} \frac{1}{s_{34}}\; P_{q\bar{q}\to G}(z)\; G_3^0(1,2,(34)) + \text{ang.}\,. \qquad (8.67)
\end{aligned}$$

8.5 Angular terms

Angular terms manifest themselves in collinear limits of antenna functions and matrix elements when a final state gluon splits into a quark-antiquark pair or into two gluons. Several examples were listed in section 8. To obtain local subtraction terms (i.e. subtraction terms which approach the full multi-parton matrix element in its unresolved limits before any integrations are carried out), it is necessary to take proper account of these angular terms. In this section, we illustrate an algorithmic procedure to reconstruct the angular terms appearing in the simple collinear limits of four-parton antenna functions. The same procedure can be generalised in principle to reconstruct angular terms appearing in the single and double unresolved limits of multi-parton matrix elements. First steps in this direction were performed in [29].

In the collinear limits arising from gluon splitting, the four-parton antenna functions do not yield the unpolarised splitting functions (8.2) multiplied by a spin-averaged three-parton antenna function. Instead, one finds that the four-parton antenna functions factorise into the corresponding spin-dependent tensorial splitting functions and tensorial three-parton antenna functions [40, 19].

JHEP09(2005)056

In constructing the subtraction terms for two colour-connected unresolved partons, section 2.3.2, we used the difference between four-parton antenna function and products of three-parton antenna functions (2.17). The former are intended to subtract all singularities in the double unresolved region, while the latter ensure that the whole subtraction term is free of singularities in all single unresolved regions. If the four-parton antenna appearing in (2.17) has simple unresolved limits where angular terms are present, the product of two three-parton antenna functions in the same equation will no longer subtract its simple collinear behaviour locally. The left-over terms are however vanishing after integration over the antenna phase space, thus not affecting the cancellation of infrared poles.

To access these angular terms correctly, one has to keep track of the transverse momentum components of the collinear partons. The collinear limit of partons p_1 and p_2 is defined [40] as the limit $k_\perp \to 0$ of

$$\begin{aligned} p_1^\mu &= z\, P^\mu + k_\perp^\mu - \frac{k_\perp^2}{z}\,\frac{n^\mu}{2\,P\cdot n}\,, \\ p_2^\mu &= (1-z)\, P^\mu - k_\perp^\mu - \frac{k_\perp^2}{(1-z)}\,\frac{n^\mu}{2\,P\cdot n}\,, \end{aligned} \tag{8.68}$$

with

$$s_{12} \equiv 2\,p_1\cdot p_2 = -\frac{k_\perp^2}{z\,(1-z)}\,. \tag{8.69}$$

In these equations the vector P^μ ($P^2 = 0$) denotes the collinear direction, while n^μ is an auxiliary light-like vector, which is necessary to specify the transverse component $k_\perp$ ($k_\perp \cdot P = k_\perp \cdot n = 0$). In the small $k_\perp$ limit (i.e. neglecting terms that are less singular than $1/k_\perp^2$), we find the following factorisation formulae of the four-parton antenna functions:

$$\begin{aligned} A_4^0(1,3,4,2) &\stackrel{3_g\|4_g}{\longrightarrow} \frac{1}{s_{34}}\, P^{\mu\nu}_{gg\to G}(z)\,(A_3^0)_{\mu\nu}(1,(34),2)\,, \\ B_4^0(1,3,4,2) &\stackrel{3_q\|4_{\bar q}}{\longrightarrow} \frac{1}{s_{34}}\, P^{\mu\nu}_{q\bar q\to Q}(z)\,(A_3^0)_{\mu\nu}(1,(34),2)\,, \\ D_4^0(1,3,4,5) &\stackrel{3_g\|4_g}{\longrightarrow} \frac{1}{s_{34}}\, P^{\mu\nu}_{gg\to G}(z)\,(D_3^0)_{\mu\nu}(1,(34),5)\,, \\ D_4^0(1,3,4,5) &\stackrel{4_g\|5_g}{\longrightarrow} \frac{1}{s_{45}}\, P^{\mu\nu}_{gg\to G}(z)\,(D_3^0)_{\mu\nu}(1,3,(45))\,, \\ E_4^0(1,3,4,5) &\stackrel{3_q\|4_{\bar q}}{\longrightarrow} \frac{1}{s_{34}}\, P^{\mu\nu}_{q\bar q\to G}(z)\,(D_3^0)_{\mu\nu}(1,(34),5)\,, \\ F_4^0(1,2,3,4) &\stackrel{i_g\|j_g}{\longrightarrow} \frac{1}{s_{ij}}\, P^{\mu\nu}_{gg\to G}(z)\,(F_3^0)_{\mu\nu}((ij),k,l)\,, \\ G_4^0(1,3,4,2) &\stackrel{1_g\|2_g}{\longrightarrow} \frac{1}{s_{12}}\, P^{\mu\nu}_{gg\to G}(z)\,(G_3^0)_{\mu\nu}((12),3,4)\,, \\ G_4^0(1,3,4,2) &\stackrel{3_q\|4_{\bar q}}{\longrightarrow} \frac{1}{s_{34}}\, P^{\mu\nu}_{q\bar q\to G}(z)\,(F_3^0)_{\mu\nu}(1,(34),2)\,, \\ H_4^0(1,2,3,4) &\stackrel{1_q\|2_{\bar q}}{\longrightarrow} \frac{1}{s_{12}}\, P^{\mu\nu}_{q\bar q\to G}(z)\,(G_3^0)_{\mu\nu}((12),3,4)\,, \\ H_4^0(1,2,3,4) &\stackrel{3_q\|4_{\bar q}}{\longrightarrow} \frac{1}{s_{34}}\, P^{\mu\nu}_{q\bar q\to G}(z)\,(G_3^0)_{\mu\nu}((34),1,2)\,. \end{aligned} \tag{8.70}$$

The spin-dependent splitting functions $P^{\mu\nu}$ appearing in these equations were given in [19]. The tensorial three-parton antenna functions $(X_3^0)_{\mu\nu}$ can be derived by analogy with the scalar three-parton antenna functions of sections 5–7 from physical squared matrix elements. Their tensorial structure is obtained by leaving the polarisation index of the gluon associated with the momentum P^μ uncontracted. On contraction of the tensorial three-parton antenna functions with a physical gluon polarisation average, we recover their scalar counterparts.

It should be noted that the collinear factorisation (8.70) of four-parton antenna functions in spin-dependent splitting functions and tensorial three-parton antenna functions prevents us a priori from using the scalar (spin-independent) antenna functions derived in the previous sections to construct local subtraction terms. It seems that tensorial antenna functions are required. However this problem can be circumenvented by explicitly isolating the angular terms as follows.

For each four-parton antenna function X_4^0 yielding angular terms in a given simple collinear limit (gluon splitting into two partons i and j in the final state), one considers an angular function denoted by $\Theta_{X_3^0}$. This function must fulfil two properties: (1) it yields the correct local behaviour in this particular limit and (2) it integrates to zero over the corresponding unresolved phase space. The second requirement is particularly important, since it ensures that the analytic integration will not be modified by the presence of these angular functions, and that the integrated scalar antennae are sufficient to fully describe the pole structure of the antenna subtraction. In principle, a local counterterm is not even required for the numerical implementation; it does however allow a point-by-point check of the correct numerical behaviour of the subtraction terms, and guarantees considerable improvement of the numerical stability.

We find that the local counterterms are obtained by the replacement

$$X_4^0(1,i,j,2) \rightarrow X_4^0(1,i,j,2) - \Theta_{X_3^0}(i,j,z,k_\perp)\,, \tag{8.71}$$

where the angular function $\Theta_{X_3^0}(i,j,z,k_\perp)$ is given by,

$$\Theta_{X_3^0}(i,j,z,k_\perp) = \left[\frac{1}{s_{ij}}\, P^{\mu\nu}_{ij\to(ij)}(z,k_\perp)(X_3^0)_{\mu\nu}(1,(ij),2) \; - \frac{1}{s_{ij}}\, P_{ij\to(ij)}(z)\; X_3^0(1,(ij),2)\right]. \tag{8.72}$$

In this equation, X_3^0 is the appropriate three-parton antenna function obtained from X_4^0 when partons i and j build the parent parton (ij). $P^{\mu\nu}_{ij\to(ij)}$ stands for the spin-dependent splitting function while $P_{ij\to(ij)}$ stands for the spin averaged splitting function appropriate to the limit under consideration. The collinear momentum fraction z can be expressed in terms of invariants formed by the momenta appearing in the four-parton antenna phase space. Its precise definition is irrelevant, as long as it yields the correct expression in the collinear limit. After the replacement (8.71), the resulting four-parton antenna function is locally free from singular terms in the single unresolved regions.

On the other hand, the term $\Theta_{X_3^0}(i,j,z,k_\perp)$ integrates to zero if integrated over the unresolved phase space, since

$$\int \mathrm{d}\phi\; k_\perp^\mu k_\perp^\nu\; f(k_\perp^2) = -\frac{d^{\mu\nu}}{d-2}\, k_\perp^2\; f(k_\perp^2)\,, \tag{8.73}$$

with

$$d^{\mu\nu} = g^{\mu\nu} - \frac{P^\mu n^\nu + n^\mu P^\nu}{n \cdot P}$$

being the gluon polarisation sum in the axial gauge. Applied to the spin-dependent splitting function $P^{\mu\nu}_{ij\to(ij)}$, relation (8.73) yields the spin-averaged splitting function $d^{\mu\nu}P_{ij\to(ij)}$. Contraction with the tensorial antenna function $(X_3^0)_{\mu\nu}$ then reproduces the product of the spin-averaged splitting function with the scalar antenna function $P_{ij\to(ij)}\,(X_3^0)$. Integration of $\Theta_{X_3^0}$ over the three-parton antenna phase space made from momenta (i), (j) and either (1) or (2) yields zero by construction.

To illustrate the angular replacement (8.71) on a specific example, we consider the four-parton antenna function $B_4^0(1_q, 3_{q'}, 4_{\bar{q}'}, 2_{\bar{q}})$ in the $(3 \parallel 4)$ limit:

$$B_4^0(1,3,4,2) \to B_4^0(1,3,4,2) - \Theta_{A_3^0}(i,j,z,k_\perp)\,, \tag{8.74}$$

with

$$\Theta_{A_3^0}(i,j,z,k_\perp) = \frac{1}{s_{34}}\, P^{\mu\nu}_{q\bar{q}\to Q}(z,k_\perp)\, (A_3^0)_{\mu\nu}(1,(34),2) - \frac{1}{s_{34}}\, P_{q\bar{q}\to Q}(z) A_3^0(1,(34),2)\,, \tag{8.75}$$

where z is the momentum fraction carried by one of the collinear partons in the angular dependent function $\Theta_{A_3^0}(i,j,z,k_\perp)$.

In the colour-connected double unresolved subtraction term (2.17), B_4^0 appears in the combination

$$B_4^0(1,3,4,2) - E_3^0(1,3,4)\, A_3^0(1,(34),2)\,.$$

In the collinear $(3 \parallel 4)$ limit, this expression is not vanishing, but yields some residual angular terms. After substituting (8.74), this becomes

$$\begin{aligned} &B_4^0(1,3,4,2) - \left[\frac{1}{s_{34}}\, P^{\mu\nu}_{q\bar{q}\to Q}(z,k_\perp)\, (A_3^0)_{\mu\nu}(1,(34),2) - \frac{1}{s_{34}}\, P_{q\bar{q}\to Q}(z) A_3^0(1,(34),2)\right] - \\ &- E_3^0(1,3,4)\, A_3^0(1,(34),2)\,, \end{aligned} \tag{8.76}$$

which is free of singularities in the $3 \parallel 4$ limit, since (8.70) holds and,

$$E_3^0(1,3,4) \stackrel{3_q \parallel 4_{\bar{q}}}{\longrightarrow} \frac{1}{s_{34}}\, P_{g\to q\bar{q}}(z)\,. \tag{8.77}$$

The term $\Theta_{A_3^0}(i,j,z,k_\perp)$ vanishes when integrated over the unresolved phase space, because of (8.73).

9. The $1/N^2$ contribution to $e^+e^- \to 3$ jets at NNLO

To illustrate the application of antenna factorisation on a non-trivial example, in this section we derive the $1/N^2$-contribution to the NNLO corrections to $e^+e^- \to 3$ jets. For completeness, and also for future reference, we will first discuss all NNLO contributions to $e^+e^- \to 3$ jets in section 9.1. We construct the $1/N^2$ double real radiation subtraction term in section 9.2 and the $1/N^2$ virtual single real radiation subtraction term in section 9.3. In section 9.4, we then show how the integrated subtraction terms cancel the $1/N^2$-poles of the two-loop virtual corrections. Some details of the numerical implementation are discussed in section. 9.5. Finally, to illustrate the power of our approach, in section 10 we show that the infrared poles of the two-loop (including one-loop times one-loop) correction to $\gamma^* \to q\bar{q}g$ are cancelled in all colour factors by a combination of integrated three-parton and four-parton antenna functions.

The $\mathcal{O}(1/N^2)$ colour or QED-like contribution to three jet production in electron positron collisions receives contributions from several different partonic channels. There are contributions from $\gamma^* \to q\bar{q}ggg$ and $\gamma^* \to q\bar{q}q\bar{q}g$ at tree-level, $\gamma^* \to q\bar{q}gg$ and $\gamma^* \to q\bar{q}q\bar{q}$ at one-loop and $\gamma^* \to q\bar{q}g$ at two-loops. The four-parton and five-parton final states contain infrared singularities, which need to be extracted using the antenna subtraction formalism.

9.1 The matrix elements

First we list the tree, one-loop and two-loop amplitudes for $\gamma^* \to n$ partons where $n \leq 5$.

9.1.1 Tree-level matrix elements for up to five partons

The tree-level amplitude $M^0_{q\bar{q}(n-2)g}$ for a virtual photon to produce a quark-antiquark pair and $(n-2)$-gluons,

$$\gamma^*(q) \to q(p_1)\bar{q}(p_2)g(p_3)\dots g(p_n)$$

can be expressed as sum over the permutations of the colour-ordered amplitude $\mathcal{M}^0_{A,n}$ of the possible orderings for the gluon colour indices

$$M^0_{q\bar{q}(n-2)g} = ie(\sqrt{2}g)^{n-2} \sum_{(i,\dots,k)\in P(3,\dots,n)} (T^{a_i}\cdots T^{a_n})_{i_1 i_2}\, \mathcal{M}^0_{A,n}(p_1,p_3,\dots,p_n,p_2)\,. \tag{9.1}$$

The squared matrix elements for $n = 3,\dots,5$, summed over gluon polarisations, but excluding symmetry factors for identical particles, are given by,

$$\left|M^0_{q\bar{q}g}\right|^2 = N_3\, A^0_3(1_q,3_g,2_{\bar{q}})\,, \tag{9.2}$$

$$\left|M^0_{q\bar{q}gg}\right|^2 = N_4 \left[\sum_{(i,j)\in P(3,4)} N A^0_4(1_q,i_g,j_g,2_{\bar{q}}) - \frac{1}{N}\tilde{A}^0_4(1_q,3_g,4_g,2_{\bar{q}})\right]\,, \tag{9.3}$$

$$\begin{aligned}\left|M^0_{q\bar{q}ggg}\right|^2 = N_5 \Bigg[&\sum_{(i,j,k)\in P(3,4,5)} \Big(N^2 A^0_5(1_q,i_g,j_g,k_g,2_{\bar{q}}) - \tilde{A}^0_5(1_q,i_g,j_g,k_g,2_{\bar{q}})\Big) + \\ &+ \left(\frac{N^2+1}{N^2}\right) \bar{A}^0_5(1_q,3_g,4_g,5_g,2_{\bar{q}})\Bigg]\,,\end{aligned} \tag{9.4}$$

where,

$$N_n = 4\pi\alpha \sum_q e_q^2 \left(g^2\right)^{(n-2)} \left(N^2-1\right) \left|\mathcal{M}^0_{q\bar{q}}\right|^2\,, \tag{9.5}$$

and

$$\left|\mathcal{M}^0_{q\bar{q}}\right|^2 = 4(1-\epsilon)q^2. \tag{9.6}$$

The squared colour-ordered matrix elements A_3^0, A_4^0 and $\tilde{A}_4^0$ are given in eqs. (5.5), (5.27) and (5.28) respectively. For the five parton case,

$$A_5^0(1_q, i_g, j_g, k_g, 2_{\bar{q}}) \left|\mathcal{M}_{q\bar{q}}^0\right|^2 = \left|\mathcal{M}_{A,5}^0(p_1, p_i, p_j, p_k, p_2)\right|^2 \tag{9.7}$$

$$\begin{aligned}\tilde{A}_5^0(1_q, i_g, j_g, k_g, 2_{\bar{q}}) \left|\mathcal{M}_{q\bar{q}}^0\right|^2 &= \\ &= \left|\mathcal{M}_{A,5}^0(p_1, p_i, p_j, p_k, p_2) + \mathcal{M}_{A,5}^0(p_1, p_i, p_k, p_j, p_2) + \mathcal{M}_{A,5}^0(p_1, p_k, p_i, p_j, p_2)\right|^2,\end{aligned} \tag{9.8}$$

$$\bar{A}_5^0(1_q, i_g, j_g, k_g, 2_{\bar{q}}) \left|\mathcal{M}_{q\bar{q}}^0\right|^2 = \left|\sum_{(i,j,k)\in P(3,\ldots,5)} \mathcal{M}_{A,5}^0(p_1, p_i, p_j, p_k, p_2)\right|^2 . \tag{9.9}$$

In the sub-leading colour contribution $\tilde{A}_5^0$, gluon k is effectively photon-like, while in the sub-sub-leading colour contribution (also called abelian contribution), $\bar{A}_5^0$, all three gluons are effectively photon-like. Photon-like gluons do not couple to three- and four-gluon vertices, and there are no simple collinear limits as any two photon-like gluons become collinear. As a consequence, the only colour connected pair in $\bar{A}_5^0$ are the quark and antiquark. All subtraction terms for this five-parton contribution are therefore based on quark-antiquark antennae.

The tree-level amplitude for

$$\gamma^*(q) \to q(p_1)\bar{q}(p_2)q'(p_3)\bar{q}'(p_4)$$

is given by

$$\begin{aligned}M_{q\bar{q}q'\bar{q}'}^0 &= ie_1 g^2 \delta_{q_1q_2}\delta_{q_3q_4}\left(\delta_{i_1i_4}\delta_{i_3i_2} - \frac{1}{N}\delta_{i_1i_2}\delta_{i_3i_4}\right)\mathcal{M}_{B,4}^0(p_1, p_2, p_3, p_4) + \\ &\quad + (1 \leftrightarrow 3, 2 \leftrightarrow 4)\,,\end{aligned} \tag{9.10}$$

where $\delta_{q_1q_2}\delta_{q_3q_4}$ indicates the quark flavours. The amplitude $\mathcal{M}_{B,4}^0(p_1, p_2, p_3, p_4)$ thus denotes the contribution from the $q_1\bar{q}_2$–pair coupling to the vector boson. The identical quark amplitude is obtained

$$M_{q\bar{q}q\bar{q}}^0 = M_{q\bar{q}q'\bar{q}'}^0 - (2 \leftrightarrow 4)\,. \tag{9.11}$$

The resulting four-quark squared matrix elements, summed over final state quark flavours and including symmetry factors are given by

$$\begin{aligned}\left|M_{4q}^0\right|^2 &= \sum_{q,q'} \left|M_{q\bar{q}q'\bar{q}'}\right|^2 + \sum_q \left|M_{q\bar{q}q\bar{q}}\right|^2 \\ &= N_4\left[N_F B_4^0(1_q, 3_q, 4_{\bar{q}}, 2_{\bar{q}}) - \frac{1}{N}\left(C_4^0(1_q, 3_q, 4_{\bar{q}}, 2_{\bar{q}}) + C_4^0(2_{\bar{q}}, 4_{\bar{q}}, 3_q, 1_q)\right) + \right. \\ &\qquad \left. + N_{F,\gamma}\,\hat{B}_4^0(1_q, 3_q, 4_{\bar{q}}, 2_{\bar{q}})\right],\end{aligned} \tag{9.12}$$

where

$$B_4^0(1_q, 3_q, 4_{\bar{q}}, 2_{\bar{q}}) \left|\mathcal{M}_{q\bar{q}}^0\right|^2 = \left|\mathcal{M}_{B,4}^0(p_1, p_2, p_3, p_4)\right|^2,$$

$$C_4^0(1_q,3_q,4_{\bar q},2_{\bar q})\left|\mathcal{M}^0_{q\bar q}\right|^2 = -\mathrm{Re}\Big(\mathcal{M}^0_{B,4}(p_1,p_2,p_3,p_4)\mathcal{M}^{0,\dagger}_{B,4}(p_1,p_4,p_3,p_2)\Big)\,, \quad (9.13)$$

$$\hat B_4^0(1_q,3_q,4_{\bar q},2_{\bar q})\left|\mathcal{M}^0_{q\bar q}\right|^2 = \mathrm{Re}\Big(\mathcal{M}^0_{B,4}(p_1,p_2,p_3,p_4)\mathcal{M}^{0,\dagger}_{B,4}(p_3,p_4,p_1,p_2)\Big)\,. \quad (9.14)$$

Explicit expressions for B_4^0 and C_4^0 are given in eqs. (5.37) and (5.42) respectively. The last term, $\hat B_4^0$, is proportional to the charge weighted sum of the quark flavours, $N_{F,\gamma}$, which for electromagnetic interactions is given by,

$$N_{F,\gamma} = \frac{(\sum_q e_q)^2}{\sum_q e_q^2}\,. \quad (9.15)$$

It is relevant only for observables where the final state quark charge can be determined.

There are four colour structures in the tree-level amplitude for

$$\gamma^*(q)\to q(p_1)\bar q(p_2)q'(p_3)\bar q'(p_4)g(p_5)$$

which reads

$$\begin{aligned}M_{q\bar q q'\bar q' g} &= ie_1 g^3\sqrt{2}\delta_{q_1q_2}\delta_{q_3q_4}\times\\ &\times\Big[T^{a_5}_{i_1i_4}\delta_{i_3i_2}\mathcal{M}^{0,a}_{B,5}(p_1,p_2,p_3,p_4,p_5) - \frac{1}{N}T^{a_5}_{i_1i_2}\delta_{i_3i_4}\mathcal{M}^{0,c}_{B,5}(p_1,p_2,p_3,p_4,p_5) +\\ &\quad + T^{a_5}_{i_3i_2}\delta_{i_1i_4}\mathcal{M}^{0,b}_{B,5}(p_1,p_2,p_3,p_4,p_5) - \frac{1}{N}T^{a_5}_{i_3i_4}\delta_{i_1i_2}\mathcal{M}^{0,d}_{B,5}(p_1,p_2,p_3,p_4,p_5)\Big]\\ &\quad + (1\leftrightarrow 3, 2\leftrightarrow 4)\,. \end{aligned} \quad (9.16)$$

The amplitude $\mathcal{M}^{0,x}_{B,5}(p_1,p_2,p_3,p_4,p_5)$ for $x=a,\ldots,d$ denotes the contribution from the $q_1\bar q_2$–pair coupling to the vector boson. Due to the colour decomposition, the following relation holds between the leading and subleading colour amplitudes:

$$\begin{aligned}\mathcal{M}^{0,e}_{B,5}(p_1,p_2,p_3,p_4,p_5) &= \mathcal{M}^{0,a}_{B,5}(p_1,p_2,p_3,p_4,p_5) + \mathcal{M}^{0,b}_{B,5}(p_1,p_2,p_3,p_4,p_5)\\ &= \mathcal{M}^{0,c}_{B,5}(p_1,p_2,p_3,p_4,p_5) + \mathcal{M}^{0,d}_{B,5}(p_1,p_2,p_3,p_4,p_5)\,. \end{aligned} \quad (9.17)$$

As before, the identical quark matrix element is obtained by permuting the antiquark momenta,

$$M^0_{q\bar q q\bar q g} = M^0_{q\bar q q'\bar q' g} - (2\leftrightarrow 4)\,. \quad (9.18)$$

The squared matrix element, summed over flavours and including symmetry factors is given by,

$$\begin{aligned}\left|M^0_{4qg}\right|^2 &= \sum_{q,q'}|M_{q\bar q q'\bar q' g}|^2 + \sum_q |M_{q\bar q q\bar q g}|^2 \quad (9.19)\\ &= N_5\Big[NN_F\Big(B_5^{0,a}(1_q,5_g,4_{\bar q'};3_{q'},2_{\bar q}) + B_5^{0,b}(1_q,4_{\bar q'};3_{q'},5_g,2_{\bar q})\Big) +\\ &\quad + \frac{N_F}{N}\Big(B_5^{0,c}(1_q,5_g,2_{\bar q};3_{q'},4_{\bar q'}) + B_5^{0,d}(1_q,2_{\bar q};3_{q'},5_g,4_{\bar q'}) - 2B_5^{0,e}(1_q,2_{\bar q};3_{q'},4_{\bar q'};5_g)\Big) -\\ &\quad - C_5^0(1_q,3_q,4_{\bar q},5_g,2_{\bar q}) + \left(\frac{N^2+1}{N^2}\right)\Big(\tilde C_5^0(1_q,3_q,4_{\bar q},5_g,2_{\bar q}) + \tilde C_5^0(2_{\bar q},4_{\bar q},3_q,5_g,1_q)\Big) -\\ &\quad - NN_{F,\gamma}\Big(\hat B_5^{0,a}(1_q,5_g,4_{\bar q'};3_{q'},2_{\bar q}) + \hat B_5^{0,b}(1_q,4_{\bar q'};3_{q'},5_g,2_{\bar q}) - \hat B_5^{0,e}(1_q,4_{\bar q'};3_{q'},2_{\bar q},5_g)\Big) +\\ &\quad + \frac{N_{F,\gamma}}{N}\Big(\hat B_5^{0,c}(1_q,5_g,2_{\bar q};3_{q'},4_{\bar q'}) + \hat B_5^{0,d}(1_q,2_{\bar q};3_{q'},5_g,4_{\bar q'}) + \hat B_5^{0,e}(1_q,2_{\bar q};3_{q'},4_{\bar q'};5_g)\Big)\Big]\,,\end{aligned}$$

where for $x = a, \ldots, e$

$$B_5^{0,x}(\ldots)\left|\mathcal{M}^0_{q\bar{q}}\right|^2 = |\mathcal{M}^{0,x}_{B,5}(p_1,p_2,p_3,p_4,p_5)|^2\,, \tag{9.20}$$

$$\hat{B}_5^{0,x}(\ldots)\left|\mathcal{M}^0_{q\bar{q}}\right|^2 = \mathrm{Re}\left(\mathcal{M}^{0,x}_{B,5}(p_1,p_2,p_3,p_4,p_5)\mathcal{M}^{0,x,\dagger}_{B,5}(p_3,p_4,p_1,p_2,p_5)\right), \tag{9.21}$$

and

$$\begin{aligned}
C_5^0(1_q,3_q,4_{\bar{q}},5_g,2_{\bar{q}})\left|M^0_{q\bar{q}}\right|^2 = -2\mathrm{Re}\Big(&\mathcal{M}^{0,a}_{B,5}(p_1,p_2,p_3,p_4,p_5)\mathcal{M}^{0,c,\dagger}_{B,5}(p_1,p_4,p_3,p_2,p_5)+\\
&+\mathcal{M}^{0,b}_{B,5}(p_1,p_2,p_3,p_4,p_5)\mathcal{M}^{0,d,\dagger}_{B,5}(p_1,p_4,p_3,p_2,p_5)+\\
&+\mathcal{M}^{0,a}_{B,5}(p_1,p_2,p_3,p_4,p_5)\mathcal{M}^{0,d,\dagger}_{B,5}(p_3,p_2,p_1,p_4,p_5)+\\
&+\mathcal{M}^{0,b}_{B,5}(p_1,p_2,p_3,p_4,p_5)\mathcal{M}^{0,c,\dagger}_{B,5}(p_3,p_2,p_1,p_4,p_5)\Big)\,,\\
\tilde{C}_5^0(1_q,3_q,4_{\bar{q}},5_g,2_{\bar{q}})\left|M^0_{q\bar{q}}\right|^2 = -\mathrm{Re}\Big(&\mathcal{M}^{0,e}_{B,5}(p_1,p_2,p_3,p_4,p_5)\mathcal{M}^{0,e,\dagger}_{B,5}(p_1,p_4,p_3,p_2,p_5)\Big)
\end{aligned} \tag{9.22}$$

9.1.2 One-loop matrix elements for up to four partons

The renormalised one-loop amplitude $M^1_{q\bar{q}g}$ for a virtual photon to produce a quark-antiquark pair together with a single gluon,

$$\gamma^*(q) \to q(p_1)\bar{q}(p_2)g(p_3)$$

contains a single colour structure such that

$$M^1_{q\bar{q}g} = ie\sqrt{2}g\left(\frac{g^2}{16\pi^2}\right)T^{a_3}_{i_1i_2}\mathcal{M}^1_{A,3}(p_1,p_3,p_2)\,. \tag{9.23}$$

Unless stated otherwise, the renormalisation scale is set to $\mu^2 = q^2$.

The interference of the one-loop amplitude with the three-parton tree-level amplitude (9.1) is given by

$$2\mathrm{Re}\left(M^{0,\dagger}_{q\bar{q}g}M^1_{q\bar{q}g}\right) = N_3\left(\frac{\alpha_s}{2\pi}\right)A_3^{(1\times 0)}(1_q,3_g,2_{\bar{q}})\,, \tag{9.24}$$

where

$$\begin{aligned}
A_3^{(1\times 0)}(1_q,3_g,2_{\bar{q}}) = &\Big(N\left[A_3^1(1_q,3_g,2_{\bar{q}}) + \mathcal{A}_2^1(s_{123})A_3^0(1_q,3_g,2_{\bar{q}})\right] - \\
&-\frac{1}{N}\left[\tilde{A}_3^1(1_q,3_g,2_{\bar{q}}) + \mathcal{A}_2^1(s_{123})A_3^0(1_q,3_g,2_{\bar{q}})\right] + N_F\hat{A}_3^1(1_q,3_g,2_{\bar{q}})\Big)\,,
\end{aligned} \tag{9.25}$$

where A_3^1, $\tilde{A}_3^1$ and $\hat{A}_3^1$ are given up to $\mathcal{O}(\epsilon^0)$ in eqs. (5.13), (5.15) and (5.17) respectively.

The one-loop corrections to $\gamma^* \to 4$ partons have been available for some time [8]. The one-loop amplitude for

$$\gamma^*(q) \to q(p_1)\bar{q}(p_2)g(p_3)g(p_4)$$

contains two colour structures,

$$M^1_{q\bar{q}gg} = ie2g^2\left(\frac{g^2}{16\pi^2}\right)\times$$
$$\times\Bigg[\sum_{(i,j)\in P(3,4)}\left(T^{a_i}T^{a_j}\right)_{i_1i_2}\times$$
$$\times\left(N\mathcal{M}^{1,a}_{A,4}(p_1,p_i,p_j,p_2)-\frac{1}{N}\mathcal{M}^{1,b}_{A,4}(p_1,p_i,p_j,p_2)+N_F\mathcal{M}^{1,c}_{A,4}(p_1,p_i,p_j,p_2)\right)+$$
$$+\frac{1}{2}\delta^{a_ia_j}\delta_{i_1i_2}\mathcal{M}^{1,d}_{A,4}(p_1,p_3,p_4,p_2)\Bigg], \tag{9.26}$$

where

$$\mathcal{M}^{1,d}_{A,4}(p_1,p_3,p_4,p_2) = \mathcal{M}^{1,d}_{A,4}(p_1,p_4,p_3,p_2)\,. \tag{9.27}$$

The "squared" matrix element is the interference between the tree-level and one-loop amplitudes,

$$2\left|M^{0,\dagger}_{q\bar{q}gg}M^1_{q\bar{q}gg}\right| =$$
$$= N_4\left(\frac{\alpha_s}{2\pi}\right)\times$$
$$\times\Bigg[\sum_{(i,j)\in P(3,4)}\left(N^2A^{1,a}_4(1_q,i_g,j_g,2_{\bar{q}})-A^{1,b}_4(1_q,i_g,j_g,2_{\bar{q}})+NN_FA^{1,c}_4(1_q,i_g,j_g,2_{\bar{q}})\right)-$$
$$-\Bigg(\tilde{A}^{1,a}_4(1_q,3_g,4_g,2_{\bar{q}})-\tilde{A}^{1,d}_4(1_q,3_g,4_g,2_{\bar{q}})-\frac{1}{N^2}\tilde{A}^{1,b}_4(1_q,3_g,4_g,2_{\bar{q}})+$$
$$+\frac{N_F}{N}\tilde{A}^{1,c}_4(1_q,3_g,4_g,2_{\bar{q}})\Bigg)\Bigg], \tag{9.28}$$

where for $x=a,\dots,d$,

$$A^{1,x}_4(1_q,i_g,j_g,2_{\bar{q}})\left|\mathcal{M}^0_{q\bar{q}}\right|^2 = \mathrm{Re}\left(\mathcal{M}^{1,x}_{A,4}(p_1,p_i,p_j,p_2)\mathcal{M}^{0,\dagger}_{A,4}(p_1,p_i,p_j,p_2)\right), \tag{9.29}$$
$$\tilde{A}^{1,x}_4(1_q,3_g,4_g,2_{\bar{q}})\left|\mathcal{M}^0_{q\bar{q}}\right|^2 = \mathrm{Re}\left(\tilde{\mathcal{M}}^{1,x}_{A,4}(p_1,p_3,p_4,p_2)\tilde{\mathcal{M}}^{0,\dagger}_{A,4}(p_1,p_3,p_4,p_2)\right), \tag{9.30}$$

and

$$\tilde{\mathcal{M}}^{1,x}_{A,4}(p_1,p_3,p_4,p_2) = \mathcal{M}^{1,x}_{A,4}(p_1,p_3,p_4,p_2)+\mathcal{M}^{1,x}_{A,4}(p_1,p_4,p_3,p_2). \tag{9.31}$$

The renormalised singularity structure of the various contributions can be easily written in terms of the tree-level squared matrix elements multiplied by combinations of the infrared singularity operators of section 4. Explicitly, we find

$$\mathcal{P}oles(A^{1,a}_4(1_q,i_g,j_g,2_{\bar{q}})) = 2\left(\mathbf{I}^{(1)}_{qg}(\epsilon,s_{1i})+\mathbf{I}^{(1)}_{gg}(\epsilon,s_{ij})+\mathbf{I}^{(1)}_{g\bar{q}}(\epsilon,s_{j2})\right)A^0_4(1_q,i_g,j_g,2_{\bar{q}})\,,$$
$$\mathcal{P}oles(A^{1,b}_4(1_q,i_g,j_g,2_{\bar{q}})) = 2\mathbf{I}^{(1)}_{q\bar{q}}(\epsilon,s_{12})A^0_4(1_q,i_g,j_g,2_{\bar{q}})\,, \tag{9.32}$$
$$\mathcal{P}oles(A^{1,c}_4(1_q,i_g,j_g,2_{\bar{q}})) = 2\left(\mathbf{I}^{(1)}_{qg,F}(\epsilon,s_{1i})+\mathbf{I}^{(1)}_{gg,F}(\epsilon,s_{ij})+\mathbf{I}^{(1)}_{g\bar{q},F}(\epsilon,s_{j2})\right)A^0_4(1_q,i_g,j_g,2_{\bar{q}})\,,$$
$$\mathcal{P}oles(\tilde{A}^{1,a}_4(1_q,3_g,4_g,2_{\bar{q}})) =$$
$$=\left(2\mathbf{I}^{(1)}_{gg}(\epsilon,s_{34})+\mathbf{I}^{(1)}_{qg}(\epsilon,s_{14})+\mathbf{I}^{(1)}_{g\bar{q}}(\epsilon,s_{23})+\mathbf{I}^{(1)}_{qg}(\epsilon,s_{13})+\mathbf{I}^{(1)}_{g\bar{q}}(\epsilon,s_{24})\right)\tilde{A}^0_4(1_q,3_g,4_g,2_{\bar{q}})\,,$$

$$\mathcal{P}oles(\tilde{A}_4^{1,b}(1_q,3_g,4_g,2_{\bar{q}})) = 2\mathbf{I}^{(1)}_{q\bar{q}}(\epsilon,s_{12})\tilde{A}_4^0(1_q,3_g,4_g,2_{\bar{q}})\,, \tag{9.33}$$

$$\begin{aligned}\mathcal{P}oles(\tilde{A}_4^{1,c}&(1_q,3_g,4_g,2_{\bar{q}})) = \\ &= \Big(2\mathbf{I}^{(1)}_{gg,F}(\epsilon,s_{34})+\mathbf{I}^{(1)}_{qg,F}(\epsilon,s_{14})+\mathbf{I}^{(1)}_{g\bar{q},F}(\epsilon,s_{23})+\mathbf{I}^{(1)}_{qg,F}(\epsilon,s_{13})+\mathbf{I}^{(1)}_{g\bar{q},F}(\epsilon,s_{24})\Big)\times \\ &\quad\times \tilde{A}_4^0(1_q,3_g,4_g,2_{\bar{q}})\,,\end{aligned} \tag{9.34}$$

$$\begin{aligned}\mathcal{P}oles(\tilde{A}_4^{1,d}&(1_q,3_g,4_g,2_{\bar{q}})) = \\ &= \Big(2\mathbf{I}^{(1)}_{q\bar{q}}(\epsilon,s_{12})+2\mathbf{I}^{(1)}_{gg}(\epsilon,s_{34})-\mathbf{I}^{(1)}_{qg}(\epsilon,s_{14})-\mathbf{I}^{(1)}_{g\bar{q}}(\epsilon,s_{23})-\mathbf{I}^{(1)}_{qg}(\epsilon,s_{13})-\mathbf{I}^{(1)}_{g\bar{q}}(\epsilon,s_{24})\Big)\times \\ &\quad\times \tilde{A}_4^0(1_q,3_g,4_g,2_{\bar{q}})\,.\end{aligned} \tag{9.35}$$

As at tree-level, the one-loop amplitude for

$$\gamma^*(q) \to q(p_1)\bar{q}(p_2)q'(p_3)\bar{q}'(p_4)$$

contains two colour structures,

$$\begin{aligned}M^1_{q\bar{q}q'\bar{q}'} &= \\ &= ie_1 g^2\left(\frac{g^2}{16\pi^2}\right)\delta_{q_1q_2}\delta_{q_3q_4}\times \\ &\quad\times\bigg[\delta_{i_1i_4}\delta_{i_3i_2}\Big(N\mathcal{M}^{1,a}_{B,4}(p_1,p_2,p_3,p_4)-\frac{1}{N}\mathcal{M}^{1,b}_{B,4}(p_1,p_2,p_3,p_4)+N_F\mathcal{M}^{1,c}_{B,4}(p_1,p_2,p_3,p_4)\Big)- \\ &\qquad -\frac{1}{N}\delta_{i_1i_2}\delta_{i_3i_4}\Big(N\mathcal{M}^{1,d}_{B,4}(p_1,p_2,p_3,p_4)-\frac{1}{N}\mathcal{M}^{1,e}_{B,4}(p_1,p_2,p_3,p_4)+ \\ &\qquad\qquad +N_F\mathcal{M}^{1,f}_{B,4}(p_1,p_2,p_3,p_4)\Big)\bigg]+(1\leftrightarrow 3, 2\leftrightarrow 4)\,,\end{aligned} \tag{9.36}$$

where

$$\mathcal{M}^{1,a}_{B,4}(p_1,p_2,p_3,p_4)+\mathcal{M}^{1,e}_{B,4}(p_1,p_2,p_3,p_4) = \mathcal{M}^{1,b}_{B,4}(p_1,p_2,p_3,p_4)+\mathcal{M}^{1,d}_{B,4}(p_1,p_2,p_3,p_4). \tag{9.37}$$

As before, the identical quark matrix element is obtained by permuting the antiquark momenta,

$$M^1_{q\bar{q}q\bar{q}} = M^1_{q\bar{q}q'\bar{q}'} - (2\leftrightarrow 4). \tag{9.38}$$

Summing over flavours and including symmetry factors, we find that the "squared" matrix element, is given by

$$\begin{aligned}2\left|M^{0,\dagger}_{4q}M^1_{4q}\right| &= \sum_{q,q'}2\left|M^{0,\dagger}_{q\bar{q}q'\bar{q}'}M^1_{q\bar{q}q'\bar{q}'}\right| + \sum_q 2\left|M^{0,\dagger}_{q\bar{q}q\bar{q}}M^1_{q\bar{q}q\bar{q}}\right| \\ &= N_4\left(\frac{\alpha_s}{2\pi}\right)\bigg[NN_FB_4^{1,a}(1_q,3_q,4_{\bar{q}},2_{\bar{q}})-\frac{N_F}{N}B_4^{1,b}(1_q,3_q,4_{\bar{q}},2_{\bar{q}})+ \\ &\qquad +N_F^2B_4^{1,c}(1_q,3_q,4_{\bar{q}},2_{\bar{q}})-C_4^{1,d}(1_q,3_q,4_{\bar{q}},2_{\bar{q}})+ \\ &\qquad +\frac{1}{N^2}C_4^{1,e}(1_q,3_q,4_{\bar{q}},2_{\bar{q}})-\frac{N_F}{N}C_4^{1,f}(1_q,3_q,4_{\bar{q}},2_{\bar{q}})- \\ &\qquad -C_4^{1,d}(2_{\bar{q}},4_{\bar{q}},3_q,1_q)+\frac{1}{N^2}C_4^{1,e}(2_{\bar{q}},4_{\bar{q}},3_q,1_q)-\end{aligned}$$

$$- \frac{N_F}{N} C_4^{1,f}(2_{\bar{q}}, 4_{\bar{q}}, 3_q, 1_q) + N N_{F,\gamma} \hat{B}_4^{1,a}(1_q, 3_q, 4_{\bar{q}}, 2_{\bar{q}}) -$$
$$- \frac{N_{F,\gamma}}{N} \hat{B}_4^{1,b}(1_q, 3_q, 4_{\bar{q}}, 2_{\bar{q}}) + N_F N_{F,\gamma} \hat{B}_4^{1,c}(1_q, 3_q, 4_{\bar{q}}, 2_{\bar{q}}) \Big], \quad (9.39)$$

where for $x = a, b, c$

$$B_4^{1,x}(1_q, 3_q, 4_{\bar{q}}, 2_{\bar{q}}) \left|\mathcal{M}^0_{q\bar{q}}\right|^2 = \mathrm{Re}\left(\mathcal{M}^{1,x}_{B,4}(p_1, p_2, p_3, p_4)\mathcal{M}^{0,\dagger}_{B,4}(p_1, p_2, p_3, p_4)\right), \quad (9.40)$$
$$\hat{B}_4^{1,x}(1_q, 3_q, 4_{\bar{q}}, 2_{\bar{q}}) \left|\mathcal{M}^0_{q\bar{q}}\right|^2 = \mathrm{Re}\left(\mathcal{M}^{1,x}_{B,4}(p_1, p_2, p_3, p_4)\mathcal{M}^{0,\dagger}_{B,4}(p_3, p_4, p_1, p_2)\right), \quad (9.41)$$

and for $x = d, e, f$

$$C_4^{1,x}(1_q, 3_q, 4_{\bar{q}}, 2_{\bar{q}}) \left|\mathcal{M}^0_{q\bar{q}}\right|^2 = -\mathrm{Re}\left(\mathcal{M}^{1,x}_{B,4}(p_1, p_2, p_3, p_4)\mathcal{M}^{0,\dagger}_{B,4}(p_1, p_4, p_3, p_2)\right). \quad (9.42)$$

Using the infrared singularity operators of section 4, we can extract the singular contributions of the renormalised one-loop contribution as,

$$\mathcal{P}oles(B_4^{1,a}(1_q, 3_q, 4_{\bar{q}}, 2_{\bar{q}})) = 2\left(\mathbf{I}^{(1)}_{q\bar{q}}(\epsilon, s_{14}) + \mathbf{I}^{(1)}_{q\bar{q}}(\epsilon, s_{23})\right) B_4^0(1_q, 3_q, 4_{\bar{q}}, 2_{\bar{q}}), \quad (9.43)$$
$$\mathcal{P}oles(B_4^{1,b}(1_q, 3_q, 4_{\bar{q}}, 2_{\bar{q}})) =$$
$$= 2\left(2\mathbf{I}^{(1)}_{q\bar{q}}(\epsilon, s_{14}) - 2\mathbf{I}^{(1)}_{q\bar{q}}(\epsilon, s_{13}) + 2\mathbf{I}^{(1)}_{q\bar{q}}(\epsilon, s_{23}) - 2\mathbf{I}^{(1)}_{q\bar{q}}(\epsilon, s_{24}) + \mathbf{I}^{(1)}_{q\bar{q}}(\epsilon, s_{12}) + \mathbf{I}^{(1)}_{q\bar{q}}(\epsilon, s_{34})\right) \times$$
$$\times B_4^0(1_q, 3_q, 4_{\bar{q}}, 2_{\bar{q}}), \quad (9.44)$$
$$\mathcal{P}oles(C_4^{1,d}(1_q, 3_q, 4_{\bar{q}}, 2_{\bar{q}})) = 2\left(\mathbf{I}^{(1)}_{q\bar{q}}(\epsilon, s_{13}) + \mathbf{I}^{(1)}_{q\bar{q}}(\epsilon, s_{24})\right) C_4^0(1_q, 3_q, 4_{\bar{q}}, 2_{\bar{q}}), \quad (9.45)$$
$$\mathcal{P}oles(C_4^{1,e}(1_q, 3_q, 4_{\bar{q}}, 2_{\bar{q}})) =$$
$$= 2\left(\mathbf{I}^{(1)}_{q\bar{q}}(\epsilon, s_{12}) + \mathbf{I}^{(1)}_{q\bar{q}}(\epsilon, s_{14}) + \mathbf{I}^{(1)}_{q\bar{q}}(\epsilon, s_{23}) + \mathbf{I}^{(1)}_{q\bar{q}}(\epsilon, s_{34}) - \mathbf{I}^{(1)}_{q\bar{q}}(\epsilon, s_{13}) - \mathbf{I}^{(1)}_{q\bar{q}}(\epsilon, s_{24})\right) \times$$
$$\times C_4^0(1_q, 3_q, 4_{\bar{q}}, 2_{\bar{q}}), \quad (9.46)$$
$$\mathcal{P}oles(\hat{B}_4^{1,a}(1_q, 3_q, 4_{\bar{q}}, 2_{\bar{q}})) = 2\left(\mathbf{I}^{(1)}_{q\bar{q}}(\epsilon, s_{14}) + \mathbf{I}^{(1)}_{q\bar{q}}(\epsilon, s_{23})\right) \hat{B}_4^0(1_q, 3_q, 4_{\bar{q}}, 2_{\bar{q}}), \quad (9.47)$$
$$\mathcal{P}oles(\hat{B}_4^{1,b}(1_q, 3_q, 4_{\bar{q}}, 2_{\bar{q}})) =$$
$$= 2\left(2\mathbf{I}^{(1)}_{q\bar{q}}(\epsilon, s_{14}) - 2\mathbf{I}^{(1)}_{q\bar{q}}(\epsilon, s_{13}) + 2\mathbf{I}^{(1)}_{q\bar{q}}(\epsilon, s_{23}) - 2\mathbf{I}^{(1)}_{q\bar{q}}(\epsilon, s_{24}) + \mathbf{I}^{(1)}_{q\bar{q}}(\epsilon, s_{12}) + \mathbf{I}^{(1)}_{q\bar{q}}(\epsilon, s_{34})\right) \times$$
$$\times \hat{B}_4^0(1_q, 3_q, 4_{\bar{q}}, 2_{\bar{q}}). \quad (9.48)$$

9.1.3 Two-loop matrix elements for three partons

The renormalised two-loop amplitude $M^2_{q\bar{q}g}$ for a virtual photon to produce a quark-antiquark pair together with a single gluon,

$$\gamma^*(q) \to q(p_1)\bar{q}(p_2)g(p_3)$$

contains a single colour structure such that

$$M^2_{q\bar{q}g} = ie\sqrt{2}g\left(\frac{g^2}{16\pi^2}\right)^2 T^{a_3}_{i_1 i_2}\mathcal{M}^2_{A,3}(p_1, p_3, p_2). \quad (9.49)$$

At NNLO, there are two contributions. One from the interference of the two-loop and tree-level amplitudes (9.1), the other from the square of the one-loop amplitudes given in (9.23). These terms were computed in [5] and are given by,

$$2\mathrm{Re}\left(M^{0,\dagger}_{q\bar{q}g}M^{2}_{q\bar{q}g}\right) = N_3\left(\frac{\alpha_s}{2\pi}\right)^2 A_3^{(2\times 0)}(1_q,3_g,2_{\bar{q}})\,, \tag{9.50}$$

$$\mathrm{Re}\left(M^{1,\dagger}_{q\bar{q}g}M^{1}_{q\bar{q}g}\right) = N_3\left(\frac{\alpha_s}{2\pi}\right)^2 A_3^{(1\times 1)}(1_q,3_g,2_{\bar{q}})\,. \tag{9.51}$$

Following [48], we organise the infrared pole structure of the NNLO contributions renormalised in the $\overline{\mathrm{MS}}$ scheme in terms of the tree and renormalised one-loop amplitudes such that,

$$\begin{aligned}\mathcal{P}oles&\left(A_3^{(2\times 0)}(1_q,3_g,2_{\bar{q}})+A_3^{(1\times 1)}(1_q,3_g,2_{\bar{q}})\right)=\\ &=2\Bigg[-\left(\boldsymbol{I}^{(1)}_{q\bar{q}g}(\epsilon)\right)^2-\frac{\beta_0}{\epsilon}\boldsymbol{I}^{(1)}_{q\bar{q}g}(\epsilon)+e^{-\epsilon\gamma}\frac{\Gamma(1-2\epsilon)}{\Gamma(1-\epsilon)}\left(\frac{\beta_0}{\epsilon}+K\right)\boldsymbol{I}^{(1)}_{q\bar{q}g}(2\epsilon)+\boldsymbol{H}^{(2)}_{q\bar{q}g}\Bigg]\times\\ &\quad\times A_3^0(1_q,3_g,2_{\bar{q}})+2\,\boldsymbol{I}^{(1)}_{q\bar{q}g}(\epsilon)\,A_3^{(1\times 0)}(1_q,3_g,2_{\bar{q}})\,.\end{aligned} \tag{9.52}$$

Here,

$$\begin{aligned}\boldsymbol{I}^{(1)}_{q\bar{q}g}(\epsilon) &= N\left(\boldsymbol{I}^{(1)}_{qg}(\epsilon,s_{13})+\boldsymbol{I}^{(1)}_{qg}(\epsilon,s_{23})\right)-\frac{1}{N}\boldsymbol{I}^{(1)}_{q\bar{q}}(\epsilon,s_{12})+\\ &\quad+N_F\left(\boldsymbol{I}^{(1)}_{qg,F}(\epsilon,s_{13})+\boldsymbol{I}^{(1)}_{qg,F}(\epsilon,s_{23})\right),\end{aligned} \tag{9.53}$$

with the individual $\boldsymbol{I}^{(1)}_{ij}$ defined in (4.1) and

$$\begin{aligned}\boldsymbol{H}^{(2)}_{q\bar{q}g} = \frac{e^{\epsilon\gamma}}{4\,\epsilon\,\Gamma(1-\epsilon)}\Bigg[&\left(4\zeta_3+\frac{589}{432}-\frac{11\pi^2}{72}\right)N^2+\left(-\frac{1}{2}\zeta_3-\frac{41}{54}-\frac{\pi^2}{48}\right)+\\ &+\left(-3\zeta_3-\frac{3}{16}+\frac{\pi^2}{4}\right)\frac{1}{N^2}+\left(-\frac{19}{18}+\frac{\pi^2}{36}\right)NN_F+\\ &+\left(-\frac{1}{54}-\frac{\pi^2}{24}\right)\frac{N_F}{N}+\frac{5}{27}N_F^2\Bigg].\end{aligned} \tag{9.54}$$

We denote the finite contributions as,

$$\begin{aligned}\mathcal{F}inite(A_3^{(2\times 0)}(1_q,3_g,2_{\bar{q}})) &= N^2A^{(2\times 0),\mathrm{finite}}_{3,N^2}+A^{(2\times 0),\mathrm{finite}}_{3,1}+\frac{1}{N^2}A^{(2\times 0),\mathrm{finite}}_{3,1/N^2}+\\ &\quad+NN_FA^{(2\times 0),\mathrm{finite}}_{3,NN_F}+\frac{N_F}{N}A^{(2\times 0),\mathrm{finite}}_{3,N_F/N}+\\ &\quad+N_F^2A^{(2\times 0),\mathrm{finite}}_{3,N_F^2}+N_{F,\gamma}\left(\frac{4}{N}-N\right)A^{(2\times 0),\mathrm{finite}}_{3,N^2_{F,\gamma}}\,,\end{aligned} \tag{9.55}$$

$$\begin{aligned}\mathcal{F}inite(A_3^{(1\times 1)}(1_q,3_g,2_{\bar{q}})) &= N^2A^{(1\times 1),\mathrm{finite}}_{3,N^2}+A^{(1\times 1),\mathrm{finite}}_{3,1}+\frac{1}{N^2}A^{(1\times 1),\mathrm{finite}}_{3,1/N^2}+\\ &\quad+NN_FA^{(1\times 1),\mathrm{finite}}_{3,NN_F}+\frac{N_F}{N}A^{(1\times 1),\mathrm{finite}}_{3,N_F/N}+\\ &\quad+N_F^2A^{(1\times 1),\mathrm{finite}}_{3,N_F^2}\,.\end{aligned} \tag{9.56}$$

Explicit formulae for the finite remainders have been given in [5]. These are expressed in terms of one-dimensional and two-dimensional harmonic polylogarithms (HPLs and 2dHPLs) [50, 51], which are generalisations of the well-known Nielsen polylogarithms [52]. A numerical implementation, which is required for all practical applications, is available for HPLs and 2dHPLs [53].

9.2 Five-parton contribution

Two different five-parton final states contribute at $1/N^2$ to three-jet final states at NNLO: $\gamma^* \to q\bar{q}ggg$ and $\gamma^* \to q\bar{q}q\bar{q}g$ with identical quarks.

The most colour suppressed contribution to the squared matrix element for $\gamma^* \to q\bar{q}ggg$ is proportional to $1/N^2$. It is given by,

$$\left|M^0_{q\bar{q}3g}\right|^2 = N_5\,\frac{1}{N^2}\,\bar{A}^0_5(1_q,3_g,4_g,5_g,2_{\bar{q}}), \tag{9.57}$$

while the identical quark contribution is

$$\left|M^0_{4qg}\right|^2 = N_5\,\frac{1}{N^2}\,\left[\tilde{C}^0_5(1_q,2_{\bar{q}},3_q,4_{\bar{q}},5_g) + \tilde{C}^0_5(3_q,2_{\bar{q}},1_q,4_{\bar{q}},5_g)\right]. \tag{9.58}$$

The NNLO radiation term appropriate for the three jet final state is given by

$$\mathrm{d}\sigma^R_{\mathrm{NNLO}} = \mathrm{d}\sigma^R_{\mathrm{NNLO},\bar{A}} + \mathrm{d}\sigma^R_{\mathrm{NNLO},\tilde{C}}\,, \tag{9.59}$$

with

$$\mathrm{d}\sigma^R_{\mathrm{NNLO},\bar{A}} = \frac{N_5}{N^2}\,\mathrm{d}\Phi_5(p_1,\ldots,p_5;q)\,\frac{1}{3!}\,\bar{A}^0_5(1_q,3_g,4_g,5_g,2_{\bar{q}})J_3^{(5)}(p_1,\ldots,p_5)\,, \tag{9.60}$$

$$\mathrm{d}\sigma^R_{\mathrm{NNLO},\tilde{C}} = \frac{N_5}{N^2}\,\mathrm{d}\Phi_5(p_1,\ldots,p_5;q)\,2\,\tilde{C}^0_5(1_q,2_{\bar{q}},3_q,4_{\bar{q}},5_g)J_3^{(5)}(p_1,\ldots,p_5)\,, \tag{9.61}$$

where the symmetry factor in front of $\bar{A}^0_5$ is due to the inherent indistinguishability of gluons. The factor 2 in front of $\tilde{C}^0_5$ arises from the fact that two different momentum arrangements contribute to the squared matrix element (9.58). If the quarks and antiquarks are not distinguished by the jet functions, these contribute equally.

The subtraction terms for these cross sections are straightforwardly obtained using the procedure detailed in section 2. Because there is only a single colour connected pair at $1/N^2$, there are no singularities associated with almost colour-unconnected or unconnected unresolved partons for either of the two contributions. Therefore

$$\mathrm{d}\sigma^{S,c}_{\mathrm{NNLO}} = \mathrm{d}\sigma^{S,d}_{\mathrm{NNLO}} = 0\,. \tag{9.62}$$

The other two types of real radiation subtraction terms are decomposed according to (9.59) as

$$\mathrm{d}\sigma^{S,i}_{\mathrm{NNLO}} = \mathrm{d}\sigma^{S,i}_{\mathrm{NNLO},\bar{A}} + \mathrm{d}\sigma^{S,i}_{\mathrm{NNLO},\tilde{C}}\,. \tag{9.63}$$

The subtraction terms for a single unresolved parton are obtained using (2.16),

$$
\begin{aligned}
\mathrm{d}\sigma^{S,a}_{\mathrm{NNLO},\tilde{A}} &= \frac{N_5}{N^2}\,\mathrm{d}\Phi_5(p_1,\ldots,p_5;q)\,\frac{1}{3!}\times \\
&\times \sum_{i,j,k\in P_C(3,4,5)} A_3^0(1_q,i_g,2_{\bar{q}})\,\tilde{A}_4^0(\widetilde{(1i)}_q,j_g,k_g,\widetilde{(2i)}_{\bar{q}})\;J_3^{(4)}(\widetilde{p_{1i}},p_j,p_k,\widetilde{p_{2i}})\,, \\
\mathrm{d}\sigma^{S,a}_{\mathrm{NNLO},\tilde{C}} &= \frac{N_5}{N^2}\,\mathrm{d}\Phi_5(p_1,\ldots,p_5;q)\,2\times \\
&\times \Big\{ A_3^0(1_q,5_g,2_{\bar{q}})\,C_4^0(\widetilde{(15)}_q,3_q,4_{\bar{q}},\widetilde{(25)}_{\bar{q}})\,J_3^{(4)}(\widetilde{p_{15}},p_3,p_4,\widetilde{p_{25}})\,+ \\
&\quad + A_3^0(1_q,5_g,4_{\bar{q}})\,C_4^0(\widetilde{(15)}_q,3_q,\widetilde{(45)}_{\bar{q}},2_{\bar{q}})\,J_3^{(4)}(\widetilde{p_{15}},p_2,p_3,\widetilde{p_{45}})\,+ \\
&\quad + A_3^0(3_q,5_g,2_{\bar{q}})\,C_4^0(1_q,\widetilde{(35)}_q,4_{\bar{q}},\widetilde{(25)}_{\bar{q}})\,J_3^{(4)}(\widetilde{p_{35}},p_1,p_4,\widetilde{p_{25}})\,+ \\
&\quad + A_3^0(3_q,5_g,4_{\bar{q}})\,C_4^0(1_q,\widetilde{(35)}_q,\widetilde{(45)}_{\bar{q}},2_{\bar{q}})\,J_3^{(4)}(\widetilde{p_{35}},p_1,p_2,\widetilde{p_{35}})\,- \\
&\quad - A_3^0(1_q,5_g,3_q)\,C_4^0(\widetilde{(15)}_q,\widetilde{(35)}_q,4_{\bar{q}},2_{\bar{q}})\,J_3^{(4)}(\widetilde{p_{15}},p_2,p_4,\widetilde{p_{35}})\,- \\
&\quad - A_3^0(2_{\bar{q}},5_g,4_{\bar{q}})\,C_4^0(1_q,3_q,\widetilde{(45)}_{\bar{q}},\widetilde{(25)}_{\bar{q}})\,J_3^{(4)}(\widetilde{p_{25}},p_1,p_3,\widetilde{p_{45}})\Big\}\,. \qquad (9.64)
\end{aligned}
$$

The sum in the first contribution runs only over the three cyclic permutations of the gluon momenta to prevent double counting of identical configurations obtained by interchange of j and k.

The colour-connected double unresolved subtraction terms are given by (see (2.17)),

$$
\begin{aligned}
\mathrm{d}\sigma^{S,b}_{\mathrm{NNLO},\tilde{A}} &= N_5\,\mathrm{d}\Phi_5(p_1,\ldots,p_5;q)\,\frac{1}{3!}\times \\
&\times \sum_{i,j,k\in P_C(3,4,5)} \Big(\tilde{A}_4^0(1_q,i_g,j_g,2_{\bar{q}}) - A_3^0(1_q,i_g,2_{\bar{q}})\;A_3^0(\widetilde{(1i)}_q,j_g,\widetilde{(2i)}_{\bar{q}}) \\
&\qquad\qquad - A_3^0(1_q,j_g,2_{\bar{q}})\;A_3^0(\widetilde{(1j)}_q,i_g,\widetilde{(2j)}_{\bar{q}})\Big)\times \\
&\times A_3^0(\widetilde{(1ij)}_q,k_g,\widetilde{(2ij)}_{\bar{q}})\;J_3^{(3)}(\widetilde{p_{1ij}},p_k,\widetilde{p_{2ij}})\,, \qquad (9.65) \\
\mathrm{d}\sigma^{S,b}_{\mathrm{NNLO},\tilde{C}} &= N_5\,\mathrm{d}\Phi_5(p_1,\ldots,p_5;q)\,2\times \\
&\times C_4^0(1_q,3_q,4_{\bar{q}},2_{\bar{q}})\,A_3^0(\widetilde{(134)}_q,5_g,\widetilde{(234)}_{\bar{q}})\;J_3^{(3)}(\widetilde{p_{134}},p_5,\widetilde{p_{234}})\,. \qquad (9.66)
\end{aligned}
$$

In the last equation, no single unresolved terms have to be subtracted from C_4^0, which contains only a single triple collinear limit, but no single unresolved limits (8.30).

By construction, the combination

$$
\mathrm{d}\sigma^{R}_{\mathrm{NNLO}} - \mathrm{d}\sigma^{S,a}_{\mathrm{NNLO}} - \mathrm{d}\sigma^{S,b}_{\mathrm{NNLO}} \qquad (9.67)
$$

is finite in all unresolved limits.

The momentum maps used in (9.64)–(9.66) are explicit realizations of the generic momentum maps denoted in section 2. In particular, in the single unresolved subtraction term (9.64), we map the three on-shell momenta i, j and k onto the on-shell momenta $(\widetilde{ij})$ and $(\widetilde{kj})$ by using the three-to-two-parton momentum map of [25]. With this mapping, the single unresolved phase spaces in the collinear limits of the unresolved momentum k with the hard momenta i or j are treated symmetrically. This mapping is in contrast to the dipole phase space mapping [40], where one collinear limit is mapped out to a larger phase space volume than the other. In the double unresolved subtraction terms (9.65) and (9.66), we map the four on-shell momenta i, j, k and l onto the on-shell momenta $(\widetilde{ijk})$ and $(\widetilde{ljk})$ by using the ordered four-to-two-parton momentum map of [25]. This mapping guarantees that both triple collinear limits of the unresolved momenta j and k with the hard momenta i or l are treated symmetrically. The single unresolved limits of j with i and of k with l are also mapped in a symmetric manner, ensuring the correctness of the double unresolved limit obtained by combining both of them. However, the phase space mapping of [25] used here does not yield the correct single unresolved behaviour of the phase space in the simple collinear limits of k with i or of j with l (as explained in detail in [25], it is not possible to construct a single four-to-two-parton momentum map which yields the correct simple unresolved behaviour in all four limits). We therefore decompose $\tilde{A}_4^0$ into its ordered components (which contain only two of the four simple collinear limits), as explained in the context of (5.28) and use either the ordered mapping onto $(\widetilde{ijk})$ and $(\widetilde{ljk})$ or onto $(\widetilde{ikj})$ and $(\widetilde{lkj})$. For clarity, these two mappings are not distinguished in (9.65). Since C_4^0 contains no simple collinear limit, but only triple collinear limits, it does not need to be decomposed any further.

9.3 Four-parton contribution

At one-loop, there are two contributions to the colour suppressed contribution proportional to $1/N^2$, one from the four quark final state and one from the two quark-two gluon final state. We therefore decompose the virtual one-loop four-parton contribution as

$$\mathrm{d}\sigma_{\mathrm{NNLO}}^{V,1} = \mathrm{d}\sigma_{\mathrm{NNLO},\tilde{A}}^{V,1} + \mathrm{d}\sigma_{\mathrm{NNLO},\tilde{C}}^{V,1}\,, \tag{9.68}$$

with

$$\mathrm{d}\sigma_{\mathrm{NNLO},\tilde{A}}^{V,1} = \frac{N_4}{N^2}\left(\frac{\alpha_s}{2\pi}\right)\mathrm{d}\Phi_4(p_1,\ldots,p_4;q)\,\frac{1}{2!}\,\tilde{A}_4^{1,b}(1_q,3_g,4_g,2_{\bar{q}})\;J_3^{(4)}(p_1,\ldots,p_4)\,, \tag{9.69}$$

$$\mathrm{d}\sigma_{\mathrm{NNLO},\tilde{C}}^{V,1} = \frac{N_4}{N^2}\left(\frac{\alpha_s}{2\pi}\right)\mathrm{d}\Phi_4(p_1,\ldots,p_4;q)\,2\,C_4^{1,e}(1_q,3_q,4_{\bar{q}},2_{\bar{q}})\;J_3^{(4)}(p_1,\ldots,p_4)\,, \tag{9.70}$$

where the origin of the symmetry factors is as in the real radiation five-parton contributions of the previous section.

As detailed in section 2, there are three subtraction terms; the subtraction of the infrared poles in the one-loop contribution, the subtraction of the one-loop unresolved part and a compensation term outside the singular region. The first of these three terms is constructed in (2.31). Following (2.32), it is minus the integrated form of $\mathrm{d}\sigma_{\mathrm{NNLO}}^{S,a}$ given in (9.64):

$$\begin{aligned}\mathrm{d}\sigma_{\mathrm{NNLO},\tilde{A}}^{VS,1,a} = &-\frac{N_4}{N^2}\left(\frac{\alpha_s}{2\pi}\right)\mathrm{d}\Phi_4(p_1,\ldots,p_4;q)\,\frac{1}{2!}\times\\ &\times\mathcal{A}_3^0(s_{12})\,\tilde{A}_4^0(1_q,3_g,4_g,2_{\bar{q}})\,J_3^{(4)}(p_1,p_3,p_4,p_2)\,,\end{aligned} \tag{9.71}$$

$$
\begin{aligned}
\mathrm{d}\sigma^{VS,1,a}_{\mathrm{NNLO},\tilde{C}} &= -\frac{N_4}{N^2}\left(\frac{\alpha_s}{2\pi}\right)\mathrm{d}\Phi_4(p_1,\ldots,p_4;q)\,2\,\times \\
&\times\left\{\mathcal{A}^0_3(s_{12})+\mathcal{A}^0_3(s_{14})+\mathcal{A}^0_3(s_{23})+\mathcal{A}^0_3(s_{34})-\mathcal{A}^0_3(s_{13})-\mathcal{A}^0_3(s_{24})\right\}\times \\
&\times C^0_4(1_q,3_q,4_{\bar{q}},2_{\bar{q}})J^{(4)}_3(p_1,p_3,p_4,p_2)\,. \qquad (9.72)
\end{aligned}
$$

Given that $\mathcal{P}oles(\mathcal{A}^0_3(s_{ij})) = -2\boldsymbol{I}^{(1)}_{q\bar{q}}(s_{ij})$, we see that the pole structures of these subtraction terms exactly cancel the pole structure of $\tilde{A}^{1,b}_4$ given in (9.33) and of $C^{1,e}_4$ given in (9.46).

Single particle unresolved contributions have to be subtracted only from (9.69), since (9.70) vanishes in all its single unresolved limits, implying

$$
\mathrm{d}\sigma^{VS,1,b}_{\mathrm{NNLO},\tilde{C}} = \mathrm{d}\sigma^{VS,1,c}_{\mathrm{NNLO},\tilde{C}} = 0\,. \qquad (9.73)
$$

Moreover, renormalisation does not affect the colour structure considered here.

From (2.33), we find:

$$
\begin{aligned}
\mathrm{d}\sigma^{VS,1,b}_{\mathrm{NNLO},\tilde{A}} &= \frac{N_4}{N^2}\left(\frac{\alpha_s}{2\pi}\right)\mathrm{d}\Phi_4(p_1,\ldots,p_4;q)\frac{1}{2!}\,\times \\
&\times\sum_{i,j\in P(3,4)}\Bigg(\tilde{A}^1_3(1_q,i_g,2_{\bar{q}})A^0_3(\widetilde{(1i)}_q,j_g,\widetilde{(2i)}_{\bar{q}})+A^0_3(1_q,i_g,2_{\bar{q}})\,\times \\
&\qquad\qquad\times\left[\tilde{A}^1_3(\widetilde{(1i)}_q,j_g,\widetilde{(2i)}_{\bar{q}})+\mathcal{A}^1_2(s_{1234})A^0_3(\widetilde{(1i)}_q,j_g,\widetilde{(2i)}_{\bar{q}})\right]\Bigg)\times \\
&\times J^{(3)}_3(\widetilde{p_{1i}},p_j,\widetilde{p_{2i}})\,. \qquad (9.74)
\end{aligned}
$$

The previous term correctly subtracts the singularities in the unresolved limits. However away from the limit, where the jet algorithm combines the partons, it introduces spurious poles. These terms are compensated by (2.36). In this case there are only two hard radiators - the quark and antiquark so that $i\equiv n=1$ and $j\equiv p=2$:

$$
\begin{aligned}
\mathrm{d}\sigma^{VS,1,c}_{\mathrm{NNLO},\tilde{A}} &= \frac{N_4}{N^2}\left(\frac{\alpha_s}{2\pi}\right)\mathrm{d}\Phi_4(p_1,\ldots,p_4;q)\frac{1}{2!}\,\times \\
&\times\sum_{i,j\in P(3,4)}\mathcal{A}^0_3(s_{12})A^0_3(1_q,i_g,2_{\bar{q}})A^0_3(\widetilde{(1i)}_q,j_g,\widetilde{(2i)}_{\bar{q}})J^{(3)}_3(\widetilde{p_{1i}},p_j,\widetilde{p_{2i}})\,. \qquad (9.75)
\end{aligned}
$$

This term corresponds to integrating the last two terms of $\mathrm{d}\sigma^{S,b}_{\mathrm{NNLO}}$ given in (9.65).

Taken together, the explicit poles in (9.74) and (9.75) cancel. Explicitly, while dropping overall factors of phase space etc., and using the definitions given in sections 4 and 5, the pole part of (9.75) is proportional to

$$
-2\boldsymbol{I}^{(1)}_{q\bar{q}}(\epsilon,s_{12})A^0_3(1_q,i_g,2_{\bar{q}})A^0_3(\widetilde{(1i)}_q,j_g,\widetilde{(2i)}_{\bar{q}})\,,
$$

while the first term in (9.74) is

$$
\left(2\boldsymbol{I}^{(1)}_{q\bar{q}}(\epsilon,s_{12})-2\boldsymbol{I}^{(1)}_{q\bar{q}}(\epsilon,s_{12i})\right)A^0_3(1_q,i_g,2_{\bar{q}})A^0_3(\widetilde{(1i)}_q,j_g,\widetilde{(2i)}_{\bar{q}})\,.
$$

The second term in eq. (9.74) is

$$2\boldsymbol{I}^{(1)}_{q\bar{q}}(\epsilon, s_{12i}) A_3^0(1_q, i_g, 2_{\bar{q}}) A_3^0(\widetilde{(1i)}_q, j_g, \widetilde{(2i)}_{\bar{q}}) \,.$$

Adding these contributions, we see that the explicit poles cancel.

By construction, the combination

$$\mathrm{d}\sigma^{V,1}_{\mathrm{NNLO}} - \mathrm{d}\sigma^{VS,1,a}_{\mathrm{NNLO}} - \mathrm{d}\sigma^{VS,1,b}_{\mathrm{NNLO}} - \mathrm{d}\sigma^{VS,1,c}_{\mathrm{NNLO}} \tag{9.76}$$

is free of explicit $1/\epsilon$-poles. Furthermore, it is also finite in its unresolved limits.

9.4 Three-parton contribution

The three-parton contribution consists of the two-loop three-parton matrix element together with the integrated forms of the five-parton and four-parton subtraction terms,

$$\mathrm{d}\sigma^{V,2}_{\mathrm{NNLO}} + \mathrm{d}\sigma^{S}_{\mathrm{NNLO}} + \mathrm{d}\sigma^{VS,1}_{\mathrm{NNLO}} \,.$$

We have shown in the previous subsections that parts of the double real radiation subtraction term cancel already with the virtual subtraction term. To make these cancellations explicit, we introduce a function $\mathrm{d}\sigma^{T}_{\mathrm{NNLO}}$, which subtracts these terms from $\mathrm{d}\sigma^{S}_{\mathrm{NNLO}}$ and adds them to $\mathrm{d}\sigma^{VS,1}_{\mathrm{NNLO}}$. After these cancellations, we observe that the three-parton contribution reduces to

$$\mathrm{d}\sigma^{V,2}_{\mathrm{NNLO}} + \left(\mathrm{d}\sigma^{S}_{\mathrm{NNLO}} - \mathrm{d}\sigma^{T}_{\mathrm{NNLO}}\right) + \left(\mathrm{d}\sigma^{VS,1}_{\mathrm{NNLO}} + \mathrm{d}\sigma^{T}_{\mathrm{NNLO}}\right) \,.$$

Upon integration of the unresolved phase space, we find

$$\mathrm{d}\sigma^{S}_{\mathrm{NNLO}} - \mathrm{d}\sigma^{T}_{\mathrm{NNLO}} = \frac{1}{N^2}\left(\frac{1}{2}\tilde{\mathcal{A}}_4^0(s_{12}) + 2\mathcal{C}_4^0(s_{12})\right) A_3^0(1_q, 3_g, 2_{\bar{q}})\,\mathrm{d}\sigma_3 \,, \tag{9.77}$$

where we defined the three-parton normalisation factor

$$\mathrm{d}\sigma_3 = N_3 \left(\frac{\alpha_s}{2\pi}\right)^2 \mathrm{d}\Phi_3(p_1, p_2, p_3; q)\, J_3^{(3)}(p_1, p_2, p_3) \,. \tag{9.78}$$

Using the explicit formulae for $\tilde{\mathcal{A}}_4^0$ and C_4^0 presented in section 5, we find that the singular contribution is given by

$$\begin{aligned} &\mathcal{P}oles(\mathrm{d}\sigma^{S}_{\mathrm{NNLO}} - \mathrm{d}\sigma^{T}_{\mathrm{NNLO}}) = \\ &= \frac{1}{N^2}\left[2\left(\boldsymbol{I}^{(1)}_{q\bar{q}}(\epsilon, s_{12})\right)^2 - \boldsymbol{H}^{(2)}_{R,\tilde{A}}(\epsilon, s_{12}) - \boldsymbol{H}^{(2)}_{R,\tilde{C}}(\epsilon, s_{12})\right] A_3^0(1_q, 3_g, 2_{\bar{q}})\,\mathrm{d}\sigma_3. \end{aligned} \tag{9.79}$$

Similarly, integration of (9.74) yields,

$$\begin{aligned} \mathrm{d}\sigma^{VS,1}_{\mathrm{NNLO}} + \mathrm{d}\sigma^{T}_{\mathrm{NNLO}} = \frac{1}{N^2}\Big(&\tilde{\mathcal{A}}_3^1(s_{12}) A_3^0(1_q, 3_g, 2_{\bar{q}}) + \\ &+ \mathcal{A}_3^0(s_{12})\left[\tilde{A}_3^1(1_q, 3_g, 2_{\bar{q}}) + \mathcal{A}_2^1(s_{123}) A_3^0(1_q, 3_g, 2_{\bar{q}})\right]\Big)\mathrm{d}\sigma_3 \,, \end{aligned} \tag{9.80}$$

resulting in

$$\begin{aligned}&\mathcal{P}oles(\mathrm{d}\sigma^{VS,1}_{\mathrm{NNLO}}+\mathrm{d}\sigma^{T}_{\mathrm{NNLO}})= \\ &\quad=\frac{1}{N^2}\left(-\mathbf{H}^{(2)}_{V,\tilde{A}}(\epsilon,s_{12})+2\boldsymbol{I}^{(1)}_{q\bar{q}}(\epsilon,s_{12})\left[\tilde{A}^1_3(1_q,3_g,2_{\bar{q}})+\mathcal{A}^1_2(s_{123})A^0_3(1_q,3_g,2_{\bar{q}})\right]\right)\mathrm{d}\sigma_3\,,\end{aligned} \tag{9.81}$$

where it is noteworthy that the finite part of $\mathcal{A}^0_3$ in (9.80) is cancelled exactly by the terms proportional to $\mathcal{A}^1_2$ in $\tilde{\mathcal{A}}^1_3$ (5.23).

At $\mathcal{O}(1/N^2)$, the singular two-loop virtual contribution is given by expanding (9.52). We find,

$$\begin{aligned}\mathcal{P}oles(\mathrm{d}\sigma^{V,2}_{\mathrm{NNLO}}) = \frac{1}{N^2}\Bigg(&\left[-2\left(\boldsymbol{I}^{(1)}_{q\bar{q}}(\epsilon,s_{12})\right)^2+2\boldsymbol{H}^{(2)}_{q\bar{q},1/N^2}(\epsilon,s_{12})\right]A^0_3(1_q,3_g,2_{\bar{q}})+ \\ &+2\boldsymbol{I}^{(1)}_{q\bar{q}}(\epsilon,s_{12})\left[\tilde{A}^1_3(1_q,3_g,2_{\bar{q}})+\mathcal{A}^1_2(s_{123})A^0_3(1_q,3_g,2_{\bar{q}})\right]\Bigg)\mathrm{d}\sigma_3\,.\end{aligned} \tag{9.82}$$

Using relation between the hard radiation operators $\mathbf{H}$ given in (4.9), it is easy to see that

$$\mathcal{P}oles(\mathrm{d}\sigma^{S}_{\mathrm{NNLO}}+\mathrm{d}\sigma^{VS,1}_{\mathrm{NNLO}}+\mathrm{d}\sigma^{V}_{\mathrm{NNLO}})=0\,. \tag{9.83}$$

The three-parton contribution is thus free of explicit infrared poles. The remaining finite contributions are fully differential in the three-jet variables and can be integrated numerically for any given infrared-safe jet definition.

9.5 Numerical implementation

Starting from the program `EERAD2` [10], which computes four-jet production at NLO, we implemented the NNLO antenna subtraction method for the $1/N^2$ colour factor contribution to $e^+e^- \to 3j$. `EERAD2` already contains the five-parton and four-parton matrix elements relevant here, as well as the NLO-type subtraction terms $\mathrm{d}\sigma^{S,a}_{\mathrm{NNLO}}$ and $\mathrm{d}\sigma^{VS,1,a}_{\mathrm{NNLO}}$.

The implementation contains three channels, classified by their partonic multiplicity:

- in the five-parton channel, we integrate
$$\mathrm{d}\sigma^{R}_{\mathrm{NNLO}}-\mathrm{d}\sigma^{S}_{\mathrm{NNLO}}\,. \tag{9.84}$$
- in the four-parton channel, we integrate
$$\mathrm{d}\sigma^{V,1}_{\mathrm{NNLO}}-\mathrm{d}\sigma^{VS,1}_{\mathrm{NNLO}}\,. \tag{9.85}$$
- in the three-parton channel, we integrate
$$\mathrm{d}\sigma^{V,2}_{\mathrm{NNLO}}+\mathrm{d}\sigma^{S}_{\mathrm{NNLO}}+\mathrm{d}\sigma^{VS,1}_{\mathrm{NNLO}}\,. \tag{9.86}$$

The numerical integration over these channels is carried out by Monte Carlo methods using the `VEGAS` [54] implementation.

It was already demonstrated above that the integrands in the four-parton and three-parton channel are free of explicit infrared poles. In the five-parton and four-parton channel, we tested the proper implementation of the subtraction by generating trajectories of phase space points approaching a given single or double unresolved limit using the RAMBO [55] phase space generator. Along these trajectories, we observe that the antenna subtraction terms converge locally towards the physical matrix elements (it has to be pointed out that the $1/N^2$ colour structure is free of angular terms, since it does not involve any gluon splitting processes), and that the cancellations among individual contributions to the subtraction terms take place as expected in section 2. Moreover, we checked the correctness of the subtraction by introducing a lower cut (slicing parameter) on the phase space variables, and observing that our results are independent of this cut (provided it is chosen small enough). This behaviour indicates that the subtraction terms ensure that the contribution of potentially singular regions of the final state phase space does not contribute to the numerical integrals, but is accounted for analytically.

10. Infrared cancellations in $e^+e^- \to 3$ jets at NNLO

To finally illustrate the power of the antenna subtraction method at NNLO, we note that the infrared poles of the two-loop (including one-loop times one-loop) correction to $\gamma^* \to q\bar{q}g$ are cancelled in all colour factors by a combination of integrated three-parton and four-parton antenna functions.

The integrated five-parton double real radiation subtraction term for three-jet production after cancellation of terms with the virtual single unresolved subtraction term reads:

$$\mathrm{d}\sigma^S_{\mathrm{NNLO}} - \mathrm{d}\sigma^T_{\mathrm{NNLO}} = \mathcal{X}^S_{q\bar{q}g,\mathrm{NNLO}}\, A_3^0(1_q, 3_g, 2_{\bar{q}})\, \mathrm{d}\sigma_3 \tag{10.1}$$

with

$$\begin{aligned}
\mathcal{X}^S_{q\bar{q}g,\mathrm{NNLO}} = {} & N^2 \left[\frac{1}{2}\,\mathcal{D}_4^0(s_{13}) + \frac{1}{2}\,\mathcal{D}_4^0(s_{23}) - \frac{1}{8}\left(\mathcal{D}_3^0(s_{13}) - \mathcal{D}_3^0(s_{23})\right)^2 - \right.\\
& \left. \qquad - \frac{1}{2}\left(\tilde{\mathcal{A}}_4^0(s_{12}) - \mathcal{A}_3^0(s_{12})\,\mathcal{A}_3^0(s_{12})\right)\right] + \\
& + N^0 \left[-\mathcal{A}_4^0(s_{12}) - \frac{1}{2}\,\tilde{\mathcal{A}}_4^0(s_{12}) - 2\,\mathcal{C}_4^0(s_{12}) - \right.\\
& \left. \qquad - \frac{1}{2}\mathcal{A}_3^0(s_{12})\left(\mathcal{D}_3^0(s_{13}) + \mathcal{D}_3^0(s_{23})\right) + \mathcal{A}_3^0(s_{12})\,\mathcal{A}_3^0(s_{12})\right] + \\
& + \frac{1}{N^2}\left[\frac{1}{2}\,\tilde{\mathcal{A}}_4^0(s_{12}) + 2\,\mathcal{C}_4^0(s_{12})\right] + \\
& + N\,N_F \left[\mathcal{E}_4^0(s_{13}) + \mathcal{E}_4^0(s_{23}) - \frac{1}{4}\left(\mathcal{D}_3^0(s_{13})\,\mathcal{E}_3^0(s_{13}) + \mathcal{D}_3^0(s_{23})\,\mathcal{E}_3^0(s_{23})\right)\right.\\
& \left. \qquad + \frac{1}{4}\left(\mathcal{D}_3^0(s_{13})\,\mathcal{E}_3^0(s_{23}) + \mathcal{D}_3^0(s_{23})\,\mathcal{E}_3^0(s_{13})\right)\right] + \\
& + \frac{N_F}{N}\left[-\mathcal{B}_4^0(s_{12}) - \frac{1}{2}\,\tilde{\mathcal{E}}_4^0(s_{13}) - \frac{1}{2}\,\tilde{\mathcal{E}}_4^0(s_{23}) - \frac{1}{2}\mathcal{A}_3^0(s_{12})\,\left(\mathcal{E}_3^0(s_{13}) + \mathcal{E}_3^0(s_{23})\right)\right].
\end{aligned} \tag{10.2}$$

Integration of the remainder of the four-parton single real radiation subtraction term produces

$$\mathrm{d}\sigma^{VS,1}_{\mathrm{NNLO}} + \mathrm{d}\sigma^{T}_{\mathrm{NNLO}} = \Bigg\{ \mathcal{X}^{VS}_{q\bar{q}g,\mathrm{NNLO}}\, A_3^0(1_q,3_g,2_{\bar{q}}) + \mathcal{X}^{VS,\mathrm{tree}}_{q\bar{q}g,\mathrm{NNLO}}\, A_3^{(1\times 0)}(1_q,3_g,2_{\bar{q}}) + \\ + \mathcal{X}^{VS,\beta}_{q\bar{q}g,\mathrm{NNLO}}\, \frac{\beta_0}{\epsilon}\, A_3^0(1_q,3_g,2_{\bar{q}}) \Bigg\}\, \mathrm{d}\sigma_3\,, \tag{10.3}$$

with

$$\begin{aligned}
\mathcal{X}^{VS}_{q\bar{q}g,\mathrm{NNLO}} &= N^2 \left[\frac{1}{2}\,\mathcal{D}_3^1(s_{13}) + \frac{1}{2}\,\mathcal{D}_3^1(s_{23}) - \tilde{\mathcal{A}}_3^1(s_{12}) \right] + \\
&\quad + N^0 \left[-\mathcal{A}_3^1(s_{12}) - \tilde{\mathcal{A}}_3^1(s_{12}) \right] + \\
&\quad + \frac{1}{N^2} \tilde{\mathcal{A}}_3^1(s_{12}) + \\
&\quad + N\,N_F \left[\frac{1}{2}\,\hat{\mathcal{D}}_3^1(s_{13}) + \frac{1}{2}\,\hat{\mathcal{D}}_3^1(s_{23}) + \frac{1}{2}\,\mathcal{E}_3^1(s_{13}) + \frac{1}{2}\,\mathcal{E}_3^1(s_{23}) \right] + \\
&\quad + \frac{N_F}{N} \left[-\hat{\mathcal{A}}_3^1(s_{12}) - \frac{1}{2}\,\tilde{\mathcal{E}}_3^1(s_{13}) - \frac{1}{2}\,\tilde{\mathcal{E}}_3^1(s_{23}) \right] + \\
&\quad + N_F^2 \left[\frac{1}{2}\,\hat{\mathcal{E}}_3^1(s_{13}) + \frac{1}{2}\,\hat{\mathcal{E}}_3^1(s_{23}) \right], \qquad (10.4) \\
\mathcal{X}^{VS,\mathrm{tree}}_{q\bar{q}g,\mathrm{NNLO}} &= N \left[\frac{1}{2}\,\mathcal{D}_3^0(s_{13}) + \frac{1}{2}\,\mathcal{D}_3^0(s_{23}) \right] + N_F \left[\frac{1}{2}\,\mathcal{E}_3^0(s_{13}) + \frac{1}{2}\,\mathcal{E}_3^0(s_{23}) \right] - \frac{1}{N}\mathcal{A}_3^0(s_{12})\,, \\
\mathcal{X}^{VS,\beta}_{q\bar{q}g,\mathrm{NNLO}} &= N \left[\frac{1}{2}\,\mathcal{D}_3^0(s_{13})\, \left[(s_{13})^{-\epsilon} - (s_{123})^{-\epsilon} \right] + \frac{1}{2}\,\mathcal{D}_3^0(s_{23}) \left[(s_{23})^{-\epsilon} - (s_{123})^{-\epsilon} \right] \right] + \\
&\quad + N_F \left[\frac{1}{2}\,\mathcal{E}_3^0(s_{13}) \left[(s_{13})^{-\epsilon} - (s_{123})^{-\epsilon} \right] + \frac{1}{2}\,\mathcal{E}_3^0(s_{23}) \left[(s_{23})^{-\epsilon} - (s_{123})^{-\epsilon} \right] \right] - \\
&\quad - \frac{1}{N}\,\mathcal{A}_3^0(s_{12})\, \left[(s_{12})^{-\epsilon} - (s_{123})^{-\epsilon} \right]. \qquad (10.5)
\end{aligned}$$

Adding these integrated subtraction terms to the two-loop three-parton contribution to $\gamma^* \to q\bar{q}g$ [5], discussed in section 9.1.3, one observes

$$\mathcal{P}oles \left(\mathrm{d}\sigma^{S}_{\mathrm{NNLO}} + \mathrm{d}\sigma^{VS,1}_{\mathrm{NNLO}} + \mathrm{d}\sigma^{V,2}_{\mathrm{NNLO}} \right) = 0 \tag{10.6}$$

for all colour structures (9.52). This highly non-trivial cancellation clearly illustrates that the antenna functions derived in this paper correctly approximate QCD matrix elements in all infrared singular limits at NNLO. The formulae in this section also outline the structure of infrared cancellations in $e^+e^- \to 3j$ at NNLO, and indicate the structure of the subtraction terms in all colour factors.

The above formulae also illustrate several aspects of the antenna subtraction method which were discussed in more generality in the preceeding sections.

The subtraction terms for two colour-unconnected and almost colour-unconnected unresolved partons $\mathrm{d}\sigma^{S,c}_{\mathrm{NNLO}}$ (2.24) and $\mathrm{d}\sigma^{S,d}_{\mathrm{NNLO}}$ (2.26) cancel partially with the virtual one-loop single unresolved subtraction term $\mathrm{d}\sigma^{VS,1,c}_{\mathrm{NNLO}}$ (2.36). The pattern of these cancellations is different for each colour factor, as can be seen from the different products of two tree-level three-parton antenna functions in (10.2).

In sections 6 and 8.3.2, we indicated that the tree-level four-parton quark-gluon-gluon-gluon antenna function D_4^0 contains an unwanted double unresolved limit due to the cyclic nature of its colour indices. In the N^2-contribution to (10.2), we see how this limit can be removed by subtraction of the subleading colour quark-antiquark antenna function $\tilde{A}_4^0$ and its strongly ordered limits. We observe that a similar subtraction has to be carried out on the one-loop three-parton antenna function D_3^1 in (10.4).

11. Conclusions

In this paper, we presented a new method for the subtraction of infrared singularities in the calculation of jet observables at NNLO. We introduced subtraction terms for double real radiation at tree level and single real radiation at one loop based on antenna functions. These antenna functions describe the colour-ordered radiation of unresolved partons between a pair of hard (radiator) partons.

All antenna functions at NLO and NNLO can be derived from physical matrix elements: quark-antiquark antenna functions from the corrections to the process $\gamma^* \to q\bar{q}$ [44], quark-gluon antenna functions from $\tilde{\chi} \to \tilde{g}g$ [46] and gluon-gluon antenna functions from $H \to gg$ [47]. We listed all three-parton tree-level and one-loop antenna functions as well as all four-parton tree-level antenna functions in their explicit, unintegrated form. We provided all integrals of these functions over the three- and four-parton antenna phase spaces for the kinematical situation of a neutral massive particle decaying into massless partons, as is relevant to $e^+e^- \to m$ jets. Having the subtraction terms in both unintegrated and integrated form, they can now be directly implemented into a parton level NNLO event generator for jet production in electron-positron annihilation.

To demonstrate the application of our new method on a non-trivial example, we implemented the NNLO corrections to the subleading colour contribution to $e^+e^- \to 3$ jets. Starting from an existing programme for $e^+e^- \to 4$ jets at NLO [10], we constructed the newly required subtraction terms for double unresolved real radiation in the five-parton channel and for single unresolved real radiation off one-loop matrix elements in the four-parton channel. We observed that after implementation of these subtraction terms, five-parton and four-parton channels integrate to numerically finite contributions to three-jet final states, and that the four-parton channel is free from explicit infrared singularities from the loop integrations and the subtraction terms. All explicit infrared singularities obtained from integrating the newly introduced subtraction terms cancel in the three-parton channel after adding with the the genuine two-loop virtual corrections to this channel, which were computed previously [5]. A further illustration of the potential of our method is given in section 10, where we demonstrate that the infrared poles of the two-loop virtual corrections to $e^+e^- \to 3$ jets cancel in all its seven colour factors against linear combinations of integrated NNLO antenna functions.

An immediate application of the method presented here is the calculation of the full NNLO corrections to $e^+e^- \to 3$ jets [56]. The antenna subtraction method can be further generalised to NNLO corrections to jet production in lepton-hadron or hadron-hadron collisions. In these kinematical situations, the subtraction terms are constructed using the same antenna functions, but in different phase space configurations: instead of the $1 \to n$ decay kinematics considered here, $2 \to n$ scattering kinematics are required, which can also contain singular configurations due to single or double initial state radiation. These require new sets of integrated antenna functions.

Acknowledgments

We would like to thank Gudrun Heinrich and Zoltan Trócsányi for useful discussions on several of the issues presented in this paper and for very constructive criticism expressed on our earlier works.

Part of the work presented here was performed during the 2004 "QCD and Collider Physics"-programme at the Kavli Institute for Theoretical Physics (KITP), Santa Barbara. The authors would like to thank the KITP for its kind hospitality.

This research was supported in part by the Swiss National Science Foundation (SNF) under contracts PMPD2-106101 and 200021-101874, by the UK Particle Physics and Astronomy Research Council and by the National Science Foundation under Grant No. PHY99-07949.

References

[1] R.K. Ellis, W.J. Stirling and B.R. Webber, *QCD and collider physics*, Cambridge University Press, Cambridge, 1996;
G. Dissertori, I.G. Knowles and M. Schmelling, *Quantum chromodynamics: high energy experiments and theory*, Oxford University Press Oxford, 2003.

[2] E.W.N. Glover, *Progress in NNLO calculations for scattering processes*, *Nucl. Phys.* **116** *(Proc. Suppl.)* (2003) 3 [hep-ph/0211412].

[3] S. Moch, J.A.M. Vermaseren and A. Vogt, *The three-loop splitting functions in QCD: the non-singlet case*, *Nucl. Phys.* **B 688** (2004) 101 [hep-ph/0403192];
A. Vogt, S. Moch and J.A.M. Vermaseren, *The three-loop splitting functions in QCD: the singlet case*, *Nucl. Phys.* **B 691** (2004) 129 [hep-ph/0404111].

[4] Z. Bern, L.J. Dixon and A. Ghinculov, *Two-loop correction to Bhabha scattering*, *Phys. Rev.* **D 63** (2001) 053007 [hep-ph/0010075];
C. Anastasiou, E.W.N. Glover, C. Oleari and M.E. Tejeda-Yeomans, *Two-loop QCD corrections to $q\bar{q} \to q'\bar{q}'$*, *Nucl. Phys.* **B 601** (2001) 318 [hep-ph/0010212]; *Two loop QCD corrections to massless identical quark scattering*, *Nucl. Phys.* **B 601** (2001) 341 [hep-ph/0011094]; *Two-loop QCD corrections to massless quark gluon scattering*, *Nucl. Phys.* **B 605** (2001) 486 [hep-ph/0101304];
E.W.N. Glover, C. Oleari and M.E. Tejeda-Yeomans, *Two-loop QCD corrections to gluon gluon scattering*, *Nucl. Phys.* **B 605** (2001) 467 [hep-ph/0102201];
C. Anastasiou, E.W.N. Glover and M.E. Tejeda-Yeomans, *Two-loop QED and QCD corrections to massless fermion boson scattering*, *Nucl. Phys.* **B 629** (2002) 255 [hep-ph/0201274];
E.W.N. Glover and M.E. Tejeda-Yeomans, *Two-loop QCD helicity amplitudes for massless quark massless gauge boson scattering*, *JHEP* **06** (2003) 033 [hep-ph/0304169];

E.W.N. Glover, *Two-loop QCD helicity amplitudes for massless quark quark scattering*, *JHEP* **04** (2004) 021 [hep-ph/0401119];
Z. Bern, A. De Freitas and L.J. Dixon, *Two-loop amplitudes for gluon fusion into two photons*, *JHEP* **09** (2001) 037 [hep-ph/0109078]; *Two-loop helicity amplitudes for gluon gluon scattering in QCD and supersymmetric Yang-Mills theory*, *JHEP* **03** (2002) 018 [hep-ph/0201161]; *Two-loop helicity amplitudes for quark gluon scattering in QCD and gluino gluon scattering in supersymmetric yang- mills theory*, *JHEP* **06** (2003) 028 [hep-ph/0304168];
A. De Freitas and Z. Bern, *Two-loop helicity amplitudes for quark-quark scattering in QCD and gluino gluino scattering in supersymmetric Yang-Mills theory*, *JHEP* **09** (2004) 039 [hep-ph/0409007];
Z. Bern, A. De Freitas, L.J. Dixon, A. Ghinculov and H.L. Wong, *QCD and QED corrections to light-by-light scattering*, *JHEP* **11** (2001) 031 [hep-ph/0109079];
T. Binoth, E.W.N. Glover, P. Marquard and J.J. van der Bij, *Two-loop corrections to light-by-light scattering in supersymmetric QED*, *JHEP* **05** (2002) 060 [hep-ph/0202266];
T. Gehrmann and E. Remiddi, *Analytic continuation of massless two-loop four-point functions*, *Nucl. Phys.* **B 640** (2002) 379 [hep-ph/0207020];
S. Moch, P. Uwer and S. Weinzierl, *Two-loop amplitudes with nested sums: fermionic contributions to* $e^+e^- \to q\bar{q}\, g$, *Phys. Rev.* **D 66** (2002) 114001 [hep-ph/0207043].

[5] L.W. Garland, T. Gehrmann, E.W.N. Glover, A. Koukoutsakis and E. Remiddi, *The two-loop QCD matrix element for* $e^+e^- \to$ *3jets*, *Nucl. Phys.* **B 627** (2002) 107 [hep-ph/0112081]; *Two-loop QCD helicity amplitudes for* $e^+e^- \to$ *3jets*, *Nucl. Phys.* **B 642** (2002) 227 [hep-ph/0206067].

[6] F.V. Tkachov, *A theorem on analytical calculability of four loop renormalization group functions*, *Phys. Lett.* **B 100** (1981) 65;
K.G. Chetyrkin and F.V. Tkachov, *Integration by parts: the algorithm to calculate beta functions in 4 loops*, *Nucl. Phys.* **B 192** (1981) 159;
V.A. Smirnov, *Analytical result for dimensionally regularized massless on-shell double box*, *Phys. Lett.* **B 460** (1999) 397 [hep-ph/9905323];
J.B. Tausk, *Non-planar massless two-loop feynman diagrams with four on- shell legs*, *Phys. Lett.* **B 469** (1999) 225 [hep-ph/9909506];
T. Binoth and G. Heinrich, *An automatized algorithm to compute infrared divergent multi-loop integrals*, *Nucl. Phys.* **B 585** (2000) 741 [hep-ph/0004013];
S. Laporta, *High-precision calculation of multi-loop Feynman integrals by difference equations*, *Int. J. Mod. Phys.* **A 15** (2000) 5087 [hep-ph/0102033];
T. Gehrmann and E. Remiddi, *Differential equations for two-loop four-point functions*, *Nucl. Phys.* **B 580** (2000) 485 [hep-ph/9912329];
S. Moch, P. Uwer and S. Weinzierl, *Nested sums, expansion of transcendental functions and multi-scale multi-loop integrals*, *J. Math. Phys.* **43** (2002) 3363 [hep-ph/0110083];
S. Weinzierl, *Symbolic expansion of transcendental functions*, *Comput. Phys. Commun.* **145** (2002) 357 [math-ph/0201011];
C. Anastasiou and K. Melnikov, *Higgs boson production at hadron colliders in NNLO QCD*, *Nucl. Phys.* **B 646** (2002) 220 [hep-ph/0207004];
V.A. Smirnov, *Evaluating Feynman Integrals*, Springer Tracts of Modern Physics, Heidelberg, 2004

[7] Z. Bern, L.J. Dixon and D.A. Kosower, *One loop corrections to five gluon amplitudes*, *Phys. Rev. Lett.* **70** (1993) 2677 [hep-ph/9302280];

Z. Kunszt, A. Signer and Z. Trócsányi, *One loop radiative corrections to the helicity amplitudes of QCD processes involving four quarks and one gluon*, *Phys. Lett.* **B 336** (1994) 529 [hep-ph/9405386];
Z. Bern, L.J. Dixon and D.A. Kosower, *One loop corrections to two quark three gluon amplitudes*, *Nucl. Phys.* **B 437** (1995) 259 [hep-ph/9409393].

[8] E.W.N. Glover and D.J. Miller, *The one-loop QCD corrections for $\gamma^* \to q\bar{q}q\bar{q}$*, *Phys. Lett.* **B 396** (1997) 257 [hep-ph/9609474];
Z. Bern, L.J. Dixon, D.A. Kosower and S. Weinzierl, *One-loop amplitudes for $e^+e^- \to \bar{q}q\bar{q}q$*, *Nucl. Phys.* **B 489** (1997) 3 [hep-ph/9610370];
J.M. Campbell, E.W.N. Glover and D.J. Miller, *The one-loop QCD corrections for $\gamma^* \to q\bar{q}gg$*, *Phys. Lett.* **B 409** (1997) 503 [hep-ph/9706297];
Z. Bern, L.J. Dixon and D.A. Kosower, *One-loop amplitudes for e^+e^- to four partons*, *Nucl. Phys.* **B 513** (1998) 3 [hep-ph/9708239].

[9] A. Signer and L.J. Dixon, *Electron positron annihilation into four jets at next-to-leading order in α_s*, *Phys. Rev. Lett.* **78** (1997) 811 [hep-ph/9609460];
L.J. Dixon and A. Signer, *Complete $O(\alpha_s^3)$ results for $e^+e^- \to (\gamma, Z) \to$ four jets*, *Phys. Rev.* **D 56** (1997) 4031 [hep-ph/9706285];
Z. Nagy and Z. Trócsányi, *Next-to-leading order calculation of four-jet shape variables*, *Phys. Rev. Lett.* **79** (1997) 3604 [hep-ph/9707309];
S. Weinzierl and D.A. Kosower, *QCD corrections to four-jet production and three-jet structure in e^+e^- annihilation*, *Phys. Rev.* **D 60** (1999) 054028 [hep-ph/9901277];
W.B. Kilgore and W.T. Giele, *Next-to-leading order gluonic three jet production at hadron colliders*, *Phys. Rev.* **D 55** (1997) 7183 [hep-ph/9610433];
Z. Nagy and Z. Trócsányi, *Multi-jet cross sections in deep inelastic scattering at next-to-leading order*, *Phys. Rev. Lett.* **87** (2001) 082001 [hep-ph/0104315];
Z. Nagy, *Three-jet cross sections in hadron hadron collisions at next-to-leading order*, *Phys. Rev. Lett.* **88** (2002) 122003 [hep-ph/0110315]; *Next-to-leading order calculation of three-jet observables in hadron hadron collision*, *Phys. Rev.* **D 68** (2003) 094002 [hep-ph/0307268];
J. Campbell and R.K. Ellis, *Next-to-leading order corrections to W + 2jet and Z + 2jet production at hadron colliders*, *Phys. Rev.* **D 65** (2002) 113007 [hep-ph/0202176].

[10] J.M. Campbell, M.A. Cullen and E.W.N. Glover, *Four jet event shapes in electron positron annihilation*, *Eur. Phys. J.* **C 9** (1999) 245 [hep-ph/9809429].

[11] Z. Bern, L.J. Dixon, D.C. Dunbar and D.A. Kosower, *One loop n point gauge theory amplitudes, unitarity and collinear limits*, *Nucl. Phys.* **B 425** (1994) 217 [hep-ph/9403226];
D.A. Kosower, *All-order collinear behavior in gauge theories*, *Nucl. Phys.* **B 552** (1999) 319 [hep-ph/9901201];
D.A. Kosower and P. Uwer, *One-loop splitting amplitudes in gauge theory*, *Nucl. Phys.* **B 563** (1999) 477 [hep-ph/9903515];
Z. Bern, V. Del Duca and C.R. Schmidt, *The infrared behavior of one-loop gluon amplitudes at next-to-next-to-leading order*, *Phys. Lett.* **B 445** (1998) 168 [hep-ph/9810409];
Z. Bern, V. Del Duca, W.B. Kilgore and C.R. Schmidt, *The infrared behavior of one-loop QCD amplitudes at next-to-next-to-leading order*, *Phys. Rev.* **D 60** (1999) 116001 [hep-ph/9903516].

[12] S. Catani and M. Grazzini, *The soft-gluon current at one-loop order*, *Nucl. Phys.* **B 591** (2000) 435 [hep-ph/0007142].

[13] D.A. Kosower, *All-orders singular emission in gauge theories*, *Phys. Rev. Lett.* **91** (2003) 061602 [hep-ph/0301069].

[14] S. Weinzierl, *Subtraction terms for one-loop amplitudes with one unresolved parton*, *JHEP* **07** (2003) 052 [hep-ph/0306248].

[15] C. Anastasiou, Z. Bern, L.J. Dixon and D.A. Kosower, *Planar amplitudes in maximally supersymmetric Yang-Mills theory*, *Phys. Rev. Lett.* **91** (2003) 251602 [hep-th/0309040];
Z. Bern, L.J. Dixon and D.A. Kosower, *Two-loop $g \to g\ g$ splitting amplitudes in QCD*, *JHEP* **08** (2004) 012 [hep-ph/0404293];
S.D. Badger and E.W.N. Glover, *Two-loop splitting functions in QCD*, *JHEP* **07** (2004) 040 [hep-ph/0405236].

[16] C. Anastasiou, L.J. Dixon, K. Melnikov and F. Petriello, *Dilepton rapidity distribution in the Drell-Yan process at NNLO in QCD*, *Phys. Rev. Lett.* **91** (2003) 182002 [hep-ph/0306192]; *High-precision QCD at hadron colliders: electroweak gauge boson rapidity distributions at NNLO*, *Phys. Rev.* **D 69** (2004) 094008 [hep-ph/0312266].

[17] A. Gehrmann-De Ridder and E.W.N. Glover, *A complete $O(\alpha_s)$ calculation of the photon + 1jet rate in e^+e^- annihilation*, *Nucl. Phys.* **B 517** (1998) 269 [hep-ph/9707224].

[18] J.M. Campbell and E.W.N. Glover, *Double unresolved approximations to multiparton scattering amplitudes*, *Nucl. Phys.* **B 527** (1998) 264 [hep-ph/9710255].

[19] S. Catani and M. Grazzini, *Collinear factorization and splitting functions for next-to-next-to-leading order QCD calculations*, *Phys. Lett.* **B 446** (1999) 143 [hep-ph/9810389]; *Infrared factorization of tree level QCD amplitudes at the next-to-next-to-leading order and beyond*, *Nucl. Phys.* **B 570** (2000) 287 [hep-ph/9908523].

[20] F.A. Berends and W.T. Giele, *Multiple soft gluon radiation in parton processes*, *Nucl. Phys.* **B 313** (1989) 595;
V. Del Duca, A. Frizzo and F. Maltoni, *Factorization of tree QCD amplitudes in the high-energy limit and in the collinear limit*, *Nucl. Phys.* **B 568** (2000) 211 [hep-ph/9909464];
T.G. Birthwright, E.W.N. Glover, V.V. Khoze and P. Marquard, *Multi-gluon collinear limits from MHV diagrams*, *JHEP* **05** (2005) 013 [hep-ph/0503063].

[21] D.A. Kosower and P. Uwer, *Evolution kernels from splitting amplitudes*, *Nucl. Phys.* **B 674** (2003) 365 [hep-ph/0307031].

[22] D. de Florian and M. Grazzini, *The structure of large logarithmic corrections at small transverse momentum in hadronic collisions*, *Nucl. Phys.* **B 616** (2001) 247 [hep-ph/0108273]; *The back-to-back region in e^+e^- energy energy correlation*, *Nucl. Phys.* **B 704** (2005) 387 [hep-ph/0407241].

[23] A. Daleo, C.A. Garcia Canal and R. Sassot, *Order-α_s^2 corrections to one-particle inclusive processes in dis*, *Nucl. Phys.* **B 662** (2003) 334 [hep-ph/0303199];
A. Daleo, D. de Florian and R. Sassot, *$O(\alpha_s^2)$ QCD corrections to the electroproduction of hadrons with high transverse momentum*, *Phys. Rev.* **D 71** (2005) 034013 [hep-ph/0411212].

[24] K.L. Adamson, D. de Florian and A. Signer, *Gluon induced contributions to $W\ Z$ and $W\gamma$ production at NNLO*, *Phys. Rev.* **D 65** (2002) 094041 [hep-ph/0202132];
Gluon induced contributions to $Z\gamma$ production at hadron colliders, *Phys. Rev.* **D 67** (2003) 034016 [hep-ph/0211295].

[25] D.A. Kosower, *Multiple singular emission in gauge theories*, *Phys. Rev.* **D 67** (2003) 116003 [hep-ph/0212097].

[26] S. Weinzierl, *Subtraction terms at NNLO*, *JHEP* **03** (2003) 062 [hep-ph/0302180].

[27] W.B. Kilgore, *Subtraction terms for hadronic production processes at next-to-next-to-leading order*, *Phys. Rev.* **D 70** (2004) 031501 [hep-ph/0403128].

[28] S. Frixione and M. Grazzini, *Subtraction at NNLO*, *JHEP* **06** (2005) 010 [hep-ph/0411399].

[29] G. Somogyi, Z. Trócsányi and V. Del Duca, *Matching of singly- and doubly-unresolved limits of tree-level QCD squared matrix elements*, *JHEP* **06** (2005) 024 [hep-ph/0502226].

[30] G. Heinrich, *A numerical method for NNLO calculations*, *Nucl. Phys.* **116** *(Proc. Suppl.)* (2003) 368 [hep-ph/0211144];
C. Anastasiou, K. Melnikov and F. Petriello, *A new method for real radiation at NNLO*, *Phys. Rev.* **D 69** (2004) 076010 [hep-ph/0311311];
T. Binoth and G. Heinrich, *Numerical evaluation of phase space integrals by sector decomposition*, *Nucl. Phys.* **B 693** (2004) 134 [hep-ph/0402265];
G. Heinrich, *A numerical approach to infrared divergent multi-parton phase space integrals*, *Nucl. Phys.* **135** *(Proc. Suppl.)* (2004) 290 [hep-ph/0406332].

[31] A. Gehrmann-De Ridder, T. Gehrmann and G. Heinrich, *Four-particle phase space integrals in massless QCD*, *Nucl. Phys.* **B 682** (2004) 265 [hep-ph/0311276].

[32] C. Anastasiou, K. Melnikov and F. Petriello, *Real radiation at NNLO: $e^+e^- \to$ 2jets through $O(\alpha_s^2)$*, *Phys. Rev. Lett.* **93** (2004) 032002 [hep-ph/0402280].

[33] C. Anastasiou, K. Melnikov and F. Petriello, *Higgs boson production at hadron colliders: differential cross sections through next-to-next-to-leading order*, *Phys. Rev. Lett.* **93** (2004) 262002 [hep-ph/0409088]; *Fully differential Higgs boson production and the di-photon signal through next-to-next-to-leading order*, hep-ph/0501130.

[34] C. Anastasiou, K. Melnikov and F. Petriello, *The electron energy spectrum in muon decay through $O(\alpha^2)$*, hep-ph/0505069.

[35] R.K. Ellis, D.A. Ross and A.E. Terrano, *The perturbative calculation of jet structure in e^+e^- annihilation*, *Nucl. Phys.* **B 178** (1981) 421.

[36] K. Fabricius, I. Schmitt, G. Kramer and G. Schierholz, *Higher order perturbative QCD calculation of jet cross- sections in e^+e^- annihilation*, *Zeit. Phys.* **C11** (1981) 315.

[37] Z. Kunszt and P. Nason, in *Z Physics at LEP 1*, CERN Yellow Report 89-08, vol. 1, p. 373.

[38] W.T. Giele and E.W.N. Glover, *Higher order corrections to jet cross-sections in e^+e^- annihilation*, *Phys. Rev.* **D 46** (1992) 1980;
Z. Kunszt and D.E. Soper, *Calculation of jet cross-sections in hadron collisions at order α_s^3*, *Phys. Rev.* **D 46** (1992) 192;
S. Frixione, Z. Kunszt and A. Signer, *Three-jet cross sections to next-to-leading order*, *Nucl. Phys.* **B 467** (1996) 399 [hep-ph/9512328].

[39] G. Sterman and S. Weinberg, *Jets from quantum chromodynamics*, *Phys. Rev. Lett.* **39** (1977) 1436;
G. Sterman, *Mass divergences in annihilation processes, 1. Origin and nature of divergences in cut vacuum polarization diagrams*, *Phys. Rev.* **D 17** (1978) 2773; *Mass divergences in annihilation processes, 2. Cancellation Of divergences in cut vacuum polarization diagrams*, *Phys. Rev.* **D 17** (1978) 2789.

[40] S. Catani and M.H. Seymour, *A general algorithm for calculating jet cross sections in NLO QCD*, *Nucl. Phys.* **B 485** (1997) 291 [hep-ph/9605323].

[41] D.A. Kosower, *Antenna factorization of gauge-theory amplitudes*, *Phys. Rev.* **D 57** (1998) 5410 [hep-ph/9710213]; *Antenna factorization in strongly-ordered limits*, *Phys. Rev.* **D 71** (2005) 045016 [hep-ph/0311272].

[42] F.A. Berends and W. Giele, *The six gluon process as an example of weyl-van der waerden spinor calculus*, *Nucl. Phys.* **B 294** (1987) 700;
M.L. Mangano, S.J. Parke and Z. Xu, *Duality and multi-gluon scattering*, *Nucl. Phys.* **B 298** (1988) 653; *The color structure of gluon emission*, *Nucl. Phys.* **B 309** (1988) 461;
L.J. Dixon, *Calculating scattering amplitudes efficiently*, hep-ph/9601359.

[43] V. Del Duca, L.J. Dixon and F. Maltoni, *New color decompositions for gauge amplitudes at tree and loop level*, *Nucl. Phys.* **B 571** (2000) 51 [hep-ph/9910563];
F. Maltoni, K. Paul, T. Stelzer and S. Willenbrock, *Color-flow decomposition of QCD amplitudes*, *Phys. Rev.* **D 67** (2003) 014026 [hep-ph/0209271].

[44] A. Gehrmann-De Ridder, T. Gehrmann and E.W.N. Glover, *Infrared structure of $e^+e^- \to$ 2jets at NNLO*, *Nucl. Phys.* **B 691** (2004) 195 [hep-ph/0403057].

[45] A. Gehrmann-De Ridder, T. Gehrmann and E.W.N. Glover, *Infrared structure of $e^+e^- \to$ 3jets at NNLO: the C_F^2 contribution*, *Nucl. Phys.* **135** *(Proc. Suppl.)* (2004) 97 [hep-ph/0407023].

[46] A. Gehrmann-De Ridder, T. Gehrmann and E.W.N. Glover, *Quark-gluon antenna functions from neutralino decay*, *Phys. Lett.* **B 612** (2005) 36 [hep-ph/0501291].

[47] A. Gehrmann-De Ridder, T. Gehrmann and E.W.N. Glover, *Gluon gluon antenna functions from Higgs boson decay*, *Phys. Lett.* **B 612** (2005) 49 [hep-ph/0502110].

[48] S. Catani, *The singular behaviour of QCD amplitudes at two-loop order*, *Phys. Lett.* **B 427** (1998) 161 [hep-ph/9802439];
G. Sterman and M.E. Tejeda-Yeomans, *Multi-loop amplitudes and resummation*, *Phys. Lett.* **B 552** (2003) 48 [hep-ph/0210130].

[49] T. Kinoshita, *Mass singularities of feynman amplitudes*, *J. Math. Phys.* **3** (1962) 650;
T.D. Lee and M. Nauenberg, *Degenerate systems and mass singularities*, *Phys. Rev.* **133** (1964) B1549.

[50] E. Remiddi and J.A.M. Vermaseren, *Harmonic polylogarithms*, *Int. J. Mod. Phys.* **A 15** (2000) 725 [hep-ph/9905237].

[51] T. Gehrmann and E. Remiddi, *Two-loop master integrals for $\gamma^* \to$ 3jets: the planar topologies*, *Nucl. Phys.* **B 601** (2001) 248 [hep-ph/0008287]; *Two-loop master integrals for $\gamma^* \to$ 3jets: the non- planar topologies*, *Nucl. Phys.* **B 601** (2001) 287 [hep-ph/0101124].

[52] N. Nielsen, *Der Eulersche Dilogarithmus und seine Verallgemeinerungen*, *Nova Acta Leopoldiana (Halle)* **90** (1909) 123;
K.S. Kölbig, J.A. Mignaco and E. Remiddi, *On Nielsen's generalized polylogarithms and their numerical calculation*, *BIT* **10** (1970) 38.

[53] T. Gehrmann and E. Remiddi, *Numerical evaluation of harmonic polylogarithms*, *Comput. Phys. Commun.* **141** (2001) 296 [hep-ph/0107173]; *Numerical evaluation of two-dimensional harmonic polylogarithms*, *Comput. Phys. Commun.* **144** (2002) 200 [hep-ph/0111255].

[54] G.P. Lepage, *A new algorithm for adaptive multidimensional integration*, *J. Comput. Phys.* **27** (1978) 192

[55] R. Kleiss, W.J. Stirling and S.D. Ellis, *A new Monte Carlo treatment of multiparticle phase space at high-energies*, *Comput. Phys. Commun.* **40** (1986) 359.

[56] A. Gehrmann-De Ridder, T. Gehrmann, E.W.N. Glover and G. Heinrich, work in progress.

Received: *August 18, 2006*

Erratum

Some formulae in the article unfortunately contained typographical errors. The corrected formulae are given below.

The sub-antennae for quark-gluon-gluon-antiquark final states at leading and subleading colour should read correctly:

$$
\begin{aligned}
a_4^0(1,3,4,2) \;=\; & \frac{1}{s_{1234}}\Bigg\{\frac{1}{2s_{13}s_{24}s_{34}}\left[2s_{12}s_{14}+2s_{12}s_{23}+2s_{12}^2+s_{14}^2+s_{23}^2\right]\\
&+\frac{1}{2s_{13}s_{24}s_{134}s_{234}}\left[3s_{12}s_{34}^2-4s_{12}^2s_{34}+2s_{12}^3-s_{34}^3\right]\\
&+\frac{1}{s_{13}s_{24}s_{134}}\left[3s_{12}s_{23}-3s_{12}s_{34}+4s_{12}^2-s_{23}s_{34}+s_{23}^2+s_{34}^2\right]\\
&+\frac{3}{2s_{13}s_{24}}\left[2s_{12}+s_{14}+s_{23}\right]+\frac{1}{s_{13}s_{34}}\left[4s_{12}+3s_{23}+2s_{24}\right]\\
&+\frac{1}{s_{13}s_{134}^2}\left[s_{12}s_{34}+s_{23}s_{34}+s_{24}s_{34}\right]\\
&+\frac{1}{s_{13}s_{134}s_{234}}\left[3s_{12}s_{24}+6s_{12}s_{34}-4s_{12}^2-3s_{24}s_{34}-s_{24}^2-3s_{34}^2\right]\\
&+\frac{1}{s_{13}s_{134}}\left[-6s_{12}-3s_{23}-s_{24}+2s_{34}\right]\\
&+\frac{1}{s_{24}s_{34}s_{134}}\left[2s_{12}s_{14}+2s_{12}s_{23}+2s_{12}^2+2s_{14}s_{23}+s_{14}^2+s_{23}^2\right]\\
&+\frac{1}{s_{24}s_{134}}\left[-4s_{12}-s_{14}-s_{23}+s_{34}\right]+\frac{1}{s_{34}^2}\left[s_{12}+2s_{13}-2s_{14}-s_{34}\right]\\
&+\frac{1}{s_{34}^2s_{134}^2}\left[2s_{12}s_{14}^2+2s_{14}^2s_{23}+2s_{14}^2s_{24}\right]-\frac{2s_{12}s_{14}s_{24}}{s_{34}^2s_{134}s_{234}}\\
&+\frac{1}{s_{34}^2s_{134}}\left[-2s_{12}s_{14}-4s_{14}s_{24}+2s_{14}^2\right]\\
&+\frac{1}{s_{34}s_{134}s_{234}}\left[-2s_{12}s_{14}-4s_{12}^2+2s_{14}s_{24}-s_{14}^2-s_{24}^2\right]\\
&+\frac{1}{s_{34}s_{134}}\left[-8s_{12}-2s_{23}-2s_{24}\right]+\frac{1}{s_{134}^2}\left[s_{12}+s_{23}+s_{24}\right]\\
&+\frac{3}{2s_{134}s_{234}}\left[2s_{12}+s_{14}-s_{24}-s_{34}\right]+\frac{1}{2s_{134}}+\mathcal{O}(\epsilon)\Bigg\}\,, \qquad (5.29)\\
\tilde{a}_4^0(1,3,4,2) \;=\; & \frac{1}{s_{1234}}\Bigg\{\frac{1}{s_{13}s_{24}s_{134}s_{234}}\left[\frac{3}{2}s_{12}s_{34}^2-2s_{12}^2s_{34}+s_{12}^3-\frac{1}{2}s_{34}^3\right]\\
&+\frac{1}{s_{13}s_{24}s_{134}}\left[3s_{12}s_{23}-3s_{12}s_{34}+4s_{12}^2-s_{23}s_{34}+s_{23}^2+s_{34}^2\right]\\
&+\frac{s_{12}^3}{s_{13}s_{24}(s_{13}+s_{23})(s_{14}+s_{24})}+\frac{1}{s_{13}s_{24}(s_{13}+s_{23})}\left[\frac{1}{2}s_{12}s_{14}+s_{12}^2\right]
\end{aligned}
$$

JHEP09(2005)056

$$
\begin{aligned}
&+\frac{1}{s_{13}s_{24}(s_{14}+s_{24})}\left[\frac{1}{2}s_{12}s_{23}+s_{12}^2\right]+\frac{1}{s_{13}s_{24}}\left[3s_{12}+\frac{3}{2}s_{14}+\frac{3}{2}s_{23}\right]\\
&+\frac{1}{s_{13}s_{134}^2}\left[s_{12}s_{34}+s_{23}s_{34}+s_{24}s_{34}\right]+\frac{2s_{12}^3}{s_{13}s_{134}s_{234}(s_{13}+s_{23})}\\
&+\frac{1}{s_{13}s_{134}s_{234}}\left[3s_{12}s_{34}-s_{24}s_{34}-2s_{34}^2\right]\\
&+\frac{1}{s_{13}s_{134}(s_{13}+s_{23})}\left[s_{12}s_{24}+s_{12}s_{34}+2s_{12}^2\right]\\
&+\frac{1}{s_{13}s_{134}}\left[-s_{23}-s_{24}+2s_{34}\right]+\frac{1}{s_{13}s_{234}(s_{13}+s_{23})}\left[s_{12}s_{14}+s_{12}s_{34}+2s_{12}^2\right]\\
&+\frac{1}{s_{13}s_{234}}\left[-2s_{12}-2s_{14}+s_{24}+2s_{34}\right]\\
&+\frac{2s_{12}^3}{s_{13}(s_{13}+s_{23})(s_{14}+s_{24})(s_{13}+s_{14})}\\
&+\frac{1}{s_{13}(s_{13}+s_{23})(s_{13}+s_{14})}\left[s_{12}s_{24}+2s_{12}^2\right]\\
&+\frac{1}{s_{13}(s_{14}+s_{24})(s_{13}+s_{14})}\left[s_{12}s_{23}+2s_{12}^2\right]\\
&+\frac{2s_{12}}{s_{13}(s_{13}+s_{14})}-\frac{2}{s_{13}}+\frac{1}{s_{134}^2}\left[s_{12}+s_{23}+s_{24}\right]\\
&\left.+\frac{1}{s_{134}s_{234}}\left[s_{12}-s_{34}\right]+\frac{1}{s_{134}}+\mathcal{O}(\epsilon)\right\}. \qquad (5.30)
\end{aligned}
$$

The sub-antennae for quark-antiquark-quark-antiquark final states should be

$$
\begin{aligned}
b_4^0(1,3,4,2) = &\frac{1}{s_{1234}}\left\{\frac{1}{s_{34}^2s_{134}^2}\left[s_{12}s_{13}s_{14}+s_{13}s_{14}s_{23}-s_{13}^2s_{24}\right]\right.\\
&+\frac{1}{s_{34}^2s_{134}s_{234}}\left[-s_{12}s_{13}s_{24}+s_{13}s_{14}s_{23}-s_{13}s_{24}^2\right]+\frac{1}{s_{34}s_{134}^2}\left[s_{12}s_{13}+s_{13}s_{23}\right]\\
&\left.+\frac{1}{2s_{34}s_{134}s_{234}}\left[2s_{12}s_{13}+s_{12}^2\right]+\frac{s_{12}}{2s_{134}s_{234}}+\mathcal{O}(\epsilon)\right\}. \qquad (5.38)
\end{aligned}
$$

$$
\begin{aligned}
c_4^0(1,2,3,4) = &\frac{1}{s_{1234}}\left\{-\frac{s_{12}s_{13}s_{14}}{2s_{23}s_{34}s_{123}s_{134}}+\frac{1}{2s_{23}s_{34}s_{134}s_{234}}\left[-s_{12}s_{13}s_{24}+s_{13}s_{14}s_{24}\right]\right.\\
&-\frac{s_{13}s_{24}^2}{2s_{23}s_{34}s_{234}^2}-\frac{s_{12}s_{13}}{s_{23}s_{123}s_{134}}\\
&+\frac{1}{2s_{23}s_{123}s_{234}}\left[-s_{12}s_{14}-s_{12}s_{34}-s_{12}^2+s_{13}s_{24}\right]\\
&+\frac{1}{2s_{23}s_{134}s_{234}}\left[s_{12}s_{14}+s_{12}s_{34}+s_{12}^2+s_{13}s_{24}\right]-\frac{s_{13}}{2s_{123}s_{134}}\\
&\left.+\frac{1}{s_{23}s_{234}^2}\left[s_{12}s_{24}+s_{14}s_{24}\right]+\frac{1}{2s_{123}s_{234}}\left[-s_{12}+s_{14}\right]+\mathcal{O}(\epsilon)\right\}. \qquad (5.43)
\end{aligned}
$$

These all agree with [57].

The finite part of the one-loop quark-quark-antiquark antenna function at leading colour should read:

$$\mathcal{F}inite\left(E_3^1(1_q,3_{q'},4_{\bar{q}'})\right) = -\Bigg(R(y_{13},y_{34})+R(y_{14},y_{34})+\frac{3}{2}\log y_{13}+\frac{3}{2}\log y_{14} +\frac{13}{6}\log y_{34}-\frac{40}{9}\Bigg)E_3^0(1,3,4) +R(y_{13},y_{34})\frac{s_{13}}{s_{134}^2}+R(y_{14},y_{34})\frac{s_{14}}{s_{134}^2}\,. \tag{6.29}$$

In the expression (6.44) for $d_4^0(1,3,4,5)$ the overall normalization of the right hand side should be $1/s_{1345}^2$ instead of $1/s_{1345}$.

The leading colour quark-quark-antiquark-gluon antenna should read:

$$\begin{aligned}
E_4^0(1_q,3_{q'},4_{\bar{q}'},5_g) = \frac{1}{s_{1345}^2}\Bigg\{ & -\frac{s_{13}s_{14}}{s_{15}s_{345}}+\frac{s_{14}}{s_{15}s_{34}s_{45}}\left[s_{13}s_{35}+s_{13}^2+s_{14}^2\right] \\
&+\frac{s_{14}}{s_{15}s_{34}s_{134}}\left[2s_{14}s_{35}+2s_{14}s_{45}-s_{35}^2+s_{45}^2\right] \\
&+\frac{s_{14}}{s_{15}s_{45}s_{345}}\left[s_{13}s_{35}+s_{13}^2+s_{14}^2\right]+\frac{s_{14}}{s_{15}s_{45}}\left[2s_{13}+2s_{14}+s_{35}\right] \\
&-\frac{4s_{14}s_{15}^2s_{35}}{s_{34}^2s_{134}s_{345}}+\frac{s_{14}}{s_{34}^2s_{134}}\Big[-4s_{14}s_{15}-4s_{14}s_{35}-4s_{14}s_{45} \\
&+8s_{15}s_{45}+4s_{15}^2+4s_{35}s_{45}+4s_{45}^2\Big] \\
&+\frac{s_{14}}{s_{34}s_{45}s_{134}}\left[-2s_{14}s_{15}-s_{14}s_{35}-2s_{14}^2-s_{15}s_{35}-s_{15}^2\right] \\
&+\frac{s_{14}}{s_{34}s_{134}^2}\left[-4s_{15}s_{35}-4s_{15}s_{45}-2s_{15}^2-4s_{35}s_{45}-2s_{35}^2-2s_{45}^2\right] \\
&-\frac{s_{14}}{s_{345}}+\frac{s_{14}^2}{s_{34}^2s_{134}^2}\left[-4s_{15}s_{35}-4s_{15}s_{45}-2s_{15}^2-4s_{35}s_{45}-2s_{35}^2-2s_{45}^2\right] \\
&+\frac{1}{s_{15}s_{34}s_{345}}\left[s_{13}s_{14}^2+s_{13}^2s_{14}+s_{13}^2s_{35}+s_{13}^3-s_{14}^2s_{35}+s_{14}^3\right] \\
&+\frac{1}{s_{15}s_{34}}\Big[s_{13}s_{14}+3s_{13}s_{35}+s_{13}s_{45}+2s_{13}^2-s_{14}s_{35}+s_{14}s_{45} \\
&+4s_{14}^2+s_{35}s_{45}+s_{35}^2\Big]+\frac{1}{s_{15}s_{134}}\Big[-s_{13}s_{45}+s_{14}s_{35} \\
&+2s_{14}s_{45}-s_{35}s_{45}+s_{45}^2\Big]+\frac{1}{s_{15}}\left[s_{13}+2s_{14}+s_{35}+s_{45}\right] \\
&+\frac{s_{15}}{s_{34}s_{134}s_{345}}\left[-2s_{14}s_{35}+8s_{14}^2-2s_{15}s_{35}+2s_{15}^2+2s_{35}^2\right] \\
&+\frac{s_{35}}{s_{34}^2s_{345}}\Big[4s_{13}s_{14}+8s_{13}s_{15}-4s_{13}s_{35}+4s_{13}^2-4s_{14}s_{35}-4s_{15}s_{35} \\
&+4s_{15}^2\Big]+\frac{s_{35}^2}{s_{34}^2s_{345}^2}\left[-4s_{13}s_{14}-4s_{13}s_{15}-2s_{13}^2-4s_{14}s_{15}-2s_{14}^2-2s_{15}^2\right] \\
&+\frac{1}{s_{34}^2}\Big[-4s_{13}s_{15}+4s_{13}s_{35}-4s_{13}s_{45}-2s_{13}^2+4s_{14}s_{15}+4s_{14}s_{35} \\
&+4s_{14}s_{45}+4s_{15}s_{35}-4s_{15}s_{45}-2s_{15}^2-2s_{45}^2\Big]
\end{aligned}$$

$$
\begin{aligned}
&+\frac{1}{s_{34}s_{134}}\Big[-s_{14}s_{15}-7s_{14}s_{35}+s_{14}s_{45}+7s_{14}^2+s_{15}s_{35}+7s_{15}s_{45}\\
&+6s_{15}^2+2s_{35}s_{45}+s_{35}^2+3s_{45}^2\Big]+\frac{1}{s_{34}s_{345}}\Big[6s_{13}s_{15}+2s_{13}s_{35}+4s_{13}^2\\
&-4s_{14}s_{35}+6s_{14}^2+5s_{15}^2\Big]+\frac{1}{s_{34}}\left[3s_{13}+2s_{14}+6s_{15}+6s_{35}+s_{45}\right]\\
&+\frac{s_{35}}{s_{45}s_{345}^2}\left[2s_{13}s_{14}+2s_{13}s_{15}+s_{13}^2+2s_{14}s_{15}+s_{14}^2+s_{15}^2\right]\\
&+\frac{1}{s_{45}s_{134}s_{345}}\Big[-s_{13}s_{14}s_{15}+s_{13}s_{14}s_{35}-s_{13}s_{14}^2+s_{13}s_{15}s_{35}+3s_{14}s_{15}^2\\
&+3s_{14}^2s_{15}+s_{14}^3+s_{15}^3\Big]+\frac{1}{s_{45}s_{134}}\left[-s_{13}s_{15}+s_{14}s_{15}-s_{14}^2+s_{15}^2\right]\\
&+\frac{1}{s_{45}s_{345}}\Big[-2s_{13}s_{15}+2s_{13}s_{35}-s_{13}^2+3s_{14}s_{15}+s_{14}s_{35}+4s_{14}^2\\
&+s_{15}s_{35}\Big]+\frac{1}{s_{45}}\left[-2s_{13}+2s_{14}-s_{34}\right]\\
&+\frac{1}{s_{134}^2}\left[-2s_{15}s_{35}-2s_{15}s_{45}-s_{15}^2-2s_{35}s_{45}-s_{35}^2-s_{45}^2\right]\\
&+\frac{1}{s_{134}s_{345}}\left[s_{13}s_{14}-3s_{13}s_{15}-s_{13}^2+4s_{14}s_{15}-s_{14}^2-3s_{15}^2\right]\\
&+\frac{1}{s_{134}}\left[-3s_{13}+6s_{14}-3s_{35}+2s_{45}\right]+2+\mathcal{O}(\epsilon)\Bigg\}\,. \qquad (6.48)
\end{aligned}
$$

The decomposition of the gluon-gluon-gluon antenna function should read as:

$$
f_3^0(1,3,2)=\frac{1}{s_{123}^2}\left(2\frac{s_{123}^2s_{12}}{s_{13}s_{23}}+\frac{s_{12}s_{13}}{s_{23}}+\frac{s_{12}s_{23}}{s_{13}}+\frac{8}{3}s_{123}+\mathcal{O}(\epsilon)\right). \qquad (7.13)
$$

The sub-antennae for gluon-gluon-quark-antiquark final states at leading and subleading colour should be

$$
\begin{aligned}
g_4^0(1,3,4,2)\;=\;&\frac{1}{s_{1234}^2}\Bigg\{\frac{1}{s_{12}^2s_{34}^2}\left[2s_{13}s_{14}s_{23}s_{24}-s_{13}^2s_{24}^2-s_{14}^2s_{23}^2\right]+\frac{s_{23}}{s_{12}s_{13}s_{34}}\left[s_{23}^2+s_{24}^2\right]\\
&+\frac{s_{23}}{s_{12}s_{13}s_{134}}\left[s_{23}^2-2s_{24}s_{34}+s_{24}^2+s_{34}^2\right]+\frac{s_{23}}{s_{12}s_{13}}\left[s_{14}+2s_{24}-s_{34}\right]\\
&-\frac{s_{13}}{s_{12}}+\frac{1}{s_{12}s_{34}s_{134}}\Big[-2s_{14}s_{23}^2+2s_{14}s_{24}^2+2s_{14}^2s_{23}+2s_{14}^2s_{24}+s_{23}s_{24}^2\\
&+s_{23}^2s_{24}+s_{23}^3+s_{24}^3\Big]+\frac{1}{s_{12}s_{34}}\Big[2s_{13}s_{14}+4s_{13}s_{23}+3s_{13}s_{24}+2s_{13}^2\\
&-s_{14}s_{23}+4s_{14}^2\Big]+\frac{1}{s_{12}s_{134}}\left[2s_{14}s_{24}-4s_{23}s_{24}+s_{23}s_{34}+s_{24}s_{34}\right]\\
&+\frac{s_{12}}{s_{34}s_{134}s_{234}}\left[2s_{12}s_{14}+s_{12}^2+4s_{14}s_{24}+4s_{14}^2+4s_{24}^2\right]\\
&+\frac{s_{12}}{s_{134}s_{234}}\left[6s_{14}+6s_{24}+3s_{34}\right]+\frac{2s_{12}^2s_{14}s_{24}}{s_{34}^2s_{134}s_{234}}+\frac{1}{2s_{13}s_{24}}\left[s_{12}s_{34}-s_{14}s_{23}\right]\\
&+\frac{s_{24}}{s_{13}s_{34}s_{234}}\left[-2s_{12}s_{24}+s_{12}^2+2s_{24}^2\right]+\frac{1}{s_{13}s_{34}}\Big[-2s_{12}s_{23}+2s_{12}s_{24}
\end{aligned}
$$

$$
\begin{aligned}
&-s_{12}^2+2s_{23}s_{24}-2s_{23}^2-2s_{24}^2\Big]+\frac{s_{34}}{s_{13}s_{134}^2}\Big[-2s_{12}s_{23}-2s_{12}s_{24}-s_{12}^2\\
&-2s_{23}s_{24}-s_{23}^2-s_{24}^2\Big]+\frac{1}{s_{13}s_{134}s_{234}}\Big[6s_{12}s_{24}s_{34}+4s_{12}s_{24}^2+3s_{12}s_{34}^2\\
&-3s_{12}^2s_{24}-3s_{12}^2s_{34}+s_{12}^3-3s_{24}s_{34}^2-4s_{24}^2s_{34}-2s_{24}^3-s_{34}^3\Big]\\
&+\frac{1}{s_{13}s_{134}}\Big[8s_{12}s_{23}-4s_{12}s_{24}-4s_{12}s_{34}+4s_{12}^2-2s_{23}s_{34}+6s_{23}^2+2s_{24}^2\\
&+2s_{34}^2\Big]+\frac{1}{s_{13}s_{234}}\left[-4s_{12}s_{24}-2s_{12}s_{34}+s_{12}^2+3s_{24}s_{34}+4s_{24}^2+s_{34}^2\right]\\
&+\frac{1}{s_{13}}\left[2s_{12}+2s_{23}-2s_{24}-2s_{34}\right]+\frac{s_{14}}{s_{34}^2s_{134}}\Big[-4s_{12}s_{14}+8s_{12}s_{24}+2s_{12}^2\\
&-4s_{14}s_{23}-4s_{14}s_{24}+4s_{23}s_{24}+4s_{24}^2\Big]+\frac{s_{14}^2}{s_{34}^2s_{134}^2}\Big[-4s_{12}s_{23}-4s_{12}s_{24}\\
&-2s_{12}^2-4s_{23}s_{24}-2s_{23}^2-2s_{24}^2\Big]+\frac{1}{s_{34}^2}\Big[-4s_{12}s_{13}+4s_{12}s_{14}-s_{12}^2\\
&+4s_{13}s_{23}-2s_{13}s_{24}-2s_{13}^2+2s_{14}s_{23}\Big]+\frac{1}{s_{34}s_{134}}\Big[4s_{12}s_{23}+2s_{12}s_{24}+5s_{12}^2\\
&-8s_{14}s_{23}+6s_{14}s_{24}+6s_{14}^2+6s_{23}^2+4s_{24}^2\Big]+\frac{1}{s_{34}}\left[2s_{12}+2s_{13}+6s_{14}\right]\\
&+\frac{1}{s_{134}^2}\left[-2s_{12}s_{23}-2s_{12}s_{24}-s_{12}^2-2s_{23}s_{24}-s_{23}^2-s_{24}^2\right]\\
&+\frac{1}{s_{134}}\left[-4s_{12}+4s_{14}-4s_{23}-2s_{24}+3s_{34}\right]-\frac{7}{2}+\mathcal{O}(\epsilon)\Bigg\}\,, \qquad (7.50)
\end{aligned}
$$

$$
\begin{aligned}
\tilde{g}_4^0(1,3,4,2) = \frac{1}{s_{1234}^2}\Bigg\{&\frac{s_{12}^2+2s_{23}^2+2s_{12}s_{23}}{s_{13}s_{14}}+\frac{s_{12}s_{24}}{2s_{13}s_{23}s_{134}s_{234}}\left[s_{24}^2+s_{12}^2\right]\\
&+\frac{s_{12}}{2s_{13}s_{23}s_{134}}\left[s_{24}s_{34}-s_{24}^2-s_{34}^2-s_{12}^2\right]+\frac{1}{2s_{13}s_{24}}\left[s_{12}s_{34}-s_{14}s_{23}\right]\\
&+\frac{s_{34}}{s_{13}s_{134}^2}\left[-2s_{12}s_{23}-2s_{12}s_{24}-s_{12}^2-2s_{23}s_{24}-s_{23}^2-s_{24}^2\right]\\
&+\frac{1}{s_{13}s_{134}s_{234}}\Big[\frac{7}{2}s_{12}s_{24}s_{34}+\frac{1}{2}s_{12}s_{24}^2+\frac{5}{2}s_{12}s_{34}^2-3s_{12}^2s_{34}+\frac{1}{2}s_{12}^3-2s_{24}s_{34}^2\\
&-2s_{24}^2s_{34}-s_{34}^3\Big]+\frac{1}{s_{13}s_{134}}\Big[-2s_{12}s_{24}-4s_{12}s_{34}-s_{12}^2-2s_{23}s_{34}+s_{23}^2\\
&+2s_{24}s_{34}-s_{24}^2\Big]+\frac{1}{s_{13}s_{234}}\Big[-2s_{12}s_{24}-2s_{12}s_{34}+s_{12}^2+2s_{24}s_{34}\\
&+2s_{24}^2+s_{34}^2\Big]+\frac{1}{s_{13}}\left[2s_{12}+2s_{23}-2s_{24}\right]+\frac{1}{s_{134}^2}\Big[-2s_{12}s_{23}-2s_{12}s_{24}\\
&-s_{12}^2-2s_{23}s_{24}-s_{23}^2-s_{24}^2\Big]+\frac{s_{12}}{s_{134}s_{234}}\left[-2s_{34}-s_{12}\right]\\
&+\frac{1}{s_{134}}\left[-2s_{12}-s_{23}-s_{24}-s_{34}\right]-\frac{1}{2}+\mathcal{O}(\epsilon)\Bigg\}\,. \qquad (7.51)
\end{aligned}
$$

The content of the paper is unaffected by these errors.

Added acknowledgments

We would like to thank Alejandro Daleo and Stefan Weinzierl for pointing out these errors to us.

Added references

[57] S. Weinzierl, *NNLO corrections to 2-jet observables in electron positron annihilation*, *Phys. Rev.* **D 74** (2006) 014020 [hep-ph/0606008].